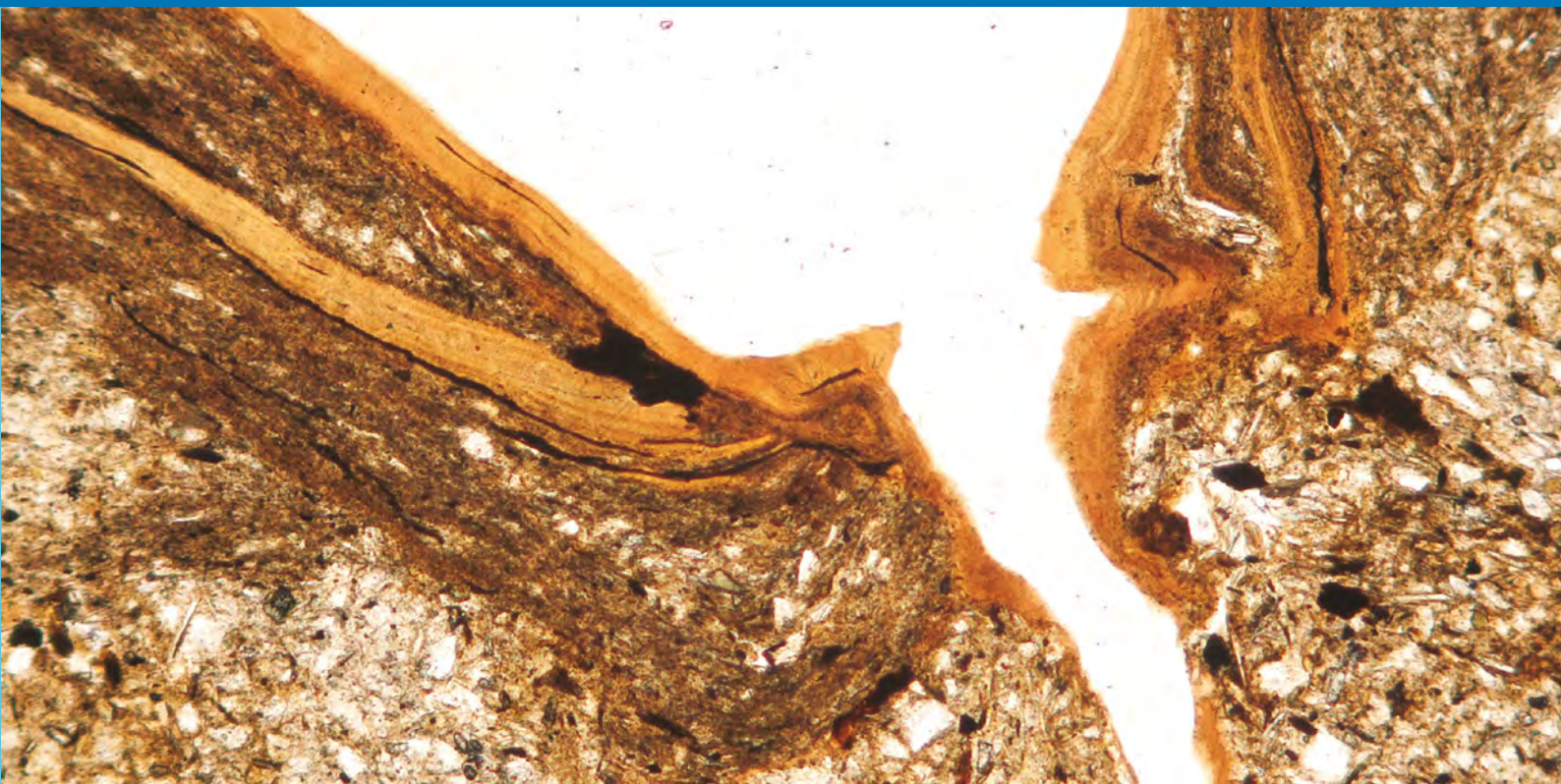


# E&G

Eiszeitalter und Gegenwart  
Quaternary Science Journal



Vol. 62  
No 1  
2013

## MIDDLE TO UPPER PLEISTOCENE PALEOSOLS IN AUSTRIA

**GUEST EDITOR** Birgit Terhorst

# E & G

## Eiszeitalter und Gegenwart Quaternary Science Journal

Volume 62 / Number 1 / 2013 / DOI: 10.3285/eg.62.1 / ISSN 0424-7116 / www.quaternary-science.net / Founded in 1951

### EDITOR

DEUQUA  
Deutsche Quartärvereinigung e.V.  
Office  
Stilleweg 2  
D-30655 Hannover  
Germany  
Tel: +49 (0)511-643 36 13  
E-Mail: info [at] deuqua.de  
www.deuqua.org

### PRODUCTION EDITOR

SABINE HELMS  
Geozon Science Media  
Postfach 3245  
D-17462 Greifswald  
Germany  
Tel. +49 (0)3834-80 14 60  
E-Mail: helms [at] geozon.net  
www.geozon.net

### EDITOR-IN-CHIEF

HOLGER FREUND  
ICBM – Geoecology  
Carl-von-Ossietzky Universität Oldenburg  
Schleusenstr. 1  
D-26382 Wilhelmshaven  
Germany  
Tel.: +49 (0)4421-94 42 00  
Fax: +49 (0)4421-94 42 99  
E-Mail: holger.freund [at] uni-oldenburg.de

### ASSOCIATE EDITORS

PIERRE ANTOINE, Laboratoire de Géographie  
Physique, Université Paris i Panthéon-  
Sorbonne, France

MARKUS FUCHS, Department of Geography,  
Justus-Liebig-University Giessen, Germany

RALF-DIETRICH KAHLKE, Senckenberg  
Research Institute, Research Station of  
Quaternary Palaeontology Weimar, Germany

THOMAS LITT, Steinmann-Institute of Geology,  
Mineralogy and Paleontology, University of  
Bonn, Germany

LESZEK MARKS, Institute of Geology, University  
of Warsaw, Poland

HENK J. T. WEERTS, Physical Geography Group,  
Cultural Heritage Agency Amersfoort, The  
Netherlands

### FORMER EDITORS-IN-CHIEF

PAUL WOLDSTEDT [1951–1966]

MARTIN SCHWARZBACH [1963–1966]

ERNST SCHÖNHALS [1968–1978]

REINHOLD HUCKRIEDE [1968–1978]

HANS DIETRICH LANG [1980–1990]

JOSEF KLOSTERMANN [1991–1999]

WOLFGANG SCHIRMER [2000]

ERNST BRUNOTTE [2001–2005]

### ADVISORY EDITORIAL BOARD

FLAVIO ANSELMETTI, Department of Surface  
Waters, Eawag [Swiss Federal Institute of  
Aquatic Science & Technology], Dübendorf,  
Switzerland

KARL-ERNST BEHRE, Lower Saxonian Institute  
of Historical Coastal Research, Wilhelmshaven,  
Germany

PHILIP GIBBARD, Department of Geography,  
University of Cambridge, Great Britain

VOLLI E. KALM, Institute of Ecology and Earth  
Sciences, University of Tartu, Estonia

CESARE RAVAZZI, Institute for the Dynamics of  
Environmental Processes, National Research  
Council of Italy, Italy

JAMES ROSE, Department of Geography, Royal  
Holloway University of London, Great Britain

CHRISTIAN SCHLÜCHTER, Institute of  
Geological Sciences, University of Bern,  
Switzerland

DIRK VAN HUSEN, Altmünster, Austria

JEF VANDENBERGHE, Faculty of Earth and  
Life Sciences, VU University Amsterdam, The  
Netherlands

ANDREAS VÖTT, Institute of Geography,  
Johannes Gutenberg-Universität Mainz,  
Germany

### AIMS & SCOPE

The *Quaternary Science Journal* publishes original articles of quaternary geology, geography, palaeontology, soil science, archaeology, climatology etc.; special issues with main topics and articles of lectures of several scientific events.

### MANUSCRIPT SUBMISSION

Please upload your manuscript at the on-line submission system at our journal site [www.quaternary-science.net](http://www.quaternary-science.net). Please note the instructions for authors before.

### FREQUENCY

2 numbers per year

### SUBSCRIPTION

Free for DEUQUA-Members! Prices for standing order: single number 27,- Euro; double number 54,- Euro; plus shipping costs. We offer discounts for libraries and bookstores. Please subscribe to the journal at the publisher *Geozon Science Media*.

### JOURNAL EXCHANGE

If you are interested in exchange your journal with the *Quaternary Science Journal*, please contact: Universitätsbibliothek Halle Tauschstelle, Frau Winther August-Bebel-Straße 13 D-06108 Halle (Saale), Germany

Tel. +49 (0)345-55 22 183

E-Mail: [tausch \[at\] bibliothek.uni-halle.de](mailto:tausch[at]bibliothek.uni-halle.de)

### REORDER

Reorders are possible at the publishing house. See full list and special prices of available numbers on next to last page.

### PUBLISHING HOUSE

Geozon Science Media UG (haftungsbeschränkt)  
Postfach 3245  
D-17462 Greifswald  
Germany  
Tel. +49 (0)3834-80 14 80  
E-Mail: [info \[at\] geozon.net](mailto:info[at]geozon.net)  
[www.geozon.net](http://www.geozon.net)

### PRINT

Printed in Germany on 100% recycled paper climate neutral produced

### COVER FIGURE

Laminated clay coatings with limpid and impure microlayers. BCtg horizon, plain polarized light.

### RIGHTS

Copyright for articles by the authors

### LICENSE

Distributed under a Creative Commons Attribution License 3.0  
<http://creativecommons.org/licenses/by/3.0/>



## Middle to Upper Pleistocene paleosols in Austria

*Preface to the special issue*

Birgit Terhorst

Since the year 2000 we carry out research projects in the area of the Pleistocene Salzach glacier, the Inn terraces of the 'Innviertel', as well as in the area of the Traun-Enns Plate (Traun-Enns-Platte) in Upper Austria. Five papers of the special issue are concerned with Quaternary sediments, paleosols and recent soils in Upper Austria. The focus is placed on the Oberlaab Loess-paleosols sequence, which was studied in great detail. National as well as international working groups were successively involved and there are numerous studies, which comprise classical field and laboratory methods, microscopic, magnetic, and paleobotanic analyses. The research works started on the base of the project 'Geomorphological and Pedological Investigations in the Former Foreland Glacier of the River Salzach/Austria', which was funded by the German Research Foundation (DFG) under the guidance of Prof. Dr. Erhard Bibus, Tübingen. Moreover, subsequent studies were supported by the University of Tübingen and an international project, which was part of the ICSU Grant Program under the title 'Polygenetic Models

for the Pleistocene Paleosols: A new Approach to decoding the Paleosol-Sedimentary Records'. The research team was formed by a German-Austrian-Mexican-Russian group, of which the major part participated in the present special issue (OTTNER & SEDOV, SEDOV et al., SOLLEIRO-REBOLLEDO et al., TERHORST; this volume). A further project in the area was organised by Prof. Dr. van Husen (ÖAW; Austrian Academy of Science). In the frame of this project concerned with the stratigraphy of the Middle Pleistocene (Untersuchungen zur zeitlichen Gliederung des mittleren Abschnitts des Quartärs), detailed studies were carried out in the former brickyard of Wels-Aschet (see SCHOLGER & TERHORST, this volume).

Since 2007 the research area was extended to the east by the loess region of Lower Austria. The research team experienced an enlargement by the cooperation with Austrian archeologists in the Krems region. The extension of the research area is represented by the paper of Sprafke et al. (this volume) and deals with the well-known outcrop of Paudorf.

# A stratigraphic concept for Middle Pleistocene Quaternary sequences in Upper Austria

Birgit Terhorst

**How to cite:** TERHORST, B. (2013): A stratigraphic concept for Middle Pleistocene Quaternary sequences in Upper Austria. – E&G Quaternary Science Journal, 62 (1): 4–13. DOI: 10.3285/eg.62.1.01

**Abstract:** Three profiles of loess-palaeosol sequences on top of Middle Pleistocene fluvio-glacial terraces of the Traun-Enns-Plate are investigated in the region of Wels (Upper Austria), each of them representing characteristic Middle Pleistocene sequences for the northeastern Alpine Foreland. The sequences comprise thick pedocomplexes, providing the opportunity to distinguish and to classify specific interglacial palaeosols. The loess-palaeosol sequence of Oberlaab developed on top of the fluvio-glacial terrace of the classical Mindel (Younger Deckenschotter) shows four interglacial palaeosols. This fact suggests that the age of the terrace is at least the fifth to last glacial period, correlative to MIS 12. The cover layers on top of classical Günz terrace (Older Deckenschotter) in Neuhofer and Wels-Aschet include five palaeosols. Both sites are characterised by intense pedogenesis in the basal pedocomplex, which is considerably more pronounced than in the overlying palaeosols. Pedostratigraphic results point out that the genesis of the studied Günz Deckenschotter can be correlated to MIS 16 (minimum age).

## Ein stratigraphisches Konzept für mittelpleistozäne Quartärabfolgen in Oberösterreich

**Kurzfassung:** Auf den mittelpleistozänen fluvio-glazialen Terrassen der Traun-Enns-Platte in der Region um Wels (Oberösterreich) wurden drei Löss-/Paläobodensequenzen untersucht. Jedes dieser Profile ist für mittelpleistozäne Abfolgen im nordöstlichen Alpenvorland charakteristisch. Die Profile umfassen mächtige Pedokomplexe, welche eine Differenzierung und Einstufung von interglazialen Paläoböden erlauben. Die Löss-/Paläobodensequenz von Oberlaab ist auf der fluvio-glazialen Terrasse des Mindel-Glazials im klassischen Sinne entwickelt (Jüngere Deckenschotter) und weist vier interglaziale Paläoböden auf. Diese Tatsache macht eine Einstufung der Jüngeren Deckenschotter mindestens in die fünftletzte Kaltzeit wahrscheinlich (MIS 12). Die Deckschichten auf den Günz-Deckenschottern im klassischen Sinn (Ältere Deckenschotter) beinhalten fünf Paläoböden. Beide Lokalitäten weisen eine sehr intensive Pedogenese in ihrem basalen Pedokomplex auf, die wesentlich ausgeprägter ist, als in den überlagernden Paläoböden. Die pedostratigraphischen Ergebnisse lassen eine Einstufung der Älteren Deckenschotter mindestens ins MIS 16 zu.

**Keywords:** *Quaternary stratigraphy, Wels-Aschet, Oberlaab, landscape formation, palaeosols, loess*

**Address of author:** B. Terhorst, University of Würzburg, Institute of Geography and Geology, Am Hubland, D-97074 Würzburg, Germany. E-Mail: birgit.terhorst@uni-wuerzburg.de

## 1 Introduction

By now, numerous palaeoclimatic curves based on marine drillings give a distinct idea of the number of glacial-interglacial cycles, as well as of the palaeoclimatic evolution of the Middle Pleistocene. Terrestrial studies in Europe are unable to accomplish these targets as they lack dating methods. This is the case especially for the Middle Pleistocene time span in the northern Alpine Foreland. In this context, HABBE (2003) mentions a time gap in numerical datings between the classical Günz and the Upper Pleistocene. The palaeomagnetic boundary at the transition from Lower to Middle Pleistocene ( $\approx 780.000$  yrs) is therefore of crucial stratigraphical importance as it is one of the rare opportunities to date in the middle and lower Middle Pleistocene. The stratigraphical position as well as the ages of the four classical glacial deposits (sensu PENCK & BRÜCKNER 1901–1909) are still under discussion. The Quaternary sediments of the western and the

eastern Alpine Foreland are hardly correlative also because of the use of different stratigraphic systems and because of the fact that terrace bodies can comprise more than one formation period (DOPPLER et al. 2011, SCHELLMANN et al. 2010).

For example, on the one hand, the Matuyama/Brunhes boundary (MBB) could be proved in Günz deposits at the location Heiligenberg (ELLWANGER et al. 1995) for the western Alpine Foreland in Baden-Württemberg. On the other hand, however, the palaeomagnetic reversal occurred within the Younger Deckenschotter (classical Mindel) near Basel (ZOLLINGER 1991), which coincides with pedostratigraphical results (BIBUS 1990). Actually, the stratigraphical system of the Pleistocene Rhineglacier area classifies the formation of the Mindel Deckenschotter as a terrace complex prior to and during the MBB. Furthermore, the Günz Deckenschotter are ranked as Early Pleistocene formations there (ELLWANGER et al. 2011). DOPPLER et al. (2011) developed a stratigraphical scheme for the Bavarian Alpine Foreland, which integrates



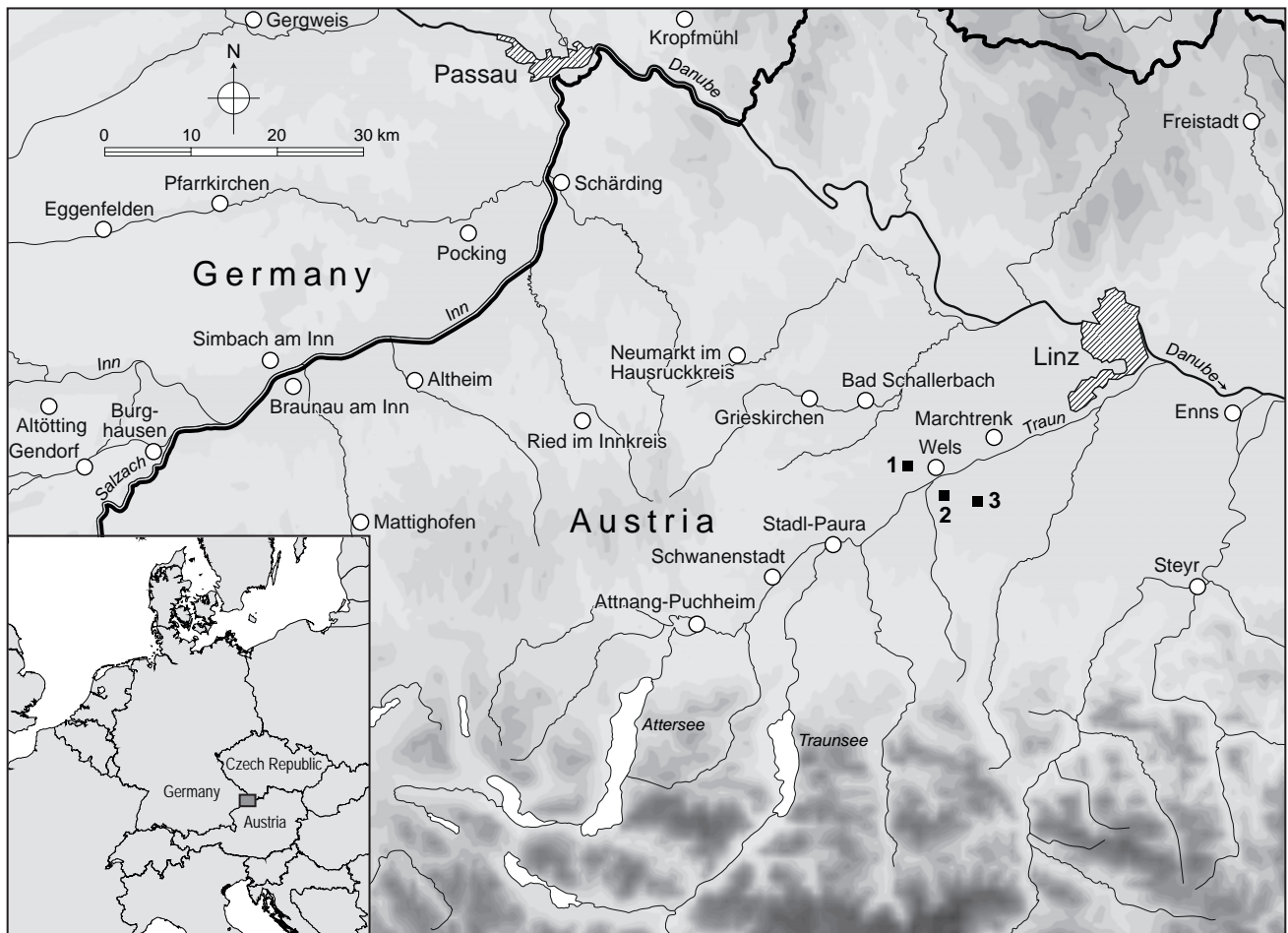


Fig. 1: Study area in Upper Austria. x1 = profile Oberlaab, x2 = profile Wels-Aschet, x3 = profile Neuhofen.

Abb. 1: Untersuchungsgebiet in Oberösterreich. x1 = Profil Oberlaab, x2 = Profil Wels-Aschet, x3 = Profile Neuhofen.

Mindel into the Brunhes-Epoch and Günz sediments mainly to the Matuyama-Epoch. The authors do not exclude that Günz sediments in parts belong to the Brunhes-Epoch. Single datings in the Bavarian foreland obtained with cosmogenic nuclides resulted in  $0.68 \pm 0.23 / -0.24$  Ma for a Mindel deposit and  $2.35 \pm 1.08 / -0.88$  Ma for a Günzian site (HÄUSELMANN et al. 2007). The error rate for the datings are remarkable high. Furthermore, it has to be mentioned that the formation period of Günz, respectively Mindel sediments in Bavaria do not correspond to those in Baden-Württemberg, in general (DOPPLER et al. 2011).

In the northeastern Alpine Foreland of Austria the “Günz complex” is assumed slightly above the MBB (VAN HUSEN 2000, VAN HUSEN & REITNER 2011b), as the transition from reverse to normal magnetisation was not yet verified in any sequence, and the studied sediments show positive magnetisation throughout (cf. KOHL 2000).

A stratigraphic classification of Quaternary forms and sediments in the northern Alpine Foreland above the MBB remains problematic. Absolute ages of Middle Pleistocene deposits are ambiguous (cf. PREUSSER & FIEBIG 2009), and detailed subdivisions are still impossible. This eventually results in the difficulty that even comparably complete Quaternary sequences are not available for a correlation on a supra-regional scale. As a consequence, this is also shown in the stratigraphic chart of the German Stratigraphic Commission (DEUTSCHE STRATIGRAPHISCHE KOMMISSION 2002), which

displays large uncertainties below the Riß complex within the chronostratigraphic correlation of glacial complexes between the northwestern and northeastern Alpine Foreland. The problem further becomes evident in the Austrian stratigraphic chart (ÖSTERREICHISCHE STRATIGRAPHISCHE KOMMISSION 2004).

For these reasons, palaeopedological/pedostratigraphical studies represent an important factor for the study area in assessing the stratigraphic position of the Younger and Older Deckenschotter. SCHOLGER & TERHORST (this volume) proposed a stratigraphic scheme for the loess-palaeosol sequence of Wels-Aschet, which is situated on top of the Günz Deckenschotter. The authors proved Middle Pleistocene palaeomagnetic excursions and classified them on the base of pedostratigraphy. According to the mentioned study, the uppermost section of the Günz Deckenschotter is older than 570–560 ka (Emperor - Big Lost - Calabrian Ridge 3 excursion) and thus is correlated with MIS 16 (SCHOLGER & TERHORST, this volume). The palaeomagnetic approach was applied for the first time in loess sequences in order to establish a chronological framework for Middle Pleistocene in the study area. In this context, it has to be mentioned that MARKOVIC et al. (2009, 2011) applied rock magnetic parameters to build up a Middle Pleistocene stratigraphy for palaeosols and loess sediments of the Middle Danube Basin. The authors were able to correlate their results to marine isotopic curves (see also BRONGER 1970).

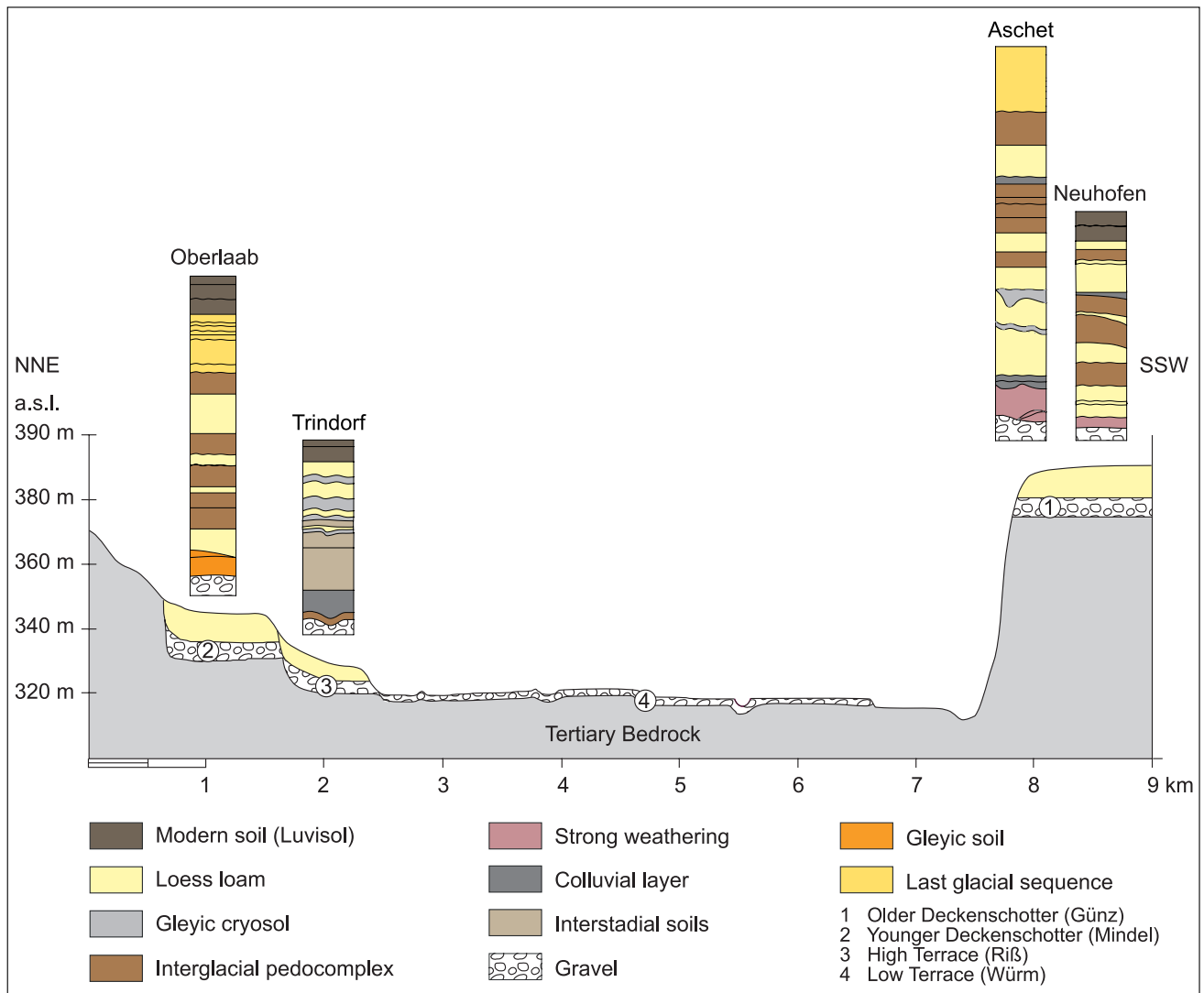


Fig. 2: Geomorphological situation of the presented profiles close to the river Traun/Wels. The uppermost interglacial pedocomplex of all profiles corresponds most probable to the Eemian interglacial soil (see also SCHOLGER & TERHORST, this volume).

Abb. 2: Geomorphologische Situation der präsentierten Profile in der Umgebung der Traun bei Wels. Der oberste interglaziale Pedokomplex entspricht mit hoher Wahrscheinlichkeit jeweils dem Eem-Interglazialboden (vgl. SCHOLGER & TERHORST, dieser Band).

In general, Middle Pleistocene terrestrial stratigraphy is still at its starting point and detailed research with palaeopedological and magnetostratigraphical methods as well as with new luminescence approaches is crucial for the development of a regional terrestrial stratigraphic framework as a first step. Moreover, for future research there is a need i) to correlate terrestrial regional results with each other and ii) to link to results of global palaeoclimatic archives.

This study is intended to propose a Middle Pleistocene stratigraphic framework for Quaternary sediments in the region of Wels.

### 1.1 Study area

The study area is situated on the Traun-Enns plate between Wels and Linz (Fig. 1). The mean annual air temperature is at 9.1°C, precipitation accounts for 821 mm per year. Holocene soils as developed in terraces, loess and loess-like sediments are Luvisols (Parabraunerde) with transitional stages to Stagnosols (Pseudogley).

The sequence of fluvio-glacial terraces is presented in Fig-

ure 2. It shows the spatial situation of the classical morphostratigraphic elements (cf. PENCK & BRÜCKNER 1901–1909). In the lowermost position, two Würmian terraces are present close to the present day floodplain of the river Traun. The Riß terrace in Figure 2 occurs at the left hand side, separated only by a small step to the next higher terrace level of the Younger Deckenschotter (~340m a.s.l.). The position of the Older Deckenschotter in Wels is at ~380 a.s.l. covered by a loess palaeosol sequence of up to 10 m thickness. Profile Neuhofen on top of the Older Deckenschotter is situated 15 km to the east.

For the maximum advances of the younger main glacial phases of Riß and Würm, marine isotopic stages MIS 6 and 2 are correlative (TERHORST et al. 2002). Most probably, Günz and Mindel occur simultaneously with phases of massive global climate decrease during MIS 16 and MIS 12 for the study area (VAN HUSEN & REITNER 2011b).

The studied Younger and Older Deckenschotter are covered with loess and loess loams, reaching a thickness up to 12 m and comprising extensive palaeosols and pedocomplexes.

Studies on Quaternary deposits in the study area are avail-

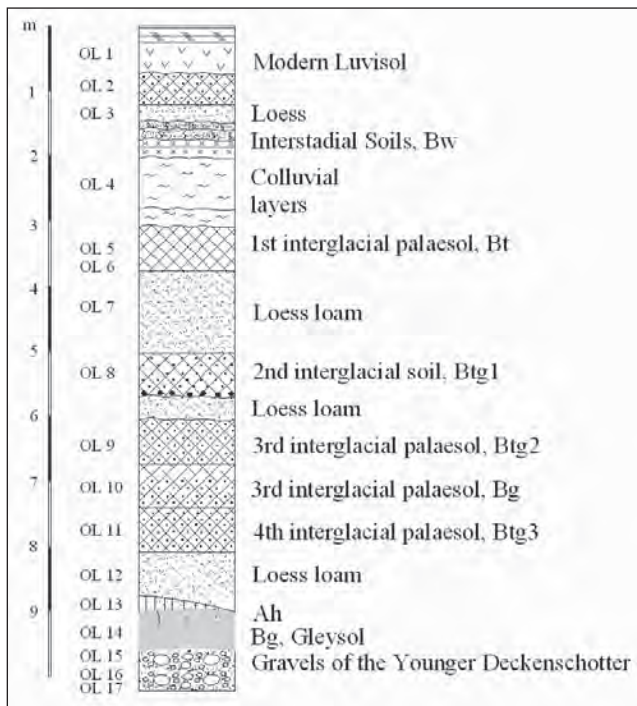


Fig. 3: Detailed palaeopedological profile of the Quaternary sequence Oberlaab on top of the Younger Deckenschotter (Mindel).

Abb. 3: Detailliertes paläopedologisches Profil der quartären Abfolge in Oberlaab auf den Jüngeren Deckenschottern (Mindel).

able by KOHL & KRENMAYR (1997), STREMMER et al. (1991) and FINK et al. (1978). Analyses on the sedimentological and mineralogical composition of the cover layers were performed by TERHORST et al. (2003) and TERHORST et al. (2011a, b).

In total, three Middle Pleistocene loess-palaeosol sequences of the Traun-Enns plate are presented, of which one profile is situated on top of the Younger Deckenschotter, while two evolved in the Older Deckenschotter. In general, the studied loess sediments are decalcified loess loams, undergone weathering processes and later redeposition. All described palaeosols have been affected by polygenetic pedogenesis and thus, correspond to pedocomplexes, although the expression partly palaeosol is used.

In order to give the complete view of Quaternary sequences in the study area, the Upper Pleistocene sequence is involved in the stratigraphic scheme, however, not described in detail here (see TERHORST et al. 2002).

## 2 Palaeopedological Results

### 2.1 The cover layers of the Younger Deckenschotter in profile Oberlaab

The loam pit Oberlaab, which is still being quarried, is located about 1.5 km north of Wels and belongs to Pichler brickyard. It represents the only pit currently accessible in the study area, in which the Younger Deckenschotter with superimposed cover layers is exposed.

The walls have been investigated several times and the situation in 2001 is presented by TERHORST (2007). Detailed field analyses were conducted in form of an international cooperation in the year 2003, of which the most complete sequence is presented in SOLLEIRO-REBOLLEDO et al. (this volume).

In 2003, excavated material showed relatively unweathered gravels and sands of the Younger Deckenschotter (Fig. 3, OL 15–17). The terrace gravels are carbonate-free in this location (Fig. 3), and debris from sedimentary rocks is weakly weathered, while crystalline debris shows almost no signs of weathering. However, KOHL (2000) also mentions the occurrence of highly weathered gravels at a former profile section. The terrace deposits are interspersed with distinct bands of iron and manganese.

In the eastern part of the pit on top of the Younger Deckenschotter an intensely greyish Gleysol (OL 14) is encountered, which shows an extraordinarily high number of root traces, and even remains of relic roots occur in places. Immediately on top of it an Ah horizon of up to 60 cm thickness appears locally (OL 13).

The gleyic horizons are covered by a silty, redoximorphic, and also weathered loess loam, which can be traced all over the exposure (OL 12).

The studied wall exhibited before 2003 showed a pedocomplex on top of the above described loess loam with a thickness of up to 2 m (OL 11–OL 9). The latter consists of the basal horizons of two single Stagnic Luvisol pedocomplexes, which were in parts multiply transformed by pedogenesis and correspond to two interglacial phases. Conspicuously, the horizon boundaries are very sharp and linear in some places and could therefore represent erosional surfaces. Interestingly, the single soil horizons (OL 11–OL 9) can be traced by their characteristic features over the entire exposure, which emphasises the independence of each palaeosol. In general, the third Btg horizon is characterised by its intense manganese precipitations and coatings. Additionally, a zone of reduced weathering intensity occurs between the third and fourth fossil soil, which is noticeable by lower clay content with simultaneously higher silt content.

On top of the third Btg horizon a loess loam (OL 8a) follows in some parts of the exposure, which is separated by a stone line from horizon OL 8. OL 8 corresponds to the second well developed Btg horizon and therefore indicates a further interglacial.

The pedocomplex is covered by a loess loam of up to 2 m thickness, which partly was affected by stagnic conditions (OL 7). Based on its stratigraphic position in the profile, the sediment most probably represents a Rißian loess loam.

On top of it the Eemian interglacial soil in form of a Bt horizon is developed (cf. SEDOV et al., this volume).

The western wall of the exposure shows a characteristic sequence of Würmian loess of up to 2 m thickness above the Eemian interglacial soil, which can be compared, even though strongly shortened in this place, to the loess-palaeosol sequences of the Last Glacial, which are present on top of the 'Hochterrasse' (classical Riß) in the study area. At the base colluvial layers are encountered (OL 4). On top of these, weakly redeposited residuals of Middle Würmian interstadials are preserved, covered by thin loess (OL 3).

The modern soil is a Stagnic Luvisol with a thickness of more than 1 m (OL 2, 1).

In conclusion, at least four interglacial pedocomplexes (OL 5/6 and OL 8 to OL 11) can be identified in the cover layers of the presented profile.



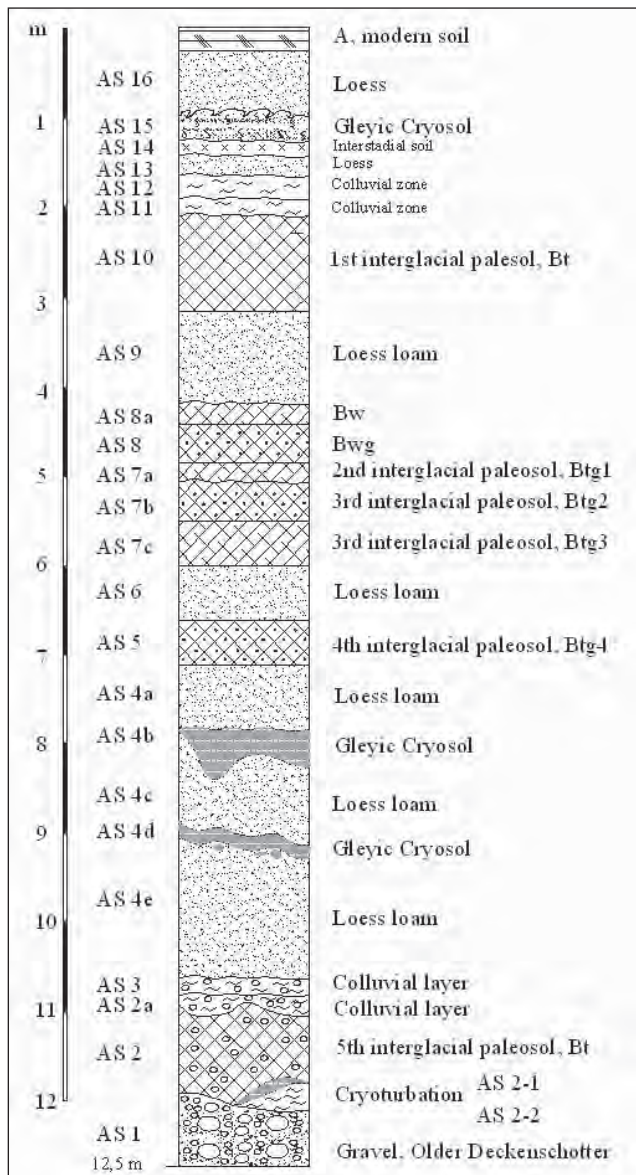


Fig. 4: Detailed palaeopedological profile of the sequence Wels-Aschet on top of the Older Deckenschotter (Günz).

Abb. 4: Detailliertes paläopedologisches Profil der quartären Abfolge in Wels-Aschet auf den Älteren Deckenschottern (Günz).

## 2.2 The cover layers of the Older Deckenschotter in profile Wels-Aschet

Profile Wels-Aschet was dug up and documented anew in 2003 by a working group headed by Prof. Dr. Dirk van Husen. Older studies on the loam pit of Pichler brickyard in Wels-Aschet are available by KOHL & KRENMAYR (1997), KOHL (2000) and STREMMER et al. (1991).

Recently, detailed descriptions are available in the study of TERHORST (2007), TERHORST et al. (2011a, b). Stratigraphical concepts have been presented by PREUSSER & FIEBIG (2009) and SCHOLGER & TERHORST (this volume).

The loess-palaeosol sequence of the studied profile reaches a thickness of 12.5 m. It is mostly decalcified while gravel deposits of the Older Deckenschotter show high lime contents.

The basal section of the profile displays an intensely red-

dish, strong weathering (Fig. 4, AS 2) with dark red clay cutans in the gravels of the Older Deckenschotter (AS 1). Fine earth shows the highest clay content of the profile. In places, the palaeosol is slightly disturbed by cryoturbations.

Above the palaeosol, which represents at least one interglacial, redeposited, gravel-bearing layers are present, which were covered by a 3.5 m thick loess loam (AS 4a–4e), which is disturbed twice by cryoturbation structures. These structures correspond to relic Cryosols and show an intense greyish brown colouring. This double subdivision of the lower loess loam of the Older Deckenschotter was already described by KOHL (2000) for Wels-Aschet, as well as for the former exposure Linz/Grabnerstraße (FINKE et al. 1978). Within the loess loam AS 4a a palaeosol developed, which is proved by an intensely stagnic, dark yellowish brown Btg horizon of interglacial intensity (AS 5). The soil texture is characterised by silty clay, and clay cutans are widely distributed across the entire horizon. The former topsoil is eroded.

A further, thin and unstructured layer of loess loam (AS 6) overlies palaeosol AS 5. Above this loam a multiply layered pedocomplex is developed (AS 8a–7c). The basal Btg horizons (AS 7b, 7c) are silty clays and contain distinct reddish brown clay coatings on aggregate surfaces. These two lower horizons of the pedocomplex can be clearly distinguished from the overlying second interglacial palaeosol (Btg horizon, AS 7a) by an erosional unconformity (wavy horizon boundary) and a change in grain sizes. Above all, the difference appears in the enhanced clay content. Additionally, the hydromorphic soil features are significantly weaker. Horizons 8 and 8a above the pedocomplex cannot be interpreted clearly. They show intensive stagnic conditions along former root channels, in which greyish reduced areas are visible.

On top of the pedocomplex loess loam with 1 m thickness is deposited, which is not subdivided any further (AS 9).

Within the loess loam an interglacial soil is developed, which is represented by an intense, 1.10 m thick, dark brown Bt horizon of a former Luvisol (AS 10), in which only weak hydromorphic features are observed. The interglacial soil corresponds largely with the first Bt horizon of the profile Oberlaab described above (TERHORST et al. 2003, SEDOV et al., this volume). This palaeosol horizon is correlative with the MIS 5e (PREUSSER & FIEBIG 2009, TERHORST et al. 2011b).

A Würmian sequence, which in comparison to other profiles is highly shortened, covers the last-mentioned palaeosol. The basal Würmian sediments of profile Wels-Aschet (AS 11, AS 12) correspond to colluvial layers. They are equally interspersed with charcoal as well as rests of the Bt-material of the underlying palaeosol. In the middle section a shortened equivalent of the “Lohne Soil” (acc. to SEMMEL 1968) (AS 14) can be documented, which is preserved as the youngest Middle Würmian interstadial in almost every Upper Austrian loess sequence (TERHORST et al. 2002). In its upper section the “Lohne Soil” is transformed by an intense Cryosol (Reductaquic). The overlying loess (AS 16) is represented by a decalcified, shallow deposit. The recent soil is missing in this profile section of the former loam pit.

Altogether, profile Wels-Aschet contains five palaeosols of interglacial intensity, while strong weathering of the lowermost palaeosol would support also the idea of six interglacial phases recorded in Wels-Aschet.



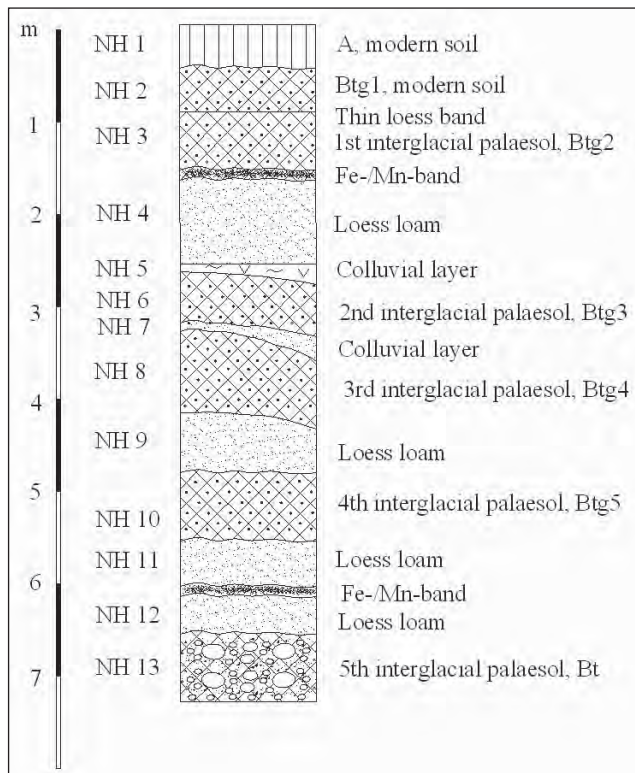


Fig. 5: Detailed palaeopedological profile of the sequence Neuhofen on top of the Older Deckenschotter (Günz).

Abb. 5: Detailliertes paläopedologisches Profil der quartären Abfolge in Neuhofen auf den Älteren Deckenschottern (Günz).

### 2.3 The cover layers of the Older Deckenschotter in profile Neuhofen

The cover layers of the Obermair loam pit in Neuhofen are on average 6.5 m thick, while in places they can reach a thickness of up to 10 m. They lead into a palaeochannel position with a stratified channel filling in northwestern direction. On the southeastern part the lower, extremely weathered Older Deckenschotter was exposed during the past years (Fig. 5).

The lowermost, intensely weathered pedocomplex has developed in the gravels and corresponds to the fifth palaeosol (Fig. 5, NH 13). Judging from its weathering status the soil horizon has to be classified as interglacial, while a formation during more than one interglacial is also probable (cf. TERHORST et al. 2003). Its surface is eroded and covered by a stagnic loess loam of about 1 m thickness (NH 12, NH 11). A distinct iron/manganese band separates this horizon.

Above the loess loam a stagnic Btg horizon has developed (NH 10). Interestingly, this horizon contains locally dark brown to black humic clay cutans, which indicate the former presence of a distinct A horizon in a superimposed position, which is not preserved to date. This Btg horizon within the presented profile corresponds to the fourth interglacial palaeosol.

On top, another loess loam was deposited (NH 9), inside of which a further interglacial palaeosol (NH 8) is developed. This soil horizon is also eroded in its uppermost section. However, the overlying redepositional zone (NH 7) can also be interpreted as marginally redeposited residue of a former E horizon.

Above, NH 6 represents another interglacial palaeosol horizon, which is in places covered by a thin redepositional zone containing soil sediment (NH 5).

A loess loam horizon of up to 1.5 m thickness follows, which is limited to the top by an iron/manganese band in some places of the profile. This band dips into the direction of the channel filling.

The uppermost section of profile Neuhofen is represented by a pedocomplex, which consists of two different superimposed Btg horizons (NH 3, NH 2). Both horizons are at the maximum 1.5 m thick. The pedocomplex is locally separated by a layer of loess loam; therefore two individual soils are recognisable.

### 3 Discussion of stratigraphic results

A highly differentiated structure of the cover layers is present in all Middle Pleistocene sequences presented here. Below a mostly shallow, characteristic Würmian sequence, which is only absent in Neuhofen, the Eemian soil is preserved as uppermost interglacial soil (Fig. 2). This soil usually is substantially less dense and stagnic than the older palaeosols of the warm stages. Underneath, at least three further, in parts highly stagnic, Btg horizons follow in all profiles. Moreover, on top of the Older Deckenschotter, a strongly weathered reddish palaeosol is present.

In general, the palaeosols are developed as pedocomplexes and represent different phases of pedogenesis and geomorphodynamics. The polypedogenetic transformation is in most cases clearly visible macromorphologically.

#### 3.1 Younger Deckenschotter

The loam pit in Oberlaab exposes one of the best structured profiles of cover layers of the Younger Deckenschotter in the entire northern Alpine Foreland. Overall four distinctly developed interglacial soils indicate a minimum age for the gravel surface of the fifth to the last glacial (MIS 12).

On the Younger Deckenschotter in Oberlaab a basal, intensely weathered Gleysol occurs in addition to the existent interglacial soils (cf. OTTNER & SEDOV, this volume). However, the palaeoclimatic meaning of this soil remains unclear. An interglacial formation cannot be fully excluded in this case, however a formation in pre-weathered flood deposits must also be discussed.

Classical ideas according to PENCK & BRÜCKNER (1909) of a formation of the Younger Deckenschotter (Mindel) in the third glacial do not apply for every case in the presented profile; however, a categorisation into the fourth to the last glacial also underestimates their age. KOHL already described three fossil interglacial soils (KOHL & KRENMAYR 1997). Therefore, the classical view on the age of the Younger Deckenschotter being set in the third to the last glacial period was already in question at that time.

Our results support the classification of Mindel Deckenschotter in the Austrian Alpine foreland as belonging to MIS 12, which is in agreement with the palaeogeographical studies of VAN HUSEN & REITNER (2011a) and palaeomagnetic results of SCHOLGER & TERHORST (this volume).

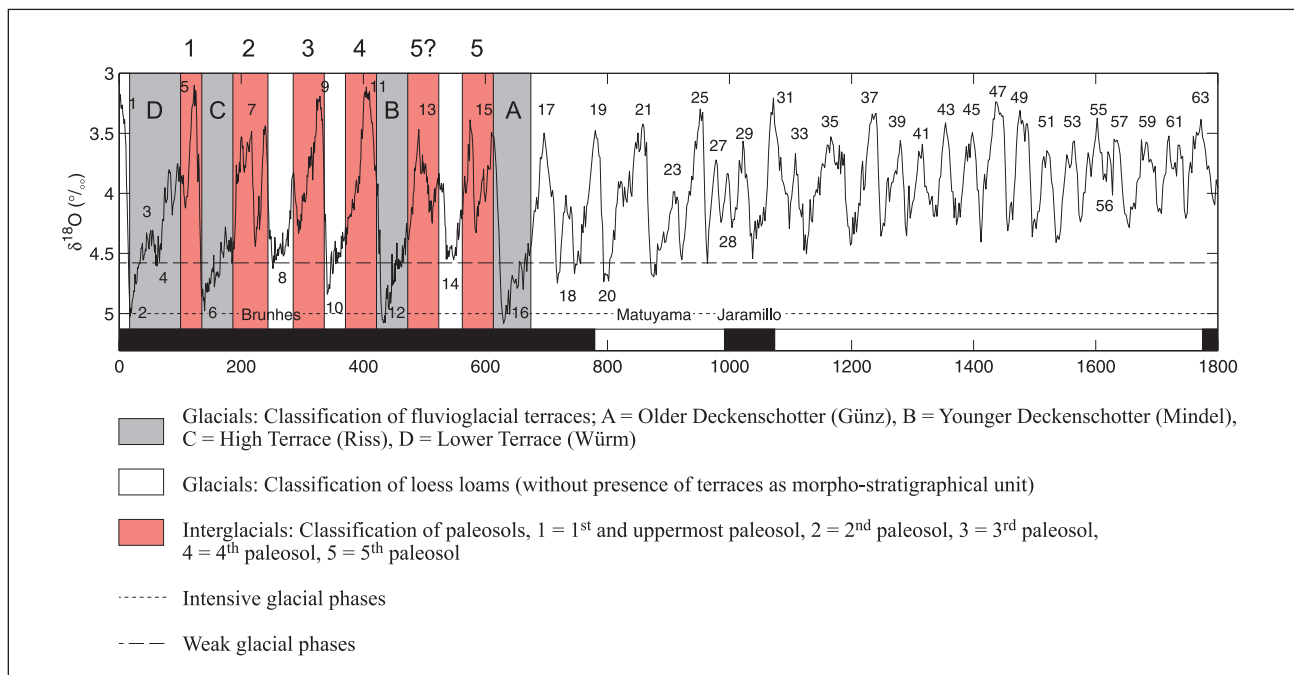


Fig. 6: Classification and correlation of palaeosols, fluvioglacial terraces and loess loams on the base of the marine oxygen isotope curve according to LISIECKI & RAYMO (2005), modified (source: TERHORST et al. 2011b).

Abb. 6: Einstufung und Korrelation von Paläoböden, fluvioglazialen Terrassen und Lösslehmen im Vergleich mit der marinen Sauerstoffisotopenkurve nach LISIECKI & RAYMO (2005), modified (source: TERHORST et al. 2011b).

### 3.2 Older Deckenschotter

The cover layers of the Older Deckenschotter in Wels-Aschet and Neuhofen contain one more interglacial palaeosol than in the Younger Deckenschotter profile of Oberlaab and consequently have to be classified as at least one glacial age older. It can be assumed that the intensely weathered basal palaeosol of both profiles contains not just one interglacial phase. The high degree of weathering in the Bt horizon of the oldest palaeosol (AS 2) is reflected in the intense red clay cutans as well as in the high clay content of about 60.0%. Furthermore, only stable minerals, such as quartz, are present. The clay fraction is dominated by mixed layer minerals, and in this palaeosol vermiculites and illites are completely weathered (TERHORST et al. 2011b).

Thus, the minimum age for the Older Deckenschotter is assumed to belong to the sixth to seventh to the last glacial phase. In this context the fact that the MBB could not yet be proved within the cover layers, leads consequently to a classification in the Brunhes epoch (SCHOLGER & TERHORST 2011). The proof of distinct palaeomagnetic excursions designated to the pedogenic phase of the basal intensely weathered palaeosol of AS 2 might be assigned to MIS15, towards whose end the geomagnetic excursion E-BL-CR3 (Emperor - Big Lost - Calabrian Ridge 3; 570–560 ka) occurs (SCHOLGER & TERHORST, this volume). Therefore, the classification according to VAN HUSEN (2000) can be confirmed by our pedostratigraphical results.

Findings of *Carya* and *Pterocarya* pollen in Wels-Aschet (KOHL 2000) yield a further stratigraphic indicator below the loess loam, which was by the author classified as Rißian. These pollen occur until the Holsteinian Interglacial, which can be parallelised with MIS 11 according to SARNTHEIN et

al. (1986, among others). The results imply a comparably old age of the basal profile sections. This fact as well as palaeopedological results were not considered in the study of PREUSSER & FIEBIG (2009). The above-discussed stratigraphic findings are in contrast to the stratigraphic approach of PREUSSER & FIEBIG (2009), who discuss much younger ages on the base of luminescence dating (IRSL). In this study, ages >200 ka do not significantly increase in the basal parts of the sequence, reflecting that the applied luminescence method can be problematic above 200 ka (cf. PREUSSER & FIEBIG 2009). Recently, methodological studies were able to extend the range of the luminescence method to 300 ka using a new post-IR IRSL protocol (290 °C) (THIEL et al. 2011), an approach not yet applied to the sequence of Wels-Aschet.

At present the Older Deckenschotter are classified as seventh to the last glacial in the Austrian Stratigraphic Chart (ÖSTERREICHISCHE STRATIGRAPHISCHE KOMMISSION 2004).

KOHL (2000) describes already four interglacial soils in Neuhofen and therefore, also in this case, assumes one interglacial more than in classical stratigraphy (acc. to PENCK & BRÜCKNER 1909).

Alltogether, the gravel surface of the Günz gravel body is younger than the MBB. This study classifies it at least to belong to MIS 16 (c.f. Van HUSEN & REITNER 2011b, SCHOLGER & TERHORST 2011).

### 3.3 Comparison of cover layers in the northern Alpine Foreland

Overall, at the present state-of-the-art it is impossible to compare stratigraphic results of the eastern Alpine Foreland with the western area in Baden-Württemberg. The most recent stratigraphic approach and nomenclature of Baden-

Württemberg deviates strongly from the Bavarian and Austrian stratigraphic system (DOPPLER et al. 2011). This fact complicates all attempts to correlate terraces of the eastern with those of the western Alpine Foreland. Furthermore, it has to be taken into account that the described single terrace bodies have to be regarded as terrace complexes, which include groups of terraces (SCHELLMANN et al. 2010). Thus, it is highly probable to obtain different ages in one terrace body.

BIBUS (1995) describes cover layers on the Iller-Lech plate and discusses the fourth or fifth to the last glacial as minimum age for the Younger Deckenschotter. Based on palaeosols in the cover layers of the Younger Deckenschotter in Allschwil brickyard near Basel he even assumes a minimum age of sixth to seventh to the last glacial (BIBUS 1990), which was later confirmed by ZOLLINGER (1991) in the verification of the MBB within the Younger Deckenschotter (cf. also discussion in BIBUS 1995). For the Upper Austrian study area no indication for a classification of the Younger Deckenschotter into seventh to the last glacial could be found so far. Thus, they are presumably younger than in the Rhine glacier area.

A comparison of the Older Deckenschotter in Upper Austria and studies on the Iller-Lech plate (BIBUS 1995) appears difficult because of the differentiated morphological structure of the terraces in the western Alpine Foreland. The Younger Deckenschotter cover layers in Roßhaupten brickyard are best compared to the sequences of the Older Deckenschotter presented here. BIBUS (1995) classifies the Younger Deckenschotter based on at least five to six the palaeosols into the seventh to the last glacial. Also the eighth to the last glacial period could be possible in this place, as the MBB could be proved above the gravels (cf. JERZ 1993). Consequently, a younger age of the Upper Austrian terraces seems to show here, too.

The classification according to pedostratigraphic investigations is consistent with glacial morphological studies in the northern Alpine Foreland by DOPPLER & JERZ (1995) and DOPPLER et al. (2011). However, it has to be taken into account critically that the sequence of the presented profiles is not preserved completely. According to DOPPLER & JERZ (1995) the lower boundary of the Günz complex has to be classified in the MIS 24 (Jaramillo), while the upper boundary is set at the transition of MIS 16 to MIS 15 based on results from the former glacial areas. Regarding the pedostratigraphic results presented here, the Older Deckenschotter of the Traun-Enns plate appear to belong to the younger most section of the Günz complex.

### 3.4 Correlation with marine curves

Regarding the marine oxygen isotope curve according to LISIECKI & RAYMO (2005), around eight interglacial soil formations respectively eight glacials are possible after the MBB, starting with MIS 19 (Fig. 5). However, based on the number of palaeosols in the studied profiles the Older Deckenschotter can be classified at the maximum into MIS 16. The generally intensive, ferretto-like weathering of the Older Deckenschotter in Upper Austria (fifth/basal palaeosol) should therefore correspond to the following interglacial (MIS 15), which is recorded in the palaeomagnetic studies as well (Emperor - Big Lost - Calabrian Ridge 3; 570–560 ka) (SCHOLGER & TERHORST, this volume). According to the results of the

palaeomagnetic analyses, loess loams deposited on top of the MIS 15 palaeosol can be correlated to MIS 14. Subsequently, five interglacials are recorded in marine curves, which should result in a sequence of five palaeosols, respectively, only four of which are clearly present in the study area on the Older Deckenschotter. If we assume that the fifth palaeosol of Wels-Aschet and Neuhofen includes the two interglacials of MIS 15 and 13, the superimposed loess sediment could also belong to MIS 12. The present stage of investigation does not allow a clear classification (SCHOLGER & TERHORST, this volume).

Pursuing these stratigraphical considerations for the Younger Deckenschotter, which also occur consistently in Oberlaab, and additionally regarding the number of palaeosols on the Younger Deckenschotter, MIS 12 or 14 can consequently be considered as probable times of origin for the Younger Deckenschotter. However, it has to be taken into account that MIS 14 is not as pronounced as the other glacials (cf. Fig. 6) and therefore may not be suitable for extensive deposition of gravel in form of an individual morphostratigraphic unit (acc. to PENCK & BRÜCKNER 1909). Further, the age classification of the younger Mindel complex can be brought into accordance with the stratigraphy by DOPPLER & JERZ (1995), who rank classical Mindel to MIS 12. In the study area four interglacial soils are still recorded on the Younger Deckenschotter, whose age of formation has to be assigned to MIS 11, 9, 7 and 5, according to the previous considerations. The intermediary glacial phases apparently did not induce the formation of independent, morphologically visible fluvioglacial terraces in the study area. Only MIS 6 is distinctly present in Rißian upper terrace deposits. The latter has to be classified as Younger Rißian stage according to datings and pedostratigraphic studies (TERHORST et al. 2002). The two older glacials MIS 8 and 10 are not represented by individual morphostratigraphic terraces here. However, during both stages sedimentation of loess loams was active. These are mostly preserved as deposits of more than 1 m thickness. According to the glacial stratigraphy for the northern Alpine Foreland (DOPPLER 2003, DOPPLER & JERZ 1995) the Riß complex can be divided into three glacial phases: Older, Middle and Younger Riß, corresponding to two terrace bodies in the western area of the Pleistocene Salzach glacier.

In this context it is remarkable, that datings by STREMMER et al. (1991) in Wels-Aschet below the Eemian soil yielded ages between 136 ka ( $\pm 13$  ka) and 128 ka ( $\pm 15$  ka). The age of the loess loam below the second palaeosol is stated in the same work as 233 ka ( $\pm 35$  ka) and 245 ka ( $\pm 51$  ka).

## 4 Conclusions

The cover layers of the studied profiles allow for the conclusion that Younger and Older Deckenschotter have to be assessed differently than it is assumed in the scope of the classical morphostratigraphic classification. The pedostratigraphic documentation over many years further proves an older formation age of the Deckenschotter than it has been reported in literature so far. The gravel surface of the Older Deckenschotter in the study area seems to be younger than the MBB and corresponds at least to MIS 16.

The Younger Deckenschotter in Oberlaab are one to two



glacial/interglacial cycles younger than the Older Deckenschotter and can, after detailed discussion, be classified at least as corresponding to MIS 12. The studies further confirm that a largely complete record of palaeosol sequences on the Traun-Enns plate can be expected.

At a supraregional level both conformities and discrepancies become obvious in the stratigraphic classifications. For basic correlations existent dating methods, such as optically stimulated luminescence (OSL), have to be further expanded, and magnetostratigraphic methods have to be applied systematically in further loess sequences.

In future it is desirable and absolutely necessary to establish a chronostratigraphy for the terrestrial Middle Pleistocene all over European loess sequences. This is the only way to enable supraregional or even global correlations. Furthermore, a reliable stratigraphy enables to decode regional landscape formation as well as the response of geosystems to climate change.

### Acknowledgement

The author is grateful for the financial support of the German Research Foundation. In this context the base for the still ongoing research in the study area has been formed by the project 'Geomorphologisch-paläopedologische Untersuchungen im Glazial- und Periglazialraum des ehemaligen Salzachgletschergebietes' (Prof. Dr. Erhard Bibus). Furthermore, the international cooperation during the studies have been financed by the ICSU Grant Programme 2003.

I would like to thank all German, Austrian and Mexican colleagues of the research team for a fruitful, long-lasting and trustful collaboration!

### References

BIBUS, E. (1990): Das Mindestalter des „jüngeren Deckenschotter“ des Rheins bei Basel aufgrund seiner Deckschichten in der Ziegelei Allschwil. – Jahreshefte Geologisches Landesamt Baden-Württemberg, 14: 223–234.

BIBUS, E. (1995): Äolische Deckschichten, Paläoböden und Mindestalter der Terrassen in der Iller-Lech-Platte. – *Geologica Bavarica*, 99: 135–164.

BRONGER, A. (1970): Zur Mikromorphologie und zum Tonmineralbestand von Böden ungarischer Lößprofile und ihre paläoklimatische Auswertung. – *Eiszeitalter und Gegenwart*, 21: 122–144.

DEUTSCHE STRATIGRAPHISCHE KOMMISSION (2002): Stratigraphische Tabelle von Deutschland. – Potsdam.

DOPPLER, G. (2003): Zur Gliederung von Ältesten Periglazialschottern und Älteren Deckenschottern im Rot-Günz-Gebiet. – *Z. dt. geol. Ges.*, 154/2–3: 255–286.

DOPPLER, G. & JERZ, H. (1995): Untersuchungen im Alt- und Ältestpleistozän des bayerischen Alpenvorlandes – Geologische Grundlagen und stratigraphische Ergebnisse. – *Geologica Bavarica*, 99: 7–53.

DOPPLER, G., KROEMER, E., RÖGNER, K., WALLNER, J., JERZ, H. & GROTTENTHALER, W. (2011): Quaternary Stratigraphy of Southern Bavaria. – *E&G Quaternary Science Journal* 60/2–3: 329–365.

ELLWANGER, D., BIBUS, E., BLUDAU, W., KÖSEL, M. & MERKT, J. (1995): Baden-Württemberg. – In: Benda, L. (ed.): *Das Quartär Deutschlands*, 255–295.

ELLWANGER, D., WIELANDT-SCHUSTER, U., FRANZ, M. & SIMON, T. (2011): The Quaternary of the southwest German Alpine Foreland (Bodensee-Oberschwaben, Baden-Württemberg, Southwest Germany). – *E&G Quaternary Science Journal*, 60/2–3: 306–328.

FINK, J., FISCHER, H., KLAUS, W., KOCI, A., KOHL, H., KUKLA, J., LOZEK, V., PIFFL, L. & RABEDER, G. (1978): Exkursion durch den österreichischen Teil des Nördlichen Alpenvorlandes und den Donaunraum zwischen Krems und Wiener Pforte. – *Mitteilungen der Kommission für Quartärforschung der österreichischen Akademie der Wissenschaften*, 1: 31 pp.

HABBE, K. A. (2003): Gliederung und Dauer des Pleistozäns im Alpenvor-

land, in Nordwesteuropa und im marinen Bereich – Bemerkungen zu einigen neueren Korrelierungsversuchen. – *Zeitschrift der Deutschen Geologischen Gesellschaft*, 154: 171–192.

HÄUSELMANN, P., FIEBIG, M., KUBIK, W., ADRIAN, H. (2007): A first attempt to date the original “Deckenschotter” of Penck and Brückner with cosmogenic nuclides. – *Quaternary International*, 164/165: 33–42.

JERZ, H. (1993): *Das Eiszeitalter in Bayern – Erdgeschichte, Gesteine, Wasser, Boden. – Geologie von Bayern II: p. 243 pp., Stuttgart (Schweizerbart).*

KOHL, H. (2000): *Das Eiszeitalter in Oberösterreich. – 429 pp., Oberösterreichischer Museal-Verein, Linz.*

KOHL, H. & KRENNMAYR, H. G. (1997): *Geologische Karte der Republik Österreich 1: 50 000, Erläuterungen zu Blatt 49 Wels. – 77 pp., Geologische Bundesanstalt Wien.*

LISIECKI, L. E. & RAYMO, M. E. (2005): A Pliocene-Pleistocene stack of 57 globally distributed benthic  $\delta^{18}O$  records. – *Palaeoceanography*, 20: 1–17.

MARKOVIĆ, S.B., HAMBACH, U., CATTO, N., JOVANOVIĆ, M., BUGGLE, B., MACHALETT, B., ZÖLLER, L., GLASER, B. & FRECHEN, M. (2009): Middle and Late Pleistocene loess sequences at Batajnica, Vojvodina, Serbia. – *Quaternary International*, 198: 255–266.

MARKOVIĆ, S.B., HAMBACH, U., STEVENS, T., KUKLA, G.J., HELLER, F., MCCOY, W.D., OCHSES, E.A., BUGGLE, B. & ZÖLLER, L. (2011): The last million years recorded at the Stari Slankamen (Northern Serbia) loess-palaeosol sequence: revised chronostratigraphy and long-term environmental trends. – *Quaternary Science Reviews*, 30: 1142–1154.

ÖSTERREICHISCHE STRATIGRAPHISCHE KOMMISSION (2004): *Stratigraphische Tabelle von Österreich. – Wien.*

OTTNER, F. & SEDOV, S. (this volume): Mineralogy and weathering intensity of the loess/paleosol sequence in Oberlaab.

PENCK A. & BRÜCKNER, E. (1901-1909): *Die Alpen im Eiszeitalter. – Vol. 1, 393 pp., Tauchnitz, Leipzig.*

PREUSSER, F. & FIEBIG, M. (2009): European Middle Pleistocene loess chronostratigraphy: Some considerations based on evidence from the Wels site, Austria. *Quaternary International*, 198/1–2: 37–45.

SARNTHEIN, M., STREMMER, H.E. & MANGINI, A. (1986): The Holstein interglaciation and the Correlation to Stable Isotope Stratigraphy of Deep-Sea-Sediments. – *Quaternary Research*, 26: 283–298.

SCHHELLMANN, G., IRMLER, R. & SAUER, D. (2010): Zur Verbreitung, geologischen Lagerung und Altersstellung der Donauterrassen auf Blatt L7141 Straubing. – *Bamberger Geographische Schriften*, 24: 89–178.

SCHOLGER, R. & TERHORST, B. (2011): Paläomagnetische Untersuchungen der pleistozänen Löss-Paläobodensequenz im Profil Wels-Aschet. – *Mitteilungen der Kommission für Quartärforschung der Österreichischen Akademie der Wissenschaften*, 19: 47–61.

SCHOLGER, R. & TERHORST, B. (this volume): Paleomagnetic investigation in the loess/paleosols sequence of Wels-Aschet.

SEMMELE, A. (1968): Studien über den Verlauf jungpleistozäner Formung in Hessen. – *Frankfurter Geographische Hefte*, 45: 133 pp.

SOLLEIRO-REBOLLEDO, E., CABADAS, H., SEDOV, S. & TERHORST, B. (this volume): Paleopedological record along the loess-paleosol sequence in Oberlaab, Austria.

SEDOV, S., SYCHEVA, S., PI, T. & DÍAZ, J. (this volume): Last Interglacial paleosols with Argic horizons in Upper Austria and Central Russia: a comparative pedogenetic and paleoecological analysis.

STREMMER, H., ZÖLLER, L. & KRAUSE, W. (1991): Bodenstratigraphie und Thermolumineszenz-Datierungen für das Mittel- und Jungpleistozän des Alpenvorlandes. – *Sonderverhandlungen des Geologischen Instituts Univ. Köln*, 82: 301–315 (Festschrift K. Brunacker).

TERHORST, B. (2007): Korrelation von mittelpleistozänen Löss-/Paläobodensequenzen in Oberösterreich mit einer marinen Sauerstoffisotopenkurve. – *E&G Quaternary Science Journal*, 56: 26–39.

TERHORST, B., FRECHEN, M. & REITNER, J. (2002): Chronostratigraphische Ergebnisse aus Lössprofilen der Inn- und Traun-Hochterrassen in Oberösterreich. – *Zeitschrift für Geomorphologie, Neue Folge Supplementband*, 127: 213–232.

TERHORST, B., OTTNER, F., POETSCH, T., KELLNER, A. & RÄHLE, W. (2003): Pleistozäne Deckschichten auf der Traun-Enns-Platte bei Linz (Oberösterreich). – In: TERHORST, B., *Exkursionsführer zur 22. Tagung des Arbeitskreises Paläoböden in Oberösterreich. Tübinger Geowissenschaftliche Arbeiten, Reihe D*, 9: 115–155.

TERHORST, B., OTTNER, F. & HOLAWA, F. (2011a): Pedostratigraphische, sedimentologische, mineralogische und statistische Untersuchungen an den Deckschichten des Profils Wels/Aschet (Oberösterreich). – *Mitteilungen der Kommission für Quartärforschung der Österreichischen Akademie der Wissenschaften*, 19: 13–35.

TERHORST, B., OTTNER, F. & WRIESSNIG, K. (2011b): Weathering intensity



- and stratigraphy of the Middle to Upper Pleistocene loess/paleosol sequence of Wels-Aschet in Upper Austria. – In: JACOBS, P., *Paleosols in the present and past landscapes*. *Quaternary International*, 265: 142–154.
- THIEL, C., BUYLAERT, J.-P., MURRAY, A., TERHORST, B., HOFER, I., TSUKAMOTO, S. & FRECHEN, M. (2011): Luminescence dating of the Stratzing loess profile (Austria) – Testing the potential of an elevated temperature post-IR IRSL protocol. – *Quaternary International*, 234: 23–31.
- VAN HUSEN, D. (2000): Geological processes during the Quaternary. – *Mitteilungen der Österreichischen Geologischen Gesellschaft*, 92: 135–156.
- VAN HUSEN, D. & REITNER, J. (2011a): Klimagesteuerte Terrassen- und Lössbildung auf der Traun-Enns-Platte und ihre zeitliche Stellung (Das Profil Wels/Aschet). – *Mitteilungen der Kommission für Quartärforschung der Österreichischen Akademie der Wissenschaften*, 19: 1–12.
- VAN HUSEN, D. & REITNER, J. (2011b): An Outline of the Quaternary Stratigraphy of Austria. – *E&G Quaternary Science Journal*, 60/2–3: 366–387.
- ZOLLINGER, G. (1991): Zur Landschaftsgenese und Quartärstratigraphie im südlichen Oberrheingraben – am Beispiel der Lössdeckschichten der Ziegelei Allschwil (Kanton Basel-Land). *Eclogae Geologicae Helvetiae*, 84/3: 739–752.

# Magnetic excursions recorded in the Middle to Upper Pleistocene loess/palaeosol sequence Wels-Aschet (Austria)

Robert Scholger, Birgit Terhorst

**How to cite:** SCHOLGER, R., TERHORST, B. (2013): Magnetic excursions recorded in the Middle to Upper Pleistocene loess/palaeosol sequence Wels-Aschet (Austria). – E&G Quaternary Science Journal, 62 (1): 14–21. DOI: 10.3285/eg.62.1.02

**Abstract:** We present the palaeomagnetic examination of the Middle to Upper Pleistocene loess/palaeosol sequence in the former pit 'Würzburger' located in Aschet near Wels. Five strongly developed palaeosols, respectively pedocomplexes alternate with interposing loess loam. By means of excavation access was gained to a profile with a thickness of 12 m. Altogether, 587 orientated samples were taken for the magnetostratigraphic analysis at the Paleomagnetic laboratory of the Montanuniversität Leoben, ensuring a near-complete sampling. The samples were demagnetised by means of alternating field as well as thermal demagnetisation. The magnetic parameters show a sequence of sections with strong magnetite formation in the soil, which can be assigned to the relatively warm climate of interglacial periods. The majority of samples showed characteristic remanence directions within the range of the normal global magnetic field of the Pleistocene. Some sections showed strongly deviating remanence directions, indicating excursions of the global magnetic field. The excursions observed in the Wels-Aschet profile are assigned to the time interval of 570 ka (Emperor-Big Lost-Calabrian Ridge) until 110 ka (Blake) due to palaeopedological-stratigraphical considerations. The Brunhes/Matuyama-Boundary (776 ka) was not reached.

## Magnetische Exkursionen in der Mittel- bis Oberpleistozänen Löss-/Paläoboden-Sequenz Wels-Aschet

**Kurzfassung:** Die vorliegende Arbeit stellt die paläomagnetische Bearbeitung der Mittel- bis Oberpleistozänen Löss-/Paläoboden-Sequenz im Areal der ehemaligen Ziegelei Würzburger in Aschet bei Wels vor. Fünf intensiv entwickelte Paläoböden, bzw. Pedokomplexe wechseln mit dazwischen geschalteten Lößlehmlagen ab. Im Rahmen einer Aufbaggerung konnte ein Profil mit einer Mächtigkeit von über 12 m erschlossen werden. Für die magnetostratigraphischen Laboruntersuchungen im Paläomagnetiklabor der Montanuniversität Leoben wurden insgesamt 587 orientierte Proben entnommen, so dass eine beinahe lückenlose Beprobung vorliegt. Die Proben wurden mit magnetischen Wechselfeldern sowie thermisch abmagnetisiert. Zur Bestimmung der magnetischen Trägerminerale in den Sedimenten wurden Curiepunkt-Bestimmungen durchgeführt, die eine Hauptträgerphase mit einem Curie-Punkt bei ca. 580°C (Magnetit), sowie untergeordnete Anteile von Hämatit mit 670°C Curie-Punkt ergaben. Die magnetischen Parameter zeigen eine Folge von Bereichen mit intensiver Magnetitbildung in den Paläoböden, die dem relativ wärmeren Klima von Interglazialen zugeordnet werden können. Die Mehrzahl der Proben zeigen charakteristische Remanenzrichtungen im Bereich des normalen pleistozänen Erdmagnetfeldes. In einigen Profilschnitten traten stark abweichende Remanenzrichtungen auf, die auf Exkursionen des Erdmagnetfeldes hinweisen. Die beobachteten Exkursionen im Profil Wels-Aschet werden aufgrund paläopedologischer-pedostratigraphischer Ergebnisse in das Zeitintervall von 570 ka (Emperor - Big Lost - Calabrian Ridge) bis 110 ka (Blake) gestellt. Die Brunhes/Matuyama-Grenze (776 ka) wurde nicht erreicht.

**Keywords:** *Pleistocene, loess, palaeosol, magnetic excursion, chronostratigraphy, rock magnetic properties, Upper Austria*

**Address of author:** R. Scholger, Montanuniversität Leoben, Paleomagnetic Laboratory Gams, Chair of Applied Geophysics, Peter-Tunner-Str. 25, A-8700 Leoben, Austria, E-mail: scholger@unileoben.ac.at; B. Terhorst, University of Würzburg, Institute of Geography and Geology, Am Hubland, D-97074 Würzburg, Germany. E-Mail: birgit.terhorst@uni-wuerzburg.de

## 1 Introduction

### 1.1 Stratigraphic framework of the study area

The Older Deckenschotter/Günz terraces of the Traun-Enns-Platte are classified according to stratigraphic considerations as belonging to the seventh-last glacial period. In this context VAN HUSEN (2000) and VAN HUSEN & REITNER (2011) proposed a chronostratigraphic framework for the glacial deposits and processes during the Middle Pleistocene of the Eastern Alps. In this study we assume that the four classic glacial periods are to be assigned to the Brunhes-Chron.

VAN HUSEN (2000) assumes that Günz is to be correlated with MIS16 and Mindel with MIS12. Furthermore, the author places the Riß-Glacial in MIS 6 and the Würmian Glacial in MIS 2. On the basis of cover layer analyses in the Linz/Wels area, TERHORST (2007) and TERHORST et al. (2011, 2012) arrive at similar results. The authors also correlated Günz with MIS16 and Mindel with MIS12. Earlier investigations in the cover layers of fluvioglacial terraces in the Linz/Wels area clearly show that too many interglacial soils occur to support the classic conceptions according to PENCK & BRÜCKNER (1909) (KOHL & KRENMAYR 1997, STREMMER et al. 1991).

## 1.2 Palaeomagnetic investigations of loess/palaeosol sequences

Climate change has an impact on weathering and sedimentation processes which affect the magnetic minerals within rocks (DEKKERS 1997). Therefore magnetic parameters such as magnetic susceptibility are sensitive indicators for climate dependant variations of the type, grain size and concentration of magnetic minerals in sediments (THOUVENY et al. 1994, VEROSUB & ROBERTS 1995). The magnetic susceptibility of rocks depends on the concentration and grain size of the magnetic mineral phases, which are part of the rock composition. In general, magnetite has the highest importance due to its high mineral specific susceptibility, and magnetic susceptibility can be used as a proxy for the magnetite content of rocks (THOMPSON & OLDFIELD 1986).

Several extensive investigations of European and Asian loess profiles document that palaeosols mainly contain finely grained magnetite as carrier mineral of the magnetic properties, while the magnetic components of loess samples are characterised by larger single-domain and multidomain grain sizes (EVANS & HELLER 2003). Since the magnetic susceptibility of SP-magnetite is significantly higher, it is possible to use the temporal variation of these parameters as an indicator for the intensity of soil formation (HELLER & LIU 1984). Model hypotheses assume that changing redox conditions in the soil during the weathering of ferrous minerals lead to the release of iron and the regeneration of ferrihydrite. At the end of a reaction chain, SP-magnetite or maghaemite regenerate in the soil under oxidising conditions (MAHER 1998). CHEN et al. (2005) refer to the importance of the organic content in connection with the activity of iron-reducing bacteria.

To date only few palaeomagnetic results of loess/palaeosol sequences in Austria are available. Earlier investigations of the clay pit of the brickyard Würzburger in Aschet/Wels are described in FINK et al. (1976). For the first attempt at a palaeomagnetic dating of these sediments, samples were taken from the cover layer above the older sheet gravels every 20 to 40 cm, which all showed a positive inclination and a declination of approximately zero. Sedimentary processes at the base of the cover layers are given as a possible reason for the absence of the expected polarity reversal (Brunhes-Matuyama Boundary) as well as the strong variation in declination values in the lowest part of the profile (FINK et al. 1976). The profile Wels-Aschet was dug up and documented anew in 2003 by a working group headed by Prof. Dr. Dirk Van Husen (SCHOLGER & TERHORST 2011).

## 2 Palaeopedological setting of the Wels-Aschet sequence

Older studies on the loam pit of Pichler brickyard in Wels-Aschet are available by KOHL & KRENMAYR (1997), KOHL (2000) and STREMMER et al. (1991). A detailed description and sedimentological analyses can be found in TERHORST et al. (2011, 2012).

Altogether, the loess/palaeosol sequence of the studied profile reaches a thickness of 12.5 m. It is mostly decalcified while gravel deposits of the Older Deckenschotter show high CaCO<sub>3</sub> contents. The sequence contains five palaeosols of

interglacial intensity, while strong weathering of the lowermost palaeosol is especially conspicuous. The basal sections of the profile display an intensely reddish-brown weathered horizon (AS 2) with dark red clay cutans in the gravels of the Older Deckenschotter (AS 1). Above the palaeosol, which represents at least one interglacial period, redeposited, gravel-bearing layers are deposited, which were later covered by a 3.5 m thick loess loam (AS 4a–4e), which intercalates two Cryosols. On top of the loess loam (AS 4a) a palaeosol developed in form of a dark yellowish brown Btg horizon of interglacial intensity (AS 5).

A further, thin and unstructured layer of loess loam (AS 6) overlies palaeosol AS 5. Above this loam a multiply layered pedocomplex is developed (AS 8a to 7c). The basal, 3<sup>rd</sup> palaeosol (AS 7b, 7c) contains distinct reddish brown clay cutans. This pedocomplex can be clearly distinguished from the overlying 2<sup>nd</sup> Btg horizon (AS 7a) by an erosional unconformity and a change in grain sizes (TERHORST et al. 2011). Two stagnic horizons (AS 8 and 8a) are superimposed on the described pedocomplex. On top of this pedocomplex, a loess loam with 1 m thickness is present, which is not subdivided any further (AS 9). Within the loess loam an interglacial soil is developed, which is represented by an intense, 1.10 m thick, dark brown Bt horizon (AS 10). This palaeosol horizon is correlative with the MIS 5e (PREUSSER & FIEBIG 2009, TERHORST et al. 2011). A Würmian sequence, which in comparison to other profiles is reduced and poorly weathered, covers the Eemian palaeosol (AS 11 to AS 16).

## 3 Methods

By means of two excavations (2001, 2003) access was gained to a profile of a thickness of more than 12 m. Samples for the palaeomagnetic laboratory analysis were collected using plastic cubes (edge length 2cm) which were pushed into the sediment either by hand or hammer along a guide rail. The orientation of the samples was measured according to routine palaeomagnetic proceedings. 162 (2001) and 425 (2003) samples were taken for the magnetostratigraphic laboratory analyses. The undetermined vertical distance between individual samples lies between 0 and 2 cm, ensuring a near-complete sampling. The continuous in situ measuring of the magnetic volume susceptibility in the profile was performed with an Exploranium KT-9 Kappameter.

Magnetic volume susceptibility as well as natural remanent magnetisation were measured at the Paleomagnetic Laboratory of the Montanuniversität Leoben as reference values for further investigations. The remanence measurements were performed with a 2G-Cryogenic-magnetometer with integrated alternating field demagnetisation, the susceptibility measurements on a Kappabridge Geofyzika KLY-2.

We first demagnetised the orientated samples with increasingly strong alternating magnetic fields (from 2 to 140 mT), and subsequently thermally demagnetised selected samples at temperatures ranging from 200° to 550°, the remaining NRM being measured after every step of the cleaning process. The demagnetisation behaviour indicates the magnetic carrier minerals and allows the separation of primary fossil magnetisation directions from secondary magnetisations created by magnetic overprints and weathering.

To determine the magnetic carrier minerals in the sediments, we performed Curie point determinations and examined the magnetic saturation behaviour. Depending on the deposit and formation conditions of the sediments and soils, different significance to the various magnetic parameters connected to certain sedimentologic or climatic processes is assigned. For the present study we chose the parameter AF@IRM according to LARRASOANA et al. (2003), which is regarded as an indicator for the haematite content within rocks. We first exposed the samples to a magnetic saturation at 0.9T and subsequently demagnetised them in an alternating field at 100mT. The remaining magnetisation is most likely due to haematite. At the same time we measured the anisotropy of the magnetic susceptibility (AMS), which determines the fabric of the magnetic minerals within the rock.

## 4 Results

### 4.1 Carrier minerals of the magnetic properties

The results of the Curie point determination yielded a magnetic carrier phase with a Curie point of approximately 580°C (magnetite) as well as a subordinate haematite content with a Curie point of 670°C. An increase in magnetic susceptibility between 280°C and 350°C most likely results from a transformation of iron sulphides or iron hydroxides into secondary magnetite or maghaemite during the heating process (GENDLER et al. 2006). The magnetic saturation indicates various magnetic minerals in the loess sediments and palaeosols of the Aschet profile. Samples from the palaeosols are characterised by a relatively low coercivity and reach magnetic saturation faster than the samples from loess horizons. The saturation behaviour of the samples indicates variations of low- and highly-coercive magnetic minerals in different concentrations. A highly coercive mineral (haematite) is present in low concentrations in all samples; the palaeo contain at least one additional low-coercive phase (magnetite) which developed during soil formation.

The measurements of the anisotropy of the magnetic susceptibility showed weakly anisotropic and in many cases isotropic magnetic fabric for all sections of the Aschet profile. The values for the magnetic fabric parameters, lineation (L) and foliation (F), lie below 2% for most samples (median value and standard deviation from 165 samples:  $L = 1,014 \pm 0,018$ ;  $F = 1,018 \pm 0,017$ ). We could not observe a preferred orientation of the Kmax direction, which would allow inferences as to palaeowind direction.

### 4.2 Characteristic magnetisation directions

The stepwise demagnetisation in an alternating field was performed in 6 to 15 stages ranging from 2 to 140mT (Figure 1). Considering the mineral magnetic results, the lower field range was examined in more detail to isolate those remanence vectors which reside in different phases of magnetite. In general we only observed a low impact of the highly coercive phases on demagnetisation behaviour. For the majority of samples the remanence could be demagnetised completely using alternating field demagnetisation. After demagnetisation in the alternating field, some samples showed remaining remanences which are due to highly coercive phases (e.g. haematite). We subsequently thermally demagnetised these

samples at temperatures ranging from 200°C to 550°C. We generally observed two magnetic phases which in most cases however yielded the same remanence direction (Figure 1 a,c).

We observed similar demagnetisation vectors in every loess and soil sample. The majority of samples showed characteristic remanence directions within the range of the normal recent or Pleistocene global magnetic field. In some sections of the profile strongly deviating remanence directions occurred (Figure 1 b,d), which indicate excursions of the global magnetic field which also occurred repeatedly during the Pleistocene (LUND et al. 1998). However, we did not observe a complete polarity reversal of the magnetic field indicating the Brunhes-Matuyama Boundary.

Up to 90% of the natural remanent magnetisation (NRM) in the Bt horizon of the 1<sup>st</sup> palaeosol (AS 10) as well as the subjacent loess loam (AS 9) were already demagnetised at low alternating fields. The subsequent thermal cleaning up to 550°C yielded further demagnetisation of the same directional component (Figure 1a). In the upper section of the 1<sup>st</sup> palaeosol (AS 10) at the transition to the colluvial layer (AS 11), we observed strongly deviating remanence directions within an interval of approximately 20 cm in the profile (1.90 to 2.10 m). Similar deviating magnetisation vectors occurred in the lower part of the loess loam AS 9 at a depth of 3.60 to 3.95 m as well as in the 2<sup>nd</sup> and 3<sup>rd</sup> palaeosols (Btg horizons, AS 7a, b) at a depth of 4.55 to 5.34 m (Figure 1b). The samples taken from AS 7 are characterised by a higher coercivity. The subsequent thermal cleaning resulted in a further loss of intensity at the temperature interval between 500°C and 550°C, which indicates magnetite as the sole carrier mineral of the remanence. In the layers AS 4 the demagnetisations indicated an additional magnetic carrier mineral both in the loess loam as well as in the Cryosols. The alternating field demagnetisation showed that only approx. 50% of the NRM were linked to lower coercive magnetic phases, most part of the remaining intensity could be removed during the first stages of thermal cleaning (Figure 1c). The samples taken from the 5<sup>th</sup> palaeosol (Bt horizon, AS2) were similar to the 2<sup>nd</sup> palaeosol in their demagnetisation behaviour. We were able to demagnetise the majority of NRM at alternating field strengths of up to 40 mT; Figure 1e). We mainly observed normal characteristic remanence directions for the whole lower part of the profile, between AS 1 and AS6, while deviating magnetisation vectors only occurred in a few samples taken from two depth sections (at approximately 9.5 m and 11.6 m; Figure 1d).

### 4.3 Variation of magnetic parameters in the profile

Magnetic susceptibility, NRM intensity, saturation intensity and the parameter AF@IRM (LARRASOANA et al. 2003), which is used as an indicator for haematite, all showed significant variations in the profile (Figure 2). The continuous susceptibility profile recorded in situ during the sampling and the measurements of the samples show a strong link between magnetic susceptibility and lithologic conditions, with the palaeosols generally emerging as areas of increased susceptibility with concurrent large variation in susceptibility values. The susceptibility values for loess loam (approx.  $150 \cdot 10^{-6}$  SI) represent the magnetic background value of the sediment, while the values in the palaeosols are as much as



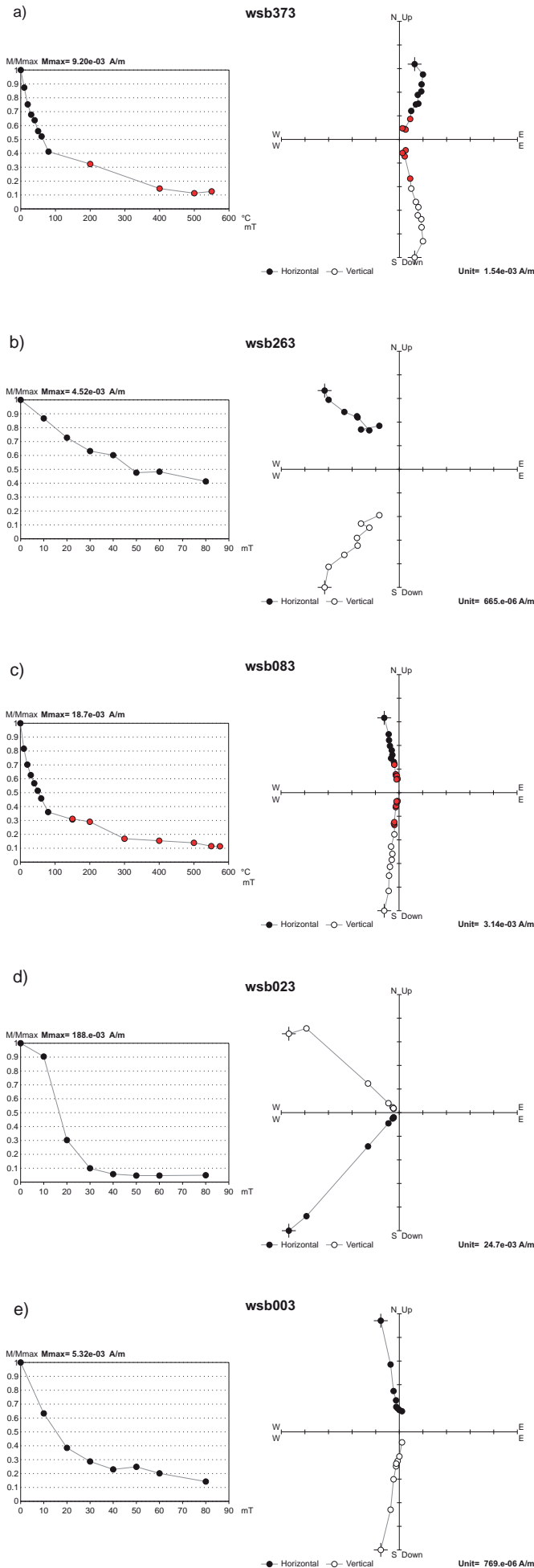


Fig. 1: Vectorplots (horizontal und vertical projection) and intensity decay during alternating field-(black) and thermal (red) cleaning. (a) WSB373 of AS 10, (b) WSB 263 of AS 7, (c) WSB83 of AS 4e, (d) WSB23 of AS 2, (e) WSB 3 of AS 2. Alternating field demagnetisation in 6 to 15 steps in the range between 2 and 140 mT, successive thermal demagnetisation at temperatures between 200°C and 550°C (a, c). In some sections of the profile strongly deviating remanence directions occurred (b,d), which indicate excursions of the global magnetic field.

Abb. 1: Vektordiagramme und Intensitätsverhalten ausgewählter Proben bei der Abmagnetisierung. Horizontale und vertikale Projektion der Remanenzvektoren, sowie Intensitätsverlauf bei der Wechselfeld- (schwarz) und thermischen (rot) Reinigung. (a) WSB373 aus AS 10, (b) WSB 263 aus AS 7, (c) WSB83 aus AS 4e, (d) WSB23 aus AS 2, (e) WSB 3 aus AS 2. Abmagnetisierung im Wechselfeld in 6 bis 15 Schritten im Bereich zwischen 2 und 140 mT, nachfolgende thermische Abmagnetisierung bei Temperaturen von 200°C bis 550°C (a, c). In einigen Bereichen des Profils traten stark abweichende Remanenzrichtungen auf die auf Exkursionen des Erdmagnetfeldes hinweisen (b, d).

ten times higher due to magnetite-formation during pedogenesis. The intensity values of NRM and SIRM largely follow the same trend. Within the loess content of the profile, the haematite indicator AF@IRM shows similar behaviour to the other magnetic parameters. In contrast, we did not observe an increase of the AF@IRM values in the palaeosols. This confirms the hypothesis that the increased values of susceptibility, NRM and SIRM in the palaeosols are due to higher magnetite content.

The intensely weathered reddish palaeosol in the basal section of the profile (12 m–11 m) with the highest loam content in the profile represents at least one interglacial period and is slightly remoulded by cryoturbation (TERHORST 2007). In this section (AS 2) the susceptibility values are generally increased. A susceptibility and SIRM-maximum at 11.5 m and diverging remanence directions may indicate a short-term excursion of the global magnetic field during soil formation or during a subsequent intense weathering period. In the superjacent loess loam complex with a thickness of 4m (AS 4a–4e), the saturation magnetisation in particular indicates an increased magnetite content in the two Cryosols. At 9.5 m we observed an indication for a magnetic excursion. In the Btg horizon (AS 5) between 7.0 m and 6.6 m, only individual samples show increased magnetic susceptibility, while the superjacent unsegmented loess loam layer AS 6 (6.6 m–6.0 m) is characterised by significantly increased susceptibility values. Within the multi-segmented pedocomplex AS 8a–7c (6 m to approx. 4.2 m), with greyish iron-reduced areas along visibly developed root traces (TERHORST 2007), increased susceptibility and SIRM values also indicate partially intense magnetite formation, which can strongly vary locally depending on the availability of organic substances. In this pedocomplex we observed a magnetic excursion over a longer profile section, the magnetisation directions in the lower part (AS 7b) indicating a possible additional subdivision.

## 5 Discussion

Saturation intensity and magnetic susceptibility strongly vary within the profile, depending on the different lithologic horizons. Several horizons with strongly increased susceptibility values occur, which are due to higher concentrations

## Profile Wels-Aschet

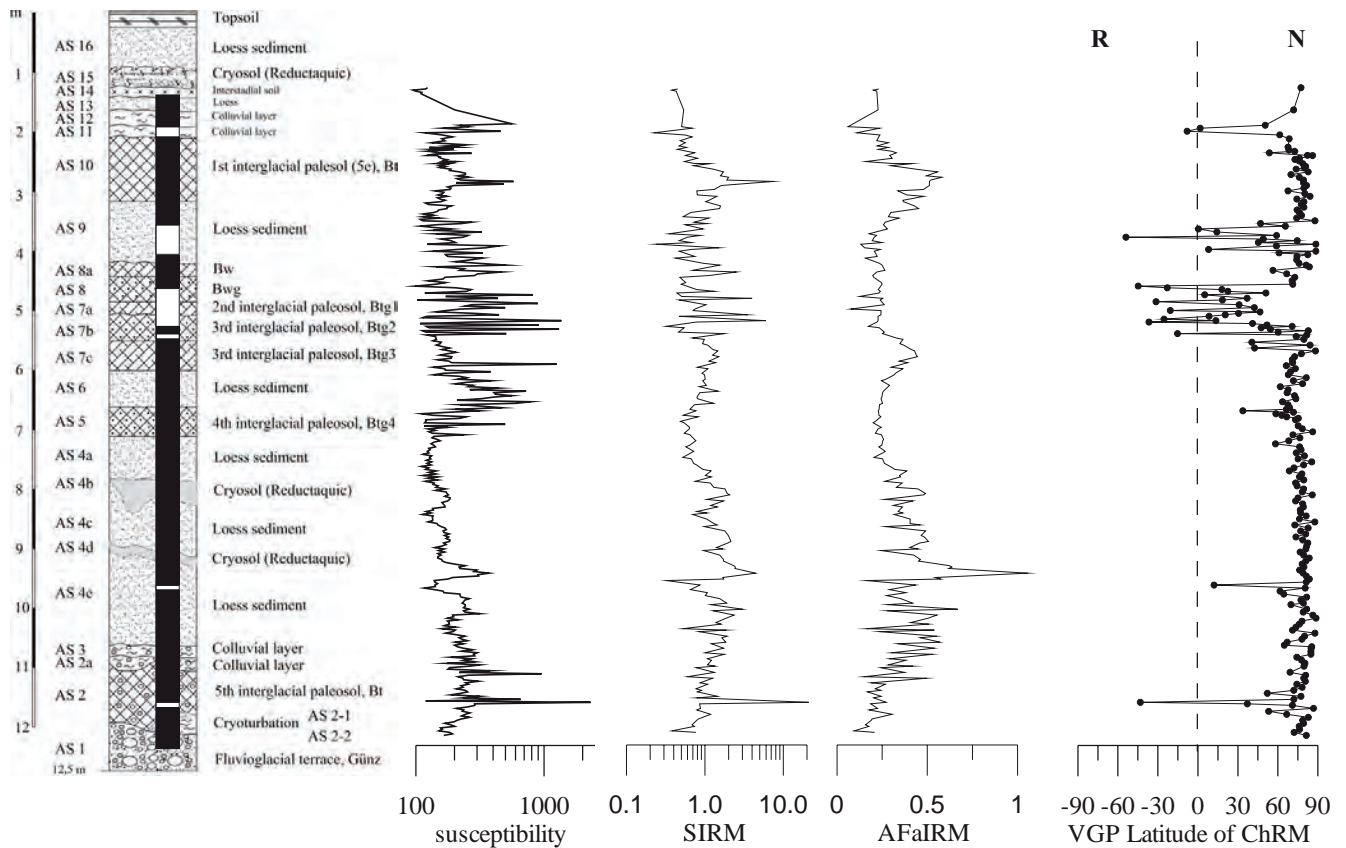


Fig. 2: Variation of magnetic parameters in the profil Wels-Aschet. Magnetic susceptibility (in  $10^6$  SI), intensity of saturation magnetisation (SIRM in A/m) and remaining remanence after successive alternating field demagnetisation (AFaIRM), VGP-Latitude calculated for the characteristic remanence component (ChRM). R, N: Inverse und Normal polarity. Geomagnetic Instability column for the profile Wels-Aschet (black: stable North direction, white: magnetic excursion).

Abb. 2: Magnetische Parameter der Proben aus dem Profil Wels-Aschet. Magnetische Suszeptibilität (in  $10^6$  SI), Sättigungsmagnetisierung (SIRM in A/m) und Rest-Remanenz nach anschließender Abmagnetisierung im Wechselfeld (AF@IRM), VGP-Breitengrad der charakteristischen Remanenzkomponente (ChRM). R, N: Inverse und Normale Pollage. Geomagnetische Zuordnung im Profil (schwarz: stabile Nordrichtung, weiß: magnetische Exkursion).

of finely grained magnetite. Such horizons indicate climate-regulated in situ soil formation during relatively warm climatic conditions. Investigations of loess profiles in China showed that palaeosol horizons are always characterised by high magnetic susceptibility and high saturation intensity (HELLER & LIU 1984, HUNT et al. 1995). EVANS & HELLER (1994) proved that the magnetic characteristics are due to magnetite and pyrrhotite, which were created by pedogenesis. For attempting a chronostratigraphic classification, the magnetic susceptibility of profile sections is used as a climate indicator and compared to the oxygen isotope curve according to LISIECKI & RAYMO (2005). For the chronostratigraphic classifications in the Aschet profile near Wels we used a current survey of internationally recognised observed excursions within the Brunhes-Chron (LAJ & CHANNELL 2007, LANGEREIS et al. 1997, SINGER et al. 2008). Geomagnetic excursions represent short-term deviations from the normal global magnetic field, which can be observed as trans-regional phenomena (SINGER et al. 2008) and are therefore suitable for chronostratigraphic correlation. Magnetic excursions or polarity reversal within the assumed stable Brunhes-Chron were first discovered at Lavas located in the French

Massif Central (Laschamp, approx. 40 ka) (BONHOMMET & BABKINE 1967). Since then numerous magnetic excursions in sediments and vulcanites, whose existence and chronostratigraphic age determination are not always beyond doubt, have been described worldwide. The various authors primarily disagree concerning the assessment of the relevance of data taken from drill cores as well as the importance of independent geochronologic datings of the examined rocks (LAJ & CHANNELL 2007). According to LUND et al. (1998) a total of 15 magnetic excursions can be observed in ODP cores within the Brunhes-Chron. According to LANGEREIS et al. (1997) 12 excursions are to be considered, 6 of which are referred to as well dated, globally observed excursions. According to SINGER et al. (2008), all excursions which have been dated radiometrically via the Ar-dating of vulcanites or astrochronological via O-isotopes in the sediments need to be considered. In contrast, LAJ & CHANNELL (2007) consider only those 7 excursions for which worldwide proof and precise dating are available: Mono Lake (33 ka), Laschamp (40 ka), Blake (120 ka), Iceland Basin (188 ka), Pringle Falls (211 ka), Big Lost (560–580 ka) and Stage 17 (670 ka).

Above the Older Deckenschotter between 11.0 and 12.0 m

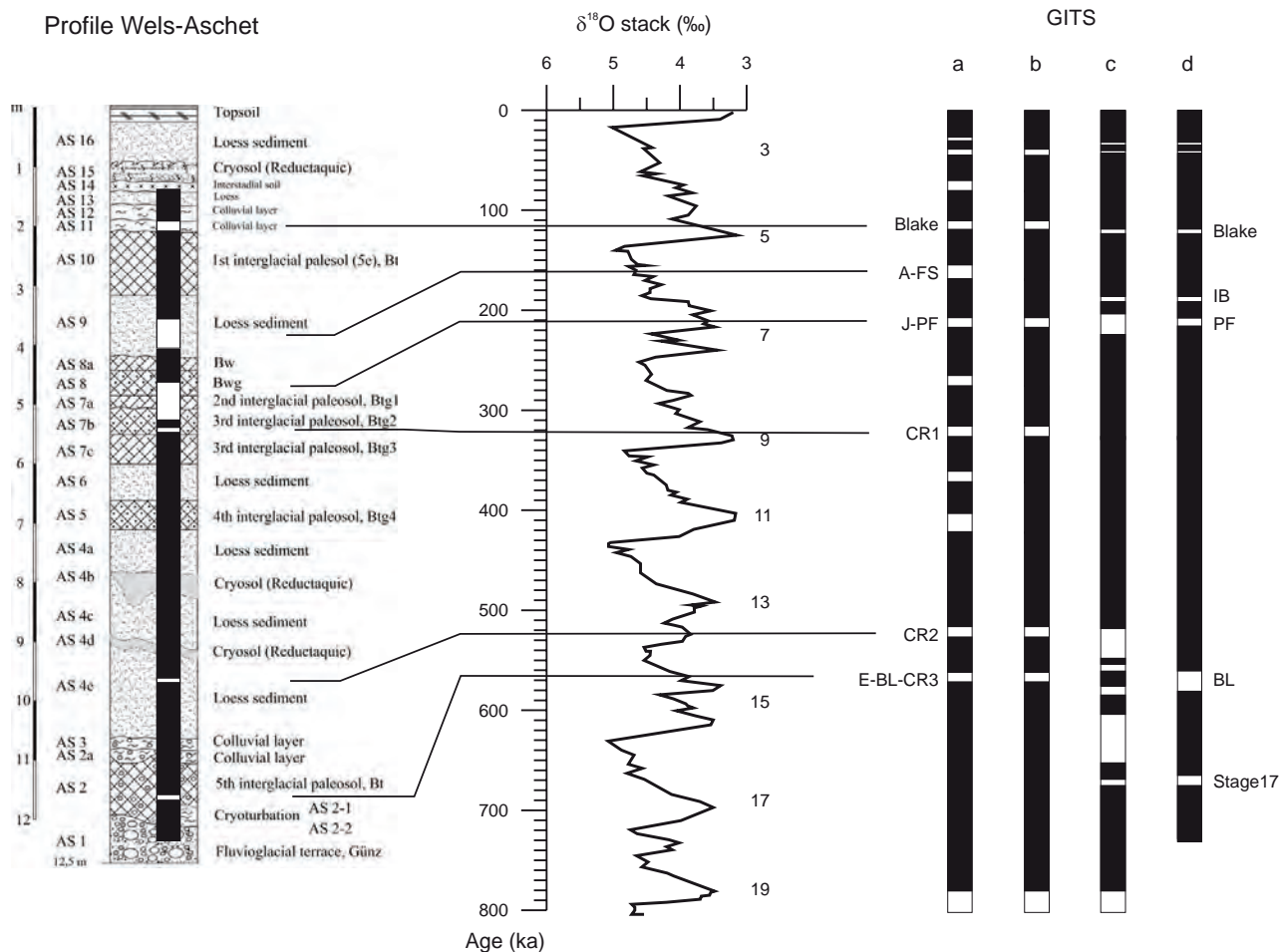


Fig. 3: Tentative correlation of magnetic parameters in the profile Wels-Aschet to chronostratigraphic reference scales. Oxygen isotopes after LISIECKI & RAYMO (2005) and Geomagnetic Instability Time Scale (GITS; (a) and (b) after LANGEREIS et al. (1997), (c) after SINGER et al. (2008), (d) after LAJ & CHAN-NEL (2007). Excursions (reversals) named after localities: Albuquerque (A), Fram Strait (FS), Iceland Basin (IB), Pringle Falls (PF), Calabrian Ridge (CR), Emperor (E), Big Lost (BL). Palaeopedologic profile after TERHORST et al. (2012).

Abb. 3: Vergleich der magnetischen Parameter im Profil Wels-Aschet mit chronostratigraphischen Referenzdaten: Sauerstoffisotopen nach LISIECKI & RAYMO (2005) und Geomagnetic Instability Time Scale (GITS; (a) und (b) nach LANGEREIS et al. (1997), (c) nach SINGER et al. (2008), (d) nach LAJ & CHAN-NEL (2007). Bezeichnung der Excursionen bzw. Umpolungen nach Fundorten: Albuquerque (A), Fram Strait (FS), Iceland Basin (IB), Pringle Falls (PF), Calabrian Ridge (CR), Emperor (E), Big Lost (BL). Paläopedologisches Profil aus TERHORST et al. (2012).

of the profile a palaeosol (AS 2) has developed, which represents at least one interglacial period and, at its lowest section at 11.6 m in the profile, contains a magnetic excursion. The pedogenic phase might be assigned to MIS15, towards whose end the geomagnetic excursion E-BL-CR3 (Emperor - Big Lost - Calabrian Ridge 3; 570–560 ka) occurs. Above the palaeosol, colluvial, gravel bearing layers were deposited (AS 3, AS 2a). The superjacent thick loess loam (AS 4) contains a further magnetic excursion in the section under a the Cryosol AS 4d at 9.5 m in the profile, for whose geological age two models need to be discussed. If the excursion is correlated with Calabrian Ridge 2 (CR2; 525–515 ka according to LANGEREIS et al. (1997)) or West Eifel 5 (528+/-16ka according to SINGER et al. (2008)) during MIS14, it ensures that the loess sedimentation (AS 4 and AS 5) encompasses a total of two glacial periods, MIS14 and MIS12, and that an erosional discordance in AS 4 removed the soil corresponding to MIS13. The alternative model for this profile section would be that the more strongly weathered palaeosol AS 2 represents two soil formation phases (MIS13 and MIS15) and that scarcely any sediments from the glacial period MIS14 have been pre-

served or they have been completely overprinted by the subsequent pedogenesis. This would mean that the whole loess loam of the layers AS 4a–e would have to be assigned to just one glacial period (MIS12).

In the loess loam AS 4a a palaeosol (AS 5) developed, which could be assigned to MIS11. The subsequent sedimentation phase in MIS10 encompasses the unsegmented loess loam (AS 6) at 6.6 to 6.0 m in the profile and the palaeosol (AS 7b–AS 7c), which developed from it in MIS9, in whose uppermost section at 5.4 m in the profile a magnetic excursion occurs which correlates with CR1 (Calabrian Ridge 1; 325–315 ka). These horizons can easily be distinguished from the superjacent soil horizon AS 7a due to a significant erosional discordance and a change in grain size (TERHORST 2007, TERHORST et al. 2011).

The loess sediments from MIS8 were completely overprinted during the subsequent soil formation phase in MIS7, so that only one segmented pedocomplex (AS 7a–AS 8a) has been preserved at 5.0 to 4.2 m in the profile. In the lower part of this profile section, in addition to the palaeomagnetic information on the soil formation phase during MIS7 with the



excursion J-PF (Jamaica - Pringle Falls; 215–205 ka), some remains of the remanent magnetisation of the original loess sediment have been preserved in a highly coercive magnetic phase, which also show vector directions deviating from the North direction.

This is followed above by a further loess loam (AS 9), which was deposited during MIS6 and contains a magnetic excursion at 4.0 m to 3.5 m in the profile which can be correlated with the A-FS excursion (Albuquerque - Fram Strait; 165–155 ka). The uppermost interglacial soil in the Aschet profile (AS 10) can be assigned to Eem (MIS5e) due to its palaeopedologic characteristics as well as by superimposed sediments of Würmian age. Due to datings at the Wels-Aschet site (PREUSSER & FIEBIG 2011) and in comparable profiles (TERHORST et al. 2002), an Early Würmian age can be presumed for the magnetic excursion in the colluvial layer AS 11 at 2.0 m in the profile. The formation of the colluvial layer AS 11 is linked to the beginning decline in climate during the close of Eem, which is why at this point, the colluvial layer correlates chronostratigraphically with the occurrence of the Blake excursion (120–110 ka).

The above-discussed stratigraphic findings are in contrast to the assumption of PREUSSER & FIEBIG (2009), who discuss much younger ages on the base of luminescence dating (IRSL). However, in this study, ages >200 ka do not significantly increase in the older sediments (c.f. PREUSSER & FIEBIG, 2009). Recently, methodological studies were able to extend the range of the luminescence method to 300 ka using a new post-IR IRSL protocol (290°C) (THIEL et al. 2010), an approach not yet applied to the sequence of Wels-Aschet.

## 6 Conclusion

The confirmation of Middle Pleistocene magnetic excursions accompanied by palaeopedologic-pedostratigraphic analyses are important implements for the development of a chronostratigraphic framework for the studied area as well as for the stratigraphical framework of Europe. For this reason, we executed a detailed magnetostratigraphic study of the plot of the former brickyard Würzburger in Aschet.

In general, for loess/palaeosol sequences, there is a methodological dependant wide gap in absolute age datings between the Matuyama/Brunhes boundary and MIS 6 in Pleistocene periglacial and glacial sediments (see discussion in TERHORST et al. 2011). Chinese loess sequences record five distinct palaeosols (S1 to S5) as well as three weak soils (S6 to S8) on top of the MBB and according to GENDLER et al. (2006), five to six pedocomplexes superimpose the MBB in the western Black Sea loess area. MARKOVIC et al. (2011) suppose seven interglacial soils for Northern Serbia and for the Russian plane, five to six interglacial soils are present in the Brunhes-Subchron including the transition close to the Matuyama/Brunhes boundary (VELICHKO 1990).

The loess deposits of the middle and lower Danube basin in southeastern Europe comprise the most comprehensive terrestrial records of the Pleistocene environmental dynamics (FITZSIMMONS et al. 2012). MARKOVIC et al. (2009) proposed a stratigraphic model for the Middle and Late Pleistocene based on magnetic susceptibility records from Loess sequences in the Vojvodina region (Serbia) that revealed a continuous record of paleoclimatic variations for the last

five glacial/interglacial cycles at least. BUGGLE et al. (2009) compared susceptibility records from pedocomplexes at Serbian, Romanian and Ukrainian loess/palaeosol sections with susceptibility data of the Chinese Loess Plateau and with the oxygen isotope record of ODP 677 and related the oldest pedocomplex in their study area to Marine Isotope Stage (MIS)17.

According to our interpretation, the oldest pedocomplex in the profile Wels-Aschet (AS2) might be assigned to MIS 15 and the thick package of AS4 represents very strong cooling in the Mindel glaziation with the most extensive glaciers in this area during the MIS 12. The Older Deckenschotter terrace apparently formed during the cold phase of MIS 16 (VAN HUSEN & REITNER 2011).

The correlation of magnetic parameters presented here (Figure 3) is based on the interpretation of sedimentation and soil formation phases on the basis of the palaeopedologic profile (TERHORST 2007, TERHORST et al. 2012). The magnetic parameters show a series of sections with intense magnetite formation in the soil, which can be assigned to the relatively warm climate of interglacial periods. In some sections of the profile the trend of the magnetic susceptibility shows a notable consistence with the oxygen isotope curve. Indications of short-term magnetic excursions can be observed in the section of the palaeosols as well as in the loess sediments. Due to sedimentologic considerations, the excursions observed in the Wels-Aschet profile are equated with the excursions Blake (120–110 ka), A-FS (Albuquerque - Fram Strait; 165–155 ka), J-PF (Jamaica - Pringle Falls; 215–205 ka), CR1 (Calabrian Ridge 1; 325–315 ka) and E-BL-CR3 (Emperor - Big Lost - Calabrian Ridge 3; 570–560 ka) of the geomagnetic reference time scales. For the excursion in the loess complex (AS4e), depending on which reference time scale is used, either CR2 (Calabrian Ridge 2; 525–515 ka), West Eifel 5 (528+-16ka) or a much younger age are up for discussion. The Brunhes-Matuyama Boundary (776 ka) was never reached.

## Acknowledgements

The palaeomagnetic investigation was performed on initiative of Prof. Dr. Dirk van Husen with financial support of the Austrian Academy of Sciences. We would like to thank Karl Stingl and Jürgen Reitner for their support during fieldwork and two anonymous reviewers for their valuable scientific and editorial support.

## References

- BUGGLE, B., HAMBACH, U., GLASER, B., GERASIMENKO, N., MARKOVIĆ, S., GLASER, I., ZÖLLER, L. (2009): Stratigraphy, and spatial and temporal paleoclimatic trends in Southeastern/Eastern European loess-palaeosol sequences. – *Quaternary International*, 196 (1–2): 86–106.
- BONHOMMET, N. & BABKINE, J. (1967): Sur la présence d'alimentation inverse dans la Chaîne Des Puys. – *Comptes Rendus Hebdomadaires des Séances de l'Académie des Sciences, Series B*, 264: 92–94.
- CHEN, T., XU, H., XIE, Q., CHEN, J., JI, J. & LU, H. (2005): Characteristics and genesis of maghemite in Chinese loess and paleosols: Mechanism for magnetic susceptibility enhancement in palaeosols. – *Earth & Planetary Science Letters*, 240: 790–820.
- DEKKERS, M.J. (1997): Environmental magnetism: an introduction. – *Geologie en Mijnbouw*, 76: 163–182, Utrecht.
- EVANS, M.E. & HELLER, F. (1994): Magnetic enhancement and paleoclimate: study of a loess/palaeosol couplet across the Loess Plateau of China. –



- Geophysical Journal International, 117: 257–264.
- EVANS, M.E. & HELLER, F. (2003): Environmental magnetism – principles and applications of Enviromagnetics. – Amsterdam (Academic press).
- FINK, J., FISCHER, H., KLAUS, W., KOCI, A., KOHL, H., KUKLA, J., LOZEK, V., PIFFL, L. & RABEDER, G. (1976): Exkursion durch den österreichischen Teil des Nördlichen Alpenvorlandes und den Donauraum zwischen Krems und Wiener Pforte. – Mitteilungen der Kommission für Quartärforschung, 1: 31 S, Wien.
- FITZSIMMONS, K., MARKOVIĆ, S., HAMBACH, U. (2012): Pleistocene environmental dynamics recorded in the loess of the middle and lower Danube basin. – Quaternary Science Reviews, 41: 104–118.
- GENDLER, T.S., SHCHERBAKOV, V.P., DEKKERS, M.J., GAPEEV, A.K., GRIBOV, S.K. & McCLELLAND, E. (2005): The lepidocrocite-maghemite-haematite rection chain- I. Acquisition of chemical remanent magnetization by maghemite, its magnetic properties and thermal stability. – Geophysical Journal International, 160: 815–832.
- HELLER, F. & LIU, T.S. (1984): Magnetism of Chinese loess deposits. – Geophys. Journal of the Royal Astronomical Society, 77: 125–141, London.
- HUNT, C.P., BANERJEE, S.K., HAN, J., SOLHEID, P.A., OCHES, E., SUN, W. & SOLHEID, P.A. (1995): Rock-magnetic proxies of climate change in the loess-paleosol sequences of the western Loess Plateau of China. – Geophysical Journal International, 123: 232–244.
- KOHL (2000): Das Eiszeitalter in Oberösterreich. Oberösterreichischer Museal-Verein, Linz, pp. 429.
- KOHL, H., KRENMAYR, H.G. (1997): Geologische Karte der Republik Österreich 1: 50 000, Erläuterungen zu Blatt 49 Wels. Geologische Bundesanstalt, Wien, pp. 77.
- LAJ, C. & CHANNEL, J.E.T. (2007): Geomagnetic Excursions. – In: Treatise on Geophysics, Vol. 5. Elsevier.
- LANGEREIS, C.G., DEKKERS, M.J., DE LANGE, G.J., PATERNE, M. & VAN SANTVOORT, P.J.M. (1997): Magnetostratigraphy and astronomical calibration of the last 1.1 Myr from a Central Mediterranean piston core and dating of short events in the Brunhes. – Geophysical Journal International, 129: 75–94.
- LARRASOANA, J.C., ROBERTS, A.P., ROHLING, E.J., WINKLHOFER, M. & WEHAUSEN, R. (2003): Three million years of monsoon variability over the northern Sahara. – Climate Dynamics, 21: 689–698.
- LISIECKI, L.E., RAYMO, M.E. (2005): A Pliocene-Pleistocene stack of 57 globally distributed benthic  $\delta^{18}O$  records. – Palaeoceanography, 20: 1–17.
- LUND, S.P., ACTON, G., HASTEDT, M., OKADA, M., WILLIAMS, T. (1998): Geomagnetic field excursions occurred often during the last million years. – EOS, 79, 14: 178–179.
- MAHER, B. (1998): Magnetic properties of modern soils and Quaternary loessic paleosols: paleoclimatic implications. – Palaeogeography, Palaeoclimatology, Palaeoecology, 137: 25–54.
- MARKOVIĆ, S., HAMBACH, U., CATTO, N., JOVANOVIĆ, M., BUGGLE, B., MACHALETT, B., ZÖLLER, L., GLASER, B., FRECHEN, M. (2009): Middle and Late Pleistocene loess sequences at Batajnica, Vojvodina, Serbia. – Quaternary International, 198 (1–2): 255–266.
- MARKOVIC, S.B., HAMBACH, U., STEVENS, T., KUKLA, G.J., HELLER, F., MCCOY, W.D., OCHES, E.A., BUGGLE, B., ZÖLLER, L. (2011): The last million years recorded at the Stari Slankamen (Northern Serbia) loess-paleosol sequence: revised chronostratigraphy and long-term environmental trends. – Quaternary Science Reviews, 30, 1142–1154.
- PENCK, A., BRÜCKNER, E. (1909): Die Alpen im Eiszeitalter, Vol. 1. – Tauchnitz, Leipzig, pp. 393.
- PREUSSER, F. & FIEBIG, M. (2009): European Middle Pleistocene loess chronostratigraphy: Some considerations based on evidence from the Wels site, Austria. – Quaternary International, 198, 37–45.
- PREUSSER, F. & FIEBIG, M. (2011): Chronologische Einordnung des Lössprofils Wels auf der Basis von Lumineszenzdatierungen. – Mitteilungen der Kommission für Quartärforschung, 19: 63–70, Wien.
- SCHOLGER, R. & TERHORST, B. (2011): Paläomagnetische Untersuchungen der pleistozänen Löss-Paläobodensequenz im Profil Wels-Aschet. – Mitteilungen der Kommission für Quartärforschung, 19: 47–61, Wien.
- SINGER, B.S., HOFFMAN, K.A., SCHNEPP, E., GUILLOU, H. (2008): Multiple Brunhes Chron excursions recorded in the West Eifel (Germany) volcanics: Support for long-held mantle control over the non-axial dipole field. – Physics of the Earth & Planetary Interiors, 169: 28–40.
- STREMMER, H., ZÖLLER, L., KRAUSE, W. (1991): Bodenstratigraphie und Thermolumineszenz-Datierungen für das Mittel- und Jungpleistozän des Alpenvorlandes. – Sonderverhandlungen des Geologischen Instituts Univ. Köln, 82: 301–315 (Festschrift K. Brunacker).
- TERHORST, B. (2007): Korrelation von mittelpleistozänen Löß-/Paläobodensequenzen in Oberösterreich mit einer marinen Sauerstoffsotopenkurve. – E & G, Quaternary Science Journal, 56/3: 172–185.
- TERHORST, B., FRECHEN, M. & REITNER, J. (2002): Chronostratigraphische Ergebnisse aus Lößprofilen der Inn- und Traun-Hochterrassen in Oberösterreich. – Zeitschrift für Geomorphologie, Suppl.-Bd. 127: 213–232.
- TERHORST, B., OTTNER, F. & HOLAWE, F. (2011): Pedostratigraphische, sedimentologische, mineralogische und statistische Untersuchungen an den Deckschichten des Profils Wels/Aschet (Oberösterreich). – Mitteilungen der Kommission für Quartärforschung, 19: 13–35, Wien.
- TERHORST, B., OTTNER, F. & WRIESSNIG, K. (2012): Weathering intensity and pedostratigraphy of the Middle to Upper Pleistocene loess/paleosol sequence of Wels-Aschet (Upper Austria). – Quaternary International, 265: 142–154.
- THOUVENY, N., DE BEAULIEU, J.L., BONIFAY, E., CREER, K.M., GUIOT, J., ICOLE, M., JOHNSEN, S., JOUZEL, J., REILLE, M., WILLIAMS, T. & WILLIAMSON, D. (1994): Climate variations in Europe over the past 140 kyr deduced from rock magnetism. – Nature, 371: 503–506.
- VAN HUSEN, D. (2000): Geological processes during the Quaternary. – Mitteilungen der Österreichischen Geologischen Gesellschaft, 92: 135–156, Wien.
- VAN HUSEN, D., REITNER, J. (2011): Klimagesteuerte Terrassen- und Lössbildung auf der Traun-Enns-Platte und ihre zeitliche Stellung (Das Profil Wels-Aschet). – Mitteilungen der Kommission für Quartärforschung, 19: 1–12, Wien.
- VELICHKO, A.A. (1990): Loess-Paleosol formation on the Russian Plain. – Quaternary International, 7–8: 103–114.
- VEROSUB, K.L. & ROBERTS, A.P. (1995): Environmental magnetism: Past, present, and future. – Journal of Geophysical Research, 100: 2175–2192, Washington.

# Paleopedological record along the loess-paleosol sequence in Oberlaab, Austria

Elizabeth Solleiro-Rebolledo, Hector Cabadas, Birgit Terhorst

## How to cite:

SOLLEIRO-REBOLLEDO, E., CABADAS, H., TERHORST, B. (2013): Paleopedological record along the loess-paleosol sequence in Oberlaab, Austria. Paleopedological record along the loess-paleosol sequence in Oberlaab, Austria. – E&G Quaternary Science Journal, 62 (1): 22–33. DOI: 10.3285/eg.62.1.03

## Abstract:

A detailed study of a loess-paleosol sequence in Oberlaab, Upper Austria, is presented with emphasis on macro- and micromorphological features, grain size distribution, rock magnetism properties, and weathering degree that allows correlation with other loess-paleosol sequences in neighboring areas, and interpretation of main pedogenic trends. The studied sequence comprises four paleosol complexes, which likely developed during four interglacial stages MIS 11, 9, 7 and 5e, and a modern soil. The oldest paleosol complex (OL5) represents three phases of soil formation, and distinct sedimentary events never reported in the area, with strong reductomorphic properties. The OL4 profile also results from three phases of pedogenesis with increased reductomorphic features in the deepest zone (affected by cryoturbation events). OL3 has abundant features related to gleyic/stagnic processes, but shows signs of clay illuviation. OL2 (Eemian soil) correlates with the MIS 5e. This paleosol shows higher degrees of clay illuviation and weathering, and fewer features related to reductomorphic processes. The modern soil is also polygenetic and constitutes a pedocomplex. Its lowermost part is formed by Würmian glacial deposits, where no well-developed soils are found; only reworked materials and pedosediments. Main pedogenic trends in the sequence are clearly differentiated. All of the paleosols were formed in humid environments, but differing in drainage conditions. The base, with OL5 and OL4 paleosols, was more affected by gleyic processes, while in the upper paleosols, especially OL2, clay illuviation is dominant. We interpret such differences to be caused by the topographic position. The basal paleosols were more affected by fluvio-glacial processes due to their position on top of the terrace. The upper paleosols received increased amounts of sediment through fluvial, colluvial and aeolian (loess) input.

## Das paläopedologische Archiv der Löss-Paläoboden-Sequenz in Oberlaab, Österreich

## Kurzfassung:

Eine detaillierte Untersuchung einer Löss-Paläoboden-Sequenz in Oberlaab, Oberösterreich, wird vorgestellt, deren Schwerpunkt auf makro- und mikromorphologischen Merkmalen, der Korngrößenverteilung, magnetischen Gesteinseigenschaften und dem Verwitterungsgrad liegt. Die untersuchten Aspekte ermöglichen einerseits eine Korrelation mit anderen Löss-Paläoboden-Sequenzen in benachbarten Gebieten und andererseits die Interpretation wichtiger pedogenetischer Entwicklungen. Die untersuchte Sequenz besteht aus vier Paläoboden-Komplexen, deren Entwicklung sehr wahrscheinlich während der vier Interglaziale MIS 11, 9, 7 und 5e stattfand, sowie einem rezenten Boden. Der ältere Paläobodenkomplex (OL5) beinhaltet drei Phasen der Bodenbildung mit unterschiedlichen Sedimentationsereignissen, die in diesem Gebiet bislang noch nicht beschrieben wurden. Darüber hinaus finden sich stark redoximorphe Merkmale. Das Profil OL4 zeigt ebenfalls drei Bodenbildungsphasen mit zunehmend redoximorpher Prägung im unteren Bereich, wobei eine Überprägung durch kryoturbate Prozesse sichtbar ist. Auch an OL3 konnten Merkmale grund- bzw. stauwasserbeeinflusster Prozesse dokumentiert werden, es finden sich aber auch Hinweise auf Tonverlagerung. Der Eemboden OL2 entspricht dem MIS 5e. Hier zeigen sich die intensivste Tonverlagerung und der stärkste Verwitterungsgrad, sowie ein Rückgang der redoximorphen Merkmale. Auch der rezente Boden ist polygenetisch und stellt sich als Pedokomplex dar. Der unterste Bereich besteht aus würmzeitlichen glazialen Ablagerungen. In diesem Profilteil finden sich keine gut entwickelten Böden, sondern ausschließlich umgelagertes Material und Pedosedimente.

Die vorherrschenden pedogenetischen Prozesse in der Sequenz können klar abgegrenzt werden. Alle Paläoböden entstanden unter humiden Bedingungen, wobei aber jeweils eine unterschiedliche Drainage vorhanden war. Die Profilbasis, die durch die Paläoböden OL5 und OL4 gebildet wird, ist stärker von Grundwasser beeinflusst, während in den oberen Paläoböden, v.a. in OL2, die Tonverlagerung dominiert. Es ist anzunehmen, dass diese Unterschiede in der topographischen Position begründet sind. Die unteren Paläoböden sind aufgrund der tieferen Lage der Terrasse stärker von glazifluvialen Prozessen betroffen, während die oberen Paläoböden nach der Sedimentation von großen Materialmengen (fluvial, kolluvial und/oder Löss) eine höhere Position einnehmen.

## Keywords:

*Middle Pleistocene, loess, paleosol, Oberlaab, pedogenesis*

**Addresses of authors:** E. Solleiro-Rebolledo, Universidad Nacional Autónoma de México, Instituto de Geología. Circuito de la Investigación Científica, 04510, México DF, Mexico. E-Mail: solleiro@geologia.unam.mx; H. Cabadas, Universidad Autónoma del Estado de México, Facultad de Geografía, Cerro de Coatepec s/n, Cd. Universitaria, Toluca, México. E-Mail: hvcabadasb@uaemex.com; B. Terhorst, University of Würzburg, Institute of Geography and Geology, Am Hubland, D-97074 Würzburg/Germany. E-Mail: birgit.terhorst@uni-wuerzburg.de

## 1 Introduction

Loess/paleosol sequences are a valuable source of information about past climatic and environmental conditions during the Quaternary, and are one of the most complete terrestrial records of glacial-interglacial cycles (PÉCSI 1990; PÉCSI & SCHWEITZER 1993; MUHS & BETTIS 2003) successfully correlated to the global climate proxies as marine isotope curves (KUKLA 1978; BRONGER et al. 1998). In temperate zones they have provided reliable information about paleoenvironmental change, particularly for the last glacial/interglacial cycle, as in Eurasia (LIU 1985; ROZYCKI 1991; SUN et al. 1997; MUHS & BETTIS 2003; FENG et al. 2007), United States (MUHS & BETTIS 2000; BETTIS et al. 2003), and South America (MUHS & ZÁRATE 2001; QUATTROCCHIO et al. 2008). In Austria, several works contain detailed descriptions for loess-paleosol sequences (e.g. FINK 1976; KOHL 1976; HAESAERTS et al. 1996; NEUGEBAUER-MARESCH 1996; NIEDERHUBER 1997; TERHORST 2007). However, our understanding of the pedostratigraphy and pedogenesis of loessic paleosols remains incomplete. In particular, in Upper Austria, where over a century of research on Pleistocene landscape history has been conducted since the classical works of PENCK & BRÜCKNER (1909), loess-paleosol records are still yielding new data for regional paleoenvironmental reconstructions.

We studied a loess-paleosol sequence in Upper Austria, situated on the top of a Mindel fluvioglacial terrace. The Austrian stratigraphic table classifies the classical Mindel glacial as belonging to the MIS 12 (ÖSTERREICHISCHE STRATIGRAPHISCHE KOMMISSION 2004). VAN HUSEN (2000) and VAN HUSEN & REITNER (2011) correlate Mindel glacial sediments in the Eastern Alpine Foreland with the MIS 12, while the Rissian deposits are associated to the MIS 6. On the basis of pedostratigraphical analyses in the Linz/Wels area, TERHORST (2007; 2013, this volume) and TERHORST et al. (2011) propose a similar correlation for the loess/paleosol sequence of Oberlaab, which includes four interglacial paleosols located on top of the Mindel terrace. These paleosols are linked to MIS 11, 9, 7 and 5, respectively (TERHORST et al. 2011, 2013), and span parts of the Middle to the Upper Pleistocene. According to TERHORST (2007) and TERHORST et al. (2011, 2013) Middle Pleistocene sequences in Upper Austria are the result of an alternation of geomorphogenetic-pedogenic processes. During Middle Pleistocene times, geomorphodynamics in the region were controlled by unstable glacial periods (causing phases of erosion and sedimentation), which alternated with stable interglacial periods and soil formation. Using the concept of “soil memory” (in the sense of TARGULIAN & GORYACHKIN 2004) the resulting paleosols contain information about environmental conditions of the interglacials.

In Oberlaab, we conducted a paleopedological survey, which involved a multidisciplinary approach to identify types of pedogenesis and degrees of paleosol development. Previously, TERHORST (2007) studied a similar sequence in the loam pit of Oberlaab, which comprises thick pedocomplexes, related to four interglacial periods, covering a time span of >400 ka. In this paper, we contribute a detailed morphological description of pedostratigraphic units accompanied by a set of quantitative pedogenetic characteristics:

morphometric analysis of diagnostic pedofeatures, grain size distribution, magnetic parameters (magnetic susceptibility and frequency dependence of susceptibility), as well as geochemical indicators of weathering. These characteristics provide a base for reliable comparison between buried paleosols and the Holocene surface soil, in order to establish differences in the typology and grade of development of the main pedogenic processes. The resulting paleopedological record contributes to the reconstruction of the environmental conditions of the four last interglacials and provides complementary data for the regional geomorphological and stratigraphic schemes.

## 2 Materials and methods

The study site is situated in a quarry exploited for clay for brick production, 1.5 km to the north of Wels, Austria (for details see TERHORST 2013, this volume). The general stratigraphy was presented by TERHORST (2007), who has recognized four interglacial paleosols. The loess/paleosol sequence of Oberlaab was developed on a Mindel terrace (Younger Deckenschotter). The basement of the sequence is formed by gravels, exposed previously in a cut operation during 2003. The whole sequence has a thickness of 15.80 m, which has been sectioned and labeled as the units OL1, OL2, OL3, OL4 and OL5. Each of these sections contains a soil/paleosol/pedocomplex unit (Figure 1).

Genetic horizons of modern soil and paleosols were defined according to their morphology following the World Reference Base (IUSS WORKING GROUP WRB 2007). We observed ped features under a 10X lens in the field. In all cases, interpretation was based on comparison of paleosols with the modern soil.

### 2.1 Micromorphology

For micromorphological studies we took undisturbed samples from every genetic horizon (Figure 1). Thin sections were prepared and described with the guide of BULLOCK et al. (1985).

To quantify the proportion of pedofeatures in different horizons, selected thin sections were scanned with high resolution (4800 and 9600 dots per inch); the digital image was later analyzed with the Image Pro Plus v.6.0 software. A contrast enhancement of every image was produced to distinguish zones with diffuse contacts to the groundmass, using the blue RGB channel acquisition. The false color was used for the segmentation of areas occupied by each pedofeature with a previous conversion to shades of grey. The most important features analyzed were: 1) iron nodules and impregnations, 2) bleaching areas and 3) clay coatings. However, in most of the thin sections the complex mixture of iron and clay was very difficult to separate by the software algorithms. Thus, we decided to study clay coatings semi-quantitatively using visual schematic petrographic diagrams (CASTRO 1989). Porosity was not estimated in the total average, because in some thin sections voids had the same color as felsic minerals.

Besides micromorphometric analysis of selected pedofeatures we established the assemblage of the primary minerals, their distribution in different size fractions and their weath-



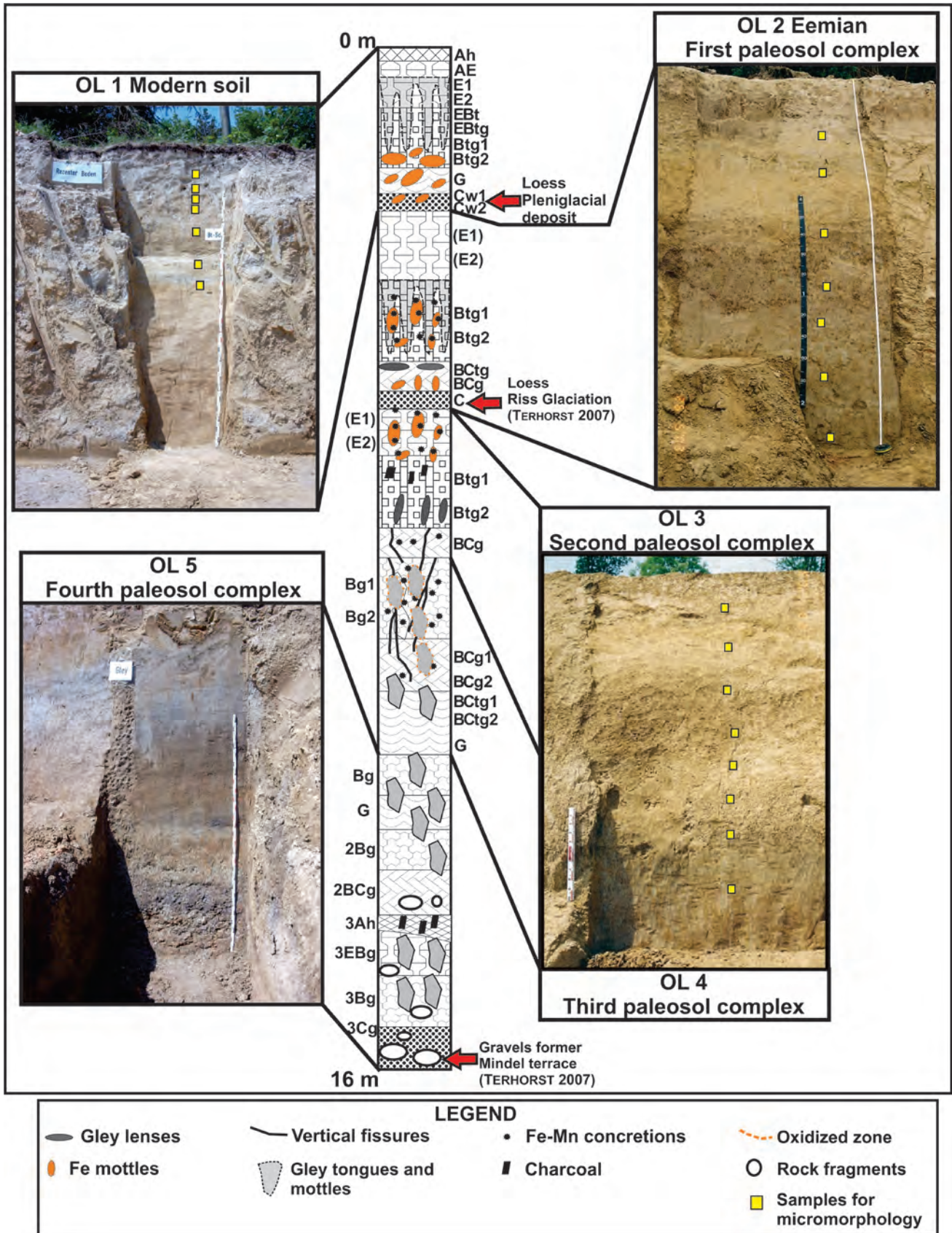


Fig. 1: Oberlaab loess/paleosol sequence on top of a Mindel terrace (Young Deckenschoter), which includes four interglacial paleosols and the modern soil.

Abb. 1: Stratigraphie der Löss-Paläoboden-Sequenz Oberlaab, sowie ein allgemeiner Überblick über alle vier Paläoböden und den rezenten Boden.

ering status basing on the crystalloptical properties under magnification with a petrographic microscope.

## 2.2 Laboratory analyses

Size fractions were separated in OL1, OL2, OL4 and OL5. OL3 was not evaluated due to the lack of samples. The sand fraction (2–0.063 mm) was separated by sieving; silt (0.063–0.002 mm) and clay (<0.002 mm) fractions by gravity sedimentation with previous destruction of aggregating agents; H<sub>2</sub>O<sub>2</sub> (15%) was used for organic matter, and dithionite-citrate-bicarbonate (DCB) for iron oxides. As the deposits had no carbonates, no additional pre-treatments were necessary for their destruction.

For magnetic measurements, 200 g samples were collected at roughly 20 cm intervals, homogenized, and placed in 8 cm<sup>3</sup> acrylic boxes. Magnetic susceptibility ( $\chi$ ), which is a measure of the concentration of magnetic minerals, was registered in all samples at low (0.47 kHz) and high frequencies (4.7 kHz) with a Bartington MS2B dual sensor. We calculated frequency dependence of susceptibility  $\chi_{fd}\%$  as  $[(\chi_{lf}-\chi_{hf})/\chi_{lf}]100$ , to approximate possible ultrafine (< 0.05  $\mu\text{m}$ ) superparamagnetic (SP) contribution. DEARING (1994) and DEARING et al. (1997) suggest that values of  $\chi_{fd}\% < 2\%$  point to a content of <10% of SP (superparamagnetic) grains; values around 8% indicate a SP contribution of 75%, and between 10–14%, the material is domain by SP particles.

## 2.3 Geochemical indices of weathering

Bulk chemical composition was obtained by X-ray fluorescence in a Siemens SRS 3000 spectrometer, using powder pellets at the Institute of Geology, UNAM. All results were calculated by weight on oven dry (105° C) soil.

As the parent material of the section is mainly loess rich in silica, we decide to evaluate the degree of weathering using the chemical index of alteration (CIA). CIA measures changes in major cation content in relation to immobile alumina, instead of changes in the silica/alumina composition. This proxy was first proposed by NESBITT & YOUNG (1982) and introduced in loess studies by LIU et al. (1995). CIA is evaluated following the formula:  $\text{CIA} = (\text{Al}^{2}\text{O}_3 / (\text{Na}_2\text{O} + \text{CaO} + \text{MgO} + \text{K}_2\text{O})) * 100$ . The reason to use this weathering index is the high concentration of K-feldspar found in the mineralogical assemblage, according to BUGGLE et al. (2011) and the lack of carbonates (thus the CaO content is only associated to silicates). A value near 100 represents the highest degree of weathering, while values lower than 50 correspond to fresh sediments.

## 3 Results

### 3.1 Morphology of the Oberlaab paleosol sequence

The study sequence in Oberlaab includes a modern soil (OL1) and 4 paleosol units (OL2 to OL5) from the top to the bottom (Figure 1).

OL1. Modern soil (depth 0–190 cm). The OL1 soil shows a well-developed profile with Ah-AE-E1-E2-EBt-EBtg-Btg1-Btg2-G-Cw horizons. The Ah horizon is thin (5 cm-thick), dark brown, very porous, with a consistent granular

structure and a high density of roots. The transitional AE horizon is also thin (10 cm thick) and paler than Ah. The underlying E horizon is 30 cm thick, divided into E1 and E2. This division was made because E2 is notably darker with less silt. In general, the E horizon is light gray, silty and with subangular blocky structure. The contact with the underlying Btg1 is also transitional, through the EBt and EBtg horizons (45–100 cm). Light gray tongues of compacted, silty material, starting from the E horizon, enter into Btg (100–150 cm). These tongues are separated from each other by 15 cm in some cases, and 25 cm in others. Roots do not penetrate the tongues. The Btg1 horizon is grayish-yellowish brown, with yellowish brown mottles. Clay coatings are thick and frequent. The Btg2 horizon has a similar color, but is distinguished by a network of cracks. The cracks boundaries are gray, contrasting with the brownish color of the matrix. The lowermost G horizon (150–160 cm) is gray in color, more dense and has a silty texture. The subangular blocky peds exhibit a platy structure. The Cw horizon (160–190 cm) corresponds with the uppermost part of a pale-yellow, silty, loess-like deposit, showing horizontal gray bands.

The underlying Cw horizon corresponds to a loess-like deposit (190–390 cm). This material constitutes a pedosediment, which contains a mixture of sediments and reworked soils.

OL2. Eemian soil (depth 390–670 cm). The next stratigraphic level corresponds to the Eemian soil (Figure 1), and contains a sequence of (E1)-(E2)-Btg1-Btg2-BCtg-BCg-C horizons. Vertical cracks cross the first 200 cm (390–590 cm), filled by a gray material, of which the inner part is black. The boundary between the gray and black materials is reddish.

Because of the paler color (brownish yellow) of the first 60 cm (390–450 cm), we initially assumed that the material corresponds to an E horizon, which is divided into E1 and E2 with a silty loam texture. However, a more detailed morphological study revealed that the horizon is constituted by two layers of reworked pedosediments. The loess-like sediment is affected by weak pedogenesis, with rounded sediment grains and soil fragments. The soil fragments occur as small subangular blocks breaking into granular aggregates, with a tendency to form a weak platy structure. Moderate amounts of 2–3 mm-diameter Fe/Mn-concretions were detected, varying from dark brown to red. The transitional limit to the underlying Btg horizon (Btg1 and Btg2) is wavy. The Btg horizon (450–540 cm) is yellowish brown, darker than the reworked pedosediments of the upper part, more compact, and clayey. Btg1 has a better developed platy structure, which breaks to subangular blocks. Clay coatings are abundant. In the upper surface of the platy aggregates, discontinuous dark brown clay coatings are present. In this horizon the vertical cracks are covered by clay and silt coatings (the latter are observable with a 10X-hand lens). Fe/Mn-concretions are abundant. The horizon shows strong mottling, which consist of bright yellow areas with brownish and grayish zones. These spots are mainly oriented along the vertical cracks. In Btg2, clay coatings are fewer and more disperse. The BCtg horizon (540–570 cm) is paler and also compact. Here, fewer clay coatings and Fe-Mn concretions are detectable. Vertical



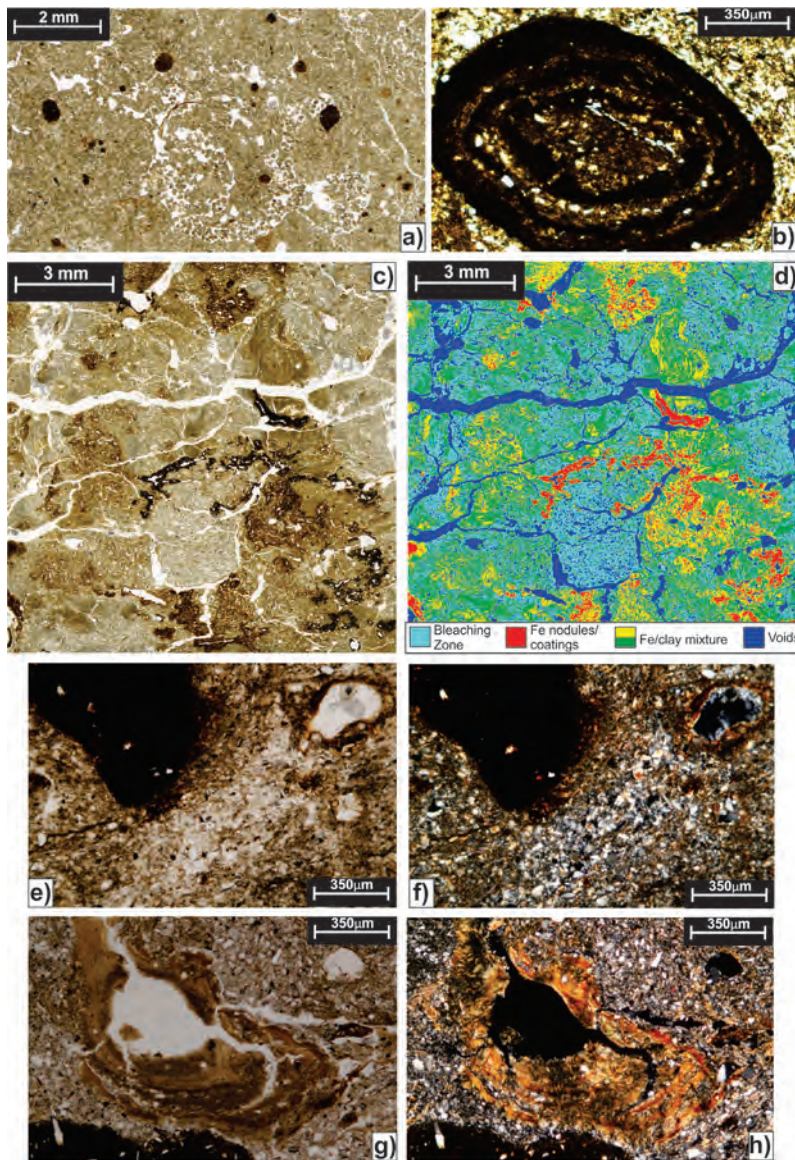


**Fig. 2: Micromorphology of the study section:**  
 a. Coalescent excremental infillings in chambers in AE horizon of the modern soil. High resolution image (4600 dpi) of scanned thin section.  
 b. Concentric iron nodule in G horizon of the modern soil, photomicrograph, plane polarized light (PPL).  
 c. Bleached zones in the groundmass of BCg1 horizon in OL4. High resolution image (4600 dpi) of a scanned thin section.  
 d. Same as 2c: Image analysis in false color.  
 e. Bleached zone (center) with sharp contact with the groundmass in OL3-BCg horizon. Fe nodules showing abrupt boundaries with the groundmass, photomicrograph (PPL).  
 f. Same as 2e, cross polarized light (XPL).  
 g. Clay coatings around a void associated with a bleached zone in OL3-Btg1 horizon. The dark-yellowish color of the clay is related to the presence of iron and coarse silt fraction, photomicrograph (PPL).  
 h. Same as g, XPL. Note the high interference color related to the presence of 2:1 clay structure.

**Abb. 2: Mikromorphologie des untersuchten Abschnitts:**  
 a. Koagulierte Exkrementfüllungen in Hohlräumen im AE-Horizont des rezenten Bodens. Hochauflösende Darstellung (4600 dpi) von gescanntem Dünnschliff.  
 b. Konzentrische Eisenkonkretion im G-Horizont des rezenten Bodens. Mikroskopaufnahme unter eben polarisiertem Licht (plane polarized light, PPL).  
 c. Gebleichte Zonierung in der Matrix des BCg1-Horizonts von OL4. Hochauflösende Darstellung (4600 dpi) von gescanntem Dünnschliff.  
 d. Wie 2c: Falschfarbenbildanalyse.  
 e. Gebleichter Bereich (Zentrum) in scharfer Abgrenzung zur Matrix im BCg-Horizont von OL3. Mikroskopaufnahme (PPL). f. Wie 2e., gekreuzte Polarisatoren (cross polarized light, XPL).  
 g. Kugelförmige Struktur (roter Rahmen rechts) in OL4. Hochauflösende Darstellung (4600 dpi) von gescanntem Dünnschliff.  
 h. Tonüberzüge in einem Hohlraum in Verbindung mit einer Bleichzone in Btg1 in OL3. Die dunkelgelbe Farbe des Tons ist bedingt durch den Eisengehalt und der Korngrößenfraktion Grobschluff. Mikroskopaufnahme (PPL).

oriented channels are also present. They are filled by laminated clay (dark brown) and silt coatings (yellow and gray). The BCg horizon (570–635 cm) is similar, but here coatings are very rare. The most conspicuous feature is the change of color as well as the intensity of gleyic characteristics throughout the horizon. Grey, horizontally oriented lenses appear in the first 15 cm. The matrix of the next 30 cm is grayish-yellowish brown with some yellow spots. The lower part is light yellowish brown and has diffuse mottles. The C horizon (635–670 cm) has a silty loam texture and a brown to yellowish brown color with rusty mottles. There are no Fe concretions. Structure is weak varying from subangular blocky to massive.

OL3. Second paleosol complex (depth 670–900 cm). Similar to the Eemian soil in OL2 (Figure 1) this unit has two levels of reworked pedosediments (E1 and E2) on the top (670–730 cm), which are superimposed on the following compact horizons: Btg1-Btg2-BCg. The first pedosediment level (30 cm thick) is strongly mottled. Matrix has a light brownish yellow color with gray stagnic mottles and round rusty patches (1 to 1.4 cm in diameter). Structure shows large subangular blocks and inside the block aggregates

there is a tendency to form a thin platy structure. Vertical cracks are frequent and filled by clay pellets. There are bleached areas with light colors that contrast with darker stagnic zones. The second level of reworked pedosediments (30 cm thick) corresponds to a strongly patchy silty loam. In this case the color is paler because of dominant grayish mottles. Rounded mottles are covered by dark brown clay coatings. Btg1 (730–790 cm) is characterized by a dark brown matrix with even darker mottles that alternate with brownish gray spots. Structure is very well developed in strong angular blocks, which break into smaller angular aggregates. Dark brown Fe/Mn-concretions with a size from 1 to 5 mm diameter are frequent. Dark brown clay coatings are present; however, they are very rare and appear in few peds. Small quantities of charcoal are present and associated to thin root channels. Due to an increase of vertically oriented gley mottles, Btg2 (790–860 cm) has a clear change in color as well as in structure (subangular blocks). In this horizon we detect a decrease in the abundance of clay coatings, and in the quantity and size of the Fe-concretions. Some rounded rock fragments are found. The BCg horizon (860–900 cm) is strongly patchy. Matrix is



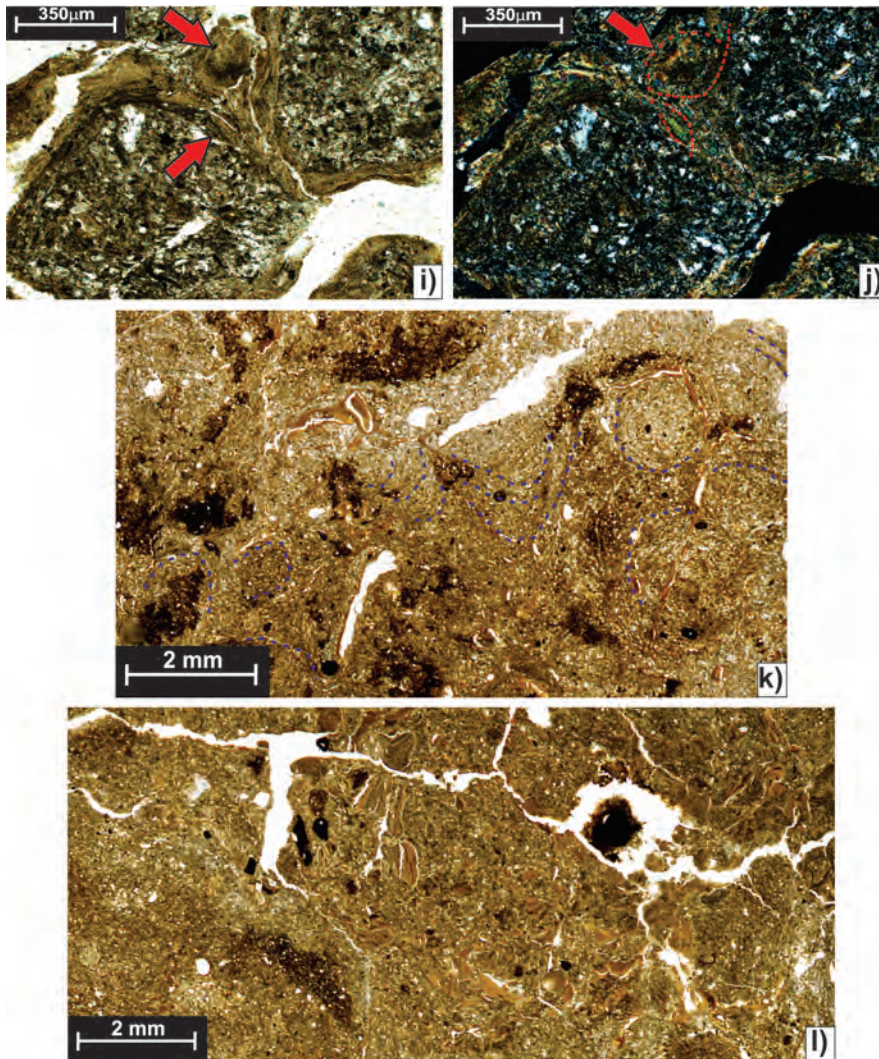


Fig. 2: Micromorphology of the study section: i. Deformed pedofeatures. Deformed clay coatings showing a "twisted" morphology and displacing the groundmass (red arrow) around blocky microstructure in Btg2 horizon of OL3, photomicrograph (PPL).

j. same as 2j, (XPL). The red discontinuous lines show the "twisted" morphology with the displacing of the groundmass. Note the high interference color inside and outside of the blocky microstructure, related to a primary phase of clay illuviation (2:1 clay structure).

k. Orbiclic fabric (blue discontinuous line) in Bg2 horizon in OL4. High resolution image (4600 dpi) of scanned thin section.

l. Fragmented clay cutans possibly associated to bioturbation in Bg2 horizon of OB4. High resolution image (4600 dpi) of scanned thin section.

Abb. 2: Mikromorphologie des untersuchten Abschnitts:

i. Wie h., gekreuzte Polarisatoren. Man beachte die hohen Interferenzfarben aufgrund der 2:1-Struktur der Tonminerale.

j. Fragmente illuvialer Tonüberzüge verdrängen die Matrix im Btg2-Horizont von OL3. Mikroskopaufnahme, (PPL).

k. Wie 2j., gekreuzte Polarisatoren. Auch hier ist die hohe Interferenzfarbe innerhalb des primär illuvial verlagerten Fragments zu beachten. Der rote Pfeil kennzeichnet teilweise in der Matrix assimilierte Toncutane.

l. In der Bildmitte Fragmentierung von Toncutanen in Bg2 (OB4), möglicherweise durch Bioturbation. Hochauflösende Darstellung (4600 dpi) von gescanntem Dünnschliff.

yellowish brown with mottles varying from gray to brownish gray and red. The structure is subangular blocky and platy. Vertical cracks filled by grayish material cross the horizon. Fe/Mn-concretions are frequent (0.1 to 0.5 in diameter).

OL4. Third paleosol complex (depth 900–1200 cm). This unit is constituted by Bg1-Bg2-BCg1-BCg2-BCTg1- BCTg2-G horizons (Figure 1), which are very compact and have silty loam textures. The unit is crossed by vertical fissures filled by dark gray, stagnic materials. In the central part of the fissures we observe clay and silt coatings (the latest distinguish by their coarser texture). The Bg1 horizon is strongly patchy and wavy (900–950 cm). Dark brown material alternates with light grey vertically oriented mottles. The exterior part of the mottles is surrounded by yellow-brown oxidized zones. Structure is platy and angular blocky. Abundant Fe/Mn-concretions (0.5–1cm in diameter) are found. Dark coatings are present, especially on the surface of platy blocks. Bg2 (950–990 cm) clearly differs from the previous horizon by the increase of gray areas (stagnic) on the ped surfaces. Fe/Mn-concretions are also present but in lesser amounts. BCg1 (990–1030 cm) is patchy, paler than the previous Btg, but with a similar structure. In this horizon the vertical fissures are thicker than in the upper part. Fe and Mn coatings are frequent. BCg2 (1030–1100 cm) is very similar to BCg1 but less patchy. BCTg1 (1100–1140

cm) and BCTg2 (1140–1180 cm) are alike, but BCTg1 is more clayey and shows dark clay coatings. Round vertical channels are common. G (1180–1200 cm) is more homogeneous in color with a grey matrix, showing small brown rusty mottles. Structure is well developed and consists of small subangular blocks. It is clear that vertical channels do not enter into this horizon.

OL5. Fourth paleosol sequence (1200–1520). This lowest stratigraphic level is clearly a pedocomplex, composed by Bg-G-2Bg-2BCg-3Ah-3EBg-3Bg-3Cg horizons (Figure 1). The upper Bg (1200–1250 cm) is pale brownish yellow with rusty and grey mottles. It is constituted by very fragile subangular blocks with a silty clay texture. Its transition to the G horizon is wavy and gradual. The G horizon (1250–1290 cm) is bluish gray with black and rusty mottles. Due to the occurrence of small subangular blocks the structure is better developed than in the Bg horizon. Mn segregations are common. The boundary with the next 2Bg horizon (1290–1370 cm) is clear and wavy. It is pale brown with brown, rusty and black mottles. It has a silty loam texture. Friable subangular blocky structure is dominant with a tendency to break into crumbly, granules. Mn is segregated in pores and channels. Very few clay coatings are present in channels and on ped surfaces. The boundary with the less structured 2BCg (1370–1415 cm) is wavy and gradual. Rounded rock fragments are present in this



horizon marking a clear and straight limit to the next 3Ah horizon (1415–1430 cm), which has a very dark gray color with rusty and brown mottles. It is a silty clay loam with a very fragile subangular blocky-granular structure. Charcoal fragments and few clay coatings are found in channels and pores. The transition to the 3EBg horizon is clear and slightly wavy. 3EBg (1430–1450 cm) is pale gray. Rusty, brown, and black mottles are present. Its structure is constituted by fragile, small subangular blocks and gravels are frequent. 3Bg1 (1450–1490 cm) is yellowish brown with grayish mottles. It is a silty clay with a fragile structure composed of subangular blocks. Mn segregations and ferruginous hypocoatings are abundant in pores and channels. The lower part of this horizon is more grayish. Its contact with the underlying 3Cg (1490–1520 cm) is abrupt. It is build up by gravels with abundant Mn segregations and dark-brown mottles around the gravels, which increase in size with depth.

### 3.2 Micromorphology

The main micromorphological features observed in the Oberlaab section can be divided into four kinds: biogenic components and features, redoximorphic pedofeatures, clay coatings, and deformed pedofeatures. In most cases the proportions are obtained by using the scanned thin sections and the Image Pro software.

Biogenic components and features. These materials include root traces, humus, coprolites, channels, and charcoal. They are clearly recognizable in both the modern soil and the OL4 profiles. The Ah and AE horizons of the modern soil (OL1) are characterized by strong bioturbation including the presence of chambers with loose and discontinuous coalescent excremental infillings (Figure 2a) associated with root traces (in some cases more or less degraded). Dark humus impregnates the matrix, in cases where a granular structure dominates. Biogenic materials in OL4 are less diverse. They are presented only by charcoal fragments with a well preserved cellular structure, as well as passage features of mesofauna.

Redoximorphic pedofeatures. These kinds of pedofeatures include ferruginous concretions, hypocoatings, and bleached areas. Paleosols contain the highest concentrations in comparison to the modern soil (Figure 3). However, Fe concretions are frequent in the G horizons of the modern soil, where they show sharp boundaries to the matrix (Figure 2b). Fe concretions and hypocoatings reach the maximum (19%) in the BCg1 horizon of OL4. The highest proportion of bleached areas (65%), which permit the estimation of zones where iron has been removed, was found in the Bg2 horizon of OL4 (Figures 2c and 2d, Figure 3). It is interesting that the contact between bleached zones and groundmass is diffuse in surficial horizons, however, in the lower part of the profiles, boundaries are more abrupt. Figures 2e and 2f clearly

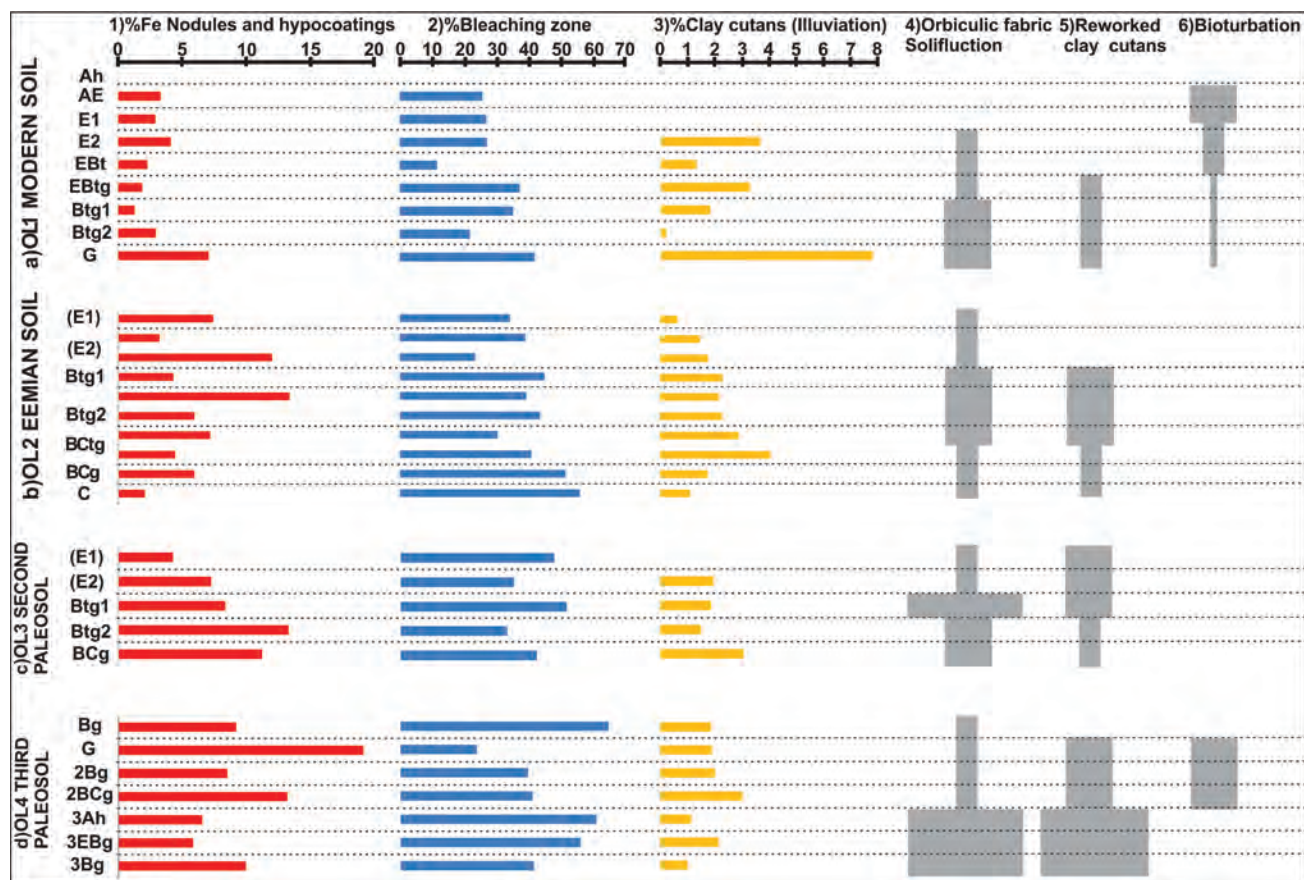


Fig. 3: Proportion of micropedofeatures in the Oberlaab sequence, according to the image analysis using the software Image Pro in high resolution image (4600 dpi) of scanned thin section.

Abb. 3: Quantifizierung von Mikrobodenmerkmalen, basierend auf der Bildanalyse mit der Software Image Pro, in hochauflösender Darstellung (4600 dpi) von gescanntem Dünnschliff.

show this kind of contact in the BCg horizon of OL3.

**Clay coatings.** Clay coatings are common in the modern soil; coating content varies from 1 to 3.5%. Surprisingly, the G horizon reaches a 7% the maximum in the whole sequence (Figure 3). In the Eemian paleosol (OL2), particularly in the Btg and BCtg horizons, the amounts are also high (2.1 to 4%). The lowest concentration of clay coatings is present in the OL3 and OL4 profiles (Figure 3). The “impurity” of the clay coatings varies in the profiles. In the modern soil most of the coatings are pure and limpid (with yellowish colors), meanwhile in the paleosols coatings show Fe microlaminations and pigmentations (Figure 2g and 2h).

**Deformed pedofeatures.** All studied paleosols, as well as the modern soil show deformation of some pedofeatures. This deformation is more evident in Btg horizons, where

the clay coatings are assimilated inside the bleached, silty groundmass and exhibit a “twisted” morphology (Figure 2i and 2j). The presence of fragmented and displaced groundmass blocks with “cloud” structures as well as orbiculate fabrics are also common (Figure 2k). Additionally, in OL3 and OL4 small blocks are fragmented and displaced. In such blocks we observe two different generations of clay coatings: the first one (thin and discontinuous clay coatings) is inside the blocks; the second one (with thicker coatings) covers the aggregates. Another kind of “deformed” coatings is present in BCg horizons (particularly in BCg horizon of OL4). These coatings are fragmented and rounded, indicating reworking processes (Figure 2l).

Besides the micromorphological descriptions made for the thin sections we analyzed the bulk mineral com-

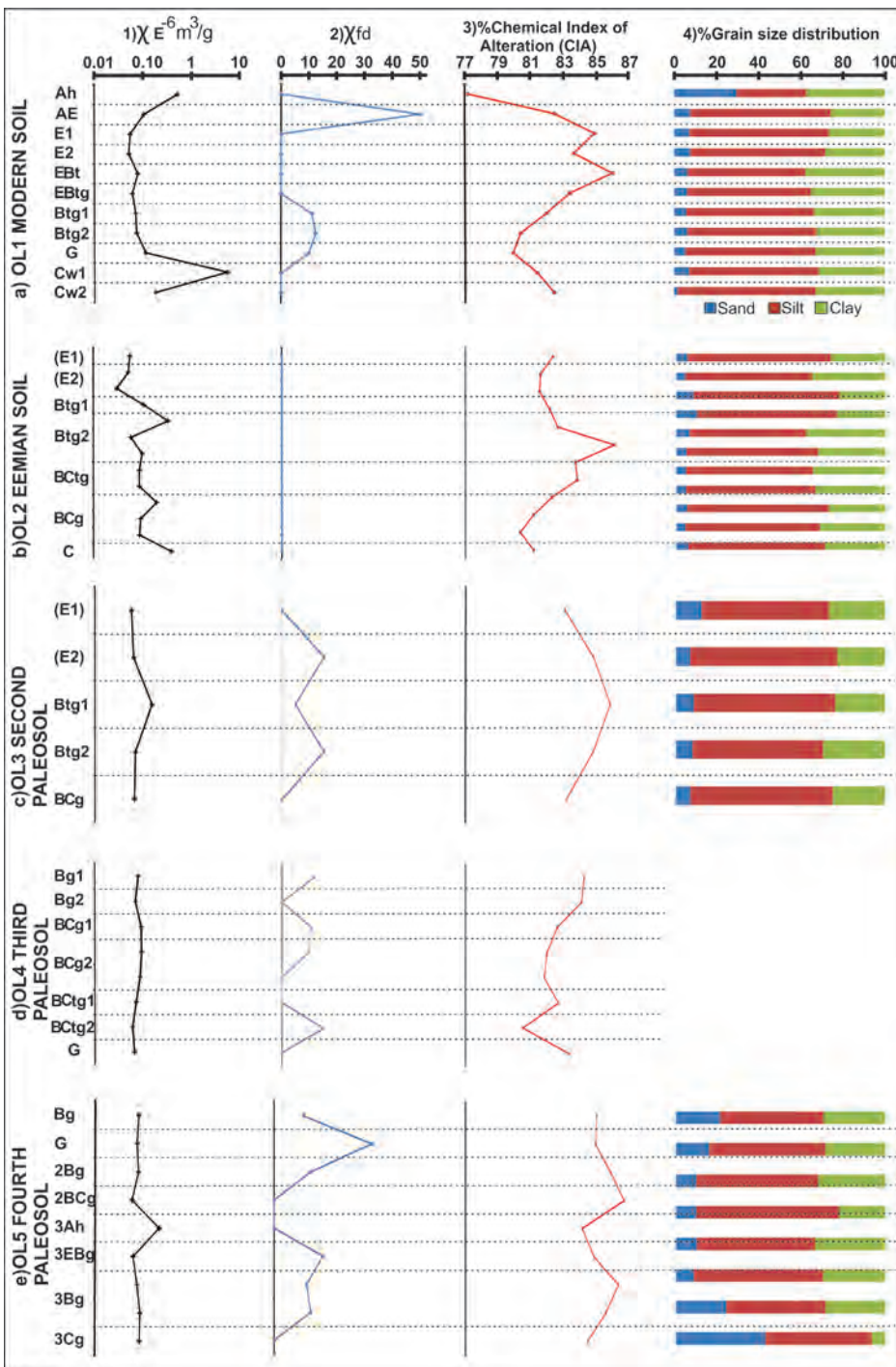


Fig. 4: Selected analytical properties of the study sequence: Magnetic susceptibility ( $\chi E^{-6} m^3/g$ ); frequency dependence of susceptibility ( $\chi fd\%$ ); grain size distribution (%).

Abb. 4: Ausgewählte Analyseergebnisse des untersuchten Abschnitts.



position of sand and silt fractions. The mineral content is mostly constituted by quartz, potassium feldspar, and mica (muscovite), which are moderately to well sorted. Biotite is present in low quantities and mostly concentrated in the sand fraction. Heavy minerals such as amphiboles (in some cases with “serrated” morphology), epidote, and garnet are concentrated in the silt fraction and demonstrate angular shape. Some schist fragments are recognizable in primary sedimentary layers. This mineralogical assemblage coincides well with the reports from other loess-paleosols sequences of Upper Austria (TERHORST et al. 2011).

### 3.3 Analytical properties

The silt fraction in the modern soil ranges from 33 to 67%. The surficial Ah horizon shows a high amount of sand (30%), contrasting to that obtained in the rest of the profile (Figure 4). The clay fraction exhibits similar proportions in all horizons, however, it increases in EBT and Btg horizons. The Cw horizon contains the highest proportion of silt (64–66%). Magnetic susceptibility ( $\chi$ ) is generally low in all horizons, but with high values in Cw1 and Ah horizons. The low values of the frequency dependence of susceptibility  $\chi_{fd}\%$  indicate a null contribution of super paramagnetic (SP), ultrafine grains ( $<0.05\ \mu\text{m}$ ). To the contrary, SP particles dominate in AE horizon (Figure 4). CIA values (chemical index of alteration) are high, increasing from 77% in Ah to 85% in EBT (Figure 4). The lowermost part of the profiles records slightly lower percentages.

In the Eemian soil (OL2) the silt fraction is dominant (55–70%). The whole profile shows a low proportion of sand. Clay content reaches a maximum in Btg2 horizon, although (E1) and (E2) horizons on the top show a high proportion as well (Figure 4). The values of magnetic susceptibility ( $\chi$ ) are very low in (E1) and (E2) but increase in Btg.  $\chi_{fd}\%$  values are very low in the whole profile, revealing that none of the horizons has SP contribution (Figure 4). CIA pattern shows a maximum in the Btg2 horizon (87%) and reach the lowest value in BCg (80.3%).

OL3 has a higher percentage of sand (7 to 12%) than the Eemian soil, however, silt still dominates (61 to 70%). In this unit the clay amount is lower (25–29%) and there is no significant difference among the horizons, although a slightly higher content is obvious in Btg2 (Figure 4). In case of magnetic parameters,  $\chi$  has similar values, while  $\chi_{fd}\%$  shows strong differences varying from zero in the (E1) to 14% in (E2), 5% in Btg1, 14% in Btg2, and zero in BCg. This contrast evidences the presence of discontinuities (Figure 4). CIA values are also very similar (83–85%). The highest weathering degree corresponds to Btg1 (Figure 4).

OL4 profile shows very low and homogeneous  $\chi$  values, but high percentages of  $\chi_{fd}\%$  indicate an elevated contribution in SP particles. However, this behavior is not continuous, because in Bg2, in the lowermost part of BCg2 (in 180–200 cm depth), and in the G horizon,  $\chi_{fd}\%$  drops to zero (Figure 4). CIA varies from 84% in Bg horizon decreasing to 82% in BCTg2.

OL5 has high variability in the proportions of the different size fractions, which reveal the influence of alluvial sedimentation. Sand varies from 8% in the Bg horizon to 42% in the lowermost part of the profile, where gravel appears. OL5

has very low values in  $\chi$ , although an enhancement without contribution of SP grains is noted in the 3Ah horizon, which is detectable in the uppermost part of the profile in the Bg and G horizon (Figure 4). CIA is equally variable. The upper Bg as well as G horizon are slightly less weathered than 2Bg and 2BCg and 3Ah and 3Cg show the lowest CIA percentages.

## 4 Discussion

### 4.1 Chronostratigraphy and correlation of the Oberlaab profile

Although no instrumental absolute dates are available in Oberlaab it is possible to establish a local chronostratigraphic scheme taking into account the stratigraphic classification of SCHOLGER & TERHORST (2011) and TERHORST et al. (2011) developed for the Middle Pleistocene profiles in the Northwest of Austria.

TERHORST (2007) points out that the Oberlaab sequence contains four interglacial paleosols (1st, 2nd, 3rd, 4th) thus covering at least the last five glacial periods (thus the development of the Mindel terrace (Younger Deckenschotter) occurs at least during MIS 12). According to the stratigraphic schemes, Oberlaab records completely the main paleoclimatic stages from MIS 12 to MIS 5e, parts of the last glacial, as well as the Holocene soil. This interpretation is in good agreement with the pedostratigraphical schemes of the cover layers in Wels-Aschet, Neuhofen, and Oberlaab and our studies can clearly be positioned in the regional stratigraphic context of the area. This contradicts to the view of PREUSSER & FIEBIG (2009), who propose younger ages for the Wels-Aschet sequence including the Older Deckenschotter of the Günz glaciation, based on luminescence dating. For instance, they suggest an age of  $252 \pm 29\text{ky}$  for the 4th interglacial paleosol (MIS7). Paleomagnetic studies done in the same sequence also contradict the chronostratigraphy of PREUSSER & FIEBIG (2009) documenting the presence of the Calabrian Ridge excursions: CR1 (325–315 ka) and CR2 (525–515 ka) inside the 3rd and in the base of the 4th interglacial pedocomplex, respectively (SCHOLGER & TERHORST 2011). Consequently, OL5 can be attributed to MIS 11 with three phases of soil formation: Bg-G-2Bg-2BCg-3Ah-3EBg-3Bg-3Cg. The upper Bg horizon correlates with the 4th interglacial paleosol, described by TERHORST (2007) and TERHORST et al. (2011) in Oberlaab, Neuhofen, and Wels-Aschet, but in our case clay coatings are not observed in this unit as in other sequences. TERHORST (2007) mentions an underlying G horizon in Neuhofen and Wels-Aschet, but without the 2Bg-2BCg horizons, which are present in our section. Furthermore, the lower paleosol has not been described before in the area. There are clear differences in analytical properties, which reflect soil formation cycles: CIA values are low in the Bg-G, 3Ah, 3EBg, and high in 2Bg-2BCg, 3Bg horizons (Figure 4).

The subsiding stratigraphic levels of OL4 and OL3 correlate with the 3th and 2th interglacial paleosols described for Upper Austria (TERHORST 2007; 2013, this volume; TERHORST et al. 2011). OL4 is developed on sediments which are classified as MIS 10 deposits and represent an intensive glacial phase. Therefore paleosol formation could correspond best to the MIS 9 (c.f. LISIECKI & RAYMO 2005). On

the base of the pedostraphic observations, the next sedimentation events can be correlated to the MIS 8 period, which records a weaker glacial phase (c.f. LISIECKI & RAYMO 2005). Pedogenesis of the OL3 unit can be related to the interglacial period of MIS 7.

Both profiles OL3 and OL4 are pedocomplexes (TERHORST 2007; TERHORST et al. 2012). According to our field observations significant differences and discontinuities are not detectable between both units. However, some quantitative analytical characteristics clearly indicate them. In OL4 we can separate three phases of pedogenesis: the first phase corresponds to the development of the lowermost G horizon, reflected by different properties: CIA values are higher than in the overlying BCtg2,  $\chi_{fd}\%$  is zero with no contribution of SP magnetic particles. The second phase comprises the horizons BCtg1 and BCg2, which tend to have similar characteristics although CIA values are higher in BCtg1, a fact which is related to a higher amount of clay. The third phase corresponds to the formation of the upper horizons Bg1-Bg2-BCg1- BCg2. These results are not in good agreement with those obtained by TERHORST (2007), who reports the presence of a pedocomplex in Oberlaab with only 2 paleosols, one described as a Bw horizon with stagnic properties superimposed by a Btg horizon. In Wels-Aschet, TERHORST et al. (2012) find the 3th paleosol, containing two Bt horizons with moderate weathering degree. Coincidences are in terms of the gleying process, because in Oberlaab as in other sections in Lower Austria, elevated amounts of Mn have been found in different forms.

On the other hand, OL3 is another pedocomplex. Repeatedly, the profile has been characterized as monogenetic during field survey, however, analytical results could highlight specific differences, although the clay content is similar (Figure 4). CIA index and  $\chi$  reveal maxima in the Btg1 horizon, which can be related to the high amount of clay (around 30%).  $\chi_{fd}\%$  values record significant differences in the contribution of magnetic particles, and thus can be explained by the presence of discontinuities (Figure 4). We have even found charcoal in Btg1 – probably because this horizon was close to the surface. Our results exhibit a discrepancy to those obtained by TERHORST et al. (2012) for the Wels-Aschet sequence, because on the basis of mineralogical analyses the authors conclude that the 2th paleosol is less weathered than the 3th one. Similar mineralogical results were obtained for earlier studied Oberlaab profiles (TERHORST et al. 2003). However, the presented CIA values, clay contents (40–32%), as well as thick clay coatings observed in our study indicate a more advanced weathering in the OL3 unit in comparison to OL4, and that means 2nd paleosol is more weathered than the 3rd one).

The multiphase pedogenesis detected in both units, OL3 and OL4, could be linked to the climatic fluctuations within MIS 7 and MIS 9. These stages demonstrate a complex pattern in the  $\delta^{18}O$ -record with warm intervals alternating with cold episodes. Earlier BRONGER et al. (1998) supposed that pedocomplexes PKII and PKIII in loess-paleosol sequences of Tadjikistan reflect climatic fluctuations within MIS 7 and MIS 9, respectively. More detailed correlation of pedocomplexes and marine isotope curve is limited by the lack of a reliable age control.

The OL2 profile, regarded as the Eemian soil (1st inter-

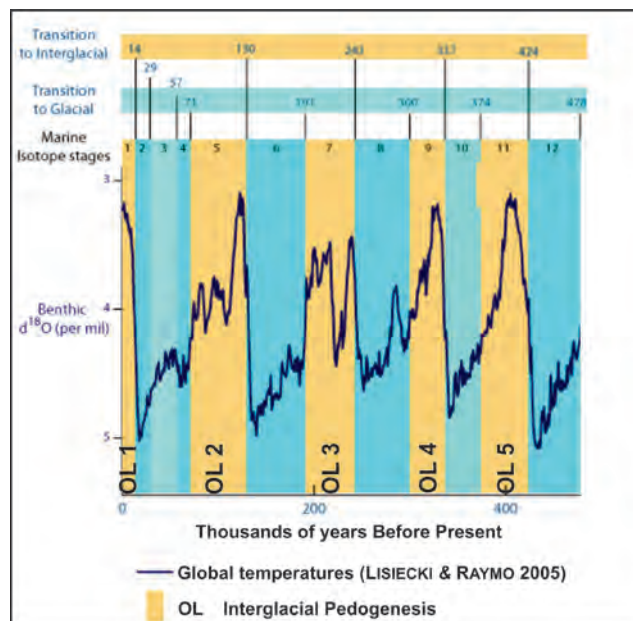


Fig. 5: Correlation of paleosols in Oberlaab with the Marine Isotope Curve.  
Abb. 5: Korrelation von Paläoböden in Oberlaab mit der marinen Isotopenkurve.

glacial paleosol), occupies the next stratigraphic level. Its age has been well established by several instrumental dates: OSL and paleomagnetism in other sections, in particular in the Wels-Aschet sequence (PREUSSER & FIEBIG 2009; SCHOLGER & TERHORST 2011), but in the case of Oberlaab such results are not available. In Wels-Aschet, the Eemian soil is developed on loessic sediments of the Riss glaciation, which is  $142 \pm 18$  ky (MIS 6) according to PREUSSER & FIEBIG (2009). On top of the MIS 5e-Eemian soil the Blake event ( $\sim 117$  ka) is proved by SCHOLGER & TERHORST (2011; 2013, this volume) in Wels-Aschet. The Eemian soil in unit OL2 is correlated to MIS 5e in this study, based on the results of further sequences in Austria. In general, the paleosol displays fewer stagnic properties and less compaction than the older paleosols. Furthermore, its stratigraphic position is situated below the Würmian sediments. From the analytical point of view the interglacial pedogenesis is proved by intensive clay illuviation, coinciding with higher CIA values.

OL1, which correspond to the Holocene soil, is separated from the Eemian paleosol by loess-like deposits characteristic for the Würmian glaciation. There is no evidence for well-developed soils in these deposits, only reworked layers are present.

According to the proposed pedostratigraphy, Figure 5 shows the correlation of the study section with the Marine Isotope Curve (acc. to LISIECKI & RAYMO 2005).

#### 4.2 Pedogenic trends in Oberlaab induced by climate change or/and geomorphic processes

The loess-paleosol sequence in Oberlaab contains several units, which developed different specific properties. Although some of the specific patterns are found in the whole section, their intensity is strongly related to pedogenic and geomorphic processes. All units are characterized as pedo-

complexes, and can be welded, thus difficulties in the recognition of every single soil cycle can emerge.

In the sequence we studied it is clear that the lower units, especially OL4 and OL5, developed under conditions produced by water saturation, which gave rise to redoximorphic processes. The lowest OL5 unit shows the formation of a diagnostic G horizon with a pale reduced soil matrix and relatively few iron segregations. These properties correspond to gleyzation in a permanently reduced soil environment, which lets us suppose a shallow groundwater table. OL4 demonstrates patchy Bg horizons, Fe-Mn concretions and hypocoatings with bleached groundmasses. In fact, the highest concentrations of ferruginous pedofeatures as well as bleached zones are found in OL4 (Figure 3). These characteristics correspond to stagnic properties related to temporary saturation with surface water. Very limited development of clay illuviation agrees with the hypothesis of pedogenesis in a poorly drained soil environment.

The stagnic and gleyic features become less frequent in the upper paleosols. Here, clay illuviation is dominant, with thick and dark clay coatings. From micromorphological results the Eemian (OL2) and Holocene soils have the highest percentages of illuvial clay (2.1 to 4%). On the other hand, coatings in OL3, OL4, and partly in OL2 (for details see SEDOV et al. 2013, this volume) are deformed and displaced, thus the material has been also affected by gleyzation and cryogenesis. In fact, only in the upper part of the modern soil clay coatings are pure with a yellow color. Its inferior part (G horizon) contains the highest amount of clay coatings, which are “dirty”, laminated or having reddish colors, with pigmentations. This horizon has also a low magnetic susceptibility value and considerably lower weathering degree. TERHORST (2007) suggests it corresponds to a previous phase of soil formation that probably occurred during MIS2 to 3.

In summary, the main trend of change of pedogenic processes in the Oberlaab sequence is the following: gleyzation at the base (OL5-OL4), stagnic processes in the central part (OL4-OL3) and clay illuviation in the upper units (OL2-OL1).

Which soil forming factors control these pedogenic trends? It seems that climate is only one factor due to the fact that all units are formed under humid climates evidenced by the formation of stagnic and gleyic features, clay neoformation and illuviation, and silt and/or iron illuviation. Differences between the pedocomplexes are well expressed in the intensity of the involved processes. Additionally, changes in temperature may be somewhat responsible. Lower units could reflect the influence of cooler environments, while the upper ones are affected by warmer climates.

The geomorphic position of the studied paleosols also evidently affected pedogenesis. The lowermost paleosols are situated at a lower level in the geoform, and were more affected by waterlogged conditions (high groundwater table or flooding). This is evident in OL5, where fluvio-glacial processes formed a gravelly alluvial deposit with a high content of Mn concretions.

The upper paleosols are located in better drained positions away from the influence of groundwater and inundations. This can be explained by the aggradation of the terrace and by lower levels of the younger terraces. In particular, the Eemian soil shows a well-developed formation stage charac-

terized by a high weathering status. The well-drained geomorphological position favors clay illuviation.

Another important process observed in the lower paleosols is related to deformation of pedofeatures, which can be caused by bioturbation, as well as by cryogenesis and gelifluction. Orbiculate fabrics, silt concentrations, and platy structures are related to such kind of processes. According to our observations these features are more frequent in OL5 and OL4 (Figure 3) due to a higher intensity of glacial periods. However, lower sedimentation and/or more intensive erosion processes cannot be neglected. According to LISIECKI & RAYMO (2005) during MIS 12 and 10 severe glacial phases occurred, after which OL5 and OL4 are formed (Figure 5). During MIS 8 the glacial phase is much weaker, thus characteristics found in OL3 are clearly less affected by cryogenesis.

## 5 Conclusion

The Oberlaab sequence on top of a Mindel terrace (Younger Deckenschotter) is constituted by four interglacial paleosols, which developed most probably during the Marine Isotope Stages MIS 11, MIS 9, MIS 7, and MIS 5, respectively. Similar to other interglacial paleosols of the same age in Upper Austria, the paleosols are formed as pedocomplexes in Oberlaab. Studied properties reveal the dominance of humid conditions in the whole section, but with differences in the intensity of pedogenic processes involved in the formation of each pedostratigraphic level. We assume that the oldest paleosol OL5 can be correlated to the 4th interglacial paleosols found in Neuhofen, Wels-Aschet, and in earlier studied profiles in Oberlaab. We correlate this soil to MIS 11. The pedocomplex is affected by strong gleyzation. OL4, which is the 3<sup>rd</sup> interglacial paleosol, is characterized by the signs of strong reductomorphic features, partly deformed and with orbiculate fabrics, which are associated with later cryogenesis, probably during MIS 8. OL3 also has properties related to stagnic processes, but clay illuviation and a higher degree of weathering are evidence of its formation under warmer conditions during MIS 7. The Eemian soil (OL2) is the best developed and reflects warm interglacial conditions.

## Acknowledgments

We thank to the financial support of the project “Polygenetic models for the Pleistocene paleosols: new approach to decoding the paleosol-sedimentary records” (International Council Science Union). We also acknowledge support from Conacyt-DLR as well as CONACYT grant for “Estancias Posdoctorales al Extranjero” to H. Cabadas. Many thanks to Lance Wallace for correcting the manuscript, and to Eligio Jiménez and Jaime Díaz for thin section preparation and the grain size separation, as well as Jorge Rivas for magnetic measurements. Rufino Lozano contributed with the X-Ray fluorescence analyses.

## References

- BETTIS, E.A. III, MUHS, D.R., ROBERTS, H.M. & WINTLE, A.G. (2003): Last glacial loess in the conterminous U.S.A. – *Quaternary Science Reviews*, 22: 1907–1946.



- BRONGER, A., WINTER, R. & HEINKELE, T. (1998): Pleistocene climatic history of East and Central Asia based on paleopedological indicators of loess-paleosol sequences. – *Catena*, 34: 1–17.
- BUGGLE, B., GLASER, B., HAMBACH, U., GERASIMENKO, N. & MARKOVIC, S. (2011): An evaluation of geochemical weathering indices in loess-paleosol studies. – *Quaternary International*, 240: 12–21.
- BULLOCK, P., FEDOROFF, N., JONGERIUS, A., STOOBS, G., TURSINA, T. & BABEL, U. (1985): Handbook for soil thin section description. – 152 p.; Wolverhampton, U.K. (Waine Research Publications).
- CASTRO, D.A. (1989): Petrografía básica: Texturas, clasificación y nomenclatura de rocas. – 143 p.; Madrid (Paraninfo).
- DEARING, J.A. (1994): Environmental Magnetic Susceptibility: Using the Bartington MS2 System. – 111 p. (Chi Publishing) Lincoln, United Kingdom.
- DEARING, J.A., BIRD, P.M., DANN, R.J.L. & BENJAMIN, S.F. (1997): Secondary ferrimagnetic minerals in Welsh soils: a comparison of mineral magnetic detection methods and implications for mineral formation. – *Geophysical Journal International*, 130: 727–736.
- FENG, Z.D., TANG, L.Y., MA, Y.Z., ZHAI, Z.X., WU, H.N., LI, F., ZOU, S.B., YANG, Q.L., WANG, W.G., DERBYSHIRE, E. & LIU, K.B. (2007): Vegetation variations and associated environmental changes during marine isotope stage 3 in the western part of the Chinese Loess Plateau. – *Palaeogeography, Palaeoclimatology, Palaeoecology*, 246: 278–291.
- FINK, J. (1976): Exkursion durch den österreichischen Teil des nördlichen Alpenvorlandes und den Donaauraum zwischen Krems und der Wiener Pforte. – Mitteilungen der Kommission für Quartärforschung der Österreichischen Akademie der Wissenschaften 1: 113 pp.
- HAESAERTS, P., DAMBLON, F., BACHNER, M. & TRNKA, G. (1996): Revised stratigraphy and chronology of the Willendorf II sequence, Lower Austria. – *Archaeologia Austriaca*, 80: 25–42.
- IUSS WORKING GROUP WRB (2007): World Reference Base for Soil Resources 2006, first update 2007. World Soil Resources Reports No.103. FAO Rome.
- KOHL, H. (1976): Lehmgrube der Ziegelei Würzburger in Aschet bei Wels. – Mitteilungen der Kommission für Quartärforschung der Österreichischen Akademie der Wissenschaften, 1: 37–41.
- Kukla, G.J. (1978): The classical European glacial stages: correlation with deep-sea sediments. – *Transactions of the Nebraska Academy of Science*, 6: 57–93.
- LIU, T. (1985): Loess in China (2nd ed.). – 224 pp.; Beijing (China Ocean Press) and Berlin, (Springer-Verlag).
- LIU, T.S., GUO, Z.T., LIU, J.Q., HAN, J.M., DING, Z.L., GU, Z.Y. & WU, N.Q. (1995): Variations of eastern Asian monsoon over the last 140,000 years. – *Bulletin de la Société Géologique de France*, 166: 221–229.
- LISIECKI, L.E. & RAYMO, M.E. (2005): A Pliocene-Pleistocene stack of 57 globally distributed benthic  $\delta^{18}O$  records. – *Palaeoceanography*, 20: 1–17.
- MUHS, D.R., & BETTIS, E.A. III. (2000): Geochemical variations in Peoria Loess of western Iowa indicate paleowinds of midcontinental North America during last glaciations. – *Quaternary Research*, 53: 49–61.
- MUHS, D.R. & ZÁRATE, M. (2001): Eolian records of the Americas and their paleoclimatic significance. – In: MARKGRAF, V. (ed.): *Interhemispheric Climate Linkages*. pp. 183–216; San Diego (Academic Press).
- MUHS, D.R. & BETTIS, E.A. III (2003): Quaternary loess-paleosol sequences as examples of climate-driven sedimentary extremes. – In: CHAN, M.A. & ARCHER, A.E. (eds.): *Extreme depositional environments: Mega end members in geologic time*. Geological Society of America Special Paper, 370: 53–74.
- NESBITT, H.W. & YOUNG, G.M. (1982): Early Proterozoic climates and plate motions inferred from major element chemistry of lutites. – *Nature*, 299: 715–717.
- NEUGEBAUER-MARESCH, C. (1996): Zur Stratigraphie und Datierung der Aurignacienstation am Galgenberg. – In: SVOBODA J. (ed.): *Paleolithic in the Middle Danube Region*. Archeologicky ustav, pp. 67, Brno.
- NIEDERHUBER, M. (1997): Stratizing/Krems-Rehberg. – In: DÖPPES, D. & RABEDER, G. (eds.): *Pliozäne und pleistozäne Faunen Österreichs*. Österreichische Akademie der Wissenschaften, pp. 56–61, Wien.
- ÖSTERREICHISCHE STRATIGRAPHISCHE KOMMISSION (2004): *Stratigraphische Tabelle von Österreich*, Wien.
- QUATTROCCHIO, M.E., BORROMEI, A.M., DESCHAMPS, C.M., GRILL, S.C. & ZAVALA, C.A. (2008): Landscape evolution and climate changes in the Late Pleistocene-Holocene, southern Pampa (Argentina): evidence from palynology, mammals and sedimentology. – *Quaternary International*, 181: 123–138.
- PÉCSI, M. (1990): Loess is not just the accumulation of dust. – *Quaternary International*, 7–8: 1–21.
- PÉCSI, M. & SCHWEITZER, F. (1993): Long-term terrestrial records of the Middle Danubian Basin. – *Quaternary International*, 17: 5–14.
- PENCK, A. & BRÜCKNER, E. (1909): *Die Alpen im Eiszeitalter*, Vol. 1, pp. 393, Tauchnitz, Leipzig.
- PREUSSER, F. & FIEBIG, M. (2009): European Middle Pleistocene loess chronostratigraphy: Some considerations based on evidence from the Wels site, Austria. – *Quaternary International*, 198: 37–45.
- ROZYCKI, S.Z. (1991): *Loess and loess-like deposits*. – 187 p. Warsaw (Osolineum Press, Polish Academy of Sciences).
- SCHOLGER, R. & TERHORST, B. (2011): Paläomagnetische Untersuchungen der pleistozänen Löss-Paläobodensequenz im Profil Wels-Aschet. – *Mitteilungen der Kommission für Quartärforschung der Österreichischen Akademie der Wissenschaften* 19, 47–61.
- SCHOLGER, R. & TERHORST, B. (2013): Magnetic excursions recorded in the Middle to Upper Pleistocene loess/paleosol sequence Wels-Aschet (Austria). – *E & G Quaternary Science Journal*, 62/1: 4–13, DOI 10.3285/eg.62.1.02, this volume.
- SEDOV, S., SYCHEVA, S., TARGULIAN, V., PI, T. & DIAZ, J. (2013): Last Interglacial paleosols with Argic horizons in Upper Austria and Central Russia: pedogenetic and paleoenvironmental inferences from comparison with the Holocene analogues. – *E & G Quaternary Science Journal*, 62/1: 44–58, this volume.
- SUN, X., SONG, C., WANG, F. & SUND, M. (1997): Vegetation history of the Loess Plateau of China during the last 100,000 years based on pollen data. – *Quaternary International*, 37: 25–36.
- TARGULIAN, V.O. & GORYACHKIN, S.V. (2004): Soil memory: types of record, carriers, hierarchy and Diversity. – *Revista Mexicana de Ciencias Geológicas*, 21: 1–8.
- TERHORST, B. (2007): Korrelation von mittelpleistozänen Löss-/Paläobodensequenzen in Oberösterreich mit einer marinen Sauerstoffisotopenkurve. – *Quaternary Science Journal*, 56: 26–39.
- TERHORST, B. (2013): Middle Pleistocene loess/paleosol sequences in Austria. – *E & G Quaternary Science Journal*, 62/1: 4–13, DOI 10.3285/eg.62.1.01, this volume.
- TERHORST, B., OTTNER, F., POETSCH, T., KELLNER, A. & RÄHLE, W. (2003): Pleistozäne Deckschichten auf der Traun-Enns-Platte bei Linz (Oberösterreich). – In: TERHORST, B., *Exkursionsführer zur 22. Tagung des Arbeitskreises Paläoböden in Oberösterreich*. Tübinger Geowissenschaftliche Arbeiten, Reihe D 9: 115–155.
- TERHORST, B., OTTNER, F. & HOLAWA, F. (2011): Pedastratigraphische, sedimentologische, mineralogische und statistische Untersuchungen an den Deckschichten des Profils Wels/Aschet (Oberösterreich). – *Mitteilungen der Kommission für Quartärforschung der Österreichischen Akademie der Wissenschaften*, 19: 13–35.
- TERHORST, B., OTTNER, F. & WRIESSNIG, K. (2012): Weathering intensity and pedostratigraphy of the Middle to Upper Pleistocene loess/paleosol sequence of Wels-Aschet (Upper Austria). – *Quaternary International*, 26: 142–154.
- VAN HUSEN, D. (2000): Geological processes during the Quaternary. – *Mitteilungen der Österreichischen Geologischen Gesellschaft*, 92: 135–156.
- VAN HUSEN, D. & REITNER, J.M. (2011): An outline of the Quaternary stratigraphy of Austria. – *E & G Quaternary Science Journal*, 60, 2–3: 366–387.

# Grain size and mineralogical indicators of weathering in the Oberlaab loess-paleosol sequence, Upper Austria

Franz Ottner, Sergey Sedov, Undrakh-Od Baatar, Karin Wriessnig

**How to cite:** OTTNER, F., SEDOV, S., BAATAR, U., WRIESSNIG, K. (2013): Grain size and mineralogical indicators of weathering in the Oberlaab loess-paleosol sequence, Upper Austria. – E&G Quaternary Science Journal, 62 (1): 34–43. DOI: 10.3285/eg.62.1.04

**Abstract:** Grain size analyses, bulk and clay mineralogical data were used to characterize weathering within the loess-paleosol-sequence of Oberlaab in Upper Austria. Soil horizons can be clearly identified by the calculation of weathering index Kd from granulometric parameters.

The mineralogical composition of the bulk samples shows increasing weathering intensity from the top to the bottom. The weakest weathering stage 1 is not present in Oberlaab, because all samples are free of carbonate minerals. Weathering stage 2 can be found in the upper part of the profile, whereas stage 3 is mainly present in the lowermost horizons. The highest weathering stages 4 and 5 are not present in Oberlaab. The clay mineral distribution in the profile is dominated by the disappearance of primary chlorite in the upper part of the profile and the neoformation of vermiculites from illite by pedogenesis in the lower part.

Two different types of mixed layer minerals were found in the pedocomplexes. An illite/chlorite mixed layer mineral occurs following the disappearance of chlorite and is present in the Eemian luvisol. The second mixed layer mineral consists of illite/vermiculite and is present in the whole profile.

The weathering stages obtained from the clay mineral composition are slightly lower than that of bulk mineralogy, but reach as well stage 3 in the lower part of the profile.

## Korngrößen und mineralogische Verwitterungsintensitäten in der Löss-Paläoboden-Sequenz von Oberlaab, Oberösterreich

**Kurzfassung:** Untersuchungen des Gesamt- und Tonmineralbestandes sowie der Korngröße wurden zur Charakterisierung der Verwitterungsstadien in einer Löss-Paläoboden-Sequenz in Oberlaab (Oberösterreich) verwendet. Durch den aus der Korngrößenzusammensetzung berechneten Verwitterungsindex Kd können Bodenhorizonte eindeutig identifiziert werden.

Der Gesamtmineralbestand zeigt, dass die Verwitterungsintensität mit der Tiefe zunimmt. Das schwächste Verwitterungsstadium tritt in Oberlaab nicht auf, da alle Proben karbonatfrei sind. Verwitterungsstadium 2 kommt in den oberen Bodenhorizonten vor und ist durch das Fehlen von primärem Chlorit in der Tonfraktion gekennzeichnet. Die untersten Horizonte entsprechen mit der Neubildung von Vermikuliten aus Illit Verwitterungsstadium 3. Die intensivsten Verwitterungsstadien 4 und 5 treten in diesem Profil nicht auf.

In den Pedokomplexen wurden zwei verschiedene Mixed-layer-Mineralen gefunden. Ein Illit-Chlorit-Mixed layer kommt in der Parabraunerde des Eem-Interglazials vor, ein Illit-Vermikulit-Mixed layer ist im gesamten Profil nachweisbar.

Die aus der Zusammensetzung der Tonfraktion ermittelten Verwitterungsstadien sind etwas niedriger als die aus dem Gesamtmineralbestand, erreichen aber im untersten Teil des Profils ebenfalls Stufe 3.

**Key words:** *Paleosols, clay minerals, vermiculite, secondary chlorite, weathering index Kd*

**Addresses of authors:** Franz Ottner, Undrakh-Od Baatar, Karin Wriessnig, Institute of Applied Geology, Department of Civil Engineering and Natural Hazards, University of Natural Resources and Life Sciences Vienna, Peter Jordan Strasse 70, 1190 Wien, Austria; Sergey Sedov, Instituto de Geología, Universidad nacional Autónoma de México (UNAM), Ciudad Universitaria, Del. Coyoacán, C.P. 04510, DF Mexico.

## 1 Introduction

The weathering status of Pleistocene loessic paleosols provides an important proxy for interglacial paleoenvironments as the processes of primary mineral breakdown and neoformation of secondary components are strongly dependent upon the bioclimatic conditions of pedogenesis, (TERHORST, 2013, this volume). Geochemical indicators (various coefficients based on ratios of different major and trace element concentrations) are widely used to evaluate weathering (BUGGLE et al., 2011). For the Oberlaab sequence this

approach was applied by SOLLEIRO-REBOLLEDO et al. (2013, this volume). Paleomagnetic stratigraphy of the Middle to Upper Pleistocene loess/paleosol sequence of Wels-Aschet is presented by SCHOLGER & TERHORST (2013, this volume). A detailed overview, as geographical position and geology of Oberlaab as well as the detailed profile description can be found in TERHORST (2013, this volume).

An important additional set of weathering indicators is related to the grain size distribution and mineralogical composition of total soil samples and clay fraction. The products of pedogenic silicate alteration are concentrated mostly in

the fine material. This justifies to use the ratios of different size fractions as an estimate of this process. PÉCSI & RICHTER (1996) proposed the weathering index Kd as an integral measure of weathering intensity in paleosols and pedocomplexes. Additional information can be obtained from the proportion of the clay fraction and specifically of the fine clay fraction. The latter consists mostly of products of more advanced transformation and synthesis of secondary minerals, whereas coarse clay is produced mostly from physical breakdown accompanied by moderate chemical transformation (CHAMLEY, 1989).

The mineralogical composition of total soil samples (although only semi-quantitative) provides hints to estimate the weathering status, through the relative abundance of weatherable components (e.g. chlorite, amphiboles, etc.) and stable minerals (especially quartz). Clay mineral assemblages are sensitive indicators of paleopedogenesis and paleoenvironments. The formation of different clay minerals in modern soils is highly dependent upon the soil processes and regimes, which in turn are controlled by climatic conditions (DIXON & WEED, 1989). Clay mineral studies in loess-paleosol sequences thus provide important proxies for the Pleistocene climatic history (BRONGER & HEINKELE, 1990; BRONGER et al., 1998).

The aim of this study is to estimate the weathering status of the Pleistocene paleosols in the Oberlaab loess profile using grain size, bulk mineralogy and clay mineral assemblages. We further compare these data with other proxies available for this profile to incorporate them into the integral paleoecological interpretation.

## 2 Methodology

### 2.1 Grain size distribution

The grain size distribution was determined by combination of wet sieving of the fraction >20 µm and automatic sedimentation analysis with a Micromeritics SEDIGRAPH III 5120.

50 g of the dried sample were treated with 200 ml 10% H<sub>2</sub>O<sub>2</sub>. The purpose was the oxidation of organic components and a proper dispersion of the sample. After approximately 24 hours reaction time the unused H<sub>2</sub>O<sub>2</sub> was removed by heating. After ultrasonic treatment the sample was sieved with a set of 2 mm, 630 µm, 200 µm, 63 µm and 20 µm sieves. The coarse fractions were dried at 105°C and stated in mass percent. The <20 µm portion was treated with 0.05% sodium polyphosphate and analyzed in the sedigraph by X-rays, according to Stoke's Law. From the cumulative curve of the sedigraph and the sieving data the grain size distribution of the entire sample was calculated.

A general overview of the grain size distribution in Oberlaab is presented by SOLLEIRO-REBOLLEDO et al. (2013). In this paper we present mostly the data relevant for the evaluation of the soil weathering index Kd. Silt (2–63 µm) including coarse silt (20–63µm) and clay (<2 µm) including fine clay (<0.2 µm) fractions are evaluated.

### 2.3 Total mineral analysis

The dried samples, ground in a rock mill to analytical size, were prepared according to the backloading method and X-rayed with a Panalytical XPert Pro MPD diffractometer with

an automatic divergence slit, Cu LFF tube, 45 kV, 40 mA, and an X'Celerator detector. The samples were measured from 2° to 70° 2Θ. The X-ray diffraction patterns served as the basis for calculating the qualitative mineral content.

### 2.4 Clay mineral analysis

The samples were dispersed with 10% hydrogen peroxide. After the reaction had subsided and the extra H<sub>2</sub>O<sub>2</sub> was removed, they were exposed to ultrasonic sounding for 15 minutes. The <63 µm fraction was obtained by wet sieving, and out of this the 2 µm fraction by centrifugation.

The next step was cation exchange. 40 ml of the clay suspension were each mixed with 10 ml 4 N KCl solution and 4 N MgCl<sub>2</sub> solution, respectively, and shaken for 12 hours. The texture specimens were placed on ceramic platelets, onto which the clay suspension was sucked via low pressure.

After treatment with ethylene glycol, DMSO (dimethyl sulfoxide) and heating 2 hours at 550 °C the samples were measured in the diffractometer and evaluated according to the same principle as the total mineral analysis. In general, the identification of the minerals and clay minerals was carried out according to BRINDLEY & BROWN (1980) and MOORE & REYNOLDS (1997).

### 2.5 Weathering intensity

In the context of this study, the data collected from the total as well as the clay mineral analysis serve as a basis for estimation of the weathering intensity of the individual horizons. It is assumed that the most sensitive minerals, such as carbonates and chlorite, will be dissolved or replaced first, and, along with increasing weathering, the more stable minerals, such as mica and feldspars.

This method was used for the first time in the loess paleosol profile Wels-Aschet (TERHORST et al., 2012) and slightly modified for the Oberlaab profile (Tables 1 and 2).

Based on the clay mineral analysis, a classification of the weathering intensity was carried out with the presence of primary chlorite on the one hand, and vermiculite varieties on the other hand TERHORST et al. (2012).

## 3 Results and discussion

### 3.1 Grain size analyses of silt and clay

The variation in clay content (<2 µm) is relatively high. The lowest clay content was found in a loess sample of OL4 with 22.7 mass%, the highest amount of clay was found in clay cutans from the same OL4 profile and is 64.3 mass% (Table 3). Apart from the clay cutans the highest clay contents occur in the Middle Pleistocene paleosols of profile OL5 (Table 3 and Fig. 1).


The Eemian interglacial Luvisol (OL2) in 120–140 cm has a very high clay content of 51.3 mass%, and especially in the deepest part of the profile the clay content is high.

The paleosols of the OL4 profile section are characterized by slightly lower clay contents; only in one sample more than 40 mass% of the clay fraction were detected. The more recent loess samples of the upper profile sections (OL1) have a clay content of less than 30 mass%.




Tab. 1: Weathering intensity according to bulk mineralogy after TERHORST et al. (2012).

Tab. 1: Verwitterungsintensität auf der Basis der mineralogischen Ergebnisse nach TERHORST et al. (2012).

Degree of weathering		Index minerals
Stage 1		Carbonate minerals present
Stage 2		Carbonates weathered, chlorites traceable
Stage 3		Micas present, chlorite absent
Stage 4		Micas absent [weathered]
Stage 5		Micas and feldspars absent [weathered]

Tab. 2: Weathering intensity according to the clay mineralogy, after TERHORST et al. (2012), slightly modified.

Tab. 2: Verwitterungsintensität auf der Basis der tonmineralogischen Ergebnisse nach TERHORST et al. (2012), leicht verändert.

Degree of weathering		Index Minerals
Stage 1		Primary chlorite present
Stage 2		Primary chlorite absent, illite or vermiculite 14Å dominant
Stage 3		Vermiculite 18 Å dominant, smectite from lessivation dominant
Stage 4		Vermiculite 18Å dominant, vermiculite 14 Å completely transformed
Stage 5		Illite totally weathered

The fine clay content (< 0.2 µm) varies much more than the total clay. The clay cutans from the OL4 profile section contain 54.6 mass% fine clay, the Eemian paleosol from 120–140 cm (OL2) 31.7 mass%. In the younger loess samples the value for the fine clay is below 10 mass%, the lowest value of 3.7 mass% was found in a loess sample of OL3 (Table 3 and Fig. 2).

As expected, the silt fraction is predominant in most samples and reaches values up to 74.0 mass% (OL4). By contrast, contents of the silt fraction in the paleosols are significantly lower. In the basal parts of the sequence (OL5), the silt fraction diminishes far below 50 mass%. The lowest silt value (33.6 mass%) can be found in the clay cutans of profile section OL4.

The decrease of the silt fraction within the paleosol horizons is significant. This trend is particularly obvious in the Eemian interglacial paleosol (OL2), in which the silt fraction is only 45.6 mass% (Table 3).

Generally speaking, the silt content is higher in the upper part of the profile and lower in the deeper parts because of the known clay enrichment during pedogenesis (Table 3).

### 3.2 Kd-values and weathering intensity

The grain size distribution can be used as an indicator for the degree of weathering. Clay illuviation in Bt horizons causes an enhancement of the fine fraction at the expense of the coarse fraction. The individual soil horizons can be recognized either by the increased values of the clay and fine clay fraction respectively (Figs.1 and 2), or by significantly lower values of the silt and coarse silt fraction.

According to PÉCSI & RICHTER (1996), the weathering index Kd allows to measure the weathering intensity of pale-

osols and pedocomplexes. It is calculated by dividing of the coarse and middle silt content by the fine silt and total clay content. In general, the lower the Kd-value is, the more weathered is the soil horizon (Fig. 3). The lowest Kd-value (0.32), and thus by far the highest degree of weathering, is obtained in the paleosols of profile OL5 and in the clay cutans.

In the Eemian paleosol (OL2) the Kd-value of 0.55 shows that the weathering process – caused by an intensive pedogenesis – is remarkable in this part of the profile as well.

Figure 3 shows clearly the less weathered upper part, a mixed part in the middle and the highly altered deepest part of the OL5 profile section.

Summarizing, paleosols are indicated by the lowest Kd-values in the studied profile. The enrichment of clay at the expense of the coarse grain fraction can be observed in many samples with low Kd-values.

### 3.3 Mineralogical results

#### 3.3.1 Bulk mineral analysis

All examined samples are free of carbonate (Table 4). Neither the uppermost more recent loess samples nor the samples from the Mindel terrace contain any calcite or dolomite.

Chlorite occurs in higher amounts only in section OL1 and partly in OL2. In OL3 hardly any chlorite is detectable, but traces were present in OL4. In OL5 due to strong weathering processes no chlorite was found (Table 4).

Hornblende - also a mineral relatively sensitive to weathering - could be detected in traces in the profile sections OL1 and OL2, but not in the Eemian paleosol. In older horizons hornblende is not present because of strong weathering (Table 4).

Generally, quartz occurs as a main component throughout the profile in uniform distribution and without recogniz-

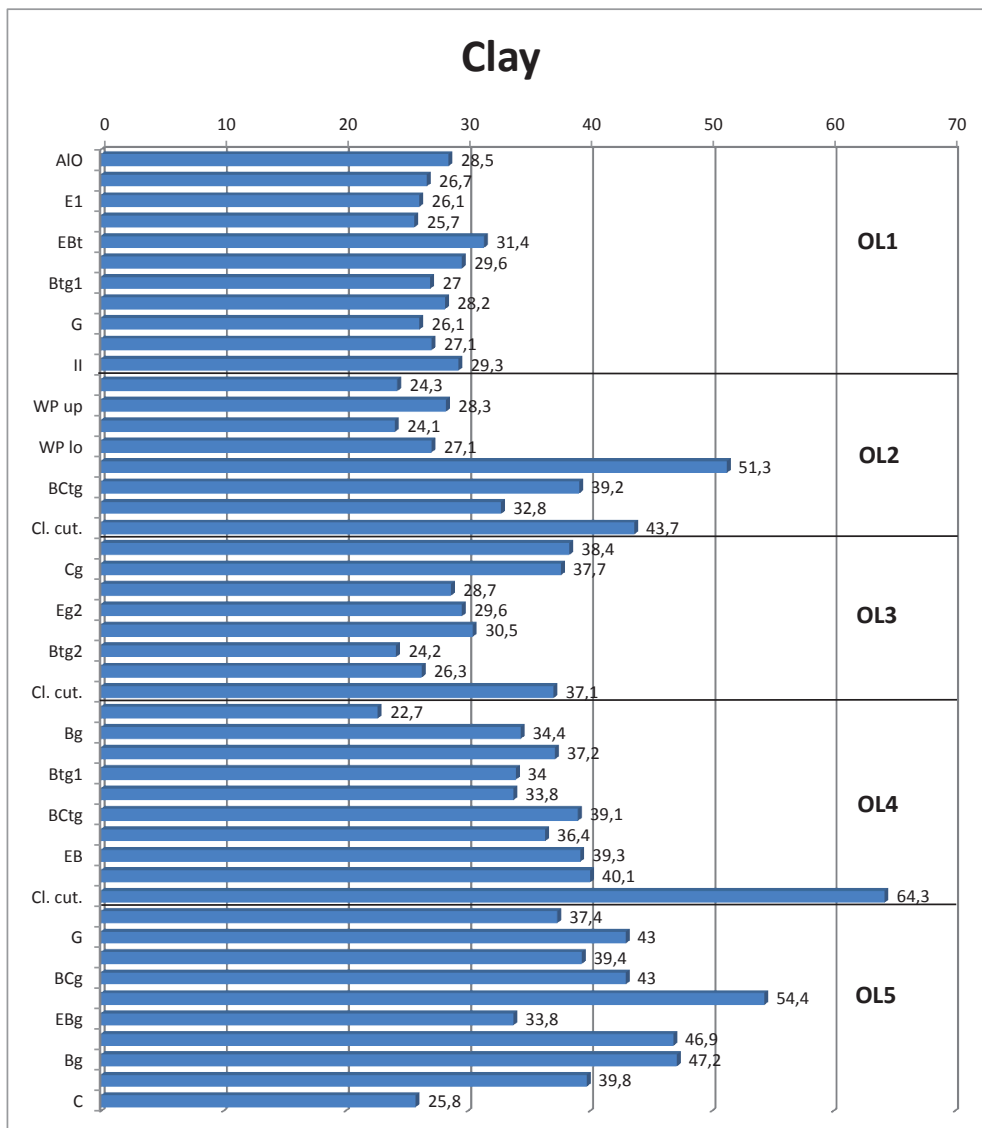


Fig. 1: Total clay content in mass% in the profile Oberlaab, WP = pedosediments.

Abb. 1: Gesamt-Tongehalt im Profil Oberlaab in Masse%, WP = Bodensedimente.

able trends. Plagioclase is detectable throughout the profile. Potassium feldspar occurs in traces only. In Table 4 the values for both types of feldspars are combined in the column “feldspars”.

The distribution of mica is also more or less homogeneous, except for clay cutans, where the amount is higher and in some samples of profile section OL5 it was found only in traces. Layer silicates, which represent the sum of all clay minerals and mica are present in all samples, whereby the highest content can be found in the Bt horizon of the Eemian interglacial paleosol (OL2). The peaks of about 14 Å originate from the clay minerals smectite and vermiculite, which will be discussed in detail in the following chapter.

The total mineral content can be used to estimate the weathering intensity of the individual horizons as based on the presence or absence of indicator minerals (cf. Tab. 1 and 2). Weathering stage 1 represents the horizons with the lowest weathering intensity. In this stage the horizons still contain carbonate minerals. In Oberlaab this stage is not present, as all samples are free of carbonate.

Most horizons can be ascribed to weathering stage 2. These horizons are characterized by the presence of chlorite with a simultaneous absence of carbonate. All samples from profile section OL1 and OL2, and few samples of section OL3

and OL4 belong to this weathering stage. Only section OL5 is totally free of chlorite.

Weathering stage 3, in which primary chlorite is absent but mica is still present, comprises the samples from OL 5 and some horizons from OL3 and 4.

The highest weathering stages 4 and 5, which are characterized by the absence of mica and feldspars and by the occurrence of high amounts of layer silicates, are not developed in the Oberlaab profile.

In all horizons, the iron hydroxide goethite could be found in varying amounts.

### 3.3.2 Clay mineral analysis

Clay minerals of the profile show strong dynamics in terms of rearrangement, particularly triggered by vermiculite.

Classical vermiculite, which expands only to 14 Å, is present in the lower part of the profile in small amounts with only few exceptions (Table 5). It occurs mainly in the moderately to stronger weathered horizons. The younger profile sections are almost free of vermiculite 14 Å.

Advanced weathering leads to the formation of the more strongly expanding vermiculite variety (vermiculite 18 Å). This mineral is present in intensely weathered horizons, in ad-

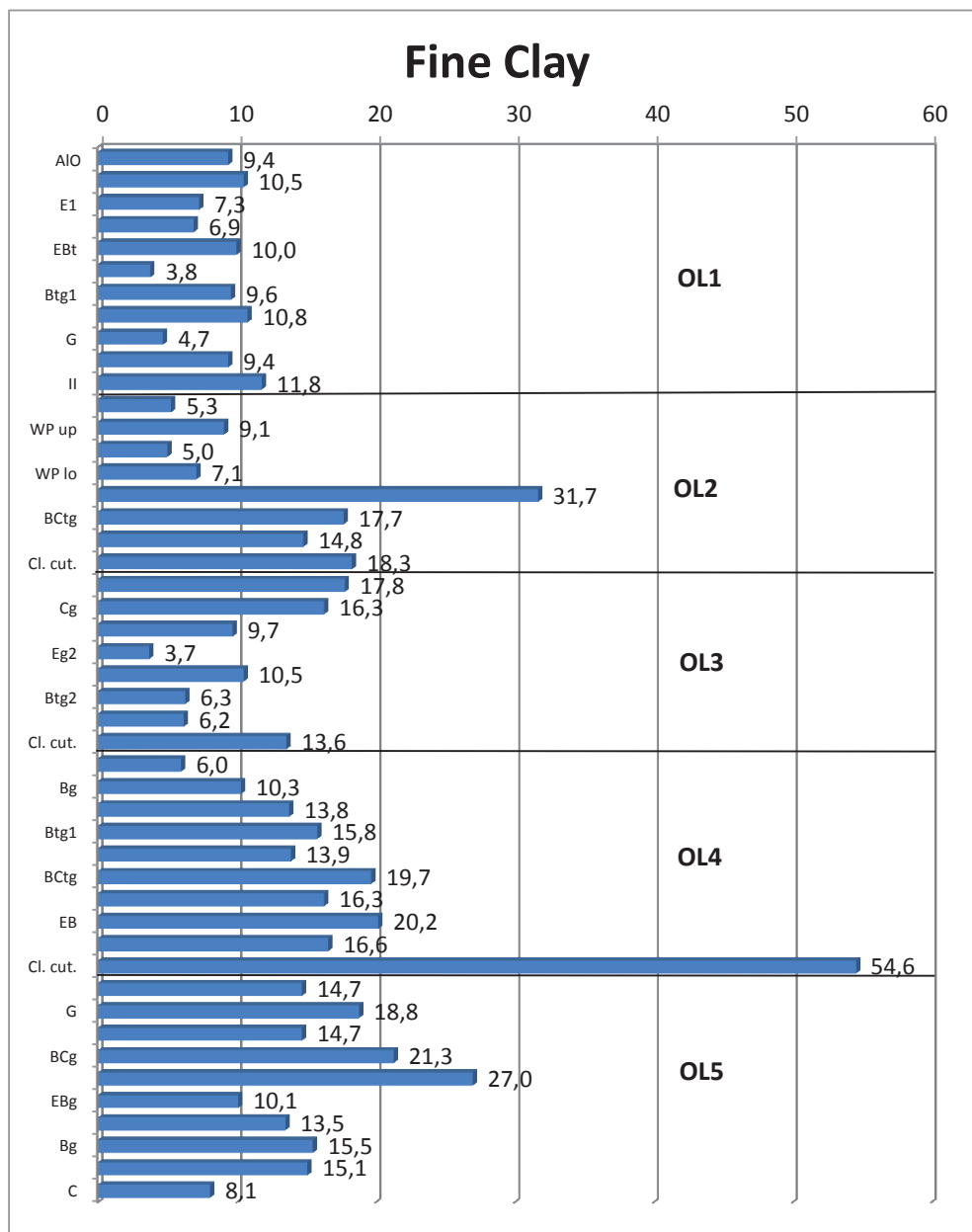


Fig. 2: Fine clay content in mass% in the profile Oberlaab, WP = pedosediments.

Abb. 2: Feintongehalt im Profil Oberlaab in Masse%, WP = Bodensedimente.

dition to vermiculite 14 Å. In the case of increasing weathering intensity it replaces vermiculite 14 Å completely. In the studied profile it is most frequently present in the older profile sections OL4 and OL5. Smaller amounts are also present in the rest of the profile but without regular distribution or trends.

In all horizons, smectite can also be found in relatively small amounts, in some parts also as a main component of the clay fraction. It is detectable both in soil horizons and in loess sediments. Its occurrence in less weathered loess layers gives reason to believe that smectite was not newly formed within the profile, but rather originates from previously weathered source material. In contrast, the occurrence of the highest amounts of smectite in the Eemian paleosol may originate in neof ormation of smectite in those horizons or is caused by lessivation.

The amount of illite, the source material for more weathered clay minerals, does not vary much in the profile, only small amounts are detectable.

Kaolinite can be found in all horizons in small amounts and does not show any recognizable trends. Kaolinite occurs

in the well crystallized form expandable with DMSO and in a poorly crystallized form (fire clay).

Primary chlorite occurs occasionally and in small amounts. It is clearly detectable only within the young loess sediments (OL1), while it is absent in all older horizons.

Secondary chlorite, which is found occasionally in paleosols, is not clearly detectable in the Oberlaab profile.

Most horizons contain two distinguishable mixed layer minerals, which consist of the components illite, chlorite or vermiculite, respectively. The chlorite containing mixed layer mineral occurs mostly in horizons of OL1 following the disappearance of chlorite. It is also present in OL2 and disappears almost completely in the lower horizons. In the clay fractions of all other horizons an additional variety of mixed layer minerals can be found, which is composed of vermiculite and most likely illite (Table 5).

The results from the clay mineral analyses were also classified according to their weathering intensity. This was mainly based on the presence of the vermiculite varieties (Tables 2 and 5).



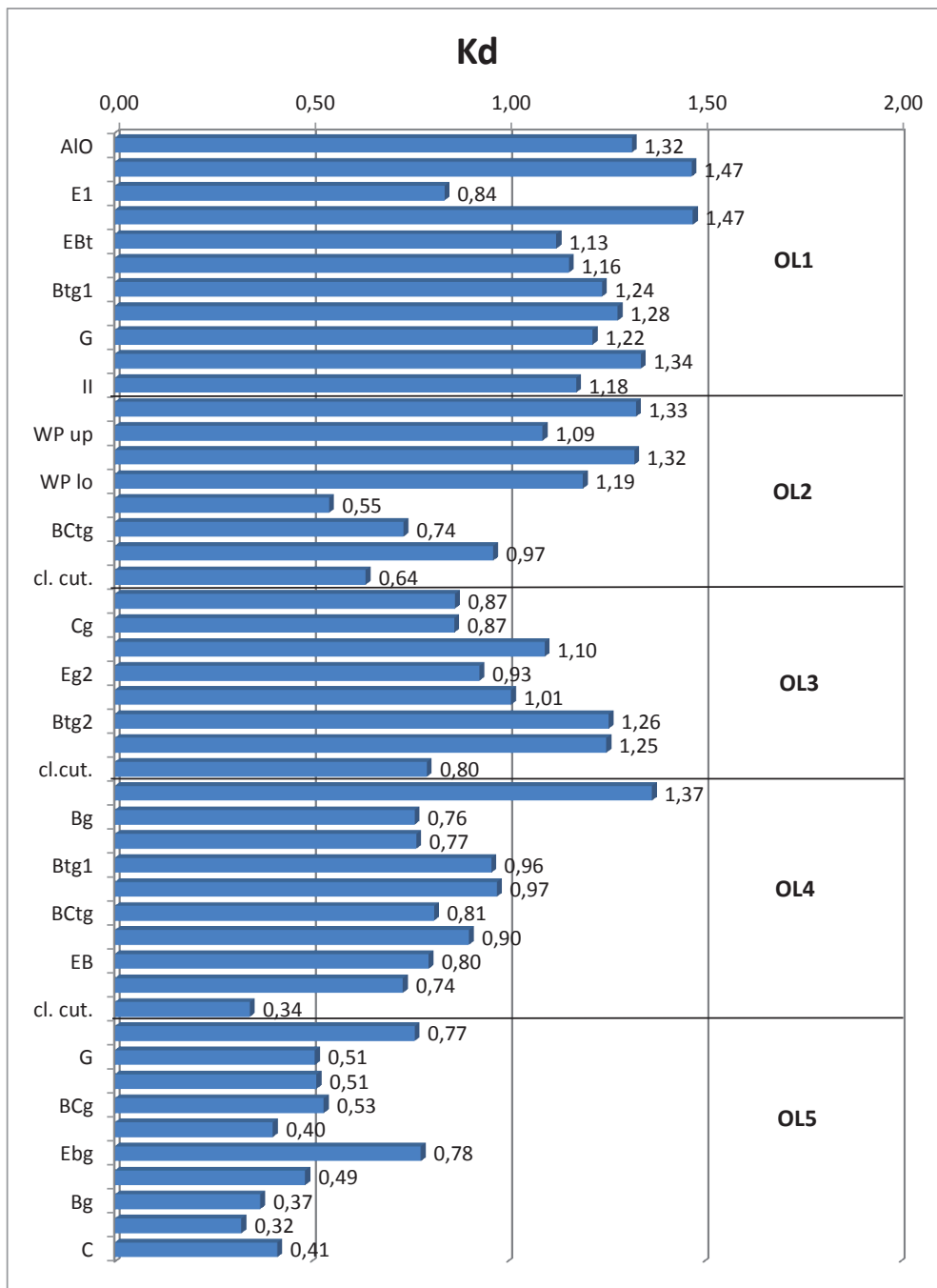


Fig. 3: Distribution of weathering index Kd in the profile Oberlaab, WP = pedosediments.  
 Abb. 3: Verteilung des Verwitterungsindex Kd im Profil Oberlaab, WP = Bodensedimente.

The weakest weathering stage 1, which is characterized by the presence of primary chlorite, only occurs in the uppermost horizons of OL1. Below that, all horizons are at least at weathering stage 2, where by definition illite or vermiculite 14 Å are the dominant clay minerals.

Most horizons below OL2 contain higher amounts of vermiculite 18 Å, which means they already belong to weathering stage 3. By means of lessivation processes, clay cutans were transported into the larger pores and fissures of the underlying loess loams. This is also reflected by the occurrence of weathering stage 3.

Weathering stage 4 is only developed in the upper part of the Middle Pleistocene paleosol OL5.

#### 4 Discussion

The results show that the paleosol units of Oberlaab are de-

veloped as pedocomplexes. The basal parts of the sequence show the highest weathering degree, although the intensity of weathering never reached the highest stages as presented for the nearby loess/paleosol sequence in Wels-Aschet (TERHORST et al., 2012).

Grain size and mineralogical indicators of weathering provide quite similar estimates of the weathering status for the different pedocomplexes of Oberlaab. All these indicators point to the lower weathering grade of the recent Luvisol as compared to all Pleistocene paleosols. The Holocene soil has a lower content of total and fine clay, a higher Kd index, and at the same time demonstrates a lower mineralogical and clay mineralogical weathering stage. The presented results show that the Kd index proposed by PÉCSI & RICHTER (1996), fits quite well to the mineralogical weathering stages used in this paper. It is remarkable that among Pleistocene paleosols the most weathered according to grain size characteristics

Tab. 3: Distribution of silt and clay fractions in the Oberlaab loess-paleosol sequence; mass%, WP = pedosediments.

Tab. 3: Verteilung der Schluff und Tonfraktionen in der Löss-Paläoboden-Sequenz Oberlaab, Masse%, WP = Bodensedimente.

IAG Lab. Nr	Horizon	Position	Silt	Clay	Fine clay
Profile OL1 Holocene Luvisol					
12401	AfD	0-5 cm	67.1	28.5	9.4
12402	EAh	5-15 cm	68.9	26.7	10.5
11212	E1	15-30 cm	71.7	26.1	7.3
11213	E2	30-40 cm	72.2	25.7	6.9
11214	EBt	45-65 cm	66.2	31.4	10.0
11215	EBtg	75-95 cm	67.7	29.6	3.8
11216	Btg1	100-120 cm	70.4	27.0	9.6
11217	Btg2	140-150 cm	69.2	28.2	10.8
11218	G	150-160 cm	70.8	26.1	4.7
11219	I	150-165 cm	70.7	27.1	9.4
11220	II	170-190 cm	61.5	29.3	11.8
Profile OL2 Eemian Luvisol					
11221	WP upper	0-20 cm	71.6	24.3	5.3
11222	WP upper	20-40 cm	68.1	28.3	9.1
11223	WP lower	40-50 cm	72.0	24.1	5.0
11224	WP lower	70-90	66.3	27.1	7.1
11225	Btg2	120-140 cm	45.6	51.3	31.7
11226/27	BCtg	160-180 cm	58.3	39.2	17.7
11228	BCtg	180-190 cm	64.1	32.8	14.8
11229	clay cutans		53.0	43.7	18.3
Profile OL3 Middle Pleistocene Paleosol					
11230	BCtg	5-20 cm	57.9	38.4	17.8
11233	Cg	25-40 cm	58.4	37.7	16.3
11234	Eg1	40-50 cm	64.0	28.7	9.7
11235	Eg2	70-90 cm	66.7	29.6	3.7
11236	Btg1	120-140 cm	66.0	30.5	10.5
11231	Btg2	180-190 cm	70.1	24.2	6.3
11232	BCg	210-220 cm	70.5	26.3	6.2
11238	clay cutans		60.7	37.1	13.6
Profile OL4 Middle Pleistocene Paleosol					
11432	BCg	10-30 cm	74.0	22.7	6.0
11433	Bg	60-70	62.6	34.4	10.3
11434	Bg	85-100 cm	60.6	37.2	13.8
11435	Btg1	120-140 cm	63.6	34.0	15.8
11436	Btg2	140-150 cm	63.9	33.8	13.6
11437	BCtg	180-200 cm	58.7	39.1	19.7
11438	BCtg	230-240 cm	61.2	36.4	16.3
11439	EB	270-280 cm	55.1	39.3	20.2
11440	G	290-300 cm	55.8	40.1	16.6
11441	clay cutans		33.6	64.3	54.6
Profile OL5 Middle Pleistocene Paleosol					
11442	BG	0-50	51.1	37.4	14.7
11443	G	50-90 cm	46.1	43.0	18.8
11444	Bg	90-170 cm	43.0	39.4	14.7
11445	BCg	170-215 cm	45.7	43.0	21.3
11446	Ah	215-230 cm	38.8	54.4	27.0
11447	EBg	230-250 cm	59.0	33.8	10.1
11448	Bg	250-260 cm	48.1	46.9	13.5
11449	Bg	265-290 cm	41.9	47.2	15.5
11450	Cg	290-310 cm	34.6	39.8	15.1
11451	C	310+	30.9	25.8	8.1

Tab. 4: Mineral composition of the bulk minerals in the Oberlaab loess-paleosol sequence, WP = pedosediments.

Tab. 4: Mineralogische Zusammensetzung der Löss-Paläoboden-Sequenz Oberlaab, WP = Bodensedimente.

IAG Lab. Nr		14Å	Mica	Chlorite	Layer sili-cates	Quartz	Feldspar	Hornbl	Calc + Dolo	Weath. stage
Profile OL1 Holocene Luvisol										
12401	AIO	.	*	*	*	**	*	.		2
12402	EAh	.	*	*	*	**	*	.		2
11212	E1	.	.	*	*	**	*	.		2
11213	E2	.	.	*	*	**	*	.		2
11214	EBt	*	*	*	*	**	*	.		2
11215	EBtg	*	*	**	*	**	*	.		2
11216	Btg1	*	*	*	*	**	*	.		2
11217	Btg2	*	*	*	*	**	*	.		2
11218	G	*	*	*	*	**	*	.		2
11219	I	*	*	*	*	**	*	.		2
11220	II	*	*	*	*	**	*	.		2
Profile OL2 Eemian Luvisol										
11221	WP upper	*	*	*	*	**	*	.		2
11222	WP upper	*	*	.	*	**	*	.		2
11223	WP lower	*	*	*	*	**	*	.		2
11224	WP lower	*	*	*	*	**	*	.		2
11225	Btg2	*	*	.	**	**	*			2
11226	BCtg	*	*	.	**	**	*			2
11228	BCtg	**	*	.	**	**	*			2
11229	clay cut.	*	**	.	**	**	*	.		2
Profile OL3 Middle Pleistocene Paleosol										
11230	BCtg	*	*	.	*	**	*	.		2
11233	Cg	**	*	.	*	**	*			2
11234	Eg1	*	*		*	**	*			3
11235	Eg2	*	*		*	**	*			3
11236	Btg1	**	*		*	**	*			3
11231	Btg2	*	*		*	**	*			3
11232	BCg	*	*		*	**	*			3
11238	clay.cut	.	.		**	**	*			3
Profile OL4 Middle Pleistocene Paleosol										
11432	BCg	.	*		*	**	*			3
11433	Bg	*	*	.	*	**	*			2
11434	Bg	*	*	.	*	**	*			2
11435	Btg1	*	*	.	*	**	*			2
11436	Btg2	**	*	.	*	**	*			2
11437	BCtg	**	*	.	*	**	*			2
11438	BCtg	**	*	.	*	**	*			2
11439	EB	*	*	.	*	**	*			2
11440	G	*	*		*	**	*			3
11441	Clay cut.	*	*		**	*	*			3
Profile OL5 Middle Pleistocene Paleosol										
11442	BG	*	*		**	**	*			3
11443	G	*	.		**	**	*			3
11444	Bg	*	.		**	**	*			3
11445	BCg	*	.		**	**	*			3
11446	Ah	*	*		**	**	*			3
11447	EBg	*	*		**	**	*			3
11448	Bg	*	*		**	**	*			3
11449	Bg	*	*		**	**	*			3
11450	Cg	*	*		**	**	*			3
11451	C	*	.		**	**	*			3

Legend:

\*\*\* : mineral in large quantity                      \* : mineral in low quantity  
 \*\* : mineral in intermediate quantity            . : mineral in traces



Tab. 5: Mineral composition of the clay fraction from the Oberlaab loess-paleosol sequence; well and poorly crystallized kaolinite are together in one column, WP = pedosediments.

Tab. 5: Mineralogische Zusammensetzung der Tonfraktion in der Löss-Paläoboden-Sequenz Oberlaab, WP = Bodensedimente.

IAG Lab. Nr	Horizon	Smectite	Vermiculite 18Å	Vermiculite 14Å	Illite	Kaolinite	Chlorite	Mixed Layer		Weath. stage
								I/Vc	I/Chl	
Profile OL1 Holocene Luvisol										
12401	Ai0				*	*	*	*		1
12402	EAh				*	*	**	*		1
11212	E1	*	*		*		**	*		1
11213	E2	*			*	*	**	*		1
11214	EBt	*			*	*	*	*		1
11215	EBtg	*			*	*	*	*		1
11216	Btg1	*			*	*	.	*	.	1
11217	Btg2	*	*		*	*		*	*	2
11218	G	*			*	*		*	*	2
11219	I	*			*	*	.	*	*	1
11220	II	*			*	*		*	.	2
Profile OL2 Eemian Luvisol										
11221	WP upper	*	*		*	*		*	*	2
11222	WP upper	*	*		*	*		*	.	2
11223	WP lower	**			*	*		*	.	2
11224	WP lower	**			*	*		*	.	2
11225	Btg2	***			*	*		*	.	3
11226	BCtg	***			*			*	.	3
11228	BCtg	***			*	.		*	.	3
11229	clay cut	**			*	*		.	.	2
Profile OL3 Middle Pleistocene Paleosol										
11230	BCtg	*	*	*	*	*		*	.	3
11233	Cg	*	*	*	*	*		*		3
11234	Eg1	*	*	*	*	*		*		3
11235	Eg2	*	*	*	*	*		*	.	3
11236	Btg1	*			*	*		*		3
11231	Btg2	*		*	*	*		*		3
11232	BCg	*	**		*	*		*		3
11238	clay.cut	*	*	*	*	*		*		3
Profile OL4 Middle Pleistocene Paleosol										
11432	BCg	*	**	*	*	*		.		3
11433	Bg	*	**		*	.		.		3
11434	Bg	*	**		*	.		.		3
11435	Btg1	*	**	*	*	*		.		3
11436	Btg2	*	**	*	*	.		.		3
11437	BCtg	*	**	*	*	*		.		3
11438	BCtg	**	**	*	*	*		.		3
11439	EB	*	**	.	*	*		.		3
11440	G	*	**	*	*	*		.		3
11441	Clay cut.		**	*	*	.		.	.	3
Profile OL5 Middle Pleistocene Paleosol										
11442	BG	**	**		*	*		.	.	4
11443	G	**	**		*	.		.		4
11444	Bg	*	**		.	.		.		4
11445	BCg	*	**		*	.		.		4
11446	Ah	*	**		*	.		.		4
11447	EBg	*	**	*	*			.		3
11448	Bg	**	**	*	*			.	.	3
11449	Bg	**	**	*	*	.		.		3
11450	Cg	**	**	*	*	.		.		3
11451	C	**	**	*	*			.	.	3

Legend:

\*\*\* : mineral in large quantity      \* : mineral in low quantity  
 \*\* : mineral in intermediate quantity      . : mineral in traces

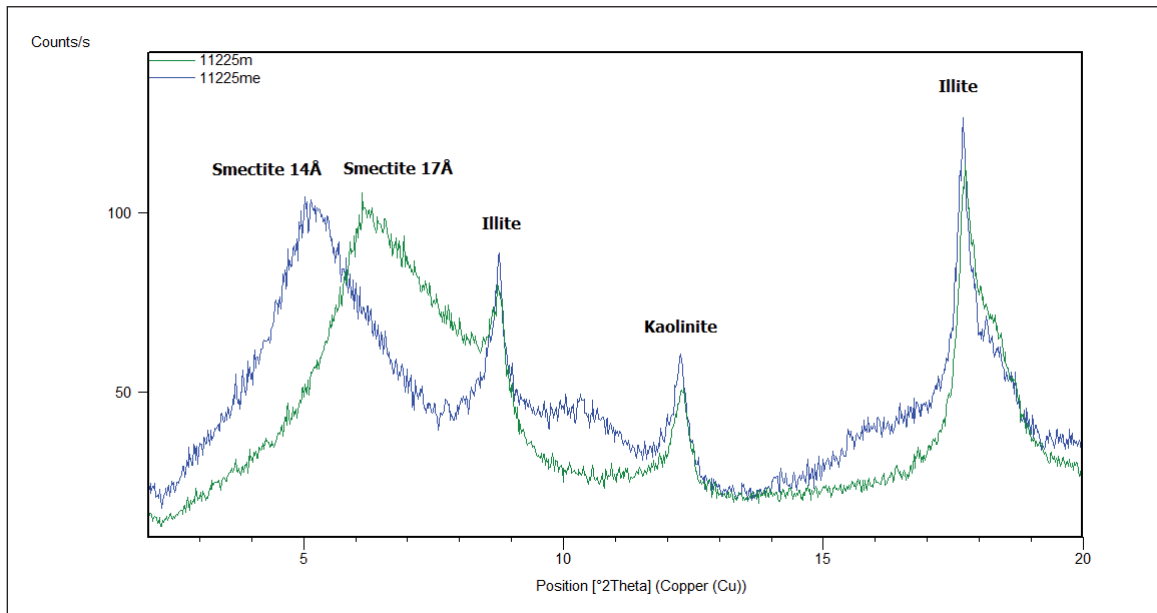


Fig. 4: X-ray diffractogram of the clay fraction <math><2\mu\text{m}</math> from OL2 Btg2 horizon. The green line is Mg treated and air dried, the blue line is Mg-treated and glycolated. The expansion of smectite from 14Å to 17Å is quite visible.

Abb. 4: Diffraktogramm der Tonfraktion <math><2\mu\text{m}</math> aus dem Btg2 Horizont von OL2. Die grüne Kurve zeigt die Mg-behandelte und lufttrockene Tonfraktion, die blaue Kurve die Mg-behandelte und glykolisierte Kurve. Deutlich ist die Aufweitung von Smektit von 14Å auf 17Å zu sehen.

are the clay illuvial Bt horizons of the Eemian paleosol OL2 and the basal gleyed paleosol OL5. We suppose that some strong chemical weathering processes should be taken into account when interpreting these maxima (CHAMLEY, 1989; SHELDON & TABOR, 2009). In the Eemian argic horizons the maximum of illuvial clay was registered by micromorphometric studies (SOLLEIRO-REBOLLEDO et al., 2013). Furthermore, detailed micromorphological observations revealed abundant multiphase clay illuvial pedofeatures (SEDOV et al., 2013, this volume). We suppose that besides weathering, strong clay illuviation could contribute to the maximum of fine fractions observed in these horizons. This is confirmed by the abundance of fine clay and smectites, which are the most mobile components in suspensions. The lower paleosol unit OL5 represents a quite different soil environment. Both abundant morphological features of redoximorphic processes and minimal values of magnetic susceptibility point to water-logged anoxic conditions. Usually such conditions hamper silicate weathering. We should pay attention to the changes in the composition of parent material in this unit – higher sand and lower silt content indicate an increase of the fluvial component. A part of the clay could be provided by slow fluvial sedimentation (overbank alluvium) being derived from the older pre-existing weathered materials of the Alpine Foreland.

In the Oberlaab sequence, grain size and mineralogical indicators of weathering provide more variable and sensitive signals of mineral transformations than the geochemical index CIA, presented by SOLLEIRO-REBOLLEDO et al. (2013).

## 5 References

AD-HOC-ARBEITSGRUPPE BODEN (2005): Bodenkundliche Kartieranleitung. – E. Schweizerbart'sche Verlagsbuchhandlung, Hannover.

- BRINDLEY, G.W. & BROWN, G. (1980): Crystal Structures of Clay Minerals and their X-Ray Identification. – Mineralogical Society, 495 pp., London.
- BRONGER, A. & HEINKELE, T. (1990): Mineralogical and clay mineralogical aspects of loess research. – *Quaternary International* 7/8, 37–51.
- BRONGER, A., WINTER, R. & SEDOV, S. (1998): Weathering and clay mineral formation in two Holocene soils and in buried paleosols in Tadjikistan: towards a Quaternary paleoclimatic record in Central Asia. – *Catena* 34: 19–34.
- BUGGLE, B., GLASER, B., HAMBACH, U., GERASIMENKO, N. & MARKOVIĆ, S.B. (2011): An evaluation of geochemical weathering indices in loess-paleosol studies. – *Quaternary International* 240, 12–21.
- CHAMLEY, H. (1989): Clay Sedimentology. – Springer Verlag, 620 pp., Berlin.
- DIXON, J.B. & WEED, S.B. (eds.) (1989): Minerals in Soil Environments. – 2nd ed. Soil Science Society of America, Madison, WI. 1244 pp.
- IUSS WORKING GROUP WRB, (2006): World Reference Base for Soil Resources. In: World Soil Resources Reports 103. FAO, Rome.
- MOORE, D.M. & REYNOLDS, R. C., JR. (1997): X – Ray Diffraction and the Identification and Analysis of Clay Minerals. – Oxford Univ. Press, 378 pp., New York.
- PÉCSI, M. & RICHTER, G. (1996): Löss Herkunft – Gliederung – Landschaften. – Zeitschrift für Geomorphologie N.F., Supplementband 98: 391 pp.
- SCHOLGER, R. & TERHORST, B. (2013): Magnetic excursions recorded in the Middle to Upper Pleistocene loess/paleosol sequence Wels-Aschet (Austria). – *E & G Quaternary Science Journal* 62 (1): 14–21, DOI: 10.3285/eg.62.1.02
- SEDOV, S., SYCHEVA, S., PI, T. & DÍAZ, J. (2013): Last Interglacial paleosols with argic horizons in Upper Austria and Central Russia: A comparative pedogenetic and paleoecological analysis. – *E & G Quaternary Science Journal* 62 (1): 44–58, DOI: 10.3285/eg.62.1.05
- SHELDON, N.D. & TABOR, N.J. (2009): Quantitative paleoenvironmental and paleoclimatic reconstruction using paleosols. – *Earth-Science Reviews*, 95: 1–52.
- SOLLEIRO-REBOLLEDO, E., CABADAS, H., SEDOV, S. & TERHORST, B. (2013): Paleopedological record along the loess-paleosol sequence in Oberlaab Austria. – *E & G Quaternary Science Journal* 62 (1): 22–33, DOI: 10.3285/eg.62.1.03
- TERHORST, B. (2013): A stratigraphic concept for Middle Pleistocene Quaternary sequences in Upper Austria. – *E & G Quaternary Science Journal* 62 (1): 4–13, DOI: 10.3285/eg.62.1.01
- TERHORST, B., OTTNER, F. & WRIESSNIG, K. (2012): Weathering intensity and pedostratigraphy of the Middle to Upper Pleistocene loess/paleosol sequence of Wels-Aschet (Upper Austria). – *Quaternary International* 265: 142–154.

# Last Interglacial paleosols with Argic horizons in Upper Austria and Central Russia – pedogenetic and paleoenvironmental inferences from comparison with the Holocene analogues

Sergey Sedov, Svetlana Sycheva, Victor Targulian, Teresa Pi, Jaime Díaz

## How to cite:

SEDOV, S., SYCHEVA, S., TARGULIAN, V., PI, T., DÍAZ, J. (2013): Last Interglacial paleosols with Argic horizons in Upper Austria and Central Russia – pedogenetic and paleoenvironmental inferences from comparison with the Holocene analogues. – E&G Quaternary Science Journal, 62 (1): 44–58. DOI: 10.3285/eg.62.1.05

## Abstract:

The paleosols of the Last Interglacial are presented in many loess sequences of the European temperate zone by soils with Argic horizon, that are considered to be the pedological response to the bioclimatic conditions of that period. We studied micromorphological, physical/chemical (bulk chemical composition, texture and dithionite-extractable iron) and mineralogical characteristics of two profiles – an Eemian Luvisol in Upper Austria (Oberlaab) and a Mikulino Albeluvisol in Central Russia (Alexandrov Quarry near Kursk) to compare them with recent analogous soils and to make further paleoecological and chronological inferences. Both profiles showed a set of characteristics indicative for weathering of primary minerals, clay transformation illuviation and surface redoximorphic (stagnic) processes. Paleosols demonstrate more advanced development than the Holocene analogues manifested however in different pedogenetic characteristics. The Eemian Luvisol in Upper Austria is characterized by stronger clay illuviation manifested in higher clay content and abundance of illuvial clay pedofeatures in the Bt horizon. Mikulino Albeluvisol in Central Russia is more strongly affected by eluvial and stagnic processes evidenced by deeper and more intensive accumulation of bleached silty material and clay depletion. We suppose that the properties of parent material are responsible for these differences. Russian Albeluvisol is formed on the Dnepr loess poor in weatherable minerals and having limited capacity for buffering acidity and clay formation. The higher development status of the Last Interglacial paleosols compared to the Holocene soils having however same type pedogenesis implies longer soil formation period, that agree with some of the paleobotanical proxies and could include besides MIS 5e part of MIS 5d; the warmer and moister paleoclimate during MIS 5e could also account for more advanced paleosol development. Several phases of clay illuviation interrupted by frost structuring and deformation are detected in the Eemian Bt horizon in Upper Austria. It suppose even longer development that could extend to the Early Würmian interstadials (late substages of MIS5).

## Letztinterglaziale Paläoböden mit Bt-Horizonten in Oberösterreich und Zentral-Russland: pedogenetische und paläoumweltbezogene Schlussfolgerungen im Vergleich mit den holozänen Analogon

## Kurzfassung:

In vielen Löss-Paläoboden-Sequenzen der gemäßigten Breiten Europas ist das letzte Interglazial (dt.: Eem, russ.: Mikulino) durch einen Bt-Horizont (Argic horizon nach WRB) repräsentiert, der als pedologisches Resultat entsprechender bioklimatischer Bedingungen dieser Zeit gedeutet wird. Wir untersuchten mikromorphologische, physikalische/chemische (Gesamtelementzusammensetzung, Korngrößenverteilung und dithionitlösliches Eisen) und mineralogische Charakteristika im Profilabschnitt des Eem-Luvisols in Oberösterreich (Oberlaab) und des Mikulino-Albeluvisols in Zentralrussland (Alexandrov Grube nahe Kursk). Aus dem Vergleich der Paläoböden mit entsprechenden rezenten Böden ergeben sich paläoökologische und chronologische Schlussfolgerungen. Beide Profile zeigen eine Reihe von Charakteristika, die auf Verwitterung primärer Minerale und Tonminerale sowie Tonverlagerung und redoximorphe Prozesse hinweisen. Die Paläoböden zeigen jeweils eine weiter fortgeschrittene Entwicklung im Vergleich zu entsprechenden holozänen Böden, jedoch anhand unterschiedlicher pedogenetischer Merkmale. Der Eem-Luvisol in Oberösterreich weist ein höheres Maß an Tonverlagerung auf, was durch einen höheren Tongehalt und zahlreiche Toncutane im Bt-Horizont gezeigt wird. Der Mikulino-Albeluvisol in Zentralrussland ist stärker von Auswaschung und Stauwasser betroffen, was sich in tieferer und stärkerer Ansammlung von gebleichtem schluffigem Material und Tonverarmung zeigt. Wir nehmen an, dass das Ausgangsmaterial diese unterschiedliche Entwicklung hervorruft. Der russische Albeluvisol bildete sich auf Dnjepr-Löss, welcher im Vergleich zu den Riss-Lössen Oberösterreichs ärmer an leicht verwitterbaren Mineralen ist und daher eine geringere Kapazität Säure zu puffern sowie Ton neu zu bilden aufweist. Das fortgeschrittenere Entwicklungsstadium des letztinterglazialen Bodens im Vergleich zu holozänen Böden, die allgemein demselben Bodentyp entsprechen, spricht für eine längere Bodenentwicklungsphase, was mit paläobotanischen Ergebnissen in Einklang steht. Einerseits könnte der letztinterglaziale Paläoboden neben dem MIS 5e auch Teile des MIS 5d umfassen, andererseits könnte eine intensivere Paläobodenentwicklung durch das wärmere und feuchtere Paläoklima während der Interglazialphase des MIS 5e verursacht werden. Mehrere Phasen der Tonverlagerung, unterbrochen durch frostdynamische Strukturierung und Deformation sind im eemzeitlichen Bt-Horizont in Oberösterreich nachweisbar. Die noch weiter reichende Entwicklung könnte bis in noch jüngere Frühwürm-Interstadiale gereicht haben.

## Keywords:

*Last Interglacial, paleosol, Argic horizon, paleoclimate*

**Adresses of authors:** S. Sedov\*, T. Pi, J. Díaz, Instituto de Geología, UNAM. Circuito de la Investigación Científica, 04510, México DF, Mexico; S. Sycheva, V. Targulian, Institute of Geography, RAS. Staromonetny 29, Moscow, 119017. Russia; \*corresponding author: sergey@geologia.unam.mx





Fig. 1: Geographical situation of the studied profiles. O – Oberlaab, A – Alexandrov.

Abb. 1: Geographische Lage der untersuchten Profile. O – Oberlaab, A – Alexandrov.

## 1 Introduction

The perspective of global climate change increased the interest to the paleoecology of earlier warmer periods, in particular to the Quaternary interglacials. The last interglacial (known in the regional stratigraphies as Riss-Würm, Eemian, Mikulino, Sangamonian) drew special attention as far as the corresponding geological objects and materials are frequent and well preserved. During the last decades a significant progress was achieved in defining the duration of this warm phase and its paleoenvironmental characteristics based on the correlations between marine and terrestrial records (SHACKLETON et al. 2003; SIER et al. 2011).

Paleosols of loess-paleosol sequences are among the most important terrestrial records of interglacial environments, especially since these sequences were thoroughly correlated with the deep sea isotope record (KUKLA 1977; BRONGER et al. 1998). In the contemporary temperate zone of Europe the paleosols of the last interglacial are often represented by soil bodies with strong clay illuviation (HAESAERTS & MESTDAGH 2000), which were considered to be, with certain limitations, the most significant response of pedogenesis to the interglacial bioclimatic conditions (STEPHAN 2000). The examples are the Ipswichian paleoargillic soils in England (CATT 1996), Rocourt Luvisol in France (ANTOINE et al. 1999) and Belgium (HAESAERTS et al. 1999; VANDENHAUTE et al. 2003; VANCAMPENHOUT et al. 2008), Erbacher Boden – Luvisol/Alfisol/Parabraunerde in Germany (MAHANAY et al. 1993; ANTOINE et al. 2001; TERHORST et al. 2001), lower Luvisol of the PK3 pedocomplex in Czechia (DEMEK & KUKLA 1969; FRECHEN et al. 1999) and Nietulisko I - GJ1 pedocomplex in Poland (JARY 2009, 2011), “brown-podzolic soil” of Pryluky-Kaydaky pedocomplex in Ukraine (ROUSSEAU et al. 2001; GERASIMENKO 2006) and Salyn paleosol, the Luvisol of Mezin pedocomplex in Central Russia (VELICHKO 1990; YAKIMENKO 1995; VELICHKO et al. 2006).

Only in areas with drier continental climate the last interglacial paleosols do not show clay illuviation: in Lower Aus-

tria (FINK 1956; BRONGER 1976; PETICZKA 2009; SPRAFKE et al. 2013, this volume) it is represented by Cambisols, whereas in the south-eastern part of the East European Plain (RUTTER et al. 2003) and the Carpatian Basin (BRONGER 1976; MARKOVIC et al. 2008) the last interglacial soils correspond to Chernozems. In fact, in the European temperate zone Luvisols occupied a larger areal in the Eemian soil cover than they do in the Holocene.

This area differs especially in the East European Plain where the zone of forest soils was much broader during the Eemian and occupied a large portion of the present day steppe zone (MOROZOVA 1981; MOROZOVA et al. 1998). In a number of sites in Central Russian and Ukrainian steppe regions one can see a striking difference between Holocene Chernozem on the surface and buried Mikulino Luvisol, separated by Valday loess, all exposed in the same cut (this is also the case in Alexandrov quarry exposure).

In the present day temperate humid forest areas both, last interglacial and Holocene soils show clay illuviation. However, they are often clearly distinguished quantitatively: stronger development of the last interglacial Argic horizons compared to the recent ones was reported in a number of case studies (BOARDMANN 1985; BULLOCK & THOMPSON 1985; MAHANAY et al. 1993). The reasons for this distinction are not so obvious: differences in bioclimatic conditions as well as in duration of pedogenesis could be involved.

We have to conclude that both paleoecological and chronological aspects of the last interglacial Luvisols development are far from being clear. Concerning the paleoenvironmental setting the assumption that the Bt horizon is a reliable sign of interglacial conditions “defined by the return of the temperate deciduous woods” (STEPHAN 2000) could be too ambitious: we know that in the present day soil cover these horizons occur in a much broader spectrum of ecosystems. In the classic zonal sequence of the Eastern Europe soils with strong clay illuviation are formed on loamy substrates from the broadleaf forests and forest-steppe till boreal coniferous northern taiga (GEROSIMOVA et al. 1996). In fact within the Eurasian forest belt only in the regions with drier extra-continental climate and permafrost in Middle and Eastern Siberia clay illuviation is hampered (GEROSIMOVA et al. 1996).

Broad ecological limits of the recent Argic horizon formation have implications for determining its timing in Europe. In the course of soil evolution during and after Last Late Glacial, clay illuviation is detected not only in the Holocene but also in the late MIS 2 interstadials (KÜHN 2003). Some authors attribute the development of Argic horizons in the European Luvisols mostly to the late glacial (BØLLING) boreal paleoenvironment (VAN VLIET LANOË 1990).

Thus the possibility should be considered that also in Mikulino/Eemian paleosols the Luvisol pedogenesis occurred not only during the interglacial *sensu stricto* but also in transitional phases of colder forest or forest-steppe ecosystems before and after it. In fact, this scenario has been already proposed by various researchers who detected several clay illuviation phases in the Eemian to Early Würmian pedocomplexes in Belgium (HAESAERTS et al. 1999; HAESAERTS & MESTDAGH 2000) and Germany (ANTOINE et al. 2001; TERHORST et al. 2001). All these authors coincided in discriminating between forest Luvisol development corresponding to the warm humid interglacial and forest-steppe

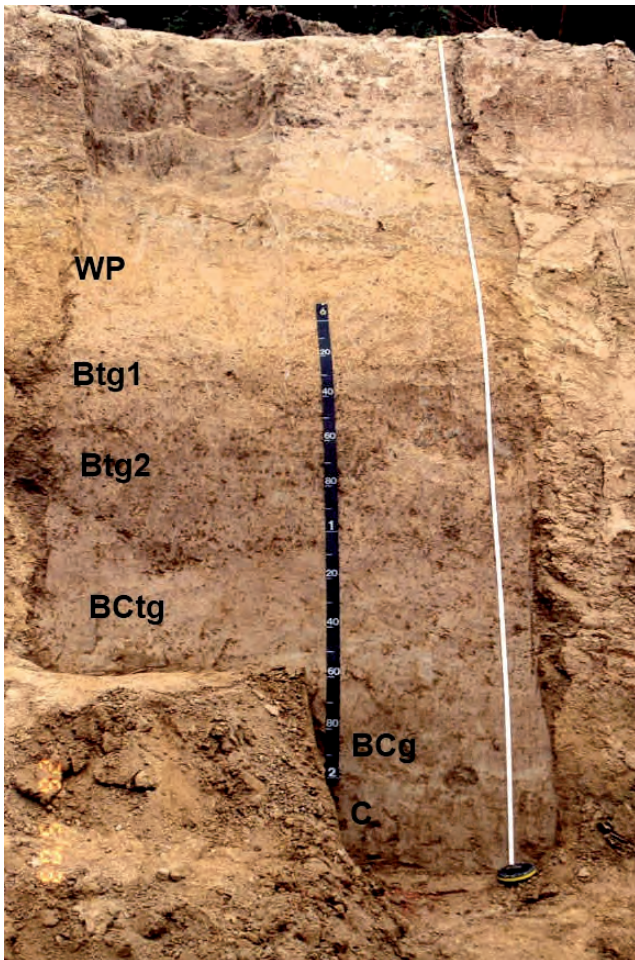


Fig. 2: Profile morphology of the Eemian paleosol of the Oberlaab profile, with the overlying Würmian pedosediment (WP).

Abb. 2: Eemzeitlicher Paläoboden im Profil Oberlaab mit darüber liegendem würmzeitlichem Bodensediment.

Grey Forest Soils attributed to cooler continental climate of the Early Weichselian interstadials. This approach revives the earlier ideas of BOARDMANN (1985) about longer pedogenesis of the Pleistocene interglacial paleosols compared to the Holocene.

However, in most works on loess stratigraphy, chronology and paleoecology the information on paleosol pedogenesis is rather limited: the conclusions are mostly based on field morphological observations, grain size and magnetic susceptibility distribution. Deeper understanding of paleoenvironmental significance of the paleosol of the last interglacial in Europe requires more detailed data about the types and succession of pedogenetic processes – which can be provided by detailed micromorphological and clay mineralogical investigation accompanied by soil chemical analyses (BRONGER 1976; BRONGER & HEINKELE 1990; KEMP 1999).

Such detailed study of the buried Luvisols promise to be effective also concerning their comparison with modern surface soils. Temperate forest soils with clay illuviation are provided with one of the most variable and detailed datasets of morphological, physical/chemical and mineralogical characteristics. In fact, these soils were one of the main “experimental polygons” of pedology to construct scenarios of pedogenesis (including polygenetic models) based on these complex datasets (e.g. TARGULIAN et al. 1974 a,b; KÜHN et

al. 2006). Thus, the actualistic approach towards paleosol interpretation was expected to be most fruitful in case of the Luvisols.

This research intends to contribute to the knowledge about the last interglacial soil evolution in Europe by carrying out a comparative pedogenetic analysis of two buried paleosols with Argic horizon formed on loess in geographically distant and ecologically dissimilar regions: Upper Austria (Oberlaab section) and Central European Russia (Alexandrov quarry section near Kursk). The final objective is to develop scenarios of paleosol genesis and evolution for both profiles and from this derive conclusions about their paleoenvironmental significance and timing.

## 2 Materials and methods

Two profiles of the last interglacial paleosols from the loess-paleosol sequences were subjected to detailed morphological analysis and sampling being selected as the key sites for the ICSU-2003 project “Polygenetic models for Pleistocene paleosols” (Fig. 1). The profile in Oberlaab (Upper Austria) is located on the fluvio-glacial terrace attributed to the Mindel glaciation, close to its bench (TERHORST 2013, this volume). The present day climate is humid providing conditions for broad leaf forest vegetation and for a development of Stagnic Luvisols as dominant modern soil type. The profile Alexandrov quarry (near Kursk, Central Russian Plain) is located at the watershed position close to the slope towards the valley of river Mlodat. The modern climate is temperate semi-humid, the surface soils are Haplic Chernozems formed under meadow-steppe vegetation. Thus, both study sites present two major cases of interrelation between last interglacial Luvisols and the Holocene soil: they belong to the same type in case of Oberlaab and they are genetically dissimilar in case of Alexandrov section.

The stratigraphic, chronological, and paleoecological aspects of both paleosol-sedimentary sequences were published earlier. For Oberlaab these data are available in the papers included in this Special Volume and some earlier publications (TERHORST 2007, 2013, this volume; SOLLEIRO et al. 2013, this volume). The Eemian soil in Oberlaab is the uppermost of 5 buried paleosols; it is separated from the modern soil by colluvial and loessic sediments with signs of weak pedogenesis, attributed to the Würmian glacial. Alexandrov section was studied by Sycheva and co-authors during the last 20 years, the results are presented in several papers (c.f. SYCHEVA 1998; GOLYEVA & SYCHEVA 2010; SYCHEVA & SEDOV 2012). Mikulino (Salyn) paleosol is developed on the Dnieper (Rissian Glacial, MIS 6) calcareous loess. The important advantage of Alexandrov section is an extensive and detailed part corresponding to the last (Valday) glaciation, overlying the Mikulino soil. The lower segment of this part is comprised by three Early Valday paleosols clearly separated by colluvial strata. Above them the Middle Valday paleosol is developed (Bryansk soil). Finally, modern Chernozem is separated from Bryansk soil by the Late Valday loess.

Detailed morphological description of the last interglacial paleosol profiles was followed by sampling of the genetic horizons: bulk samples for physical, chemical and mineralogical characteristics and blocks with undisturbed structure for thin sections were collected. Micromorpho-



logical observations were performed under petrographic microscope and the descriptions followed the terminology of BULLOCK et al. (1986). We gave special attention to the pedofeatures related to the clay eluvial-illuvial redistribution, redoximorphic processes as well as the signs of aggregation and mixing by biotic and cryogenic processes. The properties selected for paleosol laboratory analyses were those indicative of ancient pedogenetic processes and not subjected to major diagenetic changes after burial. Bulk chemical composition was estimated by X-ray fluorescence analysis. Grain size distribution – intended to estimate clay accumulation due to weathering and illuviation – included separation of sand fractions by sieving and quantification of silt and clay by pipette method. The content of free iron oxides – an important product of soil weathering – was evaluated by measuring Fe in the dithionite-citrate-bicarbonate extract ( $Fe_d$ ). Clay mineral assemblages in the soils with eluvial-illuvial differentiation are known to be specific for different horizons and strongly influenced by pedogenetic processes (TARGULIAN et al. 1974b; TONKONOGOV et al. 1987). We studied the composition of clay fraction by X-ray diffraction using a Shimadzu XRD-6000 diffractometer in oriented specimen subjected to different pretreatments: air-dry, saturated with ethylene-glycol, heated to 375 °C and 500 °C. Clay species content was estimated in semi-quantitatively, using simple peak weighting factors; for area estimation we used Fityk (WOJDYR 2010) program. Illite, smectite and mixed-layered components were identified by separating their peak areas in the glycolated XRD-trace and calculating their proportions (MOORE & REYNOLDS 1997).

All results were further integrated with other datasets – morphological, geochemical, rock magnetic, etc. published for Oberlaab by SOLLEIRO et al. (2013, this volume), for Kursk by SYCHEVA (1998), RIVAS et al. (2003) and SYCHEVA & SEDOV (2012).

The key element of interpretation consisted in the comparison of obtained results with the existing knowledge about the pedogenetic characteristics of the clay-illuvial soils formed under different environmental conditions: temperate forest of Western and Central Europe (JAMAGNE et al. 1984; KÜHN et al. 2006; SAUER et al. 2009), taiga (TARGULIAN et al. 1974 a,b; TONKONOGOV et al. 1987) and forest-steppe (MIEDEMA et al. 1999) ecosystems of European Russia. Reference profiles for comparison were modern analogues (surface soils) as close as possible to the respective studied profile for which the necessary pedogenetic characteristics were available: surface Holocene Luvisol for Oberlaab (Solleiro et al. 2013, this volume) and modern Albeluvisol of the Moscow region (TARGULIAN et al. 1974 a,b).

### 3 Results

#### *Paleosol morphology from macro- to microscale*

The Eemian soil in Oberlaab is located at a depth of about 3m below the Holocene Luvisol, formed on Würmian sediments. The lower part (60 cm) of the latter directly above Eemian Bt horizon has yellow color, silty loam texture and contains ferruginous concretions. This morphology together with gradual wavy boundary suggests that this layer could be a pedosediment that incorporated material of the Eemian eluvial horizon (indicated in the tables and

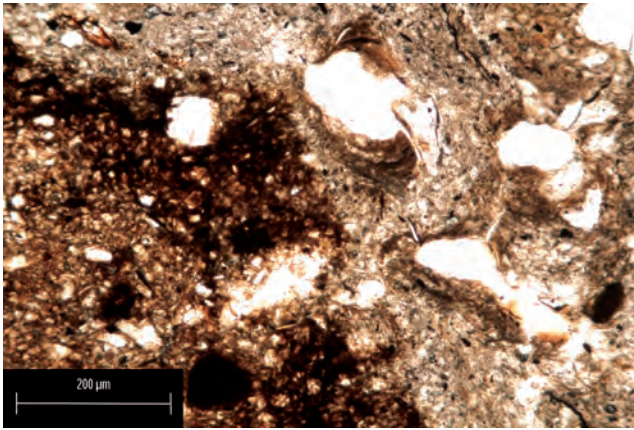
figures as WP – Würmian pedosediment). The underlying 90 cm thick brown Btg horizon (subdivided into Btg1 and Btg2) is darker, more compact and clayey than the overlying pedosediment, with platy/subangular blocky structure. Brown clay coatings cover ped surfaces and fill vertical cracks. Furthermore, few pale coatings of bleached silt, iron concretions and mottles are present. Clay illuvial features decrease in the underlying BCtg and BCg horizons (joint thickness about 1m), where larger visible cutans are restricted to very few biogenic pores – channels and chambers. Simultaneously, stagnant colour pattern appears – pale areas, often of subhorizontal lenticular shape are neighboring with yellow mottles of ferruginous pigment. Below follows the pale brown-yellow homogeneous C horizon – the loessic sediment of Riss glaciations separating the Eemian profile from the underlying Middle Pleistocene paleosol (TERHORST 2007; SOLLEIRO et al. 2013, this volume). The soil was classified in the field as Stagnic Cutanic Luvisol (Fig. 2). Under the microscope, the groundmass in all horizons is dominated by coarse silt, having rich and variable mineralogical composition: besides quartz feldspars, amphiboles and micas are abundant. Micas are represented both by colorless muscovite and dark brown biotite; in the latter at stronger magnification signs of weathering are observed – weak interference colors and pleochroism, deformation, precipitation of iron oxides.

The Würmian  $\gamma$  pedosediment (WP) has areas with banded fabric demonstrating stripes of coarse silt and fine material. Frequent ferruginous nodules – rounded, circular, compound are distributed within the groundmass, few thin clay coatings are present. Areas with banded structure were also observed in the Btg1 horizon. Clay illuvial pedofeatures become more abundant in this horizon, being presented both by undisturbed clay coatings (mostly thin and impure) (Fig. 3a) in the pores and fragmented and deformed clusters of illuvial clay incorporated into groundmass. Ferruginous nodules and mottles, mostly with irregular shape and diffuse boundaries are also abundant. Rather big anorthic iron-clay nodules of subangular fragmented shape (Fig. 3b) and charcoal fragments with the tissue structure of a conifer tree were encountered.

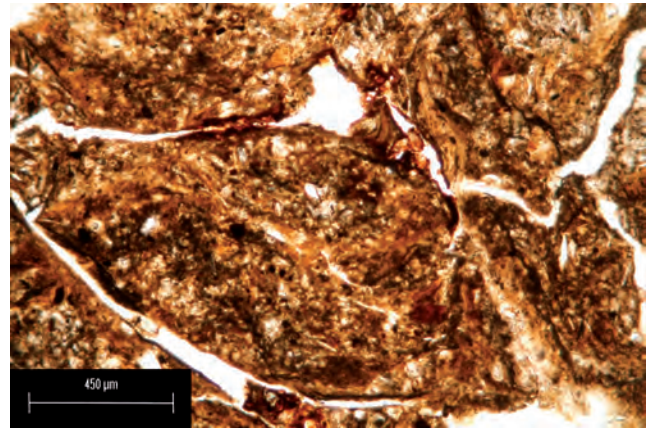
The major abundance and variety of clay illuvial materials was found in the Btg2 horizon. Undisturbed clay coatings are present, however, they are not dominant. Fragments of clay illuvial pedofeatures of different size and morphology are more frequent, some of them are larger than any of the undisturbed coatings (Fig. 3c). The Btg2 horizon is characterized by strong fracturing giving rise to angular blocky and coarse lenticular peds (Fig. 3d) and being accompanied by displacement along the cracks. The walls of these cracks support thin undisturbed coatings. Bleached irregular shaped silt concentrations depleted of clay are very rare (Fig. 3e). Few infillings with bow-like structure are of zoogenic origin (Fig. 3f) (KOOISTRA & PULLEMAN 2010).

Deeper in the BCtg horizon the number of clay illuvial pedofeatures decreases but their preservation increases – they are mostly undisturbed coatings in voids, some of them large and laminated (alternating limpid with strong interference colors and impure microlayers) (Fig. 3g,h). Further down the profile in the BCg horizon clay coatings are

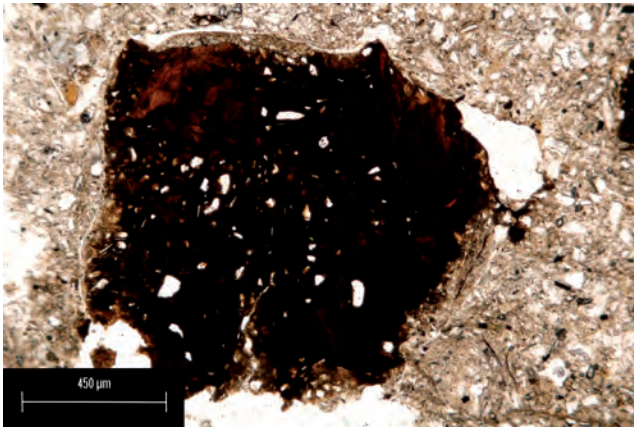




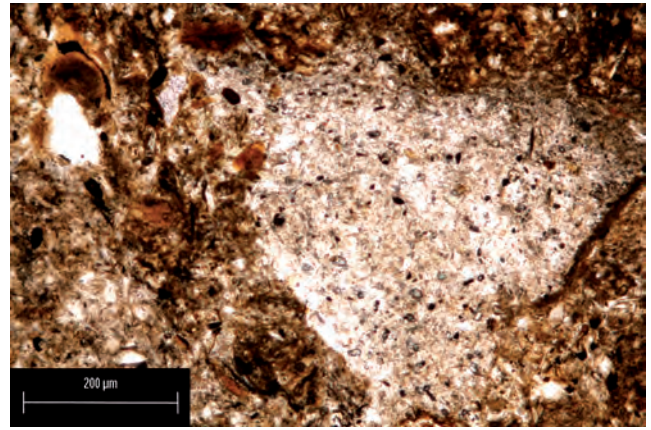
a) Impure clay coatings, Btg1 horizon, plain polarized light.



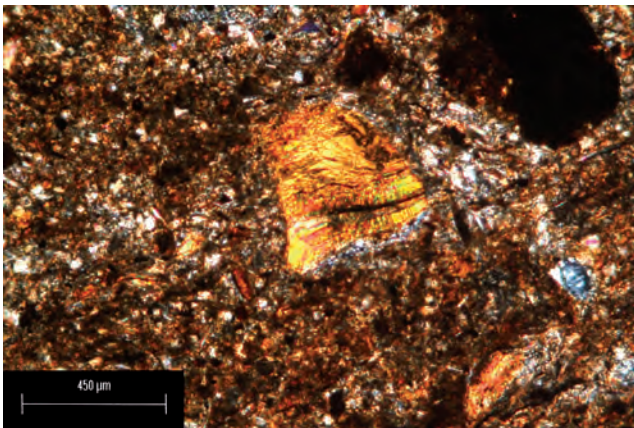
d) Angular blocky – lenticular structure produced by fracturing; note thin clay coatings on the aggregate surface. Btg2 horizon, plain polarized light.



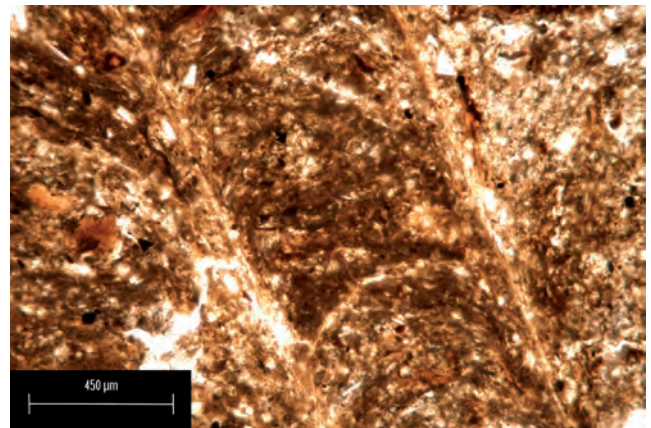
b) Anorthic ferruginous nodule, Btg1 horizon, plain polarized light.



e) Concentration of bleached silt particles. Btg2 horizon, plain polarized light.



c) Fragment of clay illuvial pedofeature, note strong interference colors and microlamination. Btg2 horizon, crossed polarizers.

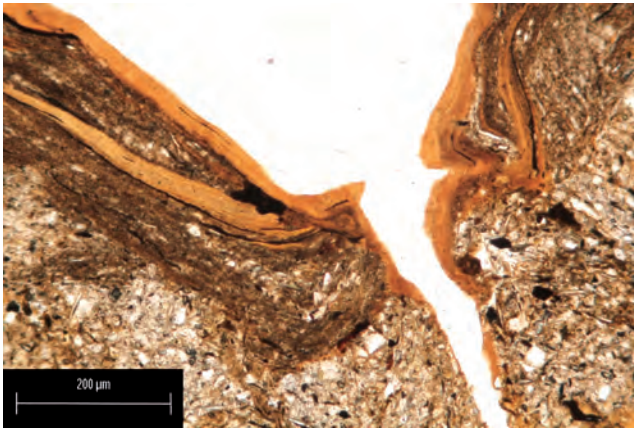


f) Infilling with bow-shaped structure. Btg2 horizon, plain polarized light.

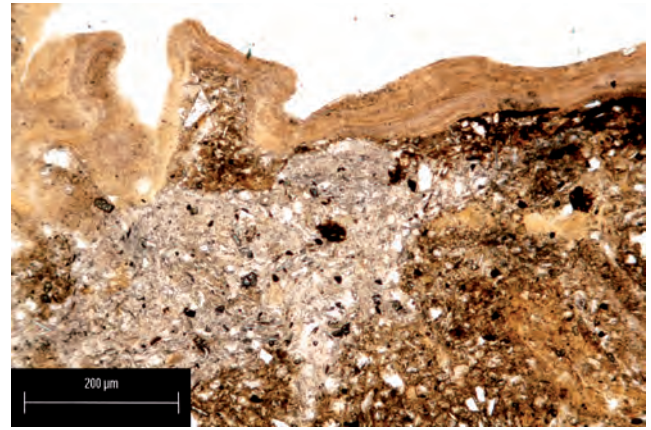
Fig. 3: Micromorphology of the Eemian paleosol in Oberlaab.

Abb. 3: Mikromorphologie des eemzeitlichen Paläobodens in Oberlaab.

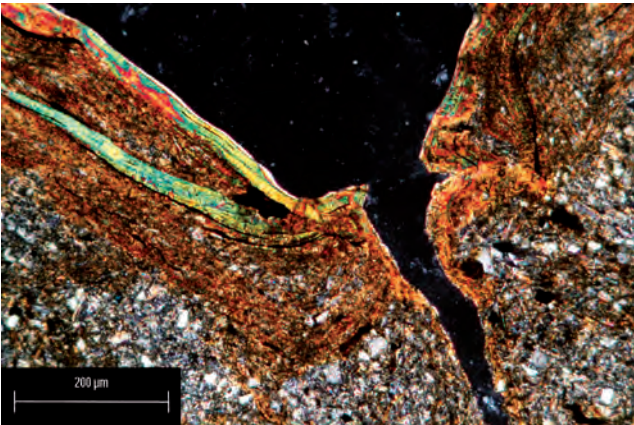




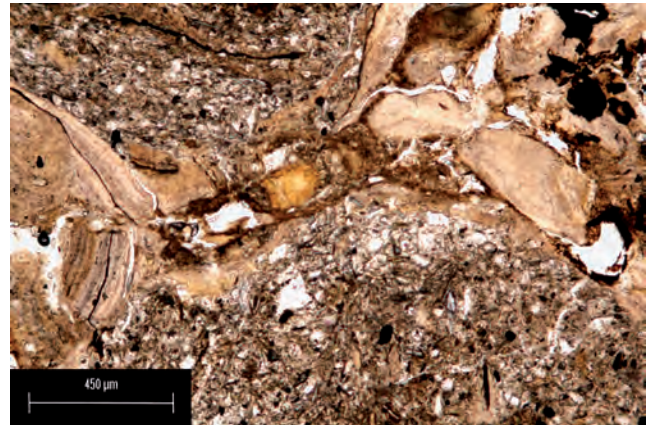
*g) Laminated clay coatings with limpid and impure microlayers. BCtg horizon, plain polarized light.*



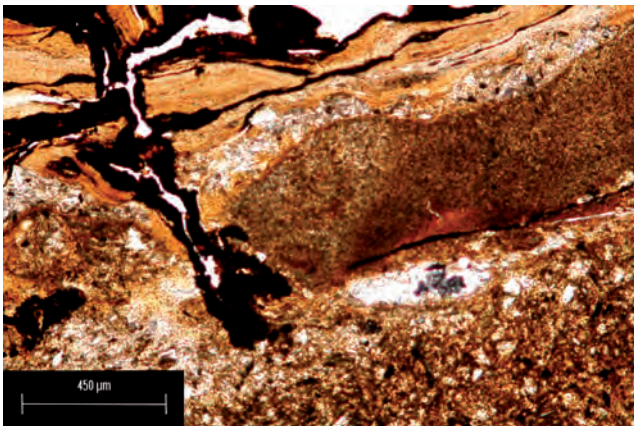
*j) Bleached area in the groundmass under clay coating. BCg horizon, plain polarized light.*



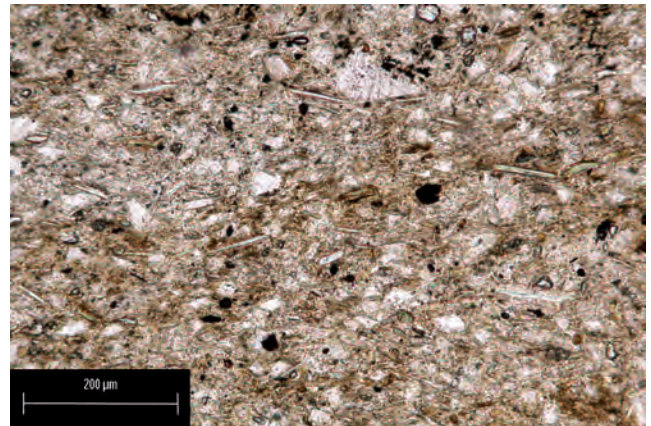
*h) Same as g), crossed polarizers; note high birefringence of limpid layers.*



*k) Disturbed clay illuvial pedofeature, fragments covered by a thin undisturbed clay coating. BCg horizon, plain polarized light.*



*i) Clay illuvial pedofeature with ferruginous coatings on the surface and in the cracks. BCg horizon, plain polarized light.*



*l) Parallel orientation of elongated mineral particles, C horizon, plain polarized light.*



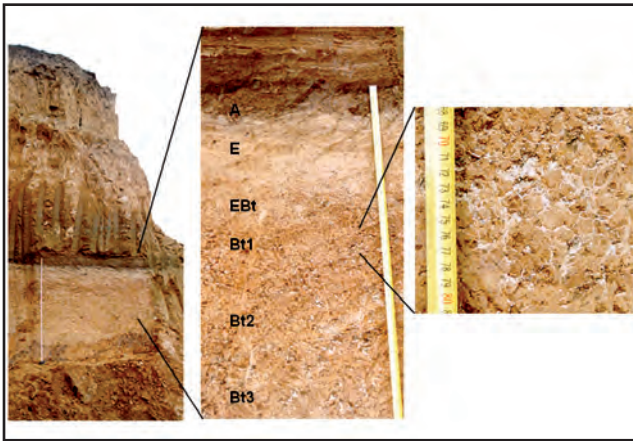


Fig. 4: Profile morphology of the Mikulino paleosol in Alexandrov: position in the sequence, eluvial-illuvial differentiation, detail of the Bt1 morphology, showing bleached areas related to the pores.

Abb. 4: Morphologie des Mikulino Paläobodens in Alexandrov: Lage im Profil, Differenzierung von Eluvial- und Illuvialbereichen, Detailaufnahme Bt1-Horizont mit gebleichten Bereichen, die im Zusammenhang mit Poren stehen.

even fewer and usually combined with ferruginous nodules and films penetrating into illuvial clay (Fig. 3i). Frequently, clay coatings in the pores overly bleached microareas adjacent to the pore walls, however, these areas although lacking ferruginous pigment are not depleted of fine clay material (Fig. 3j). In the BC horizons few clay pedofeatures are fragmented but usually not incorporated into groundmass – the fragments stay in the pores being only slightly displaced and covered by the new generation of thinner cutans (Fig. 3k). Finally in the C horizon all pedofeatures become less abundant and primary sedimentary structures are more evident – among them parallel subhorizontal orientation of the elongated mineral particles (Fig. 3l).

The profile of Mikulino paleosol as mentioned above is overlain by 6 m of Walday sediments with a Holocene Chernozem on top. The profile demonstrates a remarkable preservation of all horizons including the topsoil. It is delimited from the overlying laminated colluvial sediments by a thin (less than 1 cm) black layer of burned litter. Below it a grey-brown Ah horizon (8 cm thick) is located; it contains numerous charcoal particles (having tendency to parallel orientation) and few soft ferruginous nodules, sometimes associated with the charcoal. It is underlain by the very pale 20 cm thick E horizon with well-developed multi-order platy structure. Iron oxide nodules (soft and hard) become more abundant, whereas charcoal particles are fewer. An important diagnostic feature is the type of the lower boundary of this horizon. It is gradual with the bleached material penetrating into the underlying layer along pores and fissures and it forms thin glossic fills in the vertical cracks – known as “albeluvic tonguing”. The downward “invasion” of bleached silt material defines the 15 cm thick transitional EB horizon. It still has platy structure, however, platy aggregates are thicker and break into small subangular blocks. The bleached material concentrates on the aggregate surface whereas the internal part is darker and contains more clay. This distribution produces a heterogeneous color pattern: the network of pale veins is spread among the brown “islands”. Iron-manganese pedofeatures

are presented by small nodules and films mostly associated with the thin fissures.

The illuvial part of the profile (Bt1, 30 cm thick – Bt2, 35 cm thick – Bt3, 65 cm thick) is marked by a contrasting difference of main morphological characteristics. It has clayey loamy texture, subangular blocky to prismatic structure and predominantly brown color. However, silty bleached material is still abundant: in the Bt1 horizon it forms films on most ped surfaces. In many cases these films overly brown clay coatings. In Bt2 the pale silt component decreases and is restricted mostly to the larger vertical cracks. Aggregates are covered with continuous clay coatings. The prismatic blocky peds become coarser and clay coatings on their surfaces turn patchy in the Bt3 horizon. All Argic horizons have also ferruginous pedofeatures, in Bt1 these are mostly small nodules, whereas in Bt2 and Bt3 dendritic iron-manganese spots occur.

The BC horizons have brighter brown-yellow color and weaker pedogenic structure. Where the paleosol lies on Dnieper loess we observed a clear banded pattern in these horizons: darker clayey stripes were alternating with the pale-yellow silty bands.

All these horizons are free of carbonates and the latter appear only in the underlying loess, at the depth of 250 cm from the Mikulino surface. The paleosol was defined as Haplic Albeluvisol (Fig. 4).

Microscopic observations reveal predominance of silt grains in the groundmass. Their mineralogical composition is rather poor – quartz is clearly dominant, K-Na feldspars are present in minor quantities, micas and heavy minerals are few.

The A horizon has complex microstructure with combination of platy and isometric crumbly aggregates. Dark organic pigment with heterogeneous distribution causes interchanging of dark-colored and light-colored micro-zones. There are few signs of faunal activity: some zoogenic channels with excrement infillings were found; groundmass contains numerous charcoal particles (Fig. 5a).

In the E horizon dominant fine platy aggregates demonstrate clear textural differentiation with prevailing bleached coarse silt in the upper parts and close to the pores and fine silt and plasmic material in the central and lower parts. Frequent compact rounded simple iron nodules are widespread in the groundmass, sometimes charcoal is observed in their nucleus (Fig. 5b). We encountered fragments of clay coatings embedded in the bleached silty matrix (Fig. 5c,d).

The EB horizon also has well developed platy structure with even stronger intra-pedal differentiation of particle size. Fine silt and clay is concentrated inside the plates, while the peripheral parts consist of bleached silt. Iron pedofeatures are frequent and variable: we observed rounded nodules and incrustation of platy aggregates mainly on the bottom side (fig. 5e).

Traces of platy aggregation are still observed in the Bt1 horizon but plates are frequently neighbouring subangular blocks (Fig. 5f). The pores have common bleached silty coatings as well as infillings, whereas deformed and fragmented illuviated clay pedofeatures were found in the interior of the peds (Fig. 5g). Undisturbed clay illuvial pedofeatures still related to the pores were not observed. Small ferruginous nodules are found both, in the groundmass and silty infillings.



Horizon	Total element concentrations, %							
	SiO <sub>2</sub>	TiO <sub>2</sub>	Al <sub>2</sub> O <sub>3</sub>	Fe <sub>2</sub> O <sub>3</sub>	MgO	CaO	Na <sub>2</sub> O	K <sub>2</sub> O
Eemian paleosol [Oberlaab, Austria]								
WP upper	74.14	1.12	14.86	4.95	1.03	0.81	0.97	1.94
WP lower	74.46	1.12	14.75	4.68	1.01	0.85	1.00	1.92
Btg1	76.16	1.03	13.15	4.66	1.09	0.66	0.94	2.11
Btg2	70.26	0.94	16.49	6.38	1.60	0.67	0.79	2.60
BCtg	70.58	0.95	16.02	6.30	1.63	0.81	0.88	2.58
BCg	71.37	0.94	15.33	6.01	1.59	0.91	1.04	2.56
C	71.48	0.96	15.47	5.86	1.55	0.93	1.03	2.45
Mikulino paleosol [Alexandrov quarry, Russia]								
A	82.30	0.90	9.44	2.68	0.61	0.81	0.65	2.34
E upper	85.37	0.90	7.69	1.88	0.43	0.62	0.56	2.38
E lower	83.72	0.94	8.54	2.33	0.55	0.58	0.64	2.52
EBt	81.97	0.95	9.30	3.14	0.71	0.60	0.58	2.62
Bt1	81.30	0.92	9.70	3.40	0.73	0.62	0.55	2.63
Bt2	81.01	0.81	10.23	3.44	0.78	0.64	0.53	2.37
Bt3	80.67	0.79	10.49	3.45	0.76	0.67	0.59	2.39
BC	82.17	0.77	9.60	3.02	0.64	0.68	0.49	2.43

WP – Würmian pedosediment

Only the Bt2 and Bt3 horizons have undisturbed layered illuvial clay coatings on the pore walls (Fig. 5h). However, bleached silt concentrations are still present and concentrated mainly in fissures and large channels. They have abrupt boundaries to the groundmass, and sometimes they are juxtaposed on the clay coatings or occur in the neighboring pores (Fig. 5i,j).

In the thin sections of the banded BC horizons we observed a clear laminar structure with alternating bands enriched in coarse silt and fine clay materials. Even in these horizons we observed few thin clay coatings, which showed no clear preference for specific bands.

#### Physical and chemical characteristics

Bulk chemical composition demonstrates similar tendencies of profile differentiation in terms of element concentrations. The upper eluvial horizons have higher quantities of Si at the expense of Al and also Fe and Mg. However, it should be noted that absolute values are quite different in the two studied profiles: the material of Mikulino paleosol in Alexandrov has much higher Si content (80–85%) than that of the Eemian soil in Oberlaab (70–76%), whereas the latter is more rich in Al, Fe as well as alkaline and alkaline earths (except K that has similar concentrations in both paleosols) (Tab. 1).

Clay content shows a clear and similar distribution trend in both profiles: the maximum is observed in the Bt horizons, whereas lower values are found in the eluvial E horizon in Alexandrov and upper Würmian pedosediment in Oberlaab (in the latter – with contrasting fluctuations between upper and lower parts). The highest values of the dithionite extractable iron also correspond to the illuvial part of both profiles. However, iron and clay maxima do not coincide: iron content is highest in the upper Bt1 horizons,

whereas clay has its maximum below in the Bt2 horizons. Again, both clay and Fe<sub>d</sub> contents although having very similar distribution tendencies in both profiles, demonstrate different absolute values. For both components they are considerably higher in the Oberlaab profile (Tab. 2).

Clay mineral assemblages show very clear differentiation in both studied profiles. Interlayered illite-smectite with variable proportion of both components – (1.4–1.5 nm peak, shifting to smaller angles on glycolation) decreases strongly in the eluvial E horizons and is much higher in the illuvial stratum and parent material. In the Eemian Luvisol of Oberlaab this tendency is rather weak and expressed mostly in different proportions of smectite-rich and smectite-poor mixed layered components. The latter increase in the upper part of the profile. In the Mikulino Albeluvisol of Alexandrov this tendency is much stronger: all smectitic components decrease in the eluvial part, whereas on the contrary, illite and kaolinite (respectively 1.0 nm and 0.7 nm peak, the latter disappearing after 550 °C heating) are more abundant (see Table 3 and Fig. 6). Only in the pedosediments, eluvial and upper illuvial horizons (EB and Bt1) we found mixed-layered minerals with chloritic component (“shoulder” of 1.0 nm peak towards smaller angles after heating indicating incomplete contraction of 1.4–1.5 nm maximum), which we identify with the hydroxyl-interlayered vermiculite and smectite (HIV and HIS) (BAMHISEL & BERTSCH 1989).

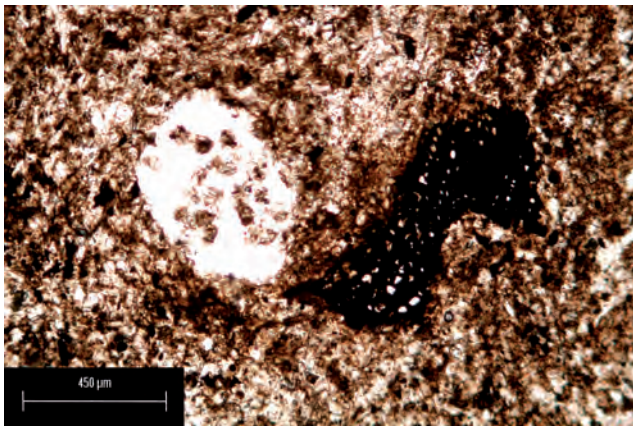
## 4 Discussion

### *Pedogenesis of paleosols – comparison with the regional modern analogues*

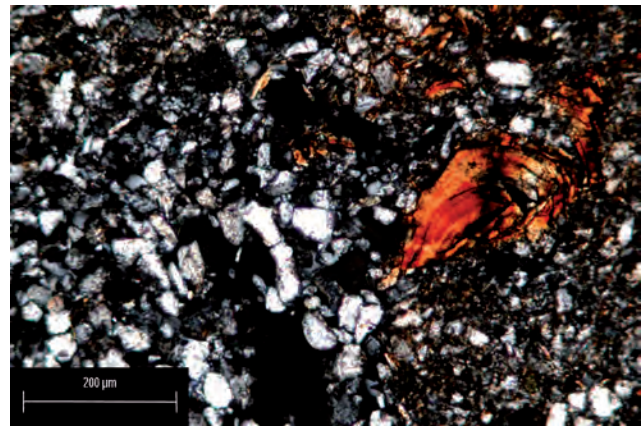
The question to be answered before soil forming processes in the paleosol can be assessed is how complete is their profile

Tab. 1: Bulk chemical composition: selected major elements.

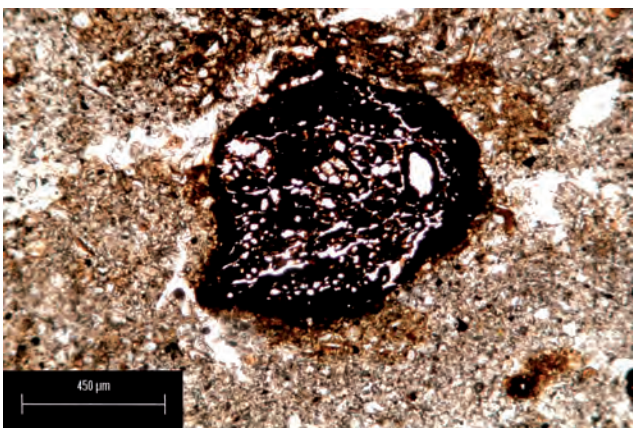
Tab. 1: Ergebnisse der Elementaranalysen: Ausgewählte Hauptelemente.



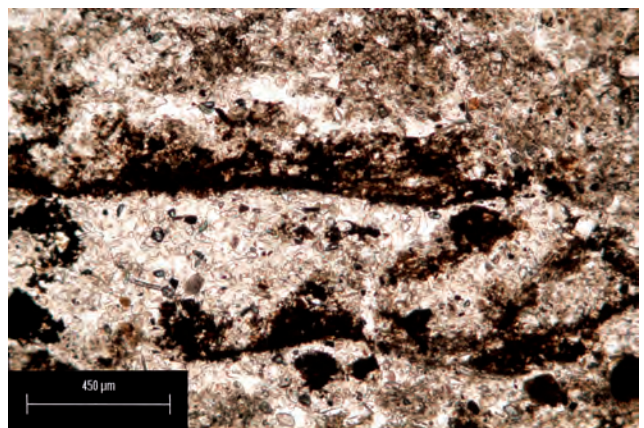
a) Pore with the excremental infilling, charcoal particle. A horizon, plain polarized light.



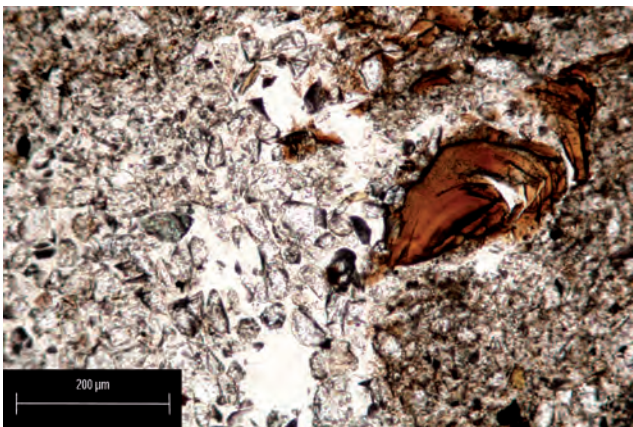
d) Same as c), crossed polarizers; note strong interference colors and undulating pattern of extinction.



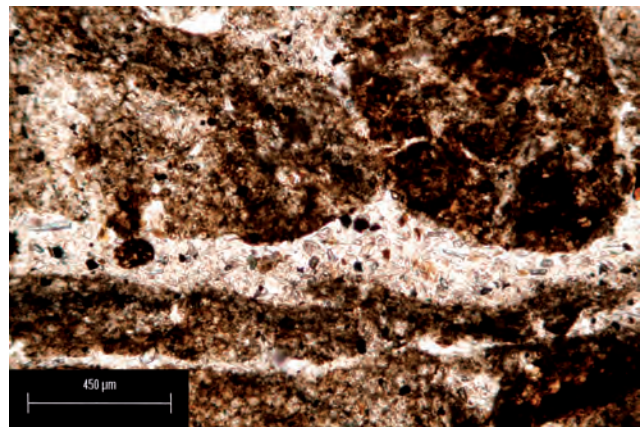
b) Ferruginous nodule with charcoal in the center. E horizon, plain polarized light.



e) Platy structure, fissures between the plates are filled with bleached silt, ferruginous hypocoatings are located on the lower surfaces of the plates. EBt horizon, plain polarized light.



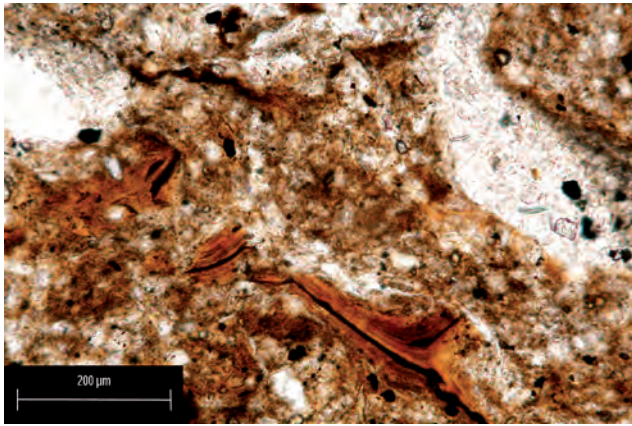
c) Fragment of clay coating surrounded by bleached silt. E horizon, plain polarized light.



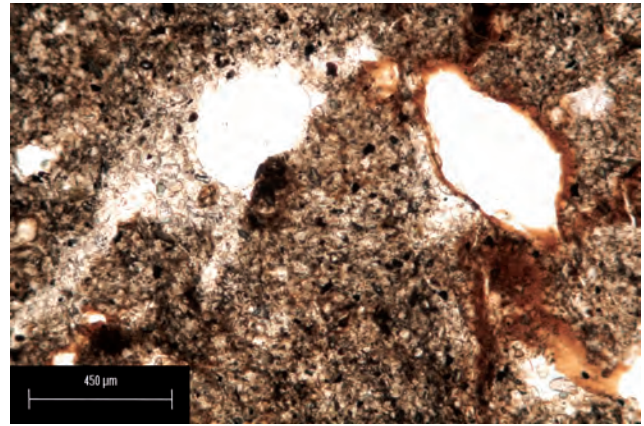
f) Platy and blocky aggregates, pores are filled with bleached silt, intrapetal matrix enriched with fine material. Bt1 horizon, plain polarized light.

Fig. 5: Micromorphology of the Mikulino paleosol in Alexandrov.  
Abb. 5: Mikromorphologie des Mikulino Paläobodens in Alexandrov.

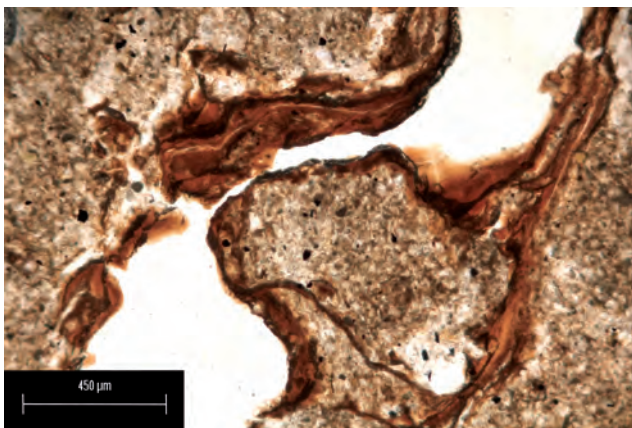




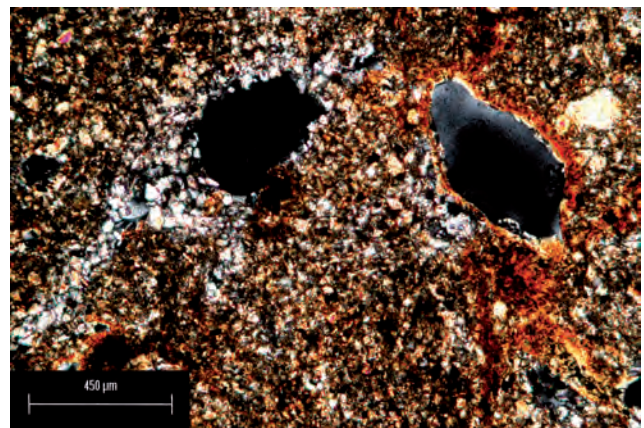
g) Fragmented and deformed clay illuvial pedofeatures incorporated into groundmass. Bt1 horizon, plain polarized light.



i) Bleached silt (left) and limpid clay coating (right) in the neighboring pores. Bt3 horizon, plain polarized light.



h) Continuous undisturbed clay coating in the pore. Bt3 horizon, plain polarized light.



j) Same as i), crossed polarizers, note strong interference colors of the clay coating.

and to what extent it is affected by post-burial (diagenetic) processes.

In the Oberlaab profile the layer directly above the Eemian Bt horizon has clear signs of sedimentation and mixing. These signs are stronger in the upper part of this horizon, where grain size fluctuations mark a lithological discontinuity; in this layer few thin clay coatings are most probably the lowermost traces of clay illuviation from the Holocene Luvisol. However, stagnic ferruginous pedofeatures and presence of the specific clay component – hydroxyl interlayered vermiculites and smectites suggest that material of the eluvial horizon, although redeposited is present in this layer. Minor signs of disturbance (anorthic iron-clay nodules, charcoal) are present even in the Bt1 horizon, and the paleosol is supposed to be intact only below the Bt1 (TERHORST et al. 2003).

In case of Alexandrov quarry the grade of preservation is high: a complete sequence of genetic horizons including the burned litter is present. Only the A horizon has signs of redeposition: oriented charcoal particles. Moreover, no effects of posterior pedogenesis are detected in this paleosol, due to its protection by a thick overlying sediment layer.

In both profiles a similar set of pedogenetic processes is detected. Clay illuviation is evidenced by clay coatings (observed both on macro- and microscale) as well as a maximum of clay content in the Bt horizon compared both to the underlying C and overlying E horizon (in situ or redepos-

ited). Clear micromorphological signs of silicate weathering are observed in the biotite particles. Increase of dithionite extractable iron, which mostly includes fine oxides produced by weathering is an important analytical indicator. An enhanced Si content in the eluvial horizons of Luvisols is often interpreted as a result of decay of all unstable silicates (including part of clay minerals) and residual accumulation of quartz (TARGULIAN et al. 1974b). Loss of smectites in the same horizons is also considered to be a result of selective destruction of the most unstable clay components (TONKONOGOV et al. 1987). However, it should be taken into account that clay illuviation could also contribute to these properties. Removal of clay from E horizon also could cause an increase of Si, due to relative accumulation of coarse components richer in this element. Smectites are most fine and dispersible components, that could be preferentially mobilized by suspension transport and removed from the eluvial horizons (VAN RANST et al. 1982). Thus, geochemical and mineralogical indicators give a mixed signal from both processes, a fact that unfortunately is rarely taken into account when elemental composition of loess-paleosol sequences is interpreted through various “weathering indices”.

More clear evidence of clay mineral transformation is provided by the HIV accumulation in the upper part of the paleosols. This component is known to be formed from 2:1 clay minerals with labile structure due to synthesis of



Tab. 2: Grain size distribution and dithionite extractable iron content.

Tab. 2: Korngrößenzusammensetzung und dithionitlöslicher Eisengehalt.

Horizon	Grain size fractions, %			Fe <sub>d</sub> , %
	sand	silt	clay	
Eemian paleosol [Oberlaab, Austria]				
WP upper	5.4	68.5	26.1	0.69
WP lower	8.2	69.8	22.0	0.65
Btg1	10.1	66.7	23.2	0.98
Btg2	6.3	55.9	37.8	0.73
BCtg	4.6	60.9	34.5	0.61
BCg	4.3	64.4	31.3	0.37
C	5.7	65.4	28.9	0.50
Mikulino paleosol [Alexandrov quarry, Russia]				
A	1.4	81.8	16.8	0.49
E upper	1.4	88.7	9.9	0.22
E lower	1.2	86.5	12.3	0.32
EBt	1.1	79.3	19.6	0.43
Bt1	1.0	78.2	20.8	0.51
Bt2	1.2	70.3	28.5	0.45
Bt3	1.5	76.1	22.4	0.43
BC	1.2	80.0	18.8	0.37

WP – Würmian pedosediment

fragmentary Al-hydroxyl layer between the 2:1 stacks. This process takes place in acid soil environment and Al for it is provided by hydrolytic alteration of silicates – primary, or the same clay components (BAMHISEL & BERTSCH 1989). Presence of these components in the eluvial horizons (in situ in Alexandrov and redeposited in Oberlaab) point to acid weathering in both interglacial paleosols. However, the alternative explanation of higher content of chloritic component in the upper horizons of acid forest soils on loess also exists. JAMAGNE et al. (1984) suppose that these minerals are not formed through the synthesis, but rather by simple breakdown and partial degradation of primary chlorites from silt fractions.

Surface redoximorphic (stagnic) processes produced ferruginous pedofeatures throughout the profile, but most abundant and variable in the eluvial and upper Bt horizons. There they are presented by nodules as well as by coatings and incrustations, indicative of iron migration (BRONNIKOVA et al. 2000). Besides intra-horizontal short-distance redistribution we suppose certain eluvial-illuvial transport of iron from E to EB and upper Bt horizons due to this process. Dithionite extractable iron is depleted in E horizons and has its maximum in the Bt1; also the abundance of the ferruginous pedofeatures is maximal in the EB and Bt1 horizons. Interestingly magnetic susceptibility also demonstrates maxima in EB (Alexandrov quarry) (RIVAS et al. 2003) and Bt1 (Oberlaab) (SOLLEIRO et al. 2013, this volume) that could also be related to the increase of pedogenic iron oxides. It should be taken into account that surface redoximorphic processes could also contribute to acid weathering and HIV neof ormation through the process of ferrollysis (BRINKMAN 1970).

Being similar regarding the set of the pedogenetic processes the studied paleosols differ greatly in their relative development. The Austrian paleosol demonstrates much stronger clay illuviation in the Bt horizon, whereas the Russian profile has much stronger evidences of eluvial and surface redoximorphic processes. This tendency becomes even clearer by comparison with the modern soils. The Eemian soil in Oberlaab has higher clay content and more abundant clay illuvial pedofeatures than the overlying Holocene Luvisol (SOLLEIRO et al. 2013, this volume). The Mikulino Albeluvisol in Alexandrov quarry compared to the local Holocene soil, a Haplic Chernozem, shows contrasting qualitative differences in the set of key pedogenetic processes. The Chernozem is characterized by high accumulation of dark humus and development of coprogenic granular structure resulting in the development of Mollic topsoil horizon. Below, in the Bk horizon abundant neof ormed carbonates are observed. Morphological features of clay translocation are very few (if any), clay content is rather uniform throughout the profile showing no tendency towards eluvial-illuvial differentiation (GERASIMOVA et al. 1996; BRONGER 2003). This set of pedogenetic properties typical for steppe pedogenesis under Ustic soil moisture regime (BRONGER 2003) provides undoubted evidence that on the local scale the Holocene climate has been drier than that of the last interglacial – in agreement with the above mentioned reconstruction for Eastern Europe by MOROZOVA (MOROZOVA 1981; MOROZOVA et al. 1998). For current research it is interesting to compare the studied Mikulino profile with the nearest analogue having similar profile organization, to assess changes in the Albeluvisol pedogenesis on the regional scale. The Mikulino Albeluvisol in Alexandrov quarry compared to the Holocene Albeluvisol of the Moscow region (TARGULIAN et al. 1974b), does not show stronger clay accumulation, which is contrary to the case study in Low Austria. However, it demonstrates major advance of eluvial and stagnic processes – bleaching and clay depletion besides E and EB horizons affected the whole Bt horizon, “attacking” the area of earlier clay illuviation. Fresh illuvial pedofeatures pointing to active clay illuviation appear only in the lower Bt2 and BtC horizons. In profiles of Holocene Albeluvisols (KÜHN et al. 2006) and Grey Forest Soils (MIEDEMA et al. 1999) this “aggression” of eluviation against degrading illuvial areas is also observed but usually is not so deep. It is strong in EBt horizon and decreases in the upper part of Bt horizons, where it is represented mostly by deep thin bleached tongues (albeluvisol tonguing), whereas the areas between the tongues are much less affected (SPIRDONOVA et al. 1999; SAUER et al. 2009). Thus, in both cases last interglacial paleosols present higher grade of development than analogous Holocene profiles in the region, however, the particular mode of this tendency is different.

These differences could be explained when linked to the classic evolution scheme for forest soil formation under temperate humid climate (PÉDRO et al. 1978). Following this scheme intensive clay illuviation develops after initial leaching phase and results in the formation of Argic horizon. However, it is succeeded by the subsequent “degradation” stage of further acidification, surface redoximorphic processes and (possibly) ferrollysis. At this stage clay illuviation is hampered and part of accumulated clay is lost due to acid weathering. We suppose that Eemian Luvisol in Oberlaab

Horizons	Types of clay minerals				
	Smectite/ illite	Illite / smectite	Chloritised 2:1 minerals	Illite	Kaolinite
Eemian paleosol [Oberlaab, Austria]					
WP upper	-	xxx	x	xxx	xx
WP lower	-	xxxx	xx	x	x
Btg 1	-	xxxx	xx	x	x
BCtg	xxxx	xx	-	x	x
BCg	xxxxx	x	-	xx	x
C	xxxxx	x	-	xx	x
Mikulino paleosol [Alexandrov quarry, Russia]					
E upper	-	xxx	xx	x	xx
E lower	-	xx	xx	xx	xxx
EBt	-	xx	xx	xx	xx
Bt2	xxxx	xx	-	x	x
C	xxxxx	-	-	x	x

Tab. 3: Clay mineral composition.

Tab. 3: Tonmineralogische Zusammensetzung.

WP – Würmian pedosediment  
 xxxxx – dominant  
 xxxx – abundant  
 xxx – frequent  
 xx – few  
 x – traces  
 - - not detected

still developed within the stage of predominant clay formation and illuviation, whereas Mikulino Albeluvisol in Alexandrov quarry already reached the stage of “degradation”.

This difference in the evolutionary status is most probably related to the composition of the paleosol parent material. The Riss loess in Austria is richer in weatherable minerals (including phyllosilicates like biotite), has more clayey texture, is enriched in bases and has lower Si content. This increases the potential for neutralizing excessive acidity as well as for the neoformation of clay and iron oxides. The Dnieper loess is much poorer, strongly enriched in quartz, thus buffering and clay generating capacities are lower.

#### **Chronological and paleoecological background of the advanced Eemian/Mikulino paleosol development**

On the local scale, especially in the border regions, qualitative differences between Mikulino/Eemian paleosol and modern soil profile are clearly related to climatic shift as shown by the case of Alexandrov exposure. The question arises, what are the reasons why last interglacial paleosols demonstrate more advanced development than Holocene soils belonging, however, to the same type of pedogenesis (proven by similarity of horizonation, main macro- and micromorphological characteristics, clay mineral association etc.)? We suppose that in many cases the duration of pedogenesis rather than “strong interglacial paleoclimates relative to the present-day climate” (as supposed by MAHANEY et al. 1993) could account for these differences. Comparison with the European paleobotanical records with high-resolution chronological scale provides insight into this problem. Detailed correlation with the deep sea isotope records and establishing the precise position of Blake paleomagnetic event allowed reliable dating of the main paleobotanic phases of Eemian established earlier in the pollen spectra from terrestrial (mostly lacustrine) sediments (ZAGWIJN 1996; TURNER 2002a). Earlier the last interglacial was associated with the Marine Isotope Stage (MIS) 5e (SHAKLETON 1969). Recently, it was shown that the spread of forest vegetation in Europe postdated the onset of MIS 5e but on the other hand

extended into the subsequent stage 5d despite the beginning of global cooling, increase of ice volume, and drop of sea level (SHAKLETON et al. 2003; SIER et al. 2011). This extension concerns in particular the last “post-temperate” paleobotanical phase of boreal forests. Thus, although the duration of the last interglacial sensu stricto is supposed by many authors to be about 11 000 yr (similar to that of the Holocene) (CASPER et al. 2002; TURNER 2002b), the total succession of the Eemian forest vegetation phases in the Western and Central Europe could reach 20,000 yr- nearly twice longer than the Holocene (KUKLA et al. 2002).

It should be stressed that all phases of humid forest ecosystems including the last one of the boreal forests provide conditions for clay illuviation and development of Argic horizons on loess-like sediments. Thus, the scenario of long-term clay illuviation during the complete succession of different forest phases during MIS5 explains more advanced development of Eemian/Mikulino paleosols compared to the Holocene analogues. Rather cold climatic conditions during the last stages of Albeluvisol profile development in Central Russia are confirmed by micromorphological observations. Typical features of eluvial-illuvial processes are combined with deep frost effects in the upper part of the profile. Lenticular structure with the microscale grain size differentiation is related to ice lensing (VAN VLIET-LANOË 2010), iron incrustations of the platy aggregates are also characteristic for seasonally deeply frozen soils (FEDOROVA & YARILOVA 1972).

An even more complex scenario for interaction of illuvial and frost processes is required for the Eemian Luvisol in Oberlaab. Here, the illuvial and frost features not only co-exist but show complex interaction. Frost fracturing propagates into the Bt horizon disrupting the older generation of the clay illuvial pedofeatures and generating blocky-lenticular structure, whereas the younger generation of clay coatings covers these aggregates. The clay translocation process itself was heterogeneous as evidenced by variable composition of illuvial pedofeatures. Impure dusty and coarse clay coatings (“mud cutans”) are attributed to the

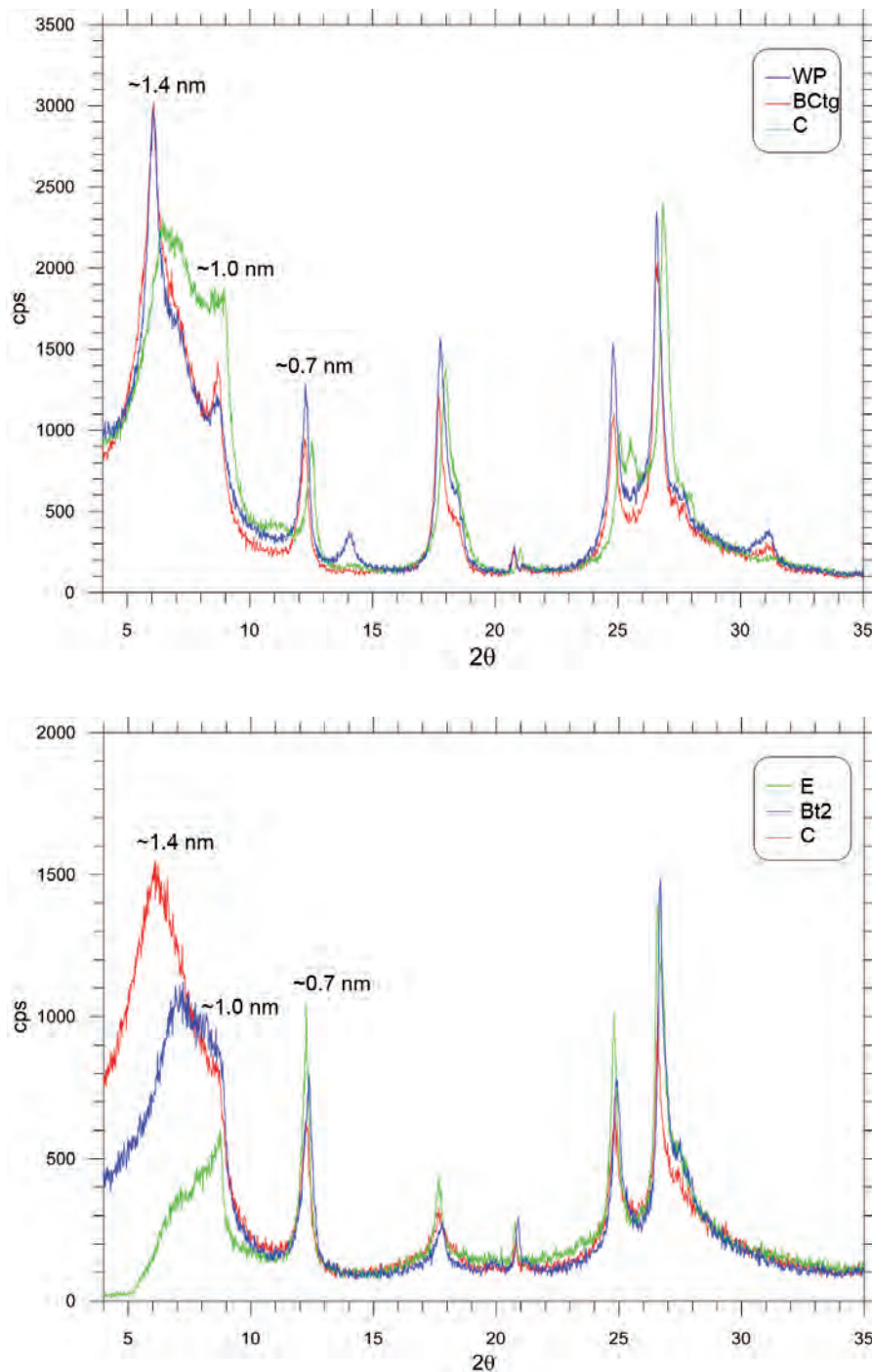


Fig. 6: X-ray diffraction patterns of oriented air-dry specimens of clay fractions from selected paleosol horizons; a) Oberlaab profile, b) Alexandrov profile.  
 Abb. 6: Röntgenbeugungsdiagramme von orientierten luftgetrockneten Proben der Tonfraktion aus ausgewählten Horizonten der Paläoböden; a) Profil Oberlaab, b) Profil Alexandrov.

fast percolation of suspensions after snowmelt in freeze-thaw soils (VAN VLIET-LANOË 2010). The laminated clay coatings (which we observed in the lower part of the Eemian Luvisol of Oberlaab) where pure limpid and impure silty microlayers are juxtaposed, could be interpreted as alternation of “normal” illuviation due to slow percolation and fast deposition from snow melt suspensions (KÜHN et al. 2010).

This suggests that clay illuviation in the Oberlaab profile was polygenetic and discontinuous, interrupted by the stages of deep frost processes. Such interplay of features is well known for Quaternary Bt horizons and could be used for pedostratigraphic inferences (summarized by VAN VLIET-LANOË 2010)

Concerning possible chronological and paleoecological implications we should take into account that no paleosols

or pedosediments clearly correspond to the Early Würmian interstadials. Thus, we could suppose that the pedogenesis of these warmer stages could contribute to the formation of the “Eemian” profile in Oberlaab. In several profiles of Europe the soils of these interstadials are characterized by dark humus accumulation and correspond to steppe environment (e.g. Mosbacher Humuszonen in Germany, Krutitsa soil in Russia, etc.). From such type of pedogenesis one would not expect contribution to the clay illuviation. However, this type of soil and landscape conditions seems to be not sole during the Early Würmian interstadials. Forest ecosystems have been also registered by various European paleoecological proxies (BIBUS et al. 2002). The warmer climate and reforestation could provide conditions for Luvisol pedogenesis, although interrupted by cold phases of the early glacial. Early Würmian Bt horizons clearly separated from the Eemian



Luvisol and correlative to Mosbacher Humuszonen were reported in the Rhine Area (LESER 1970). As mentioned above (see 'Introduction') several authors described superimposing of the Early Würmian clay illuviation (associated with Grey Forest Soil formation) over the pre-existing Eemian Luvisol producing a pedocomplex.

We suppose that Early Würmian clay illuviation could develop in the "Eemian" Argic horizon interrupted by frost processes imposed by the cold stadials in Oberlaab. Thus, its morphological and analytical (clay content, geochemical differentiation) characteristics could be an integral of longer Luvisol pedogenesis including Eemian Interglacial sensu lato (MIS 5e and part of MIS 5d) and Early Würmian interstadials (correlative to MIS 5c and MIS 5a). Such cumulative effect could be present in a number of the Eemian Luvisol profiles where Early glacial sedimentation was not sufficient to separate interglacial and interstadial soil bodies. In this way we return to the earlier ideas of BOARDMAN (1985) who stated: "Geological and palynological evidence from terrestrial, midlatitude sites suggests that temperate conditions conducive to soil formation existed for periods greatly in excess of 10,000 yr during the middle and late Pleistocene. Available data on soils formed during this interval from Western Europe and midwestern United States are best explained by relatively long interglaciations or the development of composite soils over a number of temperate periods".

## Acknowledgements

We would like to thank all colleagues – scientists and students from Austria, Germany, Mexico and Russia who took part in the field and laboratory research of the ICSU 2003 project "Polygenetic models for Pleistocene paleosols" and generated a productive and friendly atmosphere of the project sessions. We are grateful to the International Council of Science (ICSU) whose funding made possible this wonderful experience of intensive interdisciplinary and international collaboration. Special thanks are for Prof. Winfried Blum who encouraged us at the initial stage of the ICSU Project development and provided valuable advices and support.

We would also like to express our gratitude to Dirección General de Asuntos de Personal Académico, UNAM (DGAPA UNAM) for funding the sabbatical stay of S. Sedov in the University of Würzburg, allowing to finalize this research and to prepare the results for publication.

## References

- ANTOINE, P., ROUSSEAU, D.D., LAUTRIDOU, J.P. & HATTÉ, C. (1999): Last Interglacial-Glacial climatic cycle in loess-palaeosol successions of north-western France. – *Boreas*, 28: 551–563.
- ANTOINE, P., ROUSSEAU, D., ZÖLLER, L., LANG, A., MUNAUT, A.V., HATTÉ, C. & FONTUGNE, M. (2001): High-resolution record of the last Interglacial-Glacial cycle in the Nussloch loess-palaeosol sequences, Upper Rhine Area, Germany. – *Quaternary International*, 76 (77): 211–229.
- BAMHISEL, R.I. & BERTSCH P.M. (1989): Chlorites and hydroxy-interlayered vermiculite and smectite. – In: DIXON, J.B., & WEED, S.B. (eds): *Minerals in Soil Environments*: 729–788; Madison, Wisconsin (Soil Science Society of America).
- BIBUS, E., RAHLE, W. & WEDEL, J. (2002): Profilaufbau, Molluskeneinführung und Parallelisierungsmöglichkeit des Altwürmabschnittes im Lössprofil Mainz-Weisenau. – *Eiszeitalter und Gegenwart*, 51: 1–14.
- BOARDMAN, J. (1985): Comparison of soils in Midwestern United States and Western Europe with the interglacial record. – *Quaternary Research*, 23: 62–75.
- BRINKMAN, R. (1970): Ferrollysis, a hydromorphic soil forming process. – *Geoderma*, 3: 199–206.
- BRONGER, A. (1976): Zur quartären Klima- und Landschaftsgeschichte des Karpatenbeckens auf paläopedologischer und bodengeographischer Grundlage. – *Kieler Geographische Schriften*, 45: 1–268.
- BRONGER, A. (2003): Bodengeographie der Waldsteppen und Steppen. – In: BLUME, H. P., FELIX-HENNINGSEN, P., FISCHER, W. R., FREDE, H. G., HORN, R. & STAHR, K. (eds): *Handbuch der Bodenkunde*, 1–6; Landsberg/Lech (Ecomed).
- BRONGER, A. & HEINKELE, T. (1990): Mineralogical and clay mineralogical aspects of loess research. – *Quaternary International*, 7–8: 37–51.
- BRONGER, A., WINTER, R. & HEINKELE, T. (1998): Pleistocene climatic history of East and Central Asia based on paleopedological indicators of loess-paleosol sequences. – *Catena*, 34: 1–17.
- BRONNIKOVA, M.A., SEDOV, S.N. & TARGULIAN, V.O. (2000): Clay, iron-clay, and humus-clay coatings in the eluvial part of Soddy-Podzolic soils profile. – *Eurasian Soil Science*, 33(6): 577–585.
- BULLOCK, P., FEDOROFF, N., JONGERIUS, A., STOOPS, G., TURSINA, T. & BABEL, U. (1985): *Handbook for soil thin section description*. – 152 p., Wolverhampton, United Kingdom (Waine Research Publications).
- BULLOCK, P. & THOMPSON, M.L. (1985): Micromorphology of Alfisols. – In: DOUGLAS, L.A. & THOMPSON, M.L. (eds): *Soil micromorphology and soil classification*, Soil Science Society of America Special Publication, 15: 17–47; Madison.
- CASPERS, G., FREUND, H., MERKT, H., MERKT, J. & MÜLLER, H. (2002): The Eemian interglaciation in northwestern Germany. – *Quaternary Research*, 58: 49–52.
- CATT, J.A. (1996): Recent work on Quaternary paleosols in Britain. – *Quaternary International*, 3436: 183–190.
- DEMEK, J. & KUKLA, J. (eds.) (1969): *Periglazialzone, Löss und Paläolithikum der Tschechoslowakei*. – 158 p., Brno (Tschechoslowakische Akademie der Wissenschaften, Geographisches Institut).
- FEDOROVA, N.N. & YARILOVA, E.A. (1972): Morphology and genesis of prolonged seasonally frozen soils of western Siberia. – *Geoderma*, 7: 1–13.
- FINK, J. (1956): Zur Korrelation der Terrassen und Löss in Österreich. – *Eiszeitalter und Gegenwart*, 7: 49–77.
- FRECHEN, M., ZANDER, A., CILEK, V. & LOŽEK, V. (1999): Loess chronology of the Last Interglacial/Glacial cycle in Bohemia and Moravia, Czech Republic. – *Quaternary Science Reviews*, 18: 1467–1493.
- GERASIMENKO, N.P. (2006): Upper Pleistocene loess-palaeosol and vegetational successions in the Middle Dnieper Area, Ukraine. – *Quaternary International*, 149: 55–66.
- GERASIMOVA, M.I., GUBIN, S.V. & SHOBA, S.A. (1996): Soils of Russia and adjacent countries: Geography and Micromorphology. – 204 p.; Moscow-Wageningen (Moscow State University & Wageningen Agricultural University).
- GOLYEVA, A. & SYCHEVA, S. (2010): Soils, plants and climate of the Eemian Interglacial local landscapes of the Russian Plain on base of biogenic silica analysis. – *Eurasian Soil Science*, 43, 13: 1569–1573.
- HAESERTS, P., MESTDAGH, H. & BOSQUET, D. (1999): The sequence of Remicourt (Hesbaye, Belgium): new insights of the pedo- and chronostratigraphy of the Rocourt Soil. – *Geologica Belgica*, 2: 5–27.
- HAESERTS, P. & MESTDAGH, H. (2000): Pedosedimentary evolution of the last interglacial and early glacial sequence in the European loess belt from Belgium to central Russia. – *Geologie en Mijnbouw / Netherlands Journal of Geosciences*, 79 (2/3): 313–324.
- JAMAGNE, M., DE CONINCK, F., ROBET, M. & MAUCORPS, J. (1984): Mineralogy of clay fractions of some soils on loess in northern France. – *Geoderma*, 33: 319–342.
- JARY, Z. (2009): Periglacial markers within the Late Pleistocene loess-palaeosol sequences in Poland and western part of Ukraine. – *Quaternary International*, 198: 124–135.
- JARY, Z. (ed.) (2011): Closing the gap – North Carpathian loess traverse in the Eurasian loess belt. – *International Workshop, 6th Loess Seminar in Wrocław, May 16–21, 2011, Abstract and field guide book*, 80 p.; Wrocław (Institute of Geography and Regional Development, University of Wrocław).
- KEMP, R.A. (1999): Micromorphology of loess-palaeosol sequences: a record of palaeoenvironmental change. – *Catena*, 35(2–4): 179–196.
- KOOISTRA, M.J. & PULLEMAN, M.M. (2010): Features related to faunal activity. – In: STOOPS, G., MARCELINO, V. & MEES, F. (eds): *Interpretation of Micromorphological Features of Soils and Regoliths*. Chapter 18: 397–418; Amsterdam (Elsevier).
- KÜHN, P. (2003): Micromorphology and Late Glacial/Holocene genesis of

- Luvisols in Mecklenburg–Vorpommern (NE-Germany). – *Catena*, 54: 537–555.
- KÜHN, P., BILLWITZ, K., BAURIEGEL, A., KÜHN, D. & ECKELMANN, W. (2006): Distribution and Genesis of Fahlerden (Albeluvisols) in Germany. – *Journal of Plant Nutrition and Soil Science*, 169: 420–433.
- KÜHN, P., AGUILAR, J. & MIEDEMA, R. (2010): Textural pedofeatures and related horizons. – In: STOOPS, G., MARCELINO, V. & MEES, F. (eds): Interpretation of Micromorphological Features of Soils and Regoliths. Chapter 11: 217–250; Amsterdam (Elsevier).
- Kukla, G.J. (1977): Pleistocene land-sea correlations I. Europe. – *Earth-Science Reviews*, 13(4): 307–374.
- KUKLA, G.J., BENDER, M.L., DE BEAULIEU, J.L., BOND, G., BROECKER, W.S., CLEVERINGA, P., GAVIN, J.E., HERBERT, T.D., IMBRIE, J., JOUZEL, J., KEIGWIN, L.D., KNUDSEN, K.L., MCMANUS, J.F., MERKT, J., MUHS, D.R., MULLER, H., POORE, R.Z., PORTER, S.C., SERET, G., SHACKLETON, N.J., TURNER, C., TZEDAKIS, P.C. & WINOGRAD, I.J. (2002): Last interglacial climates. – *Quaternary Research*, 58: 2–13.
- Leser, H. (1970): Die fossilen Böden im Lößprofil Wallertheim (Rheinhesisches Tafel- und Hügelland). – *Eiszeitalter und Gegenwart*, 21: 108–121.
- MAHANAY, W.C., ANDRES, W. & BARENDREGT, R.W. (1993): Quaternary paleosol stratigraphy and paleomagnetic record near Dreihäusen, central Germany. – *Catena*, 20(1–2): 161–177.
- MARKOVIC, S.B., BOKHORST, M.P., VANDENBERGHE, J., MCCOY, W.D., OCHES, E.A., HAMBACH, U., GAUDENY, T., JOVANOVIC, M., ZÖLLER, L., STEVENS, T. & MACHALETT, B. (2008): Late Pleistocene loess-paleosol sequences in the Vojvodina region, North Serbia. – *Journal of Quaternary Science*, 23(1): 73–84.
- MIEDEMA, R., KOULECHOVA, I.N. & GERASIMOVA, M.I. (1999): Soil formation in Greyzems in Moscow district: micromorphology and particle size distribution. – *Catena*, 34(3–4): 315–347.
- MOROZOVA, T.D. (1981): Evolution of Late Pleistocene soil cover in Europe. – 282 p., Moscow (Nauka Press), in Russian.
- MOROZOVA, T.D., VELICHKO, A.A. & DLUSSKY, K.D. (1998): Organic carbon content in the late Pleistocene and Holocene fossil soils (reconstruction for Eastern Europe). – *Global and Planetary Change*, 16–17: 131–151.
- MOORE, D.E. & REYNOLDS, R.C.JR. (1997): X-Ray diffraction and the identification and analysis of clay minerals. – 378 p., New York (Oxford University Press).
- PÉDRO, G., JAMAGNE, M. & BÉGON, J.C. (1978): Two routes in genesis of strongly differentiated acid soils under humid, cool-temperate conditions. – *Geoderma*, 20: 173–189.
- PETICZKA, R., RIEGLER, D. & HOLAWE, F. (2009): Exkursionsführer. – 28. Jahrestagung des Arbeitskreises Paläopedologie der Deutschen Bodenkundlichen Gesellschaft, 21. bis 23. Mai 2009 in Wien, 68 p.; Wien (Universität Wien, Institut für Geographie und Regionalforschung).
- RIVAS, J., ORTEGA, B., SEDOV, S., SOLLEIRO, E. & SYCHEVA, S. (2006): Rock magnetism and pedogenetic processes in Luvisol profiles: Examples from Central Russia and Central Mexico. – *Quaternary International*, 156/157: 212–223.
- ROUSSEAU, D.D., GERASIMENKO, N., MATVIISHINA, Z.H. & KUKLA, G. (2001): Late Pleistocene environments of the Central Ukraine. – *Quaternary Research*, 56: 349–356.
- RUTTER, N.W., ROKOSH, D., EVANS, M.E., LITTLE, E.C., CHLACHULA, J. & VELICHKO, A. (2003): Correlation and interpretation of paleosols and loess across European Russia and Asia over the last interglacial-glacial cycle. – *Quaternary Research*, 60(1): 101–109.
- SAUER D., SCHÜLLI-MAURER I., SPERSTAD R., SØRENSEN R. & STAHR K. (2009): Albeluvisol development with time in loamy marine sediments of southern Norway. – *Quaternary International*, 209(1–2): 31–43.
- SCHOLGER, R. & TERHORST, B. (2013): Magnetic excursions recorded in the Middle to Upper Pleistocene loess/palaeosol sequence Wels-Aschet (Austria). – *E & G Quaternary Science Journal*, 62/1, this volume.
- SHACKLETON, N.J. (1969): The last interglacial in the marine and terrestrial records. – *Proceedings of Royal Society London B*, 174: 135–154.
- SHACKLETON, N.J., SÁNCHEZ-GOÑI, M.F., PAILLER, D. & LANCELLOT, Y. (2003): Marine isotope substage 5e and the Eemian interglacial. – *Global and Planetary Change*, 36: 151–155.
- SIER, M.J., ROEBROEKS, W., BAKELS, C.C., DEKKERS, M.J., BRÜHL, E., DE LOECKER, D., GAUDZINSKI-WINDHEUSER, S., HESSE, N., JAGISCH, A., KINDLER, L., KUIJPER, W.J., LAURAT, T., MÜCHER, H.J., PENKMAN, K.E.H., RICHTER, D. & VAN HINSBERGEN, D.J.J. (2011): Direct Terrestrial-Marine Correlation demonstrates surprisingly late onset of the last interglacial. – *Quaternary Research*, 75: 213–218.
- SOLLEIRO-REBOLLEDO, E., CABADAS, H., SEDOV, S. & TERHORST, B. (2013): Paleopedological record along the loess-paleosol sequence in Oberlaab, Austria. – *E & G Quaternary Science Journal*, 62/1, this volume.
- SPIRIDONOVA, I.A., SEDOV, S.N., BRONNIKOVA, M.A. & TARGULIAN, V.O. (1999): Arrangement, composition, and genesis of bleached components of loamy Soddy-Podzolic soils. – *Eurasian Soil Science*, 32(5): 507–513.
- SPRAFKE, T., TERHORST, B., PETICZKA, R. & THIEL, C. (2013): Middle and Late Pleistocene paleoenvironments reconstructed from the complex loess-paleosol-sequence Paudorf. – *E & G Quaternary Science Journal*, 62/1, this volume.
- STEPHAN, S. (2000): Bt-Horizonte als Interglazial-Zeiger in den humiden Mittelbreiten: Bildung, Mikromorphologie, Kriterien. – *Eiszeitalter und Gegenwart*, 50: 95–106.
- SYCHEVA, S.A. (1998): New data on composition and evolution of the Mezin Loess-Paleosol Complex in the Russian Plain. – *Eurasian Soil Science*, 31(10): 1062–1074.
- SYCHEVA, S. & SEDOV, S. (2012): Paleopedogenesis during Mikulino interglacial (MIS 5e) in East-European plain: buried toposequence of the key-section “Alexandrov quarry”. – *Boletín de la Sociedad Geológica Mexicana*, 64(2): 189–197.
- TARGULIAN, V.O., BIRINA, A.G., KULIKOV, A.V., SOKOLOVA, T.A. & TSELISHCHEVA, L.K. (1974): Arrangement, composition and genesis of sod-pale-podzolic soil derived from mantle loams. Morphological investigation – 10th International Congress in Soil Science, 47 p.; Moscow (Academy of Sciences of the USSR).
- TARGULIAN, V.O., SOKOLOVA, T.A., BIRINA, A.G., KULIKOV, A.V. & TSELISHCHEVA, L.K. (1974): Arrangement, composition and genesis of sod-pale-podzolic soil derived from mantle loams. Analytical investigation. – 10th International Congress in Soil Science., 107 p.; Moscow (Academy of Sciences of the USSR).
- TERHORST, B. (2007): Korrelation von mittelpleistozänen Löss-/Paläobodenensequenzen in Oberösterreich mit der marinen Sauerstoffisotopenkurve. – *E & G Quaternary Science Journal*, 56: 172–185.
- TERHORST, B. (2013): A stratigraphic concept for Middle Pleistocene Quaternary sequences in Upper Austria. – *E & G Quaternary Science Journal*, 62/1, this volume.
- TERHORST, B., APPEL, E. & WERNER, A. (2001): Palaeopedology and magnetic susceptibility of a loess-palaeosol sequence in southwest Germany. – *Quaternary International*, 76–77: 231–240.
- TONKONOGOV, V.D., GRADUSOV, B.P., RUBILINA, N.Y.E., TARGULIAN, V.O. & CHIZHIKOVA, N.P. (1987): Differentiation of the mineral and chemical composition in sod-podzolic and podzolic soils. – *Soviet Soil Science*, 19(4): 23–35.
- TURNER, C. (2002a): Formal status and vegetational development of the Eemian interglacial in northwestern and southern Europe. – *Quaternary Research*, 58: 41–44.
- Turner, C. (2002b): Problems of the duration of the Eemian interglacial in Europe North of the Alps. – *Quaternary Research*, 58: 45–48.
- VAN VLIET-LANOË, B. (1990): The genesis and age of the argillic horizon in Weichselian loess of northwestern Europe. – *Quaternary International*, 5: 49–56.
- VAN VLIET-LANOË, B. (2010): Frost action. – In: STOOPS, G., MARCELINO, V. & MEES, F. (eds): Interpretation of Micromorphological Features of Soils and Regoliths. Chapter 6: 81–10; Amsterdam (Elsevier).
- VAN RANST, E., DE CONINCK, F., TAVERNIER, R. & LANGOHR, R. (1982): Mineralogy in silty to loamy soils of central and high Belgium in respect of autochthonous and allochthonous materials. – *Bulletin de la Société belge de géologie*, 91(1): 27–44.
- VANCAMPENHOUT, K., WOUTERS, K., CAUS, A., BUURMAN, P., SWENNEN, R. & DECKERS, J. (2008): Fingerprinting of soil organic matter as a proxy for assessing climate and vegetation changes in last interglacial palaeosols (Veldwezelt, Belgium). – *Quaternary Research*, 69(1): 145–162.
- VANDENHOUTE, P., FRECHEN, M., BUylaERT, J.P., VANDENBERGHE, D. & DECORTE, F. (2003): The Last Interglacial palaeosol in the Belgian loess belt TL age record. – *Quaternary Science Reviews*, 22: 985–990.
- Velichko, A.A. (1990): Loess-paleosol formation on the Russian Plain. – *Quaternary International*, 7/8: 103–114.
- VELICHKO, A.A., MOROZOVA, T.D., NECHAEV, V.P., RUTTER, N.W., DLUSSKII, K.G., LITTLE, E.C., CATTO, N.R., SEMENOV, V.V. & EVANS, M.E. (2006): Loess/paleosol/cryogenic formation and structure near the northern limit of loess deposition, East European Plain, Russia. – *Quaternary International*, 152 (1): 14–30.
- WOJDYR, M. (2010): Fityk: a general-purpose peak fitting program. – *Journal of Applied Crystallography*, 43: 1126–1128.
- YAKIMENKO, E.Y. (1995): Pleistocene paleosols in the loess and loess-like sediments of the central part of the Russian Plain. – *Quaternary Science Reviews*, 14: 747–753.
- Zagwijn, W.H. (1996): An analysis of Eemian climate in western and central Europe. – *Quaternary Sciences Reviews*, 15: 451–469.

# Paudorf *locus typicus* (Lower Austria) revisited – The potential of the classic loess outcrop for Middle to Late Pleistocene landscape reconstructions

Tobias Sprafke, Birgit Terhorst, Robert Peticzka, Christine Thiel

## How to cite:

SPRAFKE, T., TERHORST, B., PETICZKA, R., THIEL, CH. (2013): Paudorf *locus typicus* (Lower Austria) revisited – The potential of the classic loess outcrop for Middle to Late Pleistocene landscape reconstructions. – E&G Quaternary Science Journal, 62 (1): 59–72. DOI: 10.3285/eg.62.1.06

## Abstract:

The more than 12 m thick loess-paleosol sequence in Paudorf, Lower Austria, has been known for decades as *locus typicus* of the “Paudorfer Bodenbildung” (Paudorf paleosol). The upper section of the outcrop contains an up to 1 m thick pedocomplex that developed during MIS 5. The differentiated sequence of loess-like sediment below, including a more than 2 m thick pedocomplex in its basal part, is an exceptional archive of landscape evolution from the Middle Pleistocene. Herein we present detailed paleopedological and sedimentological surveys, as well as first micromorphological observations to address the sequence in its entirety and the processes leading to its genesis. Furthermore, high resolution color and carbonate analyses, as well as detailed texture analyses, have resulted in a substantial database.

The studies show that the loess sediments were subject to a polygenetic development under periglacial conditions reflected in eolian silt and fine sand accumulation, admixture of local material during (mostly solifluidal) redeposition and in situ processes. Horizons with signs of pedogenesis, particularly the two pedocomplexes, document longer phases of stability; the stages of development can be correlated to equivalent sequences and seen as paleoclimatic signals where chronological data are available. The upper pedocomplex is a Chernozem of the early last glacial (MIS 5c–[a?]), which developed in a solifluidal redeposited (MIS 5d) interglacial Cambisol (MIS 5e). Cryosols, typical for MIS 6 sequences, are present in the loess sediment below. The lower pedocomplex formed during several warm stages of varying intensities, with interruptions caused by colluvial processes and admixture of eolian sediment during colder stages.

## Paudorf *locus typicus* (Niederösterreich) – Das Potential des klassischen Lössaufschlusses für die Rekonstruktion mittel- bis spätpleistozäner Paläoumwelten

## Kurzfassung:

Die über 12 m mächtige Löss-Paläoboden-Sequenz in Paudorf (Niederösterreich), ist seit Jahrzehnten bekannt als *locus typicus* für die „Paudorfer Bodenbildung“. Dieser 1 m mächtige Pedokomplex im obersten Profilabschnitt entwickelte sich eem- bis frühwürmzeitlich. Das differenzierte Lösssediment im Liegenden, mit einem über 2 m mächtigen Pedokomplex im basalen Bereich, stellt ein außergewöhnliches Archiv mittelpleistozäner Landschaftsentwicklung dar. Die paläopedologischen und sedimentologischen Untersuchungen sowie erste mikromorphologische Analysen widmen sich erstmals der Gesamtabfolge und den Prozessen, die zu ihrer Entstehung beitragen. Farb- und Karbonatanalysen in hoher Auflösung sowie detaillierte Korngrößenanalysen dienen dabei als hilfreiche Datenbasis.

Die Untersuchungen zeigen zum einen, dass die Lösssedimente einer komplexen Genese unter periglazialen Bedingungen unterlagen. Neben äolischer Akkumulation spielten (zumeist solifluidale) Umlagerungsprozesse unter Einmischung von lokalem Material ebenso wie in situ Prozesse eine Rolle. Morphodynamisch stabile Phasen sind insbesondere in den beiden Pedokomplexen nachweisbar. In Bereichen, in denen Datierungen vorliegen, können Entwicklungsphasen mit jenen anderer Sequenzen korreliert werden und als klimatische Signale interpretiert werden. Die „Paudorfer Bodenbildung“ ist vermutlich eine frühglaziale Humuszone (MIS 5c–[a?]), die sich in einer solifluidal umgelagerten (MIS 5d) eemzeitliche Braunerde (MIS 5e) gebildet hat. Im Lösssediment konnten Nassböden nachgewiesen werden, wie sie typisch für spätrisszeitliche (MIS 6) Sequenzen sind. Der untere Pedokomplex wurde offenbar über mehrere Warmphasen verschiedener Intensitäten hinweg gebildet und wiederholt von Umlagerungsprozessen und äolischer Sedimentation während Kaltphasen unterbrochen.

## Key words:

Loess, paleopedology, landscape formation, Lower Austria, Paudorf, Middle Pleistocene, micromorphology

**Addresses of authors:** T. Sprafke\*, B. Terhorst, Institute of Geography and Geology, University of Würzburg, Am Hubland, D-97074 Würzburg, Germany. E-Mail: tobias.sprafke@uni-wuerzburg.de; birgit.terhorst@uni-wuerzburg.de; R. Peticzka, Institute of Geography and Regional Research, University of Vienna, Althanstrasse 14, A-1090 Wien, Austria. E-Mail: robert.peticzka@univie.ac.at; C. Thiel, Nordic Laboratory for Luminescence Dating, Department of Earth Sciences, Aarhus University, Risø DTU, Frederiksborgvej 399, 4000 Roskilde, Denmark; Centre for Nuclear Technologies, DTU Risø Campus, Frederiksborgvej 399, DK-4000 Roskilde, Denmark. E-Mail: chrth@risoe.dtu.dk., \*corresponding author



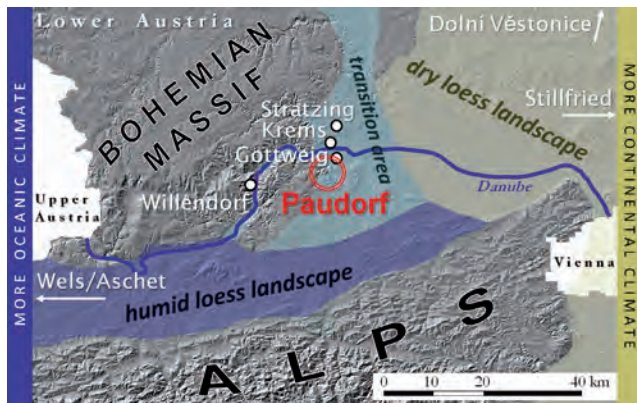


Fig. 1: Paudorf and other important loess-paleosol sequences in the loess landscapes of Lower Austria after FINK (1956). Base map: GEOinfo NÖ.

Abb. 1: Paudorf und weitere wichtige Löss-Paläoboden-Sequenzen in den österreichischen Lösslandschaften nach FINK (1956). Kartengrundlage: GEOinfo NÖ.

## 1 Introduction

Loess-paleosol sequences are the most suitable terrestrial archives to reconstruct landscape responses to Quaternary climate changes on regional to continental scale in the temperate latitudes with several  $10^3$  to  $10^4$  years resolution (cf. BRONGER 2003). For periods as far back as Marine Isotope Stage (MIS) 5 various types of records and dating methods already allow relatively detailed reconstructions. In contrast, earlier landscape responses to past climate changes remain a subject of controversial discussions (e.g. TERHORST 2007; PREUSSER & FIEBIG 2009; SCHOLGER & TERHORST 2011), despite the accurate record of global temperature fluctuations from deep-sea oxygen isotope measurements (LISIECKI & RAYMO 2005).

Reconstructions of past landscapes and climates require data from numerous localities and regions respectively, as well as reliable dating methods. For Europe, on the mentioned time scales of climate change, posterior to the Matuyama-Brunhes boundary, the most complete terrestrial archives exist in the plateau loess sediments of the Middle Danube Basin that are relatively well suited for correlations and quantitative research (BRONGER 1970, 1976, 2003; MARKOVIC et al. 2006, 2009, 2011). Geographically, Lower Austria has a key position related to paleoclimatology, between Central Europe, influenced by more marine climate, and the more continental Eastern Europe. Most thick loess deposits in Lower Austria are found on slopes in leeward positions and therefore are often influenced by hillslope processes. Due to the greater complexity of these archives, straight forward correlations and the application of quantitative methods is hampered. The need for detailed assessment of the processes leading to the formation of the archives is evident, and will give at least qualitative to semi-quantitative information about past environmental conditions.

The northeast of Lower Austria is sheltered from the moisture of the Atlantic and the Mediterranean Sea by the Bohemian Massif in the west and the Alps in the south respectively, which results in an increased continentality. Holocene Chernozems versus Eemian Bw horizons in the area give evidence for a pronounced sensitivity to climate change. This is especially true for the “transition area” around the city of

Krems a.d. Donau between the “dry loess landscape” further east and the “humid loess landscape” west of the Bohemian Massif (cf. FINK 1956; Fig. 1). The “humid loess landscape” has a present mean annual precipitation around 700–900 mm and exhibits mostly soils of the Cambisol-Luvisol group, whereas the “dry loess landscape” has an annual precipitation around 500–550 mm and exhibits mostly soils of the Phaeozem-Chernozem group.

Despite some general spatial relationships, a regional stratigraphy, as attempted by BAYER (1909, 1927), GÖTZINGER (1936), LAIS (1951), BRANDTNER (1954) and most importantly FINK (1954, 1956, 1960, 1961, 1976), has never been satisfactorily established due to a lack of suitable dating techniques as well as sequences that are polygenetic and contain gaps.

Paleomagnetic studies were carried out in the 1970s to establish stratigraphical models in the longest records of glacial-interglacial cycles of Krems Schießstätte (shooting range) and Stranzendorf (FINK 1976; FINK & KUKLA 1977; VERGINIS 1993). More recently, loess research in Lower Austria has mainly dealt with luminescence dating of some previously studied sequences (ZÖLLER et al. 1994; NOLL et al. 1994; TERHORST et al. 2011; THIEL et al. 2011a; THIEL et al. 2011b). Research is also focused on high resolution records of MIS 2 to 3, most notable for Paleolithic findings, such as at Stratzing, Willendorf and Krems-Wachtberg (NEUGEBAUER-MARESCH 1993; HAESAERTS et al. 1996; EINWÖGERER et al. 2006; THIEL et al. 2011a). Aside from that only a small number of studies have tried to unravel the very complex Middle and Late Pleistocene paleoenvironmental archives (KOVANDA et al. 1995; PETICZKA et al. 2009).

One important loess-paleosol sequence in this area is the renowned section of Paudorf, first described by GÖTZINGER (1936). In this sequence, a pedocomplex that can be correlated to MIS 5, is exposed in the upper part (ZÖLLER et al. 1994; THIEL et al. 2011b). On the basis of detailed paleopedological and sedimentological data this study aims to understand the complex pedogenetical and geomorphological processes in the interplay of local influences and climatically induced environmental changes.

## 2 The locus typicus Paudorf

Paudorf (257 m a.s.l.) is situated in the hilly transition area between the Bohemian Massif and the Molasse Basin to the east, 7 km south of the city of Krems (203 m a.s.l.). The surrounding hills consist predominantly of granulate (mostly quartz, feldspar, garnet and some mica) with sporadic lenses of ultrabasic rock (GEOLOGISCHE BUNDESANSTALT 2002; MATURA 2006). At the foot of the Waxberg (500 m a.s.l.), northwest of the village of Paudorf, the >12 m thick loess-sequence is exposed at 265–270 m a.s.l. in an approximately 70 m long outcrop facing SE and belonging to a former loampit. In Figure 2, a sketch of the outcrop with the two prominent pedocomplexes is presented. The thickness of the loess sediments between the 1 m thick upper and the > 2 m thick lower pedocomplex is increasing to the right hand side (NE).

Based on similarities to the famous paleosol of the nearby Göttweig/Furth outcrop, GÖTZINGER (1936) correlated the pedocomplex in the lower part of the Paudorf sequence with the “Göttweiger Verlehmungszone” sensu BAYER (1927). Following the German terminology, “Verleh-

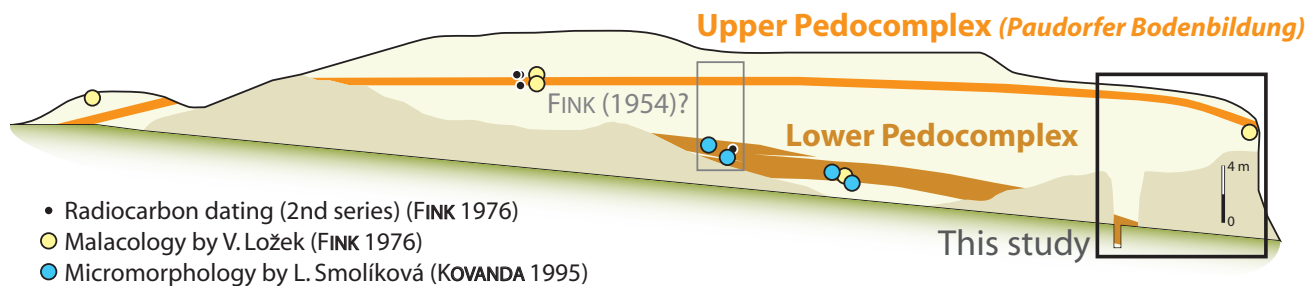


Fig. 2: Overview of the outcrop and former studies (black square: see Fig. 3). Redrawn and modified from FINK 1976, Fig. 31.

Abb. 2: Überblick über den Aufschluss und frühere Arbeiten (Schwarzes Quadrat: diese Arbeit, vgl. Abb. 3). FINK 1976, Abb. 31, neu gezeichnet und verändert.

mung” is the pedogenic process of clay neo-formation, resulting in a Bv horizon (cf. AD-HOC-ARBEITSGRUPPE BODEN 2005; Bw horizon after IUSS WORKING GROUP WRB 2006). For the upper pedocomplex, GÖTZINGER (1936) introduced the term “Paudorfer Leimenzone/Verlehmungszone”, later named “Paudorfer Bodenbildung” (Paudorf soil/paleosol) by BRANDTNER (1954) and FINK (1956). It has to be noted that the term “Paudorfer Bodenbildung” sometimes refers only to the prominent 0.3–0.4 m thick, speckled part of the ~1.0 m thick pedocomplex (e.g. in FINK 1956).

Depending on the interpretation, either both pedocomplexes in the Paudorf sequence (LAIS 1951; BRANDTNER 1954, 1956) or at least the upper one (GÖTZINGER 1936; FINK 1954, 1956) were seen to represent an interstadial of the Würm glaciation sensu PENCK & BRÜCKNER 1909. Two series of radiocarbon dating (FINK 1961, 1976) supported the idea of Paudorf being the locus typicus for a pronounced interstadial of the last glacial, the “Paudorf (Interstadial)”. In the 1960s and early 1970s this term was widely accepted and used in loess research. Interglacial mollusk assemblages in the “Paudorfer Bodenbildung”, identified by V. Ložek (FINK 1976), and the revised stratigraphy by FINK (1976), could not prevent the term “Paudorf” still being present in neighboring sciences such as paleontology and archeology as interstadial around 30 ka (PAZONYI 2004; ANGHELINU & NIȚĂ 2012).

Thermoluminescence (TL) ages presented in NOLL et al.

(1994) support the ideas of GÖTZINGER (1936), whereas the TL dating results, in combination with amino acid chronology by ZÖLLER et al. (1994), lead to a correlation of the “Paudorfer Bodenbildung” with MIS 5. Recently published post-IR infra-red optically stimulated luminescence datings (post-IR IRSL; cf. Thiel et al. 2011a) reveal ages between  $106 \pm 12$  and  $159 \pm 20$  ka for the upper pedocomplex (THIEL et al., 2011b). These results confirm its formation during the last interglacial and the early glacial, because this new dating technique is not prone to any significant over- or underestimation at this age range (BUYLAERT et al., 2012). In the loess sediment below the pedocomplex, ages of  $187 \pm 12$  and  $189 \pm 16$  ka do not suppose any major hiatus in the upper 7.5 m of the sequence. Consequently, it is most likely that most parts of the profile are of Middle Pleistocene age.

### 3 Methods

In contrast to FINK (1954, 1976), the studies were conducted in the northeastern part of the outcrop, where the sequence of loess sediments between the two pedocomplexes is thicker, thus providing higher resolution. Here, the layers/horizons are dipping 10–15° to the right hand side of the profile wall (NE). The two profiles presented in THIEL et al. (2011b), which were based on the studies of PETICZKA et al. (2009) were further extended. One composite Paudorf sequence is presented in this study, which involves the neighboring profiles Paudorf I (2.5 m thick, upper pedocomplex and surrounding loess sediments) and Paudorf II (11.8 m thick, sequence below upper pedocomplex). The presence of the upper pedocomplex in both profiles allows the correlation of the two sequences. The setting is illustrated in Figure 3. High resolution sampling of 1 dm<sup>3</sup>-blocks in 1 dm intervals (cf. Continuous Column Sampling [CCS] by ANTOINE et al. 2009) was carried out in both profiles, including some overlap in the upper pedocomplex. The color/carbonate measurements of the statistically taken samples enhance the consistency of the units and subunits clarified during the field survey. The positions of the samples for grain size analyses are indicated in Figure 6.

#### 3.1 Field survey

The description of the pedological and sedimentological parameters is based on the German Mapping Key for Soils (AD-HOC-ARBEITSGRUPPE BODEN 2005) and was adapted to

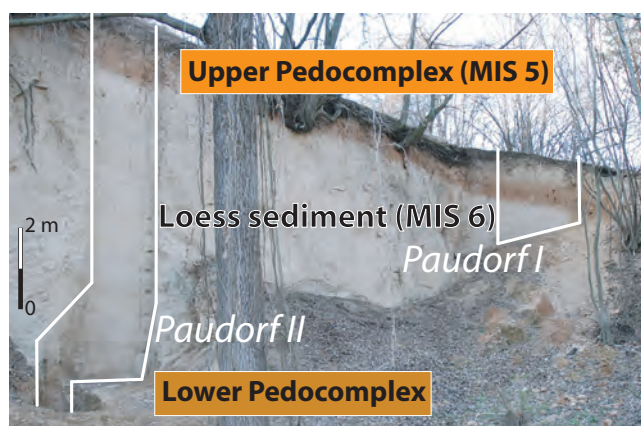


Fig. 3: Overview of the studied profiles. The lowest parts of Paudorf II in the small pit on the left hand side (cf. Fig. 4-3a) are not visible here.

Abb. 3: Überblick über die untersuchten Profile. Der untere Abschnitt von Paudorf II in der Schürfungruben linker Hand (vgl. Abb. 4-3a) ist hier nicht vollständig sichtbar.

the World Reference Base for soil resources (IUSS WORKING GROUP WRB 2006). We note that these guidelines are made for modern soils, and that many horizons exhibit features that were formed under environmental conditions different from today. Bleached horizons in loess sediment are commonly explained by iron reduction in water saturated substrates above the permafrost table in times without extreme eolian input and redeposition. These “Naßböden” sensu SCHÖNHALS et al. (1964) are close to Cryosols (Reductaquic) after WRB (IUSS WORKING GROUP WRB 2006) if assumed environmental conditions during pedogenesis are taken into account.

### 3.2 Laboratory analyses: texture, carbonate content, color

After homogenizing the samples, representative fractions (~400 g) were dried for two days at 45 °C. Half of the samples were dry-sieved to < 2000 µm to produce fine earth which was used for all analyses except the sieving procedure. Water contents were estimated gravimetrically, parallel to weighing out. 30–40 g of each corresponding sample were oven-dried (two days, 105 °C) and the results considered in weight-based calculations.

100 g of each bulk sample were without chemical pretreatment suspended in water and wet sieved for 40 min in a Ret-sch AS200 basic sieving apparatus (2000/630/200/63/40 µm). The fractions were oven-dried and weighted. The remaining suspension < 40 µm was discarded and its weight-percentage calculated. To measure the fractions of this suspension, of each fine earth sample 10–15 g (depending on the content of fractions < 40 µm) were without further pretreatment wet-sieved to < 40 µm. Treated with  $\text{Na}_4\text{P}_2\text{O}_7 \cdot 10 \text{H}_2\text{O}$  in solution, the fractions of the suspension < 40 µm (40/20/6.3/2 µm) were measured as weight-percent using a Micromeritics Sedigraph III 5120 by means of X-rays during sedimentation; the principle is based on Stokes' Law. Gravel (> 2000) is calculated in weight-percent of the whole sample. Fractions < 2000 µm are calculated in weight percent of total fine earth.

Following DIN ISO 10693 1–2 g of each air-dried fine earth sample were taken for gas-volumetric estimation of carbonate content of the sample after reaction with 10 ml of 10% HCl by means of Scheibler Apparatus.

The oven-dry fine earth used for gravimetric estimation of water content was taken for color measurement, using the Spectrophotometer SPH 850. Before the lens was placed on the samples, the aggregates were thoroughly pounded to prevent shadow effects. The resulting color values (10 nm steps from 400 to 700 nm) are calculated by dividing the ten highest summated intensities (700–600 nm) by the ten lowest values (500–400 nm). The values were normalized to the color of the most loess-like part in P3 (sample in 2.25 m depth). Values > 1.0 are “warmer” (brownish, reddish) colors, representing decalcification, oxidation as well as humification, while values < 1.0 are “colder” colors (bluish, whitish), resulting from iron reduction and carbonate illuviation. A single one-dimensional parameter adequately quantifying qualitative field perception was favored in this study of a polygenetic sequence over several published color proxies that seek for quantification of pedogenetic intensities (e.g. VISCARRA ROSSEL 2006; BÁBEK et al. 2011).

### 3.3 Microscopic studies

Microscopic studies have been carried out in order to obtain further qualitative insight into the complex genesis of the sequence. From several samples each of the five fractions obtained by sieving was studied under binocular microscope to assess their specific composition. Thin sections of the two pedocomplexes have been studied qualitatively under a Leitz DMRB polarizing microscope to principally understand their polygenetical formation. Detailed micromorphological studies are the subject of ongoing studies. The thin sections were produced from resin-impregnated undisturbed block samples.

## 4 Results

### 4.1 Field survey

Overview and detailed photographs of the outcrop are presented in Figure 4. Down to a depth of 11.80 m, the standard Paudorf sequence is differentiated into eight units, with units P2 and P7 covering the two prominent pedocomplexes. Below we highlight the main characteristics of the sequence. For field parameters, soil horizon designations and further descriptions see Figures 5 and 6.

In general, the outcrop shows a stable, wall-forming, differentiated, mostly yellowish-grey substrate dominated by silt-sized particles and a considerable percentage of sand. Both, the particles of the loess-like sediment (P1, P3–6, P8) and of the pedocomplexes (P2 and P7) form blocky to sub-polyhedral aggregates. Carbonate is abundant in all units, except the lower pedocomplex (P7). Each layer/horizon bears granulite fragments of up to gravel size. Several thin bands, rich in gravel and coarse sand, are visible. In the prominent brownish to reddish pedocomplexes rock fragments as large as several cm in length are present.

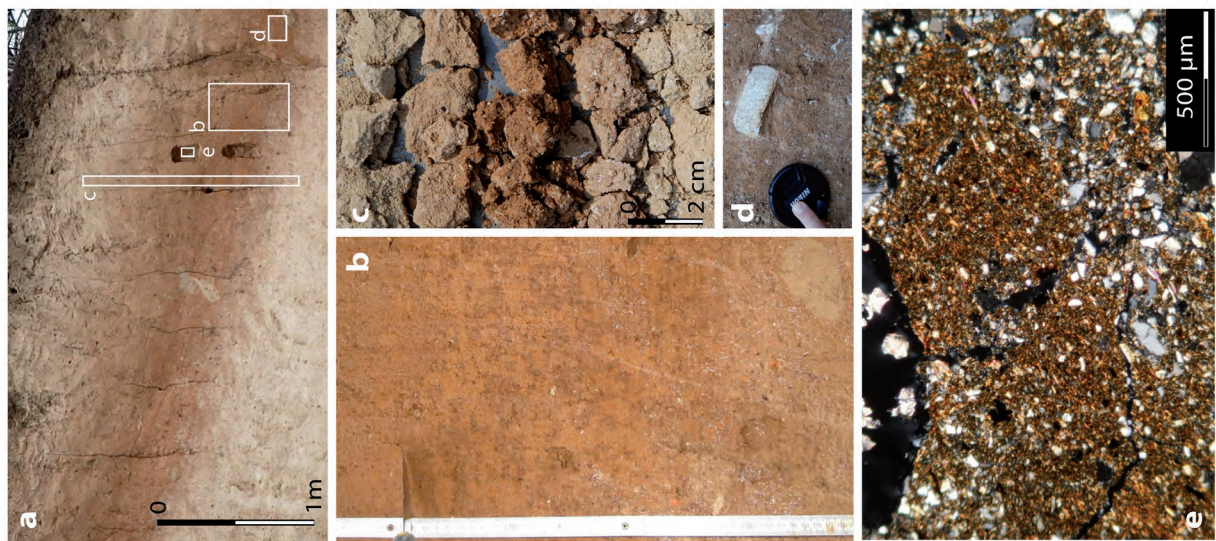
The top of the profile exhibits an approximately 0.5 m thick disturbed Cambisol (not shown in the standardized profile).

P1 has yellowish gray loess-color and loess-structure, but contains more fine sand than typical loess (cf. PYE & SHERWIN 1999). No macroscopical secondary carbonates are present. The boundary to P2, the upper pedocomplex, is gradual (Fig. 4-1a). Subunit P2a is darker and contains more clay and pseudomycelia. P2b leads into a 0.3–0.4 m thick reddish-brown horizon (P2c); this unit has a relatively regular pattern of brown interconnected irregularly shaped speckles of up to 2 cm in size and is the classical, “Paudorfer Bodenbildung” after FINK (1956) (Fig. 4-1b). The surfaces of the crumbly and porous blocks to sub-polyhedrons are free of clay coatings (Fig. 4-1c). A striking feature is the presence of several granulite cobbles (Fig. 4-1d). In addition to numerous crotovinas, the lower boundary of P2c and the entire dark-grayish subunit P2d are distorted in a complex pattern. The irregular boundaries resemble cryogenic pockets and wedges slightly deformed by hillslope processes.

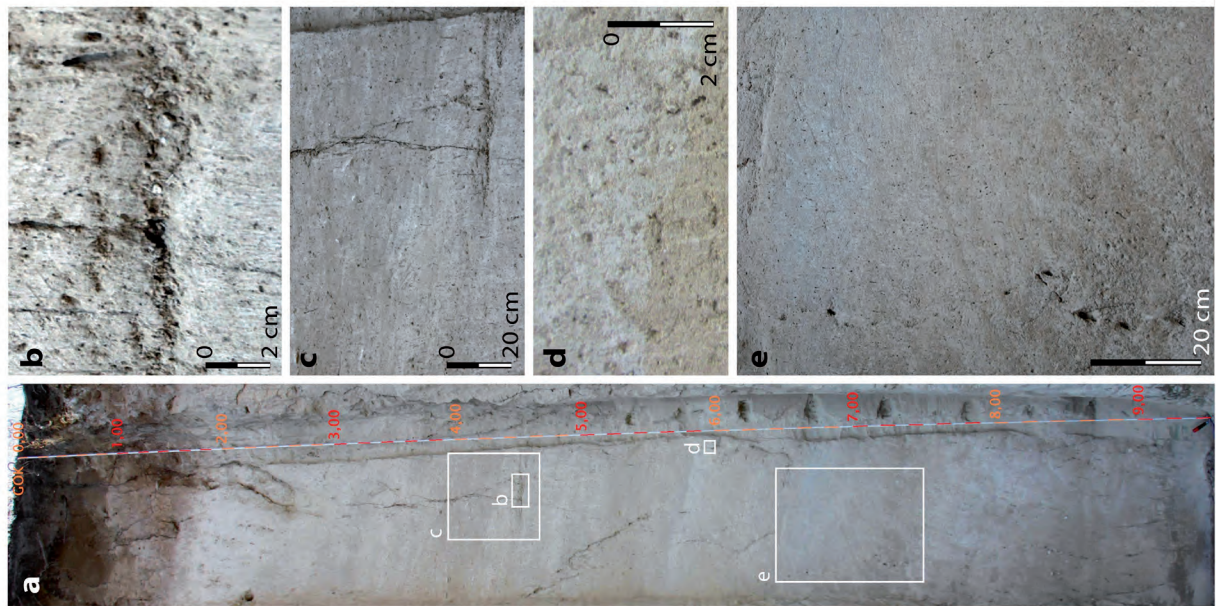
P3 to P6 are the sequence of loess sediments between the two prominent pedocomplexes (Fig. 4-2a). Evidence for eolian sedimentation, redeposition and weak pedogenesis can be found in all units. P3 is the least differentiated, most loess-like substrate, with very weak signs of soil formation and colluvial processes. P4 is more heterogeneous, striat-



### 1) Upper Pedocomplex (P2)



### 2) Loess-sediment (P3-P6)



### 3) Lower Pedocomplex (P7)

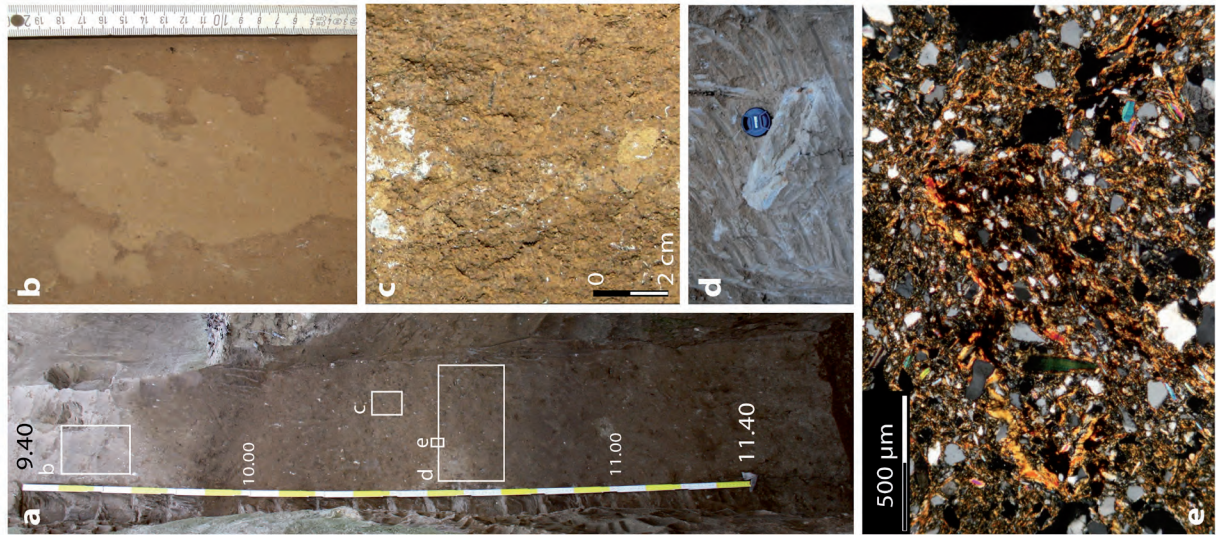


Fig. 4: Panel of macroscopic and microscopic images of characteristic parts of the Paudorf sequence. Rectangles in images 1a, 2a, 3a indicate stratigraphic position of detailed images b-d.

Abb. 4: Zusammenstellung makro- und mikroskopischer Bilder charakteristischer Abschnitte der Sequenz Paudorf. Rechtecke in den Überblicksfotos 1a, 2a, 3a zeigen die stratigraphische Position der Detailbilder b-e.



ed and contains more gravel, partly in distinct bands (Fig. 4-2b). Redeposition features can be seen clearly. A considerable amount of carbonate and silt, as well as the presence of bleached horizons, show that eolian sedimentation occurred and alternated with weak pedogenesis (Fig. 4-2c). The three Cryosols (Reductaquic) of P5 indicate clearly pedogenesis (Fig. 4-2d); especially the upper (P5a) and the lower Cryosol (P5e) are well pronounced. P6 differs considerably from the loess sediments, as it is significantly enriched in sand, has lower carbonate content and a different hue. P6b is a brownish horizon with irregular boundaries to the adjacent horizons. Striations penetrating P6a in the opposite direction to the inclination of the horizon boundary are visible (Fig. 4-2e). Further, the brownish horizon seems to be disturbed internally. Around the lower boundary and slightly below (P6c), the highest sand contents of the entire sequence are found. Sharply defined areas of darker substrate resemble crotonia, root channels or a cryogenic structure. The color of these domains is comparable to the color of P6b.

P7 exhibits the 2.8 m thick lower pedocomplex and the transitional horizons above (Fig. 4-3a). In a continuous change of substrate from P6 to P7, a 10–20 cm thick layer rich in granulite gravel up to 2 cm in size has been chosen as the boundary (P7a). In general, P7 is carbonate free, more reddish-brown in the central subunits (P7c–e) and more blackish-brown in the surrounding subunits. In P7b unevenly shaped, sharply defined lighter brown mottles are visible (Fig. 4-3b). The staining areas are bigger, but fewer, and are less regularly formed and arranged than the speckles in P2. The subunits P7c and P7e are more consolidated and the aggregates exhibit weak clay coatings (Fig. 4-3c). The intercalated P7d contains higher amounts of granulite and charcoal fragments. P7f has higher silt and less sand content, and lighter color. Pieces of granulite rock are present in this horizon (Fig. 4-3d). P7g consists of dark humic loam with areas of weak staining and crotonia, underlain by an inhomogeneous light brown horizon. P7i covers the grayish 10–20 cm thick transition horizon of P7 to P8, characterized by a dense network of pseudomycelia. P8 is the basal layer of the exposed profile, and consists of grayish, carbonate-rich sandy loess.

## 4.2 Laboratory results

### 4.2.1 Texture

The rare rock fragments in P2 and P7 were noticed in the field, but were not taken during sampling. For results of texture analyses see Figure 6 and Table 1. Sieving revealed that without exception, gravel (G, grain size > 2000 µm) is present in every sample with an average value of 1.4%. Values exceeding 2% are mainly associated with gravel bands enclosed in the samples (e.g. P4c–d and P7a–b).

In general, the sand (S) content in fine earth ranges from 20–30%. In P5 and P7a–e sand content is around 30% and in parts of P6 contents even exceed 40%. In P4 and P5, the bleached horizons (P4c–d and P5a,c,e) have significantly lower sand content than the neighboring layers. The overall minima are present in P2 and P3, especially near their boundary. In general, fine sand (fS) is the dominating fraction with bulk contents between 10–25%; its absolute content is responsible for variations in the overall sand con-

tent. Coarse sand (gS) follows this trend only marginally and is to a certain extent also independent of gravel variations. Medium sand (mS) ratios lie between those of coarse and fine sand.

On average, silt (U) makes up 50–60% of the fine earth. In P1–2a, P3 and P4c–d silt contents are higher, in the more sandy units P6 and P7 lower, sometimes as low as 40% (P6b–c). Silt contents of the bleached horizons P5a,c,e are ~5% higher than in P5b and d. Bulk coarse (gU) and medium silt (mS) contents are in general similar in both absolute contents and changes throughout the profile, with the first reaching not more than 30% and the latter not more than 25%. As fine silt (fS) varies only slightly around 14% throughout the profile, the changes in silt content are mainly reflected by the two coarser silt fractions. Fine silt shows an increase in the pedocomplexes (P2 and P7). In the sand rich P6, the three silt fractions have similar contents. It is interesting to note that the transition zone between P2 and P3 (enriched in secondary carbonate) exhibits relatively low bulk silt contents, where fine silt has a relative maximum and clay its absolute maximum.

Bulk clay (T) contents exceed 15% in each fine earth sample. In the loess sediment units P3 to P6, the values vary around 20% with no clear trend. In the pedocomplexes (P2 and P7), clay contents reach more than 25%. In general, relative clay maxima are present at the lower boundaries of the two pedocomplexes. Highest clay contents are present at the lower boundary of P2 and in the central horizons of P7. In the uppermost and lowermost units of loess-like sediment (P1 and P8) the clay contents differ strongly (16.6 and 25.2%, respectively).

### 4.2.2 Carbonate content and color

The results of carbonate and color analyses are shown in Figure 6 and Table 1. Carbonate content is significantly lower in the pedocomplexes (P2 and P7) than in all other units. In contrast, the underlying units (P3 and P8) both exhibit strongly enhanced carbonate contents. The upper four units are in general richer in carbonate than the lowest three (more sandy) units. P5 exhibits intermediate values. The lower pedocomplex is almost completely decalcified whereas the upper pedocomplex has 6–7% carbonate. P6b, the brownish colored horizon above the lower pedocomplex has >6% less carbonate content than the over- and underlying units.

Color values support the field observations in a more sensitive and quantitative way. P2 and P7 show much more “warmer” coloring, with P7c–d exhibiting slightly higher intensities than P2c. P6 is also more intensely colored than the more loess-like units. The minima are present in the bleached horizons (P5a,c,e and P4d) and in the carbonate illuvial horizons P3a and P8.

Some interesting relation is visible by direct comparison of the relative maxima of carbonate and color value. Clearly, the pedocomplexes exhibit strong coloring and low carbonate contents, in connection with high carbonate values below. But this pattern is also traceable on a smaller scale: Around P3b and the boundary of P3d–4 a, in P4b and very clear in P6b and below, we detect higher color values connected with lower carbonate values and carbonate enrichment below.

Unit Horizon No. (subunit)	Pedogenic horizon after WRB	Lower limit depth (cm)	Lower limit shape character after KA 5*	Munsell color(s)	Texture (after KA 5*)	Carbonate content	Description and further details
<b>P 1</b>	C	65	w-pl di	2.5-10 YR5/4	Uls	****	Loess (redeposited?)
<b>P 2</b>	Ah	102	pl di	7.5-10 YR4/4	Lu	*****	from top to bottom increasing intensity in color (reddish to blackish, depending on light source), some pseudomycelia
	AhBw	118	pl di	-	-	-	transition horizon, pseudomycelia
	AhBw	150	dr-mot di-cl	7.5 YR4/6 7.5 YR3/3-4	Lu	***	reddish-brown with brownish speckles, partly lighter colored interior (10 YR 4/4), color partly connected to surrounding of numerous pseudomycelia. Matrix decalcified. Slope parallel granulite rock, charcoal, crotowina
<b>P 3</b>	AhCk	163	dr-mot di-sh	10 YR4/6	Lu	****	inhomogenous, forming pockets, penetrated by crotowina, abundant pseudomycelia, brick colored concretions of max. 1-2 cm diameter
	Ck	240	pl di	2.5 Y 5/4	Uls	*****	most loess-like, carbonate rich substrate, partly secondary (pseudomycelia)
	C	254	pl di	2.5 Y 5/4	Uls	****(*)	slightly more pedogenic modification as surrounding layers (?)
	C	310	pl di	2.5 Y 5/4	Uls	****(*)	inhomogenous, some weak striations, slight bleaching possible
	C	340	pl-w di	2.5 Y 5/4	Uls	****(*)	comparable to 3b, slightly more modified
<b>P 4</b>	C(k)	390	pl cl-di	2.5 Y 5/4	Uls	****(*)	inhomogenous with darker and lighter striations, especially in lower parts (dry colors 2.5 Y 7/4 vs. 2.5 Y 8/3), gravel band (290), carbonate concretions (up to 2 cm)
	C(k)	430	pl-w sh-di	2.5 Y 5/4	Uls	****	inhomogenous, darker (greyish), striated (dry colors: 2.5 Y 7/4 vs. 2.5 Y 8/3), gravel fragments (granulite, carbonate concretions)
	C(g?)	480	pl di	2.5 Y 5/4	Uls	****	inhomogenous, striated, lighter (bleached?), gravel band + gravel lens (460)
	C(g?)	520	pl di	2.5 Y 5/4	Uls	****	comparable to 4 c, gravel band (495)
	C	577	pl-w di-sh	2.5 Y 5/4 10 YR6/6	Uls	****	inhomogenous, darker, more brownish than surrounding units, less traces for redeposition
<b>P 5</b>	Cg	593	pl cl-sh	2.5 Y 5/4	Uls	****	strongly bleached, homogenous, almost white with pale red lenses of same type of substrate (dry colors: 2.5 Y 8/2 vs. 2.5 Y 7/4)
	C	632	pl-w di	2.5 Y 6/4	Uls	****	darker, more sandy
	Cg	646	pl di	2.5 Y 5/6	Uls	****	weakly bleached, not continuous
	C	660	pl cl-di	2.5 Y 5/3	Slu	****	darker, gravel bands, especially boundary to 5 e
	Cg	690	pl cl-di	2.5 Y 5/3	Uls	****	light blueish-grey, finer substrate, relatively homogenous
<b>P 6</b>	C	722	w cl-di	10 YR4/3	Slu	****	transition horizon, more sandy, brownish stripes coming from unit 6 b
	Bw	760	dr cl-di	10 YR4/3	Slu	****(*)	inhomogenous brownish horizon (colluvial vs. in-situ ?)
	C	860	w di	10 YR5/4	Slu	****	very sandy, crotowina/root burrows, gravel band (818)
	Ah	880	pl di	10 YR4/3	Slu	****(*)	fragments of granulite, up to 2 cm in diameter
	AhBw	990	pl di	10 YR3/4 10 YR4/4	Lu	****(*)	from top to bottom: decreasing carbonate, increasing color intensity (dark brown humic) and pedogenic structure; mottles in lower parts, singular pseudomycelia, very weak clay coatings in lower parts
	AhBt	1010	pl di	10 YR3/6	Lu	*	slightly reddish color, some clay coatings
	Ah	1030	pl di	10 YR3/4	Lu	*	less reddish (more brownish), inhomogenous, gravel component, iron- and manganese concretions, charcoal
	AhBt	1060	pl di	10 YR3/6	Lu	*	slightly reddish, inhomogenous, clay coatings
	AC	1074	pl di	10 YR3/4	Lu	*	lighter colored (loess component?), granulite rock fragments
	Ah	1103	pl cl-di	10 YR3/4	Lu	*	dark humic, weak mottles, crotowina, charcoal
	AhBw	1131	pl di	10 YR4/4	Lu	*	brownish(-reddish?), inhomogenous, to the bottom increasing pseudomycelia
<b>P 8</b>	AhCk	1144	mot di	10 YR5/4	Uls	****	greyish transition horizon, pseudomycelia abundant
	Cv-Cc	1180	-	2.5 Y 5/4	Lu	****	(sandy) loess, pseudomycelia

Table legend (cf. KA 5*):		fossil loose substrate		humic bioturbated weathered containing sec. carbonate affected by retained water		dr mot w pl		drop-like mottled wavy plain		sh cl di		sharp clear diffuse		* no weak moderate strong very strong	
f	i	h	x	h	h	dr	mot	dr	drop-like	sh	sharp	*	no	*KA 5 = German mapping key for soils, 5th ed. (Ad-Hoc Arbeitsgruppe Boden 2005).	
-	+	v	v	v	v	w	w	w	wavy	cl	clear	**	weak	S = sand, U = silt, T = clay, L = loam (S+U+T).	
-	+	c	c	c	c	pl	pl	pl	plain	di	diffuse	****	strong	For grain size classes see Fig. 6	
-	+	g	g	g	g							*****	very strong		

Fig. 5: Field description of the Paudorf sequence (stratigraphy sketch in Fig. 6)

Abb. 5: Geländedaten der Löss-Paläoboden-Sequenz Paudorf (Profilskizze in Abb. 6)

### 4.3 Microscopic studies

A regular pattern of the petrographical composition of the different fractions from the sieving (for classes cf. Fig. 6) was identified under binoculars. Gravel consists mainly of small

angular to subangular rock particles bearing quartz, feldspar, garnet and other unidentified components. The composition and structure is identical to the local granulite. The surfaces of the fragments are partly oxidized and thus have yellowish to orange pigmentation. Coarse sand has a comparable com-



position. In the medium sand fraction, granulitic material is successively replaced by aggregates of feldspar, quartz and pale garnet without darker accessories. The major portion of the 40–200 µm fractions consists of unoxidized particles of disintegrated granulite. To a certain degree in the fine sand, and most obvious in the 40–63 µm fraction, the petrographic composition shows greatest variety.

As no pretreatment with hydrochloric acid has been carried out before grain size analysis, secondary carbonates typical for loess-paleosol sequences (cf. BARTA 2011) contribute to the sand and gravel fractions. Carbonate concretions of 1–2 cm in size (“loess dolls”) were found in P4a–b (cf. Fig. 5). Ochre colored, rough, branch shaped fragments of up to 3 mm in length were found in the sieves that are result of carbonate cementing (hypocoating) of pore wall substrates (mostly silt) in former root channels. Plain white calcified root cells (CRC) of 0.2–1 mm size, were also present.

The above mentioned patterns are also visible in the thin sections studied under petrographic microscopes, for example in the section of P2b (upper pedocomplex). Here, (sub-) angular coarse mineral grains of > 100 µm diameter are predominantly local clastic material (granulite rock fragments or single granulite minerals). Furthermore, secondary carbonates (CRC, mollusk shell fragments, crystallized earthworm cast) and manganese nodules can have sand size. However, the dominant fractions in the sample are silt to clay sized. It consists of a broad spectrum of minerals typical for loess (quartz, feldspar, pyroxene, amphibole, mica, primary carbonates, clay minerals), secondary (pedogenic) minerals (clay minerals, iron- and manganese oxides), including secondary carbonates (lubinite, calcitic hypocoatings). These observations are of importance with respect to the results of texture analysis.

In the upper pedocomplex, minerals are only slightly altered. Micas for example are weakly oxidized. Clay coatings are not present, and only some domains of oriented clay are traceable; in many parts the structure is granular. Fragments of more intensely colored and more clay rich substrate containing less or no carbonate are present (Fig. 4-1e). Overall the substrate is quite heterogeneous.

Apart from a higher sand content, the composition of the groundmass of the lower pedocomplex is comparable. The thin section of P7e is darker pigmented than the sections of the upper pedocomplex and contains only very few secondary carbonate (micrite). The sample contains more clay in the groundmass as well as reddish-brown colored deformed clay coatings (Fig. 4-3e). Some areas of granular structure are also present in this horizon. CRC are only present in the sample of P7b, which exhibits more granular structure.

## 5 Discussion

In the morphological setting at the foot of the Waxberg hill, slope processes contribute to the genesis of the sequence. This is best reflected in the ubiquitous presence of gravel that does not fulfill expectations regarding an eolian sediment. Furthermore, none of the renowned paleosols described earlier is monogenetic (if we understand monogenetic as development over time under relatively homogenous climatic conditions). In the following the loess sediments between the two pedocomplexes will be discussed. First correlations

with other records are attempted where chronological data are available. Afterwards the upper pedocomplex will be reviewed on the basis of existing and new data and assumptions on its genesis and its significance presented. The lower pedocomplex lacks a reliable chronological framework; therefore only preliminary concepts in respect to its genesis can be discussed.

### 5.1 Loess sediment units [P1, P3–6, P8]

P1, P3–6 and P8 are made up mostly of silt rich yellow-gray substrate that in some parts contains considerable amounts of coarser material of local origin. Next to eolian sedimentation, redepositional processes were common, creating an admixture of local materials. The substrate has blocky to subpolyhedral structure. Several paleosols that evidence phases of morphological stability were identified in the sequence between the two pedocomplexes.

A considerable part of the primary carbonate and silt rich material in P1, P3–6 and P8 can be attributed to eolian input. The finer sand fractions with a broad petrographic/mineralogical spectrum are most likely also wind-blown deposits. Saltation and reptation in environments of sparse vegetation are possible processes for the admixture of the coarser clastic particles of local origin. The partly layered appearance of the substrate and the presence of gravel bands indicates colluvial processes. The pale yellow color and the character of aggregates – most likely due to cementation by carbonate and clay in cold steppe environments (PÉCSI & RICHTER 1996) resemble typical loess of temperate latitudes. These near-surface diagenetic processes and redeposition may have occurred with seasonal alternation and are thus to be classified as syngenetic on the studied time scales.

If loess is defined genetically as wind-blown dust (e.g. PYE & SHERWIN 1999), there is clearly no loess (sub)unit present in the Paudorf sequence. Following SMALLEY et al. (2011) input of eolian dust is the most crucial element for loess genesis; the eolian dust provides physiochemical conditions, which are of great importance for the subsequent specific processes that alter the deposit in situ. In Paudorf, mineral dust is only one component of a substrate that has structural similarity to loess. Structural development, equally important for the genesis, is supposed to have taken place in situ, in a cold steppe environment. All twelve descriptive criteria for an adequate description of loess attributed to Márton Pécsi, listed in SMALLEY et al. (2011) are fulfilled to a certain grade within P1, P3–6 and P8. An exception is the very sandy P6c in which the silt content is less than 40% and therefore too low for loess after this definition. Referring to section 3 of this list, which says that loess horizons are usually unstratified, the striated appearance, especially in P4, should be noted as unusual. In PÉCSI (1990) and PÉCSI & RICHTER (1996) criteria are slightly different but the conceptual idea is identical. Acknowledging the fundamental ideas of L.S. Berg (cf. SMALLEY et al. 2011), adjusted by PÉCSI (1990; PÉCSI & RICHTER 1996), it is possible to classify this yellowish substrate with loess structure, which is dominated by silt particles as “loess”. According to KOCH & NEUMEISTER (2005), most parts of the loess sediment in Paudorf correspond to be named solifluction sand-loess (“Solifluk-tions-Sandlöss”).

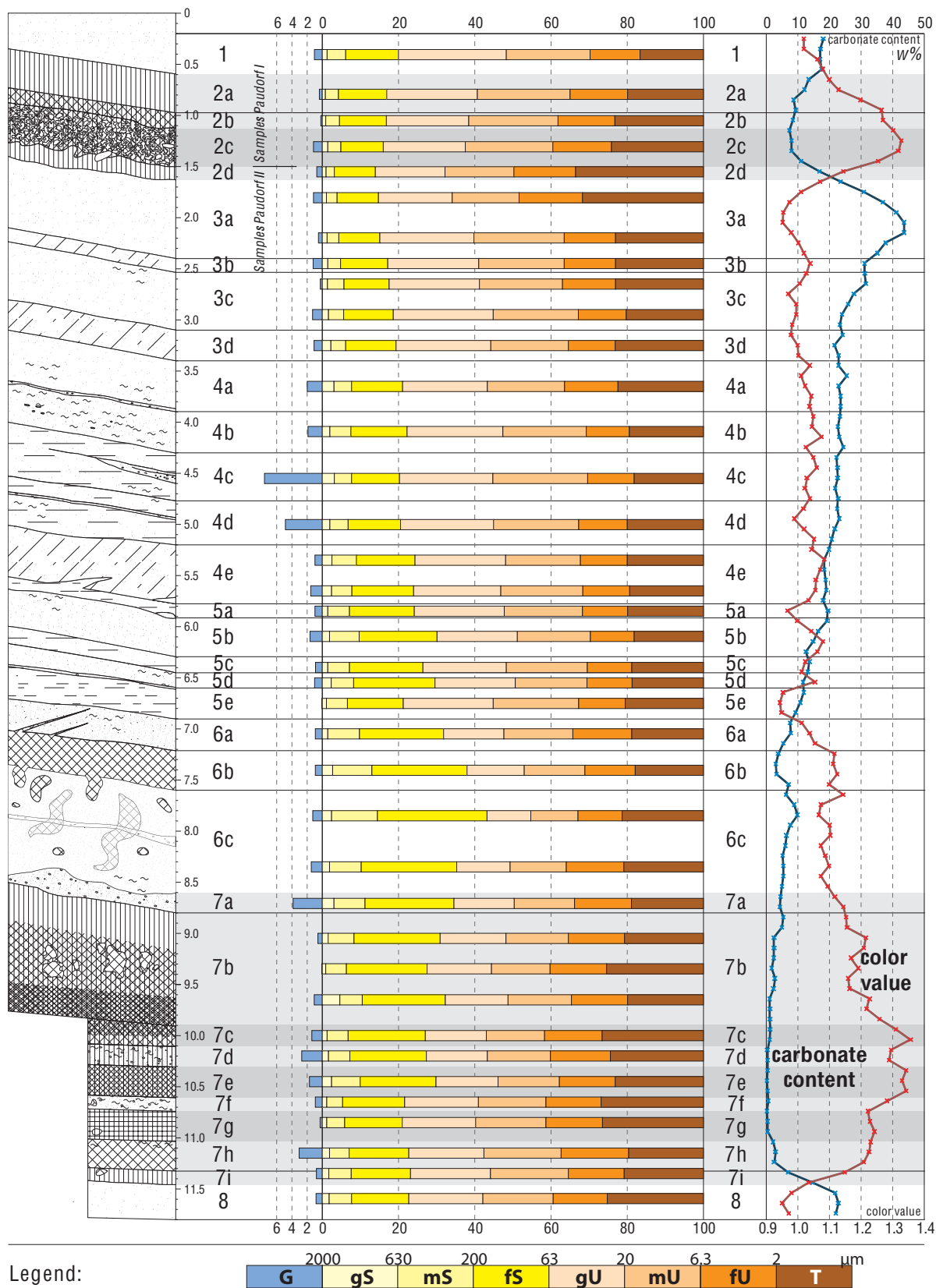


Fig. 6: Stratigraphy of the standard Paudorf sequence with texture analyses and high resolution carbonate contents and color values. The results are listed in Table 1. Grain size classes and names after KA 5 (AD-HOC-ARBEITSGRUPPE BODEN 2005).

Abb. 6: Stratigraphie der Standardsequenz Paudorf mit Ergebnissen der Korngrößenanalysen und Daten zu Carbonatgehalten und Farbwerten in hoher Auflösung. Die Ergebnisse sind in Tabelle 1 aufgelistet. Die Korngrößenklassen und -bezeichnungen folgen der KA 5 (AD-HOC-ARBEITSGRUPPE BODEN 2005).

Tab. 1: Results of laboratory analyses of texture, carbonate and color. For texture classes and names see Fig. 6. Color values and carbonate contents are calculated for the horizons of the texture analyses.

Tab. 1: Resultate der Laboranalysen von Korngrößen, Karbonatgehalten und Farbwerten. Die Korngrößenklassen und -bezeichnungen sind Abb. 6 zu entnehmen. Farbwerte und Karbonatgehalte sind auf die Horizonte der Korngrößenanalyse umgerechnet.

Sub-unit	<b>G [w%]</b>	gS [w%]	mS [w%]	fS [w%]	<b>Σ S [w%]</b>	gU [w%]	mU [w%]	fU [w%]	<b>Σ U [w%]</b>	<b>T [w%]</b>	Color value	Carbonate [w%]
P1	<b>1.0</b>	1.3	4.8	13.8	<b>20.0</b>	28.3	22.0	13.1	<b>63.4</b>	<b>16.6</b>	1.04	17.2
P2a	<b>0.4</b>	0.8	3.5	12.6	<b>16.9</b>	23.8	24.3	15.1	<b>63.2</b>	<b>19.9</b>	1.16	10.4
P2b	<b>0.2</b>	1.0	3.6	12.3	<b>16.8</b>	21.6	23.4	14.9	<b>59.9</b>	<b>23.3</b>	1.27	8.4
P2c	<b>1.2</b>	1.5	3.4	11.1	<b>16.0</b>	21.5	22.9	15.3	<b>59.8</b>	<b>24.2</b>	1.32	8.0
P2d	<b>0.7</b>	1.0	2.2	10.8	<b>14.0</b>	18.2	18.1	16.2	<b>52.5</b>	<b>33.5</b>	1.14	16.9
P3a1	<b>1.2</b>	1.2	2.7	10.9	<b>14.8</b>	19.3	17.6	16.6	<b>53.5</b>	<b>31.7</b>	0.99	34.0
P3a2	<b>0.5</b>	1.3	3.0	10.7	<b>15.1</b>	24.7	23.7	13.4	<b>61.8</b>	<b>23.1</b>	0.99	40.8
P3b	<b>1.2</b>	1.4	3.4	12.3	<b>17.2</b>	23.9	22.4	13.5	<b>59.8</b>	<b>23.1</b>	1.04	31.1
P3c1	<b>0.3</b>	1.4	4.3	11.8	<b>17.6</b>	23.7	21.8	13.9	<b>59.3</b>	<b>23.1</b>	1.01	31.6
P3c2	<b>1.3</b>	1.7	3.9	13.0	<b>18.7</b>	26.2	22.4	12.6	<b>61.1</b>	<b>20.2</b>	1.00	24.0
P3d	<b>1.1</b>	2.3	3.9	13.2	<b>19.3</b>	24.8	20.4	12.3	<b>57.5</b>	<b>23.1</b>	1.00	21.7
P4a	<b>2.0</b>	3.1	4.6	13.4	<b>21.1</b>	22.2	20.2	14.0	<b>56.4</b>	<b>22.5</b>	1.02	23.0
P4b	<b>1.9</b>	2.1	5.5	14.8	<b>22.3</b>	25.1	21.9	11.3	<b>58.2</b>	<b>19.5</b>	1.06	22.9
P4c	<b>7.6</b>	3.2	4.5	12.5	<b>20.3</b>	24.5	24.8	12.3	<b>61.6</b>	<b>18.2</b>	1.03	22.6
P4d	<b>4.8</b>	2.1	4.7	13.7	<b>20.6</b>	24.4	22.4	12.7	<b>59.5</b>	<b>20.0</b>	1.01	22.5
P4e1	<b>1.0</b>	2.6	6.4	15.4	<b>24.4</b>	23.7	19.7	12.3	<b>55.6</b>	<b>20.0</b>	1.08	18.4
P4e2	<b>1.5</b>	2.4	5.3	16.2	<b>24.0</b>	22.8	21.5	12.3	<b>56.7</b>	<b>19.4</b>	1.06	19.0
P5a	<b>1.0</b>	1.5	5.6	17.0	<b>24.1</b>	23.6	20.6	11.8	<b>56.0</b>	<b>19.9</b>	0.97	19.6
P5b	<b>1.6</b>	1.9	7.8	20.5	<b>30.1</b>	21.1	19.1	11.5	<b>51.7</b>	<b>18.2</b>	1.06	15.7
P5c	<b>0.9</b>	1.5	5.7	19.2	<b>26.4</b>	21.8	21.2	11.7	<b>54.7</b>	<b>18.8</b>	1.02	13.5
P5d	<b>1.0</b>	2.4	5.9	21.3	<b>29.6</b>	21.0	18.9	11.8	<b>51.7</b>	<b>18.7</b>	1.05	11.8
P5e	<b>0.1</b>	1.2	5.5	14.6	<b>21.2</b>	23.6	22.4	12.3	<b>58.2</b>	<b>20.5</b>	0.94	10.8
P6a	<b>0.9</b>	1.5	8.2	22.1	<b>31.8</b>	15.8	18.1	15.5	<b>49.4</b>	<b>18.8</b>	1.04	7.8
P6b	<b>0.9</b>	2.8	10.3	24.9	<b>38.0</b>	15.0	15.9	13.2	<b>44.1</b>	<b>17.9</b>	1.12	3.2
P6c1	<b>1.3</b>	2.5	12.0	28.7	<b>43.2</b>	11.5	12.4	11.6	<b>35.4</b>	<b>21.3</b>	1.07	9.9
P6c2	<b>1.5</b>	1.9	8.4	25.0	<b>35.3</b>	14.0	14.8	15.1	<b>43.8</b>	<b>20.9</b>	1.10	5.5
P7a	<b>3.8</b>	3.1	8.1	23.3	<b>34.5</b>	15.8	15.8	14.9	<b>46.5</b>	<b>19.0</b>	1.13	4.5
P7b1	<b>0.6</b>	1.6	6.8	22.6	<b>31.0</b>	17.2	16.4	14.7	<b>48.3</b>	<b>20.7</b>	1.22	2.5
P7b2	<b>0.1</b>	0.9	5.5	21.1	<b>27.5</b>	16.8	15.4	14.8	<b>47.0</b>	<b>25.4</b>	1.19	1.8
P7b3	<b>1.1</b>	4.7	5.9	21.7	<b>32.3</b>	16.5	16.7	14.7	<b>47.8</b>	<b>20.0</b>	1.23	1.1
P7c	<b>1.4</b>	1.3	5.5	20.2	<b>27.0</b>	16.0	15.2	15.1	<b>46.4</b>	<b>26.6</b>	1.33	1.2
P7d	<b>2.7</b>	1.6	5.7	20.1	<b>27.4</b>	16.0	16.5	15.8	<b>48.2</b>	<b>24.4</b>	1.29	0.4
P7e	<b>1.7</b>	2.5	7.5	19.8	<b>29.8</b>	16.3	16.1	14.6	<b>47.0</b>	<b>23.2</b>	1.33	0.3
P7f	<b>0.9</b>	1.2	4.2	16.3	<b>21.7</b>	19.3	17.7	14.5	<b>51.5</b>	<b>26.9</b>	1.28	0.6
P7g	<b>0.3</b>	1.2	4.7	15.1	<b>21.0</b>	19.3	18.4	14.8	<b>52.5</b>	<b>26.5</b>	1.23	0.5
P7h	<b>3.0</b>	1.9	5.2	15.6	<b>22.7</b>	19.7	20.3	17.7	<b>57.7</b>	<b>19.7</b>	1.23	3.0
P7i	<b>0.8</b>	1.7	5.9	15.5	<b>23.1</b>	21.0	20.4	14.7	<b>56.1</b>	<b>20.8</b>	1.15	7.0
P8	<b>0.8</b>	1.8	5.9	15.0	<b>22.7</b>	19.4	18.4	14.2	<b>52.1</b>	<b>25.2</b>	0.97	22.4

Morphologically stable phases of slightly moister conditions with reduced sedimentation rates (cf. BIBUS 1974, ANTOINE et al. 2009) are documented by Cryosols. The higher silt and lower sand contents in the bleached horizons of P5 compared to the surrounding (sub)units appear significant. They can be attributed to cryogenic weathering, but also to ongoing dust input. Post IR-IRSL ages (THIEL et al. 2011b) indicate that the major part of the sequence between the two pedocomplexes (P3–5) can be attributed to MIS 6. The formation of Cryosols in the penultimate glacial is reported for several locations from Western to Central Europe. For Belgium/Netherlands “tundrasols” are reported by MEIJIS (2002) in the “B-Loess”. This correlates to the findings of BIBUS (1974, 2002), who names a sequence of six “Naßböden” (wet soils) in the “Jungriss” loess as “Bruchköbeler Böden” (BIBUS 2002). These paleosols are labeled from base to top

B1 to B6. B1 and B3 are more pronounced (BIBUS 1974, 2002) and potentially correlate to the Cryosols P5a and P5e in Paudorf.

The genesis of P6b, a brownish horizon with reduced carbonate content in the upper part of the sandy P6 remains unclear. It appears rather inhomogeneous and could be interpreted as soil sediment. A crotovina-like pattern below can be seen as evidence for morphologic stability in a warmer phase.

The relation between carbonate content and color described in 4.2.2 could be interpreted by slight sedimentological changes. On the other hand it is possible that further phases of morphological stability were detected several times in the profile: Slight decalcification with an increase in coloring, in combination with calcification a few decimeters below, could be attributed to slight pedogenesis.



## 5.2 Upper pedocomplex (P2)

The upper pedocomplex (P2) formed during MIS 5 (ZÖLLER et al. 1994; THIEL et al. 2011b). The combination of its features points strongly to polygenesis: It is characterized by a reddish-brown color, partly in a speckled pattern, enhanced clay content and less carbonate compared to the loess sediments. However, primary carbonates can be detected. Clay coatings were not identified. Rock fragments that are oriented parallel to the inclination of the horizons and frost structures at the lower boundary are characteristic.

P2, the “Paudorfer Bodenbildung”, is contrary to previous assumptions not a Bw or Bt horizon (BRANDTNER 1954; PETICZKA et al. 2009); neither it can be classified as an Ah horizon (SEMMELE 1968; BRONGER 1976). V. Ložek (in FINK 1976) stated that the “Paudorfer Bodenbildung” is a complicated pedocomplex. However, no attempt was made to investigate the sequence in greater detail to reconstruct the processes leading to its formation. We assume the formation of a Chernozem in a redeposited Cambisol. During redeposition of the Cambisol, admixture of primary carbonate took place that was not leached during the development of the Chernozem.

### Stages of development

The first step in the genesis of the pedocomplex after deposition of the parent material (loess sediment) is the development of a Cambisol. Passive and active reddish-brown pigmentation due to carbonate leaching and formation of iron oxides respectively lead to the formation of a Bw horizon. In general, rubified soils develop in ecosystems with a pronounced dry season. However, the reddish component can also be explained by reddening after burial (RETALLACK 2001). The carbonate maximum is found directly below P2, in P3a. This could evidence relatively shallow decalcification if the Cambisol was not too much eroded. It has to be noted in this context that the role of P3a as uppermost loess-unit in the subdivision of the polygenetic loess-paleosol sequence is ambiguous. Being the Ck-horizon of the Cambisol it could be assigned also as lowermost subunit of P2. Reddish pigmentation is as shallow decalcification in general common in environments with a seasonal precipitation.

Clay contents in P2 are enhanced; therefore the question of humidity resulting in hydrolytical weathering with clay neoformation is to be discussed. It is firsthand likely that the higher fine silt and clay content at the boundary of P2 and P3 is partly due to precipitation of microcrystalline calcite that is visible in thin sections. However, some chemical weathering resulting in clay neoformation likely took place, as decalcified clay-rich material was detected in the thin section (Fig. 4-1e). V. Ložek found mollusks (*Aegopis verticillus* [LAM], *Pagodulina pagodula* [DESM.], *Cepaea vindobonensis* [FÉR.]) at the lower boundary of the “Paudorfer Bodenbildung”, which indicate humid interglacial conditions; even more humid than indicated by the Holocene fauna (in FINK 1976). Our results, however, give no evidence for pronounced humidity, which would most likely result in clay illuviation. To summarize the first phase in the genesis of the pedocomplex, the formation of a Cambisol, potentially in a temperate climate with seasonal precipitation is assumed.

Rock fragments as well as primary carbonate grains imply that the (probably decalcified) Cambisol was later trun-

cated and reworked. During redeposition wind-blown dust with carbonate component was admixed. At least one interval of periglacial conditions during this phase can be assumed; the rock fragments in P2 are oriented parallel to the inclination of the horizons, which is typical for solifluction, and the boundary to P3 is characterized by deformed wedges and pockets, which are most likely caused by cryogenic processes.

A dark pigmentation of P2, primary carbonate and a granular structure led SEMMELE (1968) and BRONGER (1976) to the conclusion that the “Paudorfer Bodenbildung” at the locus typicus is a fossilized Chernozem. In its upper part V. Ložek detected a *Tridens*-fauna that corresponds to early last glacial interstadial Chernozems (FINK 1976). This typical steppe soil is characterized by humification and bioturbation. Calcified root cells may be relics of the steppe environment. The speckles/mottles in humic horizons are likely caused by post-pedogenetical humus degradation and are a common feature in early last glacial humic horizons (ROHDENBURG 1964).

Pedogenesis in the steppe environment was successively replaced by accumulation of eolian dust and fine sand, documented in the diffuse upper boundary of P2 and increasing silt contents in P1.

### Chronology and correlation

The post-IR IRSL date of  $106 \pm 12$  ka above the “Paudorfer Bodenbildung” published by THIEL et al. (2011b) indicates that pedogenesis during MIS 5a is not documented in Paudorf. On the contrary, ZÖLLER et al. (1994) revealed TL-ages of  $54 \pm 6$  ka from a comparable stratigraphical position.

On the base of these datings and our results, the Cambisol formation is attributed to MIS 5e (Eemian), the redeposition to the cold 5d stage, and the early glacial interstadial Chernozem to MIS 5c[-a]. The processes found in P2 during Eemian and early last glacial can be correlated with standard MIS 5 pedocomplexes in Central Europe: The paleosol stack of Stillfried A, also named “Stillfrieder Komplex” exhibits a basal “Verlehmungszone” (Bw horizon) of a truncated Cambisol and three Ah horizons on top, separated by thin layers of loess sediment (FINK 1954; BRONGER 1976). In the German loess stratigraphy a comparable scheme exists. The fossil Ah horizons above the remaining Bt horizons of the truncated Eemian Luvisols are named Mosbacher Humuszonen (SCHÖNHALS et al. 1964; SEMMELE 1968). A comparable pattern of MIS 5 paleosols is found in the Czech Republic, e.g. in Dolní Věstonice (BRONGER 1976; FRECHEN et al. 1999; BÁBEK et al. 2011). In P2 of the Paudorf sequence, the paleosols of the classical MIS 5-complexes are found not superimposed but interlaced.

### Geographical significance

Pedocomplexes comparable to P2 in Paudorf are present in the region, for example in the outcrops of Stiefen, Buchberg or Göttweig-Aigen (cf. FINK 1956, 1976). At the present state of research it is likely that P2 is a typical MIS 5-pedocomplex in the transition area of the Austrian loess landscapes after FINK (1956). P2, the classical “Paudorfer Bodenbildung”, can be regarded as the missing link between the MIS 5-complexes of the “humid loess landscape” (Linzer Komplex: an Eemian fossil Bt horizon and early glacial soil sediment) and “dry loess landscape” (Stillfrieder Komplex), defined by FINK

(1956). Although FINK (1961) presented time ranges and correlations that were revised at a later stage, we agree with his early assumption that the transition area is characterized both by pedogenesis of the “dry loess landscape” as well as intensive early glacial colluvial events, which are clearly documented in the profiles of the “humid loess landscape”. In this context it should be mentioned that more recent studies have revealed that colluvial layers above Eemian paleosols in the “humid loess landscape” do not necessarily represent only the early glacial (MIS 5d–5a), but also younger stages up to MIS 3 (TERHORST et al. 2002).

In future, it has to be discussed, whether Paudorf will be again accepted as type locality, but now for the MIS 5-complex of the “transition area” in Austrian loess landscapes, and if yes, whether the term “Paudorfer Bodenbildung” should still be used or finally dismissed. It is not a monogenetic paleosol and it carries some historical burden in context of Quaternary stratigraphy.

From a broader paleoclimatological perspective, the presented findings appear promising, related to the question of Eemian (MIS 5e) paleoclimate in Central Europe. In Paudorf (and possibly in the comparable pedocomplexes of the “transition area”) as well as in Stillfried (as type profile for the “dry loess landscape”) the Eemian paleosol is a Bw horizon of a Cambisol. The climate during the Eemian in the neighboring loess regions to the west (“humid loess landscape”) and the north (Moravia) must have been significantly moister, as evidenced by Eemian Bt horizons of former Luvisols (FINK 1956; BRONGER 1976; TERHORST et al. 2002; BÁBEK et al. 2011). In contrast, in the Pannonian Basin, the last interglacial is frequently represented by Chernozems or Phaeozems (BRONGER 2003; MARKOVIĆ et al. 2011).

### 5.3 Lower pedocomplex (P7)

The overall brownish lower pedocomplex (P7) has a reddish-brown middle part. Clay content is enhanced and carbonates are almost completely leached. In parts pedogenic structure is well expressed and horizons with clay coatings reflect longer phases of morphological stability. In the upper half of the pedocomplex (P7a–e), sand contents are higher. Several horizons bear considerable amounts of granulate and even rock fragments were found in P7f, providing evidence for phases of geomorphological activity. The genesis of this over 2 m thick pedocomplex seems thus even more complex than the genesis of the upper pedocomplex (P2). The lack of chronological data however, does not allow paleoecological implications and broader correlations.

Micromorphological assessment by L. Smolíková (in KOVANDA et al. 1995) was the first approach to decipher aspects of the pedogenesis: Two superimposed paleosols were identified in the field. Microscopic analyses of both paleosols revealed clay illuviation processes and humification/bioturbation, representing forest and steppe environments respectively. Besides these findings, previous studies (e.g. FINK, 1954, 1976; VERGINIS 1993; KOVANDA et al. 1995) have not described the remarkable complexity of the lower pedocomplex.

Below, preliminary assumptions of the main formation stages are discussed. In general, several phases of pedogenesis in steppe- to forest-steppe environments, disturbed by redeposition were found:

In the lower parts of P7, a dark Ah horizon (P7g) above a weak Bw horizon (P7h) are developed. The boundary area to P8 is enriched in secondary carbonate. This succession can be interpreted as monogenetic degraded Chernozem (Phaeozem) under (forest-)steppe conditions. Intensive redeposition and input of dust and local material is attributed to a degradation phase (P7f). Both field survey and microscopical analyses indicate phases of interglacial pedogenesis and redeposition in subunits P7c–e. Deformed clay coatings and areas with clear granular structure, as observed in thin sections, reveal clay mobilization under more humid conditions (Forest ecosystem) and bioturbation/humification in a drier climate (Steppe ecosystem). Gravel and charcoal especially in P7d, can be seen as macroscopic signs of colluvial processes. P7b–a represent a complex of steppe to forest steppe soils, which were successively buried by enhanced accumulation of eolian dust and admixture of coarser sediments of local origin.

In the context of paleoclimate, the overall more intense weathering as well as the presence of clay coatings can indicate significantly moister conditions compared to the Holocene climate in the study area or the Eemian paleoclimate. However, BRONGER et al. (1998) interpret more intensive weathering in MIS13–15 soils with prolonged pedogenesis. The thickness and complexity of P7 points to a formation during more than one interglacial, but the lack of datings allows no final conclusion whether climate or time is the main factor in respect to the grade of development.

Following the assumptions of KOVANDA et al. (1995), the lower pedocomplex is at least one interglacial older than the upper pedocomplex, which was formed during the Eemian (MIS 5e) and early last glacial. ZÖLLER et al. (1994) assume as well its formation during the penultimate interglacial. As the oldest age according to THIEL et al. (2011b) in the loess sediment above the lower pedocomplex is  $189 \pm 16$  ka, the genesis of P7 in MIS 7 and/or some older interglacial(s) is most probable. In discussion of the chronology, however, possible discontinuities in P6 and P7 have to be taken into account.

It should be noted that the lower pedocomplex has been previously correlated with the “Göttweiger Verlehmungszone” (GÖTZINGER 1936; FINK 1976). However, this paleosol was dated to  $\geq 350$  ka (THIEL et al., 2011b) in Göttweig-Furth. Further, the “Göttweiger Verlehmungszone” has been correlated to the KR 4 paleosol of Krems-Schießstätte (shooting range) (GÖTZINGER 1936; FINK 1976); absolute ages are not available for that site, but in the loess below KR 4 the Brunhes/Matuyama reversal was found (FINK 1976). Therefore, it can be hypothesised that a major portion of the Middle Pleistocene interglacials could be recorded in Paudorf P7.

The two pedocomplexes in Paudorf thus cannot reflect two interstadials of the last glacial as postulated by LAIS (1951) and BRANDTNER (1954, 1956) but may be two interglacial pedocomplexes, the upper one representing the Late Pleistocene and the lower one an as yet unknown time span of Middle Pleistocene.

## 6 Conclusions

Detailed paleopedological, sedimentological and micromorphological analyses reflect the complex genesis of Paudorf locus typicus. Although this archive was seen as not favora-

ble during its scientific history (cf. FINK 1954, 1976, BRONGER 1976), it records a well resolved and thus a considerable archive to reconstruct landscape development during Middle Pleistocene and MIS 5 in the interplay of local influences and climatically driven environmental changes. This study demonstrates that process oriented research can provide valuable insights into paleoenvironmental archives even in complex morphological settings. The scientific potential of the sequence is not only focussed on the prominent pedocomplexes, but further in the sequence of loess sediments in between. In complex loess-paleosol sequences it is next to reliable datings crucial, to trace phases of pedogenesis in order to detect phases of stability, which allow for correlation with loess-paleosol sequences of the same age.

P2, the “Paudorfer Bodenbildung”, is a pedocomplex attributed to MIS 5. It is an early glacial Chernozem that developed in the redeposited (MIS 5d) Eemian Cambisol. From a paleoclimatological perspective it is important to note that P2 in Paudorf includes, like the basal soil of Stillfried a further example for Eemian Cambisols in Lower Austria.

P3–5 probably represent MIS 6. Under periglacial environmental conditions eolian dust sedimentation and (solifluidal) redeposition took place as well as pedogenesis (Cryosols) during more stable geomorphodynamic phases. To establish the genesis and age of P6, which includes a brownish horizon, micromorphological and geochronological investigations must be carried out. The thick lower pedocomplex (P7) provides research potential for the future, as it seems to represent local effects of few 100 ka of climatically driven sedimentation, pedogenesis and colluvial activity during the Middle Pleistocene.

## Acknowledgements

We would like to thank Simon Meyer-Heinze, Markus Hörschlein and Katja Wiedner for support during field work. Christa Hermann and Maxime Farin are thanked for assistance with grain size analyses. The competent advice of Karin Wriessnig was highly appreciated in the laboratory. Dr. Sergey Sedov gave valuable review comments and was always open for fruitful discussions. Furthermore, we are grateful for the helpful review of Dr. Holger Kels. Finally we thank Hazel Sprafke for linguistic support.

## References

- AD-HOC-ARBEITSGRUPPE BODEN (2005): *Bodenkundliche Kartieranleitung*, – 5. Aufl., 438 pp.; Hannover.
- ANGHELINU, M. & NIȚĂ, L. (2012): What’s in a name: The Aurignacian in Romania. – *Quaternary International*, in press. doi:10.1016/j.quaint.2012.03.013.
- ANTOINE, P., ROUSSEAU, D.-D., MOINE, O., KUNESCH, S., HATTÉ, C., LANG, A., TISSOUX, H. & ZÖLLER, L. (2009): Rapid and cyclic aeolian deposition during the Last Glacial in European loess: a high-resolution record from Nussloch, Germany. – *Quaternary Science Reviews*, 28: 2955–2973.
- BÁBEK, O., CHLACHULA, J. & GRYGAR, T.M. (2011): Non-magnetic indicators of pedogenesis related to loess magnetic enhancement and depletion: Examples from the Czech Republic and southern Siberia. – *Quaternary Science Reviews*, 30/7–8: 967–979.
- BARTA, G. (2011): Secondary carbonates in loess-paleosol sequences: a general review. – *Central European Journal of Geosciences*, 3/2: 129–146.
- BAYER, J. (1909): Jüngster Löß und paläolithische Kultur in Mitteleuropa. – *Jahrbuch für Altertumskunde III*: 149–160.
- BAYER, J. (1927): *Der Mensch im Eiszeitalter*. – 452 pp.; Wien (Deuticke).
- BIBUS, E. (1974): Abtragungs- und Bodenbildungsphasen im Rißlöß. – *Eiszeitalter und Gegenwart*, 25: 166–182.
- BIBUS, E. (2002): Zum Quartär im mittleren Neckarraum - Reliefentwicklung, Löß/Paläobodensequenzen, Paläoklima. – *Tübinger Geowissenschaftliche Arbeiten, D8*: 236 pp.
- BRANDTNER, F. (1954): Jungpleistozäner Löß und fossile Böden in Österreich. – *Eiszeitalter und Gegenwart*, 4/5: 49–82.
- BRANDTNER, F. (1956): Lößstratigraphie und paläolithische Kulturabfolge in Niederösterreich und in den angrenzenden Gebieten. – *Eiszeitalter und Gegenwart*, 7: 127–175.
- BRONGER, A. (1970): Zur Mikromorphologie und zum Tonmineralbestand von Böden ungarischer Lößprofile und ihre paläoklimatische Auswertung. – *Eiszeitalter und Gegenwart*, 21: 122–144.
- BRONGER, A. (1976): Zur quartären Klima- und Landschaftsentwicklung des Karpatenbeckens auf (paläo-)pedologischer und bodengeographischer Grundlage. – *Kieler Geographische Schriften*, 45: 268 pp.
- BRONGER, A., WINTER, R. & SEDOV, S. (1998): Weathering and clay mineral formation in two Holocene soils and in buried paleosols in Tadjikistan: towards a Quaternary paleoclimatic record in Central Asia. – *Catena*, 34/1-2: 19–34.
- BRONGER, A. (2003): Correlation of loess-paleosol sequences in East and Central Asia with SE Central Europe: towards a continental Quaternary pedomorphology and paleoclimatic history. – *Quaternary International*, 106–107: 11–31.
- BUYLAERT, J.-P., JAIN, M., MURRAY, A.S., THOMSEN, K.J., THIEL, C. & SOHBAATI, R. (2012): A robust feldspar luminescence dating method for Middle and Late Pleistocene sediments. – *Boreas*, 41/3: 435–451.
- DIN ISO 10693. Bodenbeschaffenheit – Bestimmung des Carbonatgehalts – Volumetrisches Verfahren (ISO 10693:1995).
- EINWÖGERER, T., FRIESINGER, H., HÄNDEL, M., NEUGEBAUER-MARESCH, C., SIMON, U. & TESCHLER-NICOLA, M. (2006): Upper Paleolithic infant burials. – *Nature*, 444: 285.
- FINK, J. (1954): Die fossilen Böden im österreichischen Löß. – *Quartär*, 6: 85–108.
- FINK, J. (1956): Zur Korrelation der Terrassen und Lössen in Österreich. – *Eiszeitalter und Gegenwart*, 7: 49–77.
- FINK, J. (1960): Leitlinien einer österreichischen Quartärstratigraphie. – *Mitteilungen der Geologischen Gesellschaft in Wien*, 53: 249–266.
- FINK, J. (1961): Die Gliederung des Jungpleistozäns in Oesterreich. – *Mitteilungen der Geologischen Gesellschaft in Wien*, 54: 1–25.
- FINK, J. (1976): Exkursion durch den österreichischen Teil des nördlichen Alpenvorlandes und den Donauraum zwischen Krems und der Wiener Pforte. (Mitteilungen der Kommission für Quartärforschung der Österreichischen Akademie der Wissenschaften, 1). – 113 pp.; Wien.
- FINK, J. & KUKLA, G.J. (1977): Pleistocene Climates in Central Europe: At Least 17 Interglacials after the Olduvai Event. – *Quaternary Research*, 7: 363–371.
- FRECHEN, M., ZANDER, A., CILEK, V. & LOŽEK, V. (1999): Loess chronology of the Last Interglacial/Glacial cycle in Bohemia and Moravia, Czech Republic. – *Quaternary Science Reviews*, 18: 1467–1493.
- GEONFO NÖ: NÖ-Atlas 3.0. - Karte: Geländehöhe (Laserscan). – [www.in-termap1.noel.gv.at](http://www.in-termap1.noel.gv.at).
- GEOLOGISCHE BUNDESANSTALT (ed., 2002): *Niederösterreich. Geologische Karte 1:200 000 mit Kurzerläuterung. Geologie der österreichischen Bundesländer*.
- GÖTZINGER, G. (1936): Das Lößgebiet um Göttweig und Krems an der Donau. – In: GÖTZINGER, G. (Ed.): *Führer für die Quartär-Exkursionen in Österreich*. Geologische Bundesanstalt, 1: 1–11.
- HAESAERTS, P., DAMBLON, F., BACHNER, M. & TRNKA, G. (1996): Revised stratigraphy and chronology of the Willendorf II sequence, Lower Austria. – *Archaeologia Austriaca*, 80: 25–42.
- IIUSS WORKING GROUP WRB (2006): *World reference base for soil resources 2006 (FAO - World Soil Resources Reports, 103)*. – 132 pp.; Rome.
- KOCH, R. & NEUMEISTER, H. (2005): Zur Klassifikation von Lößsedimenten nach genetischen Kriterien. – *Zeitschrift für Geomorphologie N.F.*, 49/2: 183–203.
- KOVANDA, J., SMOLÍKOVÁ, L. & HORÁČEK, I. (1995): New data on four classic loess sequences in Lower Austria. – *Sborník geologických věd, Antropozoikum*, 22: 63–85.
- LAIS, R. (1951): Über den jüngeren Löß in Niederösterreich, Mähren und Böhmen. – *Berichte der Naturforschenden Gesellschaft zu Freiburg i. Br.*, 41: 119–178.
- LISIECKI, L. E. & M. E. RAYMO (2005): A Pliocene-Pleistocene stack of 57 globally distributed benthic  $\delta^{18}O$  records. – *Paleoceanography*, 20: 1–17.
- MARKOVIĆ, S.B., OCHES, E., SÜMEGI, P., JOVANOVIĆ, M. & GAUDENYI, T.



- (2006): An introduction to the Middle and Upper Pleistocene loess-paleosol sequence at Ruma brickyard, Vojvodina, Serbia. – *Quaternary International*, 149: 80–86.
- MARKOVIĆ, S.B., HAMBACH, U., CATTO, N., JOVANOVIĆ, M., BUGGLE, B., MACHALETT, B., ZÖLLER, L., GLASER, B. & FRECHEN, M. (2009): Middle and Late Pleistocene loess sequences at Batajnica, Vojvodina, Serbia. – *Quaternary International*, 198: 255–266.
- MARKOVIĆ, S.B., HAMBACH, U., STEVENS, T., KUKLA, G.J., HELLER, F., MCCOY, W.D., OCHSES, E.A., BUGGLE, B. & ZÖLLER, L. (2011): The last million years recorded at the Stari Slankamen (Northern Serbia) loess-paleosol sequence: revised chronostratigraphy and long-term environmental trends. – *Quaternary Science Reviews*, 30: 1142–1154.
- MATURA, A. (2006): Böhmisches Massiv. – In: WESSELY, G. (Ed.): *Niederösterreich (Geologie der Österreichischen Bundesländer)*. Geologische Bundesanstalt, Wien: 25–39.
- MEIJS, E.P.M. (2002): Loess stratigraphy in Dutch and Belgian Limburg. – *Eiszeitalter und Gegenwart*, 51: 114–130.
- NEUGEBAUER-MARESCH, C. (1993): Zur altsteinzeitlichen Besiedlungsgeschichte des Galgenberges von Stratzing/Krems-Rehberg. – In: *Archäologie Österreichs. Mitteilungen der Österreichischen Gesellschaft für Ur- und Frühgeschichte*, 4: 10–19.
- NOLL, M., LEITNER-WILD, E. & HILLE, P. (1994): Thermoluminescence Dating of Loess Deposits at Paudorf, Lower Austria. – *Quaternary Geochronology (Quaternary Science Reviews)*, 13: 473–476.
- PAZONYI, P. (2004): Mammalian ecosystem dynamics in the Carpathian Basin during the last 27,000 years. – *Palaeogeography, Palaeoclimatology, Palaeoecology*, 212: 295–314.
- PÉCSI, M. (1990): Loess is not just the accumulation of dust. – *Quaternary International*, 7/8: 1–21.
- PÉCSI, M. & RICHTER, G. (1996): Löss. Herkunft - Gliederung - Landschaften. – *Zeitschrift für Geomorphologie, Supplementband*, 98: 391 pp.
- PENCK, A. & BRÜCKNER, E. (1909): *Die Alpen im Eiszeitalter 1*. – 393 pp.; Leipzig (Tauchnitz).
- PETICZKA, R., RIEGLER, D. & HOLAWA, F. (2009): *Exkursionsführer - 28. Jahrestagung des Arbeitskreises Paläopedologie der Deutschen Bodenkundlichen Gesellschaft*, 21. bis 23. Mai 2009 in Wien. – 68 pp.; Wien. Unpublished.
- PREUSSER, F. & FIEBIG, M. (2009): European Middle Pleistocene loess chronostratigraphy: Some considerations based on evidence from the Wels site, Austria. – *Quaternary International*, 198: 37–45.
- PYE, K. & SHERWIN, D. (1999): Loess. – In: Goudie, A. S., Livingstone, I. & Stokes, S. (Eds.): *Aeolian Environments, Sediments and Landforms*. Wiley & Sons: 213–238.
- RETALLACK, G.J. (2001): *Soils of the Past. An introduction to paleopedology*. – 2nd ed., 404 pp.; Oxford (Blackwell).
- ROHDENBURG, H. (1964): Ein Beitrag zur Deutung des „Gefleckten Horizontes“. – *Eiszeitalter und Gegenwart*, 15: 66–71.
- SCHOLGER, R. & TERHORST, B. (2011): Paläomagnetische Untersuchungen der pleistozänen Löss-Paläobodensequenz im Profil Wels-Aschet. – In: VAN HUSEN, D. & REITNER, J. (eds.): *Die Löss-Sequenz Wels/Aschet - Ein Referenzprofil für das Mittel- und Jungpleistozän im nördlichen Alpenvorland (MIS 16 bis MIS2)* (Mitteilungen der Kommission für Quartärforschung der Österreichischen Akademie der Wissenschaften, 19): 47–61.
- SCHÖNHALS, E., ROHDENBURG, H. & SEMMEL, A. (1964): Ergebnisse neuerer Untersuchungen zur Würmlöß-Gliederung in Hessen. – *Eiszeitalter und Gegenwart*, 15: 199–206.
- SEMMEL, A. (1968): Studien über den Verlauf jungpleistozäner Formung in Hessen. – *Frankfurter Geographische Hefte*, 45: 133 pp.
- SMALLEY, I., MARKOVIĆ, S.B. & SVIRČEV, Z. (2011): Loess is [almost totally formed by] the accumulation of dust. – *Quaternary International*, 240: 4–11.
- TERHORST, B. (2007): Korrelation von mittelpaleozänen Löss-/Paläobodensequenzen in Oberösterreich mit der marinen Sauerstoffisotopenkurve. – *E & G, Quaternary Science Journal*, 56: 172–185.
- TERHORST, B., FRECHEN, M. & REITNER, J. (2002): Chronostratigraphische Ergebnisse aus Lößprofilen der Inn- und Traun-Hochterrassen in Oberösterreich. – *Zeitschrift für Geomorphologie N.F., Supplementband*, 127: 213–232.
- TERHORST, B., THIEL, C., PETICZKA, R., SPRAFKE, T., FRECHEN, M., ROETZEL, R., NEUGEBAUER-MARESCH, C. & FLADERER, F.A. (2011): Casting new light on the chronology of the loess/paleosol sequences in Lower Austria. – *E & G, Quaternary Science Journal*, 60/2–3: 270–277.
- THIEL, C., BUYLAERT, J.-P., MURRAY, A.S., TERHORST, B., HOFER, I., TSUKAMOTO, S. & FRECHEN, M. (2011a): Luminescence dating of the Stratzing loess profile (Austria) – Testing the potential of an elevated temperature post-IR IRSL protocol. – *Quaternary International*, 234: 23–31.
- THIEL, C., BUYLAERT, J.-P., MURRAY, A. S., TERHORST, B., TSUKAMOTO, S., FRECHEN, M. & SPRAFKE, T. (2011b): Investigating the chronostratigraphy of prominent palaeosols in Lower Austria using post-IR IRSL dating. – *E & G, Quaternary Science Journal*, 60/1: 137–152.
- VERGINIS, S. (1993): Lössakkumulation und Paläoböden als Indikatoren für Klimaschwankungen während des Paläolithikums (Pleistozän). Mit ausgewählten Beispielen aus Niederösterreich. – In: NEUGEBAUER-MARESCH, C. (Ed.): *Altsteinzeit im Osten Österreichs (Wissenschaftliche Schriftenreihe Niederösterreich, 95/96/97)*, 2. Aufl.: 13–30.
- VISCARRA ROSSEL, R.A., MINASNY, B., ROUDIER, P. & McBRATNEY, A.B. (2006): Colour space models for soil science. – *Geoderma*, 133: 320–337.
- ZÖLLER, L., OCHES, E. A. & MCCOY, W. D. (1994): Towards a revised chronostratigraphy of loess in Austria with respect to key sections in the Czech Republic and in Hungary. – *Quaternary Geochronology (Quaternary Science Reviews)*, 13: 465–472.



# Instruction to Authors

Basically the manuscript shall be submitted in electronic form and has to include the name and the address of the first author. Please use a standard word processor in .rtf, .odt or .doc-format (LaTeX files on request). As character set please use the standard fonts Times Roman, Helvetica or Courier with 1.5 line spacing.

For the submission please use our online system at [www.quaternary-science.net](http://www.quaternary-science.net). After the login you can upload your manuscript as well as separate figures and tables.

## Manuscript style

The acceptable languages are English and German. Manuscripts in German have to contain an English subtitle, an abstract in English and English keywords. The rules of the new German spelling reform apply to German texts.

Manuscripts should be arranged in the following order:

- I Short but concise title
- II Full names, full address and e-mail
- III 5 to 10 keywords that describe the contents of your paper
- IV An abstract of up to 200 words in German and English.  
The translated abstract should carry the translated title in square brackets,
- V Clearly structured text. For chapter numbering use Arabic numerals.
- VI The reference list has to be arranged alphabetically and should conform to the examples given below.

References have to be inserted in the text as brief quotations, the name of the author has to be set in small CAPITALS, the year of publication in brackets e.g. MÜLLER (2006). If more than one publication of the same author in the same year is cited, identify each citation as follows: MÜLLER (2006a, 2006b). Where three or more authors are listed in the reference list, please cite in the text as MÜLLER et al. (2006). Papers with up to three authors should be cited as MÜLLER & MEYER (2006) or MÜLLER, MEYER & SCHULZ (2006). If a special page or figure of a paper should be cited, use following citation style: MÜLLER (2006: 14) or MÜLLER (2006, Fig. 14).

Scientific names of flora and fauna (*gender, sub-gender, species, sub-species*) have to be written in *italics*. Use small CAPITALS for the author (*Armeria maritima* WILLD.)

- Do not justify your text, use a ragged left alignment.
- Do not use automatic hyphenation.
- Do not use any automatic formatting.
- Do not use pagination.

Do not insert images, tables and photos into the text, it should be added as separate files. Captions of figures and tables in German and English should be placed at the end of the manuscript.

## Illustrations

Supply each figure as a separate file with the name of the author. Illustrations should be reducible to a column width (8.4 cm) or type area (17.2 x 26 cm). The lettering has to be easily readable after reduction. Where a key of symbols is required, include this in the figure, not in the caption of the figure. Avoid fine lines (hairlines) and grey-shading/halftones. All figures may be colored. There are no additional costs.

For printing all illustrations have to be supplied electronically. Please use for pixel-based images (photos) the .tif-format with a resolution of at least 450 dpi and for vector-based illustrations (graphs, maps, tables) the .eps-format. Greatly reduced .jpg-files or .pdf-files or figures included in word-documents are not accepted.

## References [examples]

### Papers:

- SCHWARZBACH, M. (1968): Neue Eiszeithypothesen. – *Eiszeitalter und Gegenwart*, 19: 250–261.
- EISSMANN, L. & MÜLLER, A. (1979): Leitlinien der Quartärenentwicklung im norddeutschen Tiefland. – *Zeitschrift für Geologische Wissenschaften*, 7: 451–462.
- ZAGWIJN, W.H. (1996): The Cromerian Complex Stage of the Netherlands and correlation with other areas in Europe. – In: TURNER, C. (ed.): *The Middle Pleistocene in Europe*: 145–172; Rotterdam (Balkema).
- MAGNY, M. & HAAS, J.N. (2004): A major widespread climatic change around 5300 cal. yr BP at the time of the Alpine Ice man. – *Journal of Quaternary Science*, 19: 423–430. DOI: 10.1002/jqs.850

### Books:

- EHLERS, J. (1994): *Allgemeine und historische Quartärgeologie*. – 358 S.; Stuttgart (Enke).

Please do not use abbreviations of the journal names.

## Specimen copies

Authors receive no printed specimen copies. The electronic version is available as download free.

For further questions about the submission of manuscripts please contact the production editor (imprint).



# Radiocarbon Dating Without Regrets



**BETA**

**Beta Analytic**  
Radiocarbon Dating  
[www.radiocarbon.com](http://www.radiocarbon.com)

- Reliable turnaround time
- High-quality, ISO 17025 accredited results
- Prompt responses within 24 hours

**Results in as little as 2-3 days**

**Australia Brazil China India Japan Korea UK USA**

Das Manuskript ist grundsätzlich in elektronischer Form einzureichen und muss mit Namen und Adresse des Erstautoren versehen sein. Bitte benutzen Sie eine Standard-Textverarbeitung im .rtf, .odt oder .doc-Format (LaTeX-Dateien auf Anfrage). Als Zeichensatz verwenden Sie bitte die Standard-Fonts Times Roman, Helvetica oder Courier mit einem 1,5-fachen Zeilenabstand.

Zur Einreichung nutzen Sie bitte unser Online Submission System unter [www.quaternary-science.net](http://www.quaternary-science.net). Nach dem Login steht Ihnen hier eine Upload-Funktion für das Manuskript und die Abbildungs-Dateien zur Verfügung.

### Manuskriptform

Als Publikationssprachen sind Englisch und Deutsch zugelassen. Manuskripte in deutscher Sprache müssen einen englischen Untertitel tragen sowie eine englische Kurzfassung und englische Keywords beinhalten. Für die deutschen Texte gelten die Regeln der neuen Rechtschreibreform.

Die Manuskripte sollen folgendem Aufbau entsprechen:

- I Kurze, aber prägnante Überschrift
- II Ausgeschriebener Vor- und Nachname, Post- und E-Mail-Adresse
- III 5 bis 10 englische Keywords, die den Inhalt des Manuskriptes widerspiegeln.
- IV Deutsche und englische Kurzfassung des Textes mit einer Länge von bis zu 200 Wörtern. Der englische Untertitel des Manuskriptes ist der englischen Kurzfassung in eckigen Klammern voranzustellen.
- V Klar gegliederter Text. Kapitelnummerierungen sind mit arabischen Ziffern zu versehen.
- VI Alphabetisch geordnete Literaturliste. Die Zitierweise muss der unten angegebenen Form entsprechen.

Im fortlaufenden Text sind Literaturhinweise als Kurzzitate einzufügen, der oder die Autorennamen sind in KAPITÄLCHEN-Schrift zu setzen, das Erscheinungsjahr in Klammern, z. B. MÜLLER (2006). Werden von einem Autor mehrere Arbeiten aus einem Jahr zitiert, so sind diese durch Buchstaben zu unterscheiden: MÜLLER (2006a, 2006b). Bei mehr als drei Autoren kann et al. verwendet werden: MÜLLER et al. (2006). Arbeiten mit bis zu drei Autoren werden folgendermaßen zitiert: MÜLLER & MEYER (2006) oder MÜLLER, MEYER & SCHULZ (2006). Sind mit der Zitierung bestimmte Seiten oder Abbildungen gemeint, müssen diese genau angegeben werden: MÜLLER (2006: 14) oder MÜLLER (2006: Fig. 14).

Die wissenschaftlichen Namen von Pflanzen und Tieren (*Gattungen*, *Untergattungen*, *Arten*, *Unterarten*) sind kursiv zu schreiben. Die den biologischen Namen folgenden Autoren werden in KAPITÄLCHEN gesetzt (*Armeria maritima* WILLD.).

Bitte keinen Blocksatz verwenden, sondern linksbündigen Satz. Bitte keine automatische Silbentrennung verwenden.

Bitte alle automatischen Formatierungen in Ihrer Textbearbeitung deaktivieren.

Bitte keine Seitenzählung.

Abbildungen, Tabellen und Fotos nicht in den Text einbauen, sondern separat als Datei beifügen. Abbildungsunterschriften in Deutsch und Englisch am Ende des Manuskripttextes platzieren.

### Abbildungen

Bitte fügen Sie jede Abbildung als separate Datei mit einem eindeutigen Namen bei. Alle Grafiken müssen eine Verkleinerung auf Spaltenbreite (= 8,4 cm) oder Satzspiegel (= 17,2 x 26 cm) zulassen. Die Beschriftung muss nach der Verkleinerung noch gut lesbar sein. Sollte eine Legende nötig sein, so binden Sie diese in die Abbildung ein. Bitte vermeiden Sie Haarlinien oder Grauwerte. Alle Abbildungen können farbig sein. Es entstehen keine Mehrkosten.

Für die Drucklegung müssen alle Abbildungen in elektronischer Form eingereicht werden. Bitte verwenden Sie für pixelbasierte Abbildungen (Fotos) das .tif-Format mit einer Auflösung von mindestens 450 dpi und für vektorbasierte Abbildungen (Diagramme, Maps, Tabellen) das .eps-Format. Stark reduzierte .jpg oder .pdf-Dateien sowie in Text-Dokumente eingebundene Abbildungen werden nicht akzeptiert.

### Zitierweise (Beispiele)

#### Aufsätze:

SCHWARZBACH, M. (1968): Neue Eiszeithypothesen. – Eiszeitalter und Gegenwart, 19: 250–261.

EISSMANN, L. & MÜLLER, A. (1979): Leitlinien der Quartärentwicklung im norddeutschen Tiefland. – Zeitschrift für Geologische Wissenschaften, 7: 451–462.

ZAGWIJN, W.H. (1996): The Cromerian Complex Stage of the Netherlands and correlation with other areas in Europe. – In: TURNER, C. (ed.): The Middle Pleistocene in Europe: 145–172; Rotterdam (Balkema).

MAGNY, M. & HAAS, J.N. (2004): A major widespread climatic change around 5300 cal. yr BP at the time of the Alpine Ice man. – Journal of Quaternary Science, 19: 423–430. DOI: 10.1002/jqs.850

#### Monographische Werke, Bücher:

EHLERS, J. (1994): Allgemeine und historische Quartärgeologie. – 358 S.; Stuttgart (Enke).

Bitte keine Abkürzungen der Zeitschriftentitel verwenden.

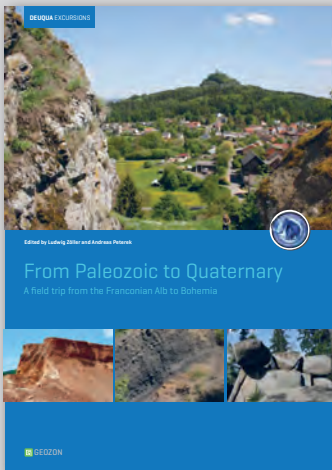
### Belegexemplare

Es werden keine gedruckten Belegexemplare verschickt. Die elektronische Version steht zum kostenlosen Download zur Verfügung.

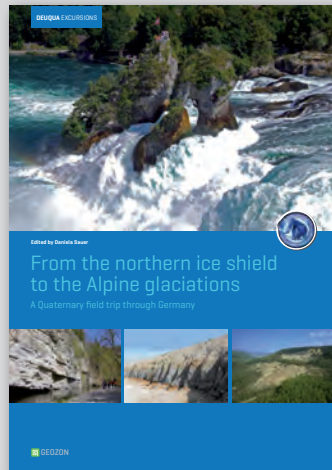
Bei weiteren Fragen zur Manuskripteinreichung wenden Sie sich bitte an die technische Redaktion (s. Impressum)



## DEUQA EXKURSIONSFÜHRER / FIELD GUIDEBOOKS



**From Paleozoic to Quaternary: A field trip from the Franconian Alb to Bohemia**  
 ISBN 978-3-941971-08-0  
 120 pp., A4, 34,- Euro



**From the northern ice shield to the Alpine glaciations**  
 ISBN 978-3-941971-06-6  
 88 pp., A4, 29,- Euro



**Eiszeitlandschaften in Mecklenburg-Vorpommern**  
 ISBN 978-3-941971-05-9  
 164 pp., A4, 34,- Euro

## REGIONALE GEOLOGIE



**Zur jungquartären Landschaftsentwicklung der Mecklenburgischen Kleinseenplatte**  
 ISBN 978-3-941971-09-7  
 78 pp., A4, 22,- Euro



**Zur Landschafts- und Gewässergeschichte der Müritz**  
 ISBN 978-3-941971-00-4  
 94 pp., A4, 29,- Euro



**Neubrandenburger Geologische Beiträge**  
 ISSN 1616-959X  
 88 pp., 17 x 24 cm, 8,50 Euro



Geozon Science Media  
 Postfach 3245  
 D-17462 Greifswald  
 Germany

Tel. 03834-80 14 80  
 Fax 03834-80 14 81  
 E-Mail: [info@geozon.net](mailto:info@geozon.net)  
 Online: [www.geozon.net](http://www.geozon.net)





## German Quaternary Association

The German Quaternary Association (DEUQUA) eV is an association of German-speaking Quaternary Scientists. The aim of the association is to promote the Quaternary Science, to represent it in public, to intensify the contact to applied science as well as to advice public and political boards in quaternary issues.

Furthermore, the association has set itself the task of operating the contacts between the Quaternary Scientists and related organizations at home and abroad.

The DEUQUA published annually several editions of "E&G – Quaternary Science Journal". In that journal research results from the field of Quaternary Science are published. In addition, developments in the DEUQUA are announced in the "Geoscience messages" (GMIT). GMIT is published quarterly.

Every two years, the German Quaternary Association held the DEUQUA-Conference. At this conference the latest research results of the Quaternary Science are presented and discussed.

## Deutsche Quartärvereinigung

Die Deutsche Quartärvereinigung (DEUQUA) e.V. ist ein Zusammenschluss deutschsprachiger Quartärwissenschaftler und wurde 1949 gegründet. Der Verein hat zum Ziel, die Quartärwissenschaft zu fördern, sie in der Öffentlichkeit zu vertreten, den Kontakt zu angewandter Wissenschaft zu intensivieren sowie öffentliche und politische Gremien in quartärwissenschaftlichen Fragestellungen zu beraten. Des Weiteren hat der Verein sich zur Aufgabe gemacht, die Kontaktpflege der Quartärforscher untereinander und zu verwandten Organisationen im In- und Ausland zu betreiben.

Die DEUQUA veröffentlicht jährlich mehrere Ausgaben von „E&G – Quaternary Science Journal“. Dort werden Forschungserkenntnisse aus dem Bereich der Quartärwissenschaft publiziert. Zusätzlich werden Entwicklungen in der DEUQUA vierteljährlich in den Geowissenschaftlichen Mitteilungen (GMIT) bekannt gemacht.

Im zweijährigen Turnus veranstaltet die Deutsche Quartärvereinigung e.V. die DEUQUA-Tagung. Diese bietet ein Forum, in welchem aktuelle Forschungsergebnisse aus dem Bereich der Quartärwissenschaften vorgestellt und diskutiert werden.

## Committee / Vorstand



### PRESIDENT / PRÄSIDENTIN

MARGOT BÖSE  
Freie Universität Berlin  
Malteserstr. 74-100  
D-12249 Berlin, Germany  
Tel.: +49 (0)30-838-70 37 3  
E-Mail: m.boese [at] fu-berlin.de

### VICE PRESIDENTS / VIZEPRÄSIDENTEN

CHRISTOPH SPÖTL  
Institut für Geologie und Paläontologie  
Universität Innsbruck  
Innrain 52  
A-6020 Innsbruck, Austria  
Tel.: +43 (0)512-507-5593  
Fax: +43 (0)512-507-2914  
E-Mail: christoph.spoetl [at] uibk.ac.at

LUDWIG ZÖLLER  
Fakultät II – Lehrstuhl für Geomorphologie  
Universität Bayreuth  
Universitätsstraße 30  
D-95440 Bayreuth, Germany  
Tel.: +49 (0)921-55 2266  
Fax: +49 (0)921-55 2314  
E-Mail: ludwig.zoeller [at] uni-bayreuth.de

### TREASURER / SCHATZMEISTER

JÖRG ELBRACHT  
Landesamt für Bergbau, Energie und Geologie  
Stilleweg 2  
D-30655 Hannover, Germany  
Tel.: +49 (0)511-643-36 13  
E-Mail: joerg.elbracht [at] lbeg.niedersachsen.de

### EDITOR-IN-CHIEF / SCHRIFTLÉITUNG (E&G)

HOLGER FREUND  
ICBM – Geoecology  
Carl-von-Ossietzky Universitaet Oldenburg  
Schleusenstr. 1  
D-26382 Wilhelmshaven, Germany  
Tel.: +49 (0)4421-94 42 00  
E-Mail: holger.freund [at] uni-oldenburg.de

### ARCHIVIST / ARCHIVAR

STEFAN WANSA  
Landesamt für Geologie und Bergwesen  
Sachsen-Anhalt  
Postfach 156  
D- 06035 Halle, Germany  
Tel. +49 (0)345-5212-12 7  
E-Mail: wansa [at] lagb.mw.sachsen-anhalt.de

### ADVISORY BOARD / BEIRAT

CHRISTIAN HOSELMANN  
Hessisches Landesamt für Umwelt und Geologie  
Postfach 3209  
D-65022 Wiesbaden, Germany  
Tel.: +49 (0)611-69 39 92 8  
E-Mail: christian.hoselmann [at] hlug.hessen.de

### DANIELA SAUER

Institut für Bodenkunde und Standortslehre  
Universität Hohenheim  
Emil-Wolff-Str. 27  
D-70593 Stuttgart, Germany  
Tel.: +49 (0)711-459-22 93 5  
E-Mail: d-sauer [at] uni-hohenheim.de

### FRANK PREUSSER

Department of Physical Geography and  
Quaternary Geology  
Stockholm University  
10961 Stockholm, Sweden  
Tel. +46 8 674 7590  
E-Mail: frank.preusser [at] natgeo.su.se

### REINHARD LAMPE

Institut für Geographie und Geologie  
Ernst-Moritz-Arndt-Universität Greifswald  
Friedrich-Ludwig-Jahn-Straße 16  
D-17487 Greifswald, Germany  
Tel: +49 (0)3834-86-45 21  
E-Mail: lampe [at] uni-greifswald.de

### BIRGIT TERHORST

Geographisches Institut  
Universität Würzburg  
Am Hubland  
D-97074 Würzburg, Germany  
Deutschland  
Tel. +49 (0)931-88 85 58 5  
E-Mail: birgit.terhorst [at] uni-wuerzburg.de

## Reorder / Nachbestellung

The volumes 6–7, 11–17, 19–28 and 30–58 are currently available. All other volumes are sold out. A reduced special price of 10,- € per edition is up to and including volume 55. The regular retail price applies from vol. 56/1–2. The prices are understood plus shipping costs. VAT is included. The complete content is searchable at [www.quaternary-science.net](http://www.quaternary-science.net).

### 1951–2006

Vol. 6–7, 11–17, 19–28, 30–55 each volume 10,- €

2007	Topics	Price
------	--------	-------

Vol. 56 No 1–2	Special issue: Stratigraphie von Deutschland – Quartär	54,- €
Vol. 56 No 3	Pfälzerwald, pollen types and taxa, Oberösterreich, Riß-Iller, Schatthausen	27,- €
Vol. 56 No 4	Nußloch, Rangsdorfer See, Lieth/Elmshorn, Gardno Endmoräne/Debina Cliff	27,- €

2008	Topics	Price
------	--------	-------

Vol. 57 No 1–2	Special issue: Recent progress in Quaternary dating methods	54,- €
Vol. 57 No 3–4	Special issue: The Heidelberg Basin Drilling Project	54,- €

2009	Topics	Price
------	--------	-------

Vol. 58 No 1	Surface Exposure Dating, Bodensee, Living Fossil, Hochgebirgsböden	27,- €
Vol. 58 No 2	Special issue: Changing environments – Yesterday, Today, Tomorrow	27,- €

2010	Topics	Price
------	--------	-------

Vol. 59 No 1–2	Baltic Sea Coast, Rodderberg Crater, Geiseltal, Wettersteingebirge, Møn, Argentina	54,- €
----------------	--	--------

2011	Topics	Price
------	--------	-------

Vol. 60 No 1	Special issue: Loess in Europe	27,- €
Vol. 60 No 2–3	Special issue: Glaciations and periglacial features in Central Europe	54,- €
Vol. 60 No 4	Special issue: Quaternary landscape evolution in the Peribaltic region	27,- €

2012	Topics	Price
------	--------	-------

Vol. 61 No 1	Calcareous Alps Austria, Löss, Holzreste Schweiz, Rinnen-Strukturen, Permafrost carbon	27,- €
Vol. 61 No 2	Rivers, Lakes and Peatlands NE Germany, Lavrado Region Brazil, Terna River Basin India	27,- €

## Subscription / Abonnement

Title: E&G – Quaternary Science Journal

Print-ISSN: 0424-7116

Issues per volume: 2

### Prices [EUR] print per volume

End customers: 50,46 € (Free for DEUQUA-Members)

Wholesalers, booksellers: 32,80 €

Scientific libraries: 47,94 €

VAT is not included.

### Postage [EUR] per volume

within Germany: 2,50 €

World (Surface): 6,80 €

World (Airmail): 7,70 €

### Special offer

Libraries which subscribe our journal can receive the volumes 1951–2006 for free. Only shipping costs have to be paid.

### Order address

Geozon Science Media

P.O. Box 3245

D-17462 Greifswald

Germany

tel.: +49 (0)3834-80 40 80

fax: +49 (0)3834-80 40 81

e-mail: [info \(at\) geozon.net](mailto:info@geozon.net)

web: [www.geozon.net](http://www.geozon.net)

## Contents

- DOI 10.3285/eg.62.1.01  
4 **A stratigraphic concept for Middle Pleistocene Quaternary sequences in Upper Austria**  
*Birgit Terhorst*
- DOI 10.3285/eg.62.1.02  
14 **Magnetic excursions recorded in the Middle to Upper Pleistocene loess/palaeosol sequence Wels-Aschet (Austria)**  
*Robert Scholger, Birgit Terhorst*
- DOI 10.3285/eg.62.1.03  
22 **Paleopedological record along the loess-paleosol sequence in Oberlaab, Austria**  
*Elizabeth Solleiro-Rebolledo, Hector Cabadas, Birgit Terhorst*
- DOI 10.3285/eg.62.1.04  
34 **Grain size and mineralogical indicators of weathering in the Oberlaab loess-paleosol sequence, Upper Austria**  
*Franz Ottner, Sergey Sedov, Undrakh-Od Baatar, Karin Wriessnig*
- DOI 10.3285/eg.62.1.05  
44 **Last Interglacial paleosols with Argic horizons in Upper Austria and Central Russia – pedogenetic and paleoenvironmental inferences from comparison with the Holocene analogues**  
*Sergey Sedov, Svetlana Sycheva, Victor Targulian, Teresa Pi, Jaime Díaz*
- DOI 10.3285/eg.62.1.06  
59 **Paudorf *locus typicus* (Lower Austria) revisited – The potential of the classic loess outcrop for Middle to Late Pleistocene landscape reconstructions**  
*Tobias Sprafke, Birgit Terhorst, Robert Peticzka, Christine Thiel*